Condition Assessment of Concrete Bridge Decks using Ground Penetrating Radar

Kien Dinh

A Thesis

In The Department

of

Building, Civil and Environmental Engineering

Presented in Partial Fulfillment of the Requirements

For the Degree of

Doctor of Philosophy (Civil and Environmental Engineering) at

Concordia University

Montreal, Quebec, Canada

September 2014

© Kien Dinh

CONCORDIA UNIVERSITY
SCHOOL OF GRADUATE STUDIES

This is to certify that the thesis prepared

By: Kien Dinh

Entitled: Condition Assessment of Concrete Bridge Decks Using Ground Penetrating Radar

and submitted in partial fulfillment of the requirements for the degree of

Doctor of Philosophy (Building Engineering)

complies with the regulations of the University and meets the accepted standards with respect to originality and quality.

Signed by the final examining committee:

Dr. Amin Hammad	Chair
Dr. Nenad Gucunski	External Examiner
Dr. Govind Gopakumar	External to Program
Dr. Osama Moselhi	Examiner
Dr. Luis Amador	Examiner
Dr. Tarek Zayed	Thesis Supervisor

Approved by

Dr. Mohammed Zaheeruddin
Chair of Department or Graduate Program Director

Sep 17, 2014

Dr. Amir Asif
Dean of Faculty

ABSTRACT

Condition Assessment of Concrete Bridge Decks using

Ground Penetrating Radar

Kien Dinh

Concordia University, 2014

Highway bridge structures play a critical role in transportation system. While one-third of Canada's 75,000 highway bridges have structural or functional deficiencies and a short remaining service life; in the United States (US), as of December 2013, more than 100 million m^2 of the total 360 million m^2 of concrete bridge decks is either structurally deficient or functionally obsolete. To eliminate that deficient backlog in US by 2028, it is estimated that an annual investment of $20.5 billion would be needed and the largest portion of this expenditure would be for bridge decks.

Condition assessment of concrete bridge decks provides required inputs for programming deck maintenance activities. In both Canada and the United States, the main approach to evaluate condition of bridge decks, as for other bridge elements, is based on visual inspection. Although this approach may be effective in finding external flaws such as cracks, scaling and spalls; it cannot detect subsurface defects such as voids, internal cracks, delaminations, or rebar corrosion. To overcome such limitation of visual inspection, this research aims at developing a condition assessment system for concrete bridge decks based on nondestructive evaluation (NDE) technology. In order to achieve that goal, three research

objectives were identified: (1) study and select the most appropriate NDE technology; (2) study methods for interpreting data of selected NDE technique; and (3) develop bridge deck corrosiveness index (BDCI) from NDE output.

Ground penetrating radar (GPR) was found to be one of the most appropriate technologies for inspecting concrete bridge decks subjected to corrosion-induced deterioration. As for GPR data interpretation, two analysis methods are proposed in this research. The first one is an integrated technique between the amplitude method and visual interpretation with threshold calibration based on K-means clustering. The second approach is a technique for analyzing time-series GPR data. Based on correlation coefficient between A-scans, this technique assesses concrete deterioration by studying the change of GPR signals over time. Expert opinions, through a structured questionnaire survey, were used to develop and interpret bridge deck corrosiveness index (BDCI) based on GPR output. After being validated by several case studies, an automated software has been developed to facilitate the implementation of the entire methodology. The developed system and models will help transportation agencies to identify critical deficiencies and focus limited funding on most deserving bridge decks.

Acknowledgements

very gratefuly to my friend, Thai-Hoa Le and my colleagues in The Automation and Construction Lab at Concordia University.

Last but not least, I express my deepest acknowledgement to my parent Mr. Phuc Dinh and Mrs. Ty Pham, my adorable wife Thuy Huynh, my two sons Anh Triet and Hoang Dan, my sister Tra Mi and her little family. Without their support, I would certainly not be able to finish this interesting but challenging research.

TABLE OF CONTENT

LIST OF FIGURES

LIST OF TABLES

CHAPTER 1   INTRODUCTION

1.1   Problem Statement and Research Motivation

Highway bridge structures play a critical role in transportation system. Consequences of highway bridge failure are usually catastrophic, both in terms of human life as well as economic loss. While one-third of Canada's 75,000 highway bridges have structural or functional deficiencies and a short remaining service life (Lounis 2013); according to the Federal Highway Administration (FHWA 2013), as of December 2013, more than 100 million m^2 of the total 360 million m^2 of concrete bridge decks in the United States is either structurally deficient (SD) or functionally obsolete (FO). American Society of Civil Engineers (ASCE 2013) estimated that an annual investment of \$20.5 billion would be needed to eliminate the nation's bridge deficient backlog by 2028. The largest portion of this expected expenditure is allocated to bridge decks (Gucunski et al. 2013) in which rebar corrosion problem is one of the most concerns (Gucunski 2013).

In Canada and the United States, the main approach to evaluate the condition of bridge decks, as for other bridge elements, is based on visual inspection. The obtained condition is then used to make decision for optimizing deck maintenance, repair and rehabilitation (MR&R). Although visual inspection approach may be effective in finding external defects, such as cracks, scaling and spalls; it cannot detect subsurface

flaws such as voids, internal cracks, delaminations, or rebar corrosion. This problem is especially more obvious for paved deck structures. Another problem associated with visual inspection is that inspection results are subjective to operators' technique and interpretation.

Many efforts have been made to solve the above problems using nondestructive evaluation (NDE) technologies. Although successful application of these techniques has been demonstrated through a number of research projects or case studies, NDE technologies have not been widely accepted partially because of less than positive experiences that may have occurred from unrealistic expectations or improper use (Gucunski 2013). Most of research efforts have still aimed at verifying the capability, or to compare the accuracy, of different NDE techniques.

1.2   Research Objectives

The ultimate goal of this research is to develop a condition assessment system for concrete bridge decks subject to corrosion-induced deterioration, based on the most appropriate NDE technology. In order to achieve that goal, the following study objectives are carried out:

1- Identify, study, and select the most appropriate NDE technology.

2- Develop inspection framework and methods for data analysis.

3- Develop bridge deck condition index (BDCI) and automate its implementation.

1.3 Research Methodology

Although detailed research methodology of this study will be described in detail in each chapter, its overall schematic representation in Fig. 1.1 can be summarized including the following steps.
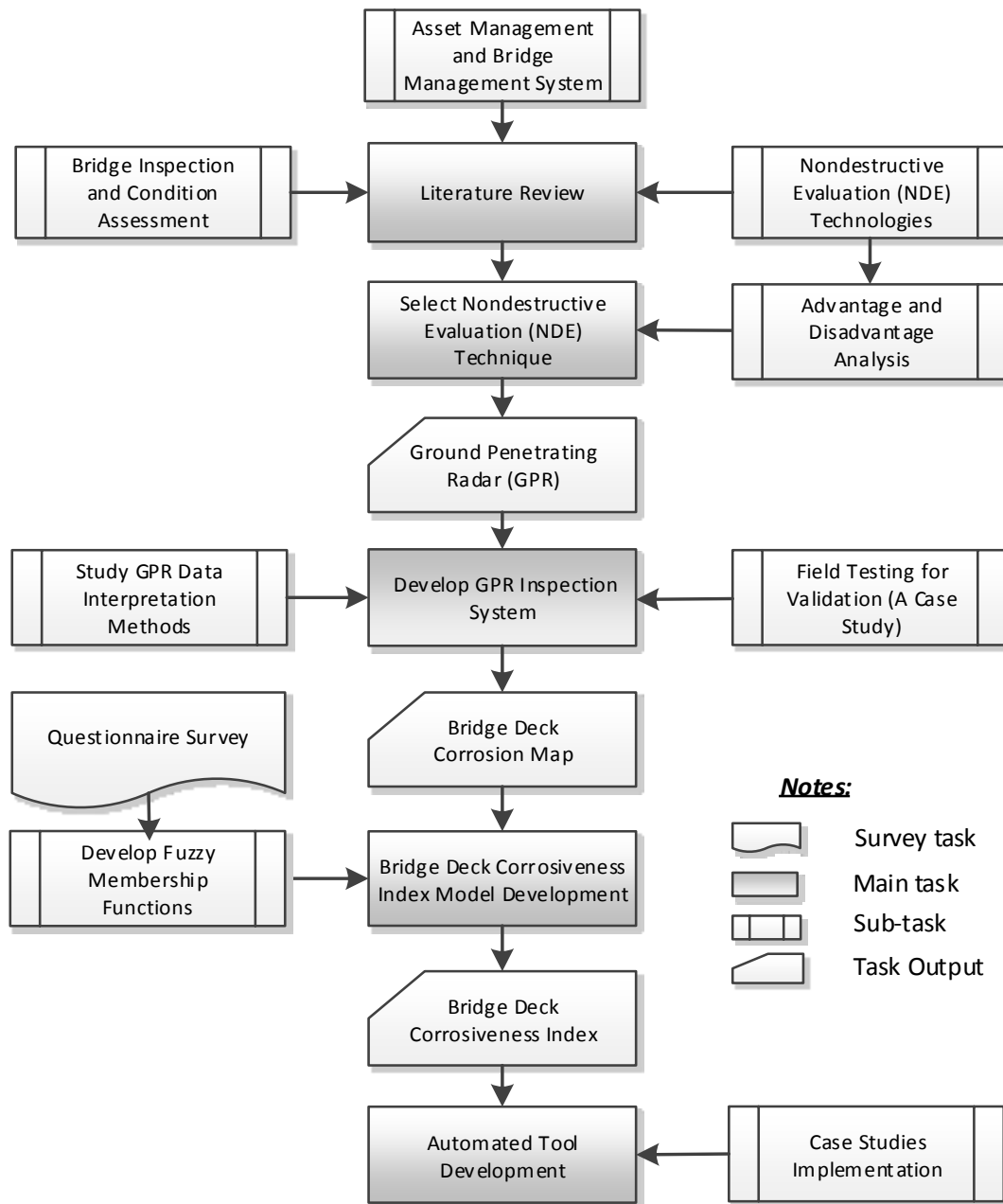
Fig. 1.1 Overall Research Methodology.

Step 1. *Literature Review*

This first step starts by extensive search of the literature regarding asset management, asset condition assessment, bridge management system, bridge inspection, bridge condition rating and nondestructive evaluation (NDE) technologies. The focus is however placed on the last items, i.e., bridge inspection, bridge condition assessment, and NDE techniques.

Step 2. *Study and select the most appropriate NDE technique*

In this step, based on studying principles and literature of various nondestructive evaluation (NDE) technologies, the research identifies and selects the most appropriate NDE technique for inspection of concrete bridge decks. Such selection is based on analyzing advantages and disadvantages of each technology from the bridge deck inspection perspective.

Step 3. *Develop inspection framework*

Through a real case study with extensive data for the selected NDE technology, the inspection framework and data interpretation methods are studied, developed and validated in this step.

Step 4. *Develop Bridge Deck Corrosiveness Index*

In this step, the method to obtain condition rating for concrete bridge deck based on NDE output is studied. In the current research, that rating is termed Bridge Deck Corrosivness Index (BDCI). This index uses the scale from 0 to 100, the same idea as

the California Bridge Health Index. However, it is developed based on fuzzy set theory through a structured questionnaire survey to solicit opinions from bridge and NDE experts.

Step 5. *Develop a software for the proposed framework*

In this last step, the software to automate the entire system is coded. This software will help transportation agencies and NDE consulting firms to easily implement the developed framework, from processing the inspection output to computation of bridge deck corrosiveness index (BDCI). Finally, in order to illustrate its functionality, the software is implemented for several real case studies.

1.4   Thesis Organization

This thesis consists of seven chapters as follows:

Chapter 1 highlights the research need by stating problem and research motivation. It then introduces the research objectives and provides brief description of proposed research methodology.

Chapter 2 proceeds with the literature review of bridge condition assessment. It first provides an introduction about asset management in general and bridge management system in particular. The focus is finally placed on bridge inspection and bridge condition rating. The chapter is concluded by briefing the limitations of current practices or research gaps.

Chapter 3 presents the research methodology in detail, which shows how data for the

selected NDE technology will be analyzed and how condition rating model will be developed in this research.

Chapter 4 describes data collection for the questionnaire survey proposed in the research methodology and NDE data collection for real concrete bridge decks as the case studies. The case studies used in this research include one bare concrete bridge deck in New Jersey, US and four asphalt-covered concrete bridge decks in Quebec, Canada.

Chapter 5 presents the implementation of the proposed models to the collected data, i.e., the responses obtained from the questionnaire survey and the NDE data for New Jersey bridge deck. The final output will be a bridge deck corrosiveness index (BDCI) that represents the overall corrosiveness of the deck structure.

Chapter 6 describes the automated tool (software) for implementing the system, i.e., GPR data analysis and condition rating model developed in this study. The software implementation will then be illustrated through its application to four concrete bridge decks in Quebec, Canada.

Finally, Chapter 7 concludes the thesis by highlighting the research contributions, research limitations and future works.

CHAPTER 2   LITERATURE REVIEW

2.1   Asset Management

2.1.1   Definition of Asset Management

Asset Management (AM), as defined by USFHA (1999), is "*a business process and a decision-making framework that covers an extended time horizon, draws from economics as well as engineering, and considers a broad range of assets*". The basic idea of its approach is based on economic assessment of trade-offs between investment alternatives, at both the project level and network level. USFHA (1999) also pointed out three reasons behind the naissance of the asset management concept, including: (1) changes in the transportation environment; (2) changes in public expectation, and (3) extraordinary advances in technologies. Specifically, the transportation sector is presently experiencing the highest ever users' demands while at the same time it has to maintain the huge number of on-going deteriorated structures. Under the condition of limited financial resources, the public expects that transportation agencies make the most effective investment decisions on their infrastructure assets and these decisions have to be understandable and justifiable to them. Finally, the advances of computer technology have made very complex analytical tools and techniques available for realization of asset management ideology.

2.1.2   Asset Management Process

Schematically, the process for asset management is illustrated in Fig. 2.1 (USFHA,

1999), while verbally, this entire process can be described including the following steps:

Step 1. *Specify agency's missions*

The AM approach recommends that transportation agencies should start managing their assets by specifying, clarifying their missions as well as their assets' goals and agencies' policies. Once these questions are answered, the agency would know exactly what they are trying to achieve and then what should be followed to achieve those goals.

Step 2. *Acquire knowledge about asset inventory*

This step is to help the transportation agencies know what assets they own and hold responsible for. This knowledge is very important and has to be acquired before the agencies can go any further in managing those assets.

Step 3. *Acquire knowledge about assets' condition & performance*

It is clear that one cannot manage his/her assets when he/she does not know how the assets are performing their intended functions. The situation is the same when it comes to transportation asset management. Transportation agencies need to know clearly the condition and performance of their assets in order to make effective management decisions, guarantying the public's value for money. This step can be considered the most important stage in the asset management process since it provides the input for the whole system, considering the well-known expression "garbage in, garbage out".

Step 4. *Alternative Evaluations and Program Optimization*

Based on inputs provided in previous steps, transportation agencies will specify

investment alternatives at both the project level and network (system) level. These alternatives will then be evaluated and compared with each other, while taking into account the available budget, to determine the project priority order for program optimization.
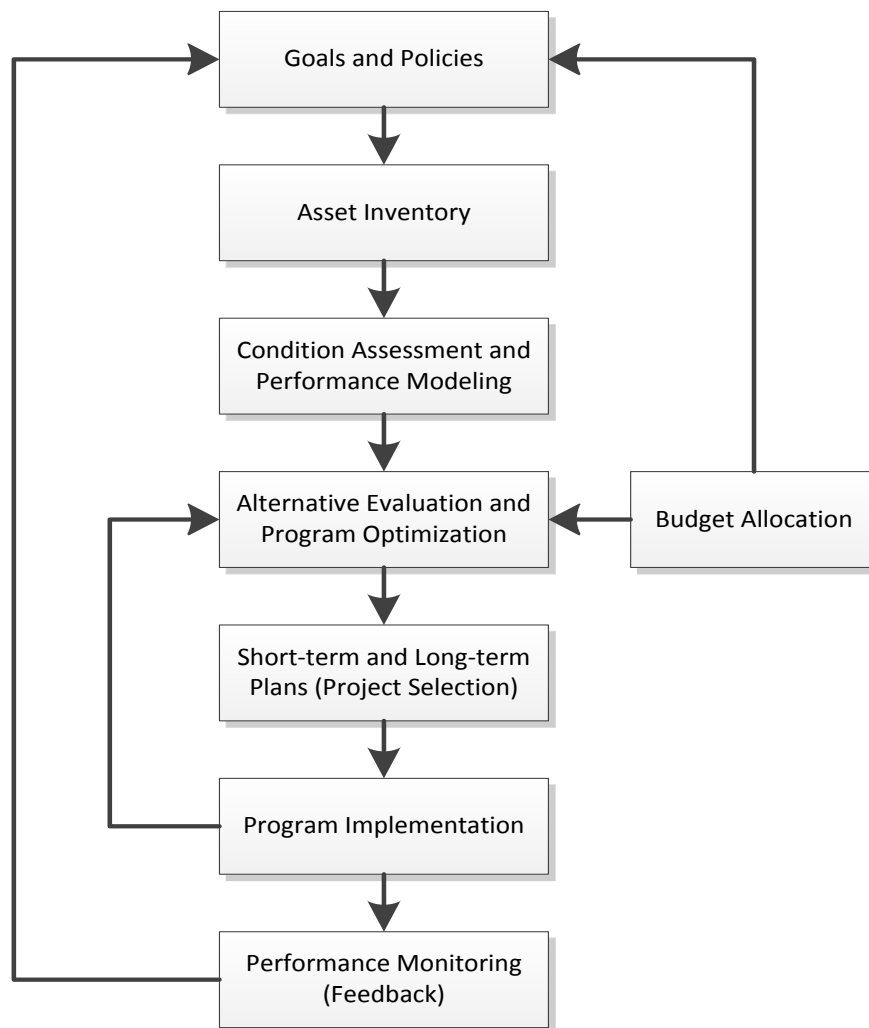
Fig. 2.1 Generic Asset Management System (USFHA 1999).

Step 5. *Select projects for short-term and long-term plans*

This step is to select specific projects for implementation in the short-term, usually within first five years of the program, and to select the projects that can be delayed for

9

implementation later during the second half of the program.

Step 6. *Program Implementation*

All the projects that have been selected in the program will be deployed and implemented in this step. The projects in the short-term plan will be selected before the projects in the long-term plan. During this implementation, any changes from forecasted constraints or environment will be taken into account, and the program as well as the alternatives may be re-evaluated.

Step 7. *Performance Monitoring*

Finally, in this last step, performance of the assets will be monitored and assessed for comparison with the agencies' expectations. This feedback provides the input for the first step of the next process and a new management cycle begins.

Above is the entire process of asset management referred from USFHA (1999). The number of steps and specific descriptions of asset management processes may vary among different literatures, however the basic ideas and processes are all the same. For example, Vanier (2000) proposed six levels of implementation for asset management using six "What" questions. Answering each of these questions corresponds to each step in the entire management process. These six "What" questions include: *(1) What do you own; (2) What is it worth; (3) What is the deferred maintenance; (4) What is its condition; (5) What is the remaining service life; and (6) What do you fix first.* As can be seen, these six "What" questions are a shorter version of the asset management process previously described.

2.2 Bridge Management Systems

2.2.1 Definition of Bridge Management System

The bridge management system (BMS) is a particular domain of asset management in general when the assets in question are bridges. Along with the pavement management system, it is the most advanced asset management system that provides state-of-the-art practices to transportation agencies all over the world. Hudson et al. (1993) defines BMS as a rational and systematic approach to organizing and carrying out all activities related to maintaining a network of bridges. The main goal of a BMS is to advise bridge managers in making consistent and justifiable decisions regarding maintenance, rehabilitation, and replacement (MR&R) of bridges and in identifying future funding needs. These management decisions include both decisions made for an individual bridge and decisions made for the entire network of bridges. And generally, they are based on the benefits of the whole network rather than the benefits of the individual bridge. At the network level, a BMS tries to establish optimal investment funding levels and performance goals for an inventory of bridges, while at the bridge level it has to identify the appropriate combinations of treatment scope and timing for each individual bridge over its life cycle (Patidar et al. 2007).

2.2.2 Components of Bridge Management Systems

To perform their stated functions, Ryall (2010) suggests that bridge management systems should include the following components: (1) Inventory; (2) Inspection; (3) Maintenance; (4) Cost; and (5) Bridge condition. These five components will form the

database for the entire system. Information contained in the database will then be processed by management control to select maintenance options. After implementation of these chosen maintenance options, new output information will be updated to the database.

There have been many bridge management systems being developed all over the world. It should be noted that the specific structure of each of them varies and the decision-making methodologies that they use may not be the same. Therefore, it is not the intention of this section to describe the components of all available bridge management systems in detail. Instead, the structure of one of the most commonly used BMS in North America, Pontis (Robert et al. 2003), is selected for that purpose. Golabi and Shepard (1997) described this BMS in great detail. As can be seen in Fig. 2.2, the main information stored in the database of Pontis comes from inventory information and the condition surveys. The other information needed in order for the system to work include: MR&R costs; improvement costs; a set of interrelated models including the deterioration model, MR&R optimization model, improvement optimization model, and the model for integrated project programming. The brief description of how Pontis is built and how it works is as follows.

First, when a completely new bridge management system is constructed, all the information about the bridges it manages will be collected and stored in its database. This type of information is called inventory data, and for each bridge it typically includes information such as owner, location, year of construction, year of rehabilitation

(if any), traffic volume, type of material, current condition and so on (Golabi and Shepard 1997).
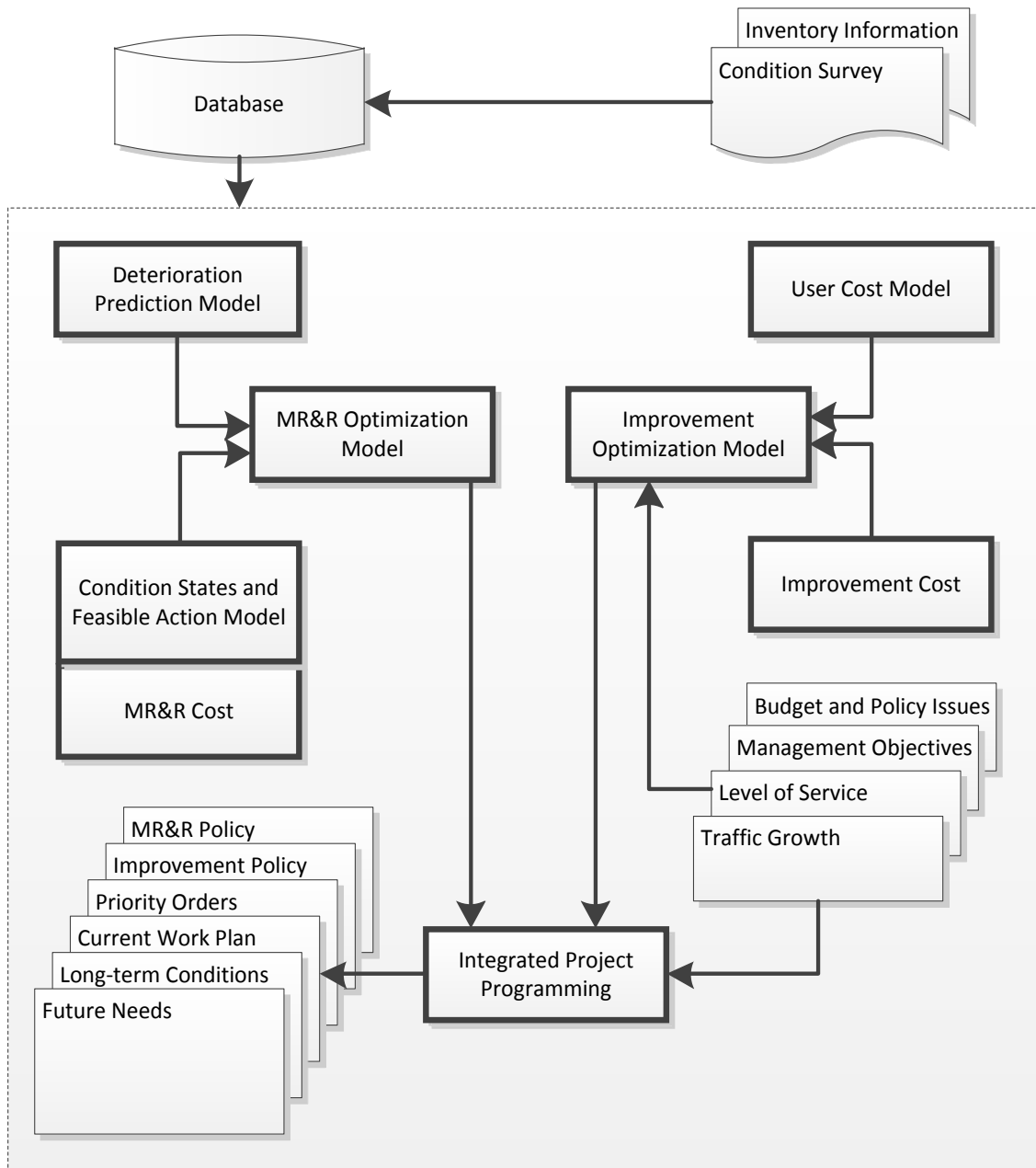
Fig. 2.2 Components of Bridge Management System (Golabi and Shepard 1997).

Periodically, these bridges will be inspected using either visual detection or

nondestructive evaluation technologies to assess their condition. The results will be updated and stored in the database to be available for data analysis. Although nondestructive evaluations can be used, current BMSs are mostly based on visual inspection to detect defects on bridges. The inspection is done on element basis and for each element the BMS will record element quantity associated with each condition state. Along with that, for each condition state of each element, the BMS will provide a list of possible actions (Golabi and Shepard 1997).

Based on inspected condition states, deterioration and action effectiveness (feasible action) models in Pontis will then be used to predict the future condition of each element in both cases, i.e., no or some action is taken on that element (Golabi and Shepard 1997). Specifically, if no action is taken, then only the deterioration model is needed to predict the element future condition, otherwise both the deterioration model and action effectiveness model are required. Basically, the action effectiveness model is the model used to predict condition of an element right after a specific action is taken on that element associated with a current condition state. So, in case there are some actions taken on the bridge, the action effectiveness models will be used first to predict the bridge's condition immediately after performing those actions. Deterioration models will be used after that to forecast condition of the bridge later on.

All the information available as described so far, along with cost data of feasible MR&R actions, will provide the input for the MR&R optimization model. Pontis uses this optimization model to recommend the best action for each condition state based on the

least long-term cost criteria (Golabi and Shepard 1997). This optimization model is one of the most important components of Pontis. Based on that, the scoping and timing of the optimal intervention for each bridge in the network will be determined.

For a bridge that is functionally obsolete, in addition to MR&R actions, Pontis also considers the possibility of bridge improvement (Golabi and Shepard 1997). Basically, the difference between the MR&R actions and improvement action is that MR&R actions only try to preserve as-built condition of the bridge while improvement actions will absolutely enhance the bridge's level-of-service. Normally, the improvement option will cost more than the MR&R options however the benefits it bring back will be the reduced cost of bridge users, safer traffic, and reduced traveling time due to the detour. This type of cost will be calculated in Pontis using the user cost model. The comprehensive cost–benefit analysis for improvement alternatives will be performed using the improvement optimization model.

After all investment alternatives for an individual bridge, including MR&R options and improvement options, have been generated, the final step will be programming interventions for the entire bridge network. In Pontis, this task is implemented using the integrated project programming module, or the network-level optimization model as it sometimes may be called. Pontis uses the Incremental Benefit – Cost (IBC) technique as its optimization method (Patidar et al. 2007). Its purpose is to select a subset of candidate projects from a network-wide candidate list that is expected to maximize the network benefits. The final outputs of this model and the entire system will include

policies for the MR&R and improvement actions, priority order of projects listed in the program, short-term work plan, long-term conditions, and predicted future needs.

Although being used by approximately 45 transportation agencies in the United State and internationally (Smadi et al. 2008), Pontis is still being considered not a comprehensive system. Most transportation agencies use the Pontis framework to exploit its strength in recording and storing detailed element-level inspection data, however for the project selection, they do not completely rely on Pontis' recommendation. One of the main reasons is that Pontis prioritizes projects based solely on cost–benefit analysis while ignoring other performance measures. An example can be taken from a study done for the Kansas Department of Transportation (KDOT). The purpose of the research was to explore whether KDOT should replace the current bridge priority formula by the Pontis system as the method for prioritizing bridge improvements and selecting bridges for major rehabilitation or replacement (Scherschligt and Kulkarni 2003).

Specifically, at the time when the research was performed, KDOT used bridge priority formula that was based totally on the National Bridge Inventory (NBI) rating, while Pontis element-level inspection data had also been collected and available since 1994. KDOT considered three following alternatives for integrating the Pontis system into the prioritization of bridge projects: (1) Translating Pontis inspection rating to NBI rating; (2) Calculating health indices from Pontis; and (3) Replacing the NBI bridge priority formula with Pontis. After analyzing and comparing three alternatives, it was concluded

that the most effective way for incorporating Pontis data into the bridge priority formula is to calculate health indices (Scherschligt and Kulkarni 2003). Also, it was determined that replacing the bridge priority formula with Pontis is unacceptable. The reason pointed out was that the two approaches utilized totally different strategies for project selection and as a result, the ranking of bridge projects by Pontis and by bridge priority formula varied widely. While Pontis selects bridge projects with the highest benefit–cost ratio, the bridge priority formula tends to select the projects with the most severe bridge deficiencies. KDOT realized that although project selection based on cost–benefit analysis is accepted by the bridge management community, it is difficult for them to explain to the public when one of the main stated objectives of their BMS is to guarantee the safety of the bridge to its users.

This section concludes by emphasizing the following findings:

1- Bridge management system is the most effective tool available for transportation agencies to manage their bridge inventories;

2- There is a need to build a comprehensive decision making methodology for current bridge management systems that can integrate all performance measures into the reasoning process; and

3- The bridge health or condition index is a very important performance measure of bridge structure and it should play the main role in the reasoning process mentioned above.

2.3 Bridge Inspection

2.3.1 Deterioration of Concrete Bridge Decks

The need for bridge inspection comes naturally because of deterioration of bridge structures. As stated in the research objectives, because this study focuses mainly on reinforced concrete bridge decks, only deterioration processes associated with this element type are described. It is known that deterioration of concrete structures is a result of combined effects of many complex phenomena. Penttala (2009) classifies two broad mechanisms of reinforced concrete bridge deterioration, namely, physically-induced and chemically-induced processes. Specifically, he defines physically-induced deteriorations are those processes caused by the factors such as freeze-thaw loads, non-uniform volume changes, temperature gradients, abrasion, erosion and cavitation while chemically-induced deteriorations happen because of carbonation, chloride ion, sulfate and acid attacks or alkali-aggregate reactions.

With such a variety of mechanisms, the deterioration of most concrete bridge decks in North America, however, is associated with corrosion of reinforcing steel bars that are caused by the de-icing salt applied on bridges during winter or by salt in seawater for structures built in marine environments (Qian 2004). In US alone, approximately 20 percent of the cost to rehabilitate its bridges is attributed to chloride-induced corrosion (Al-Qadi et al. 1993). The following paragraphs are therefore dedicated for the description of the corrosion-induced deterioration process.

According to Carino (2004), in newly constructed concrete structures, steel

reinforcements develop a protective oxide film that provides a natural barrier to the transformation of the iron to rust. This passive oxide coating film forms because of the alkaline condition in the pores of the cement paste. There are two main causes that break down this passive coating film, namely carbonation and chloride ingression.

Carbonation refers to the breakdown mechanism in which carbon dioxide (CO_2) reacts with alkalis ($Ca(OH)_2$ and $NaOH$) in the pore solution of the cement paste. The consequence of these reactions is that the alkaline condition, which is the required condition for maintaining the passive oxide coating film, is reduced when the pH of the pore solution decreases.

For chloride ingression, although the exact mechanism is not known, it is observed that when the presence of chloride reaches a certain extent, it breaks down the passive oxide film and the condition is ready for the corrosion to be initiated. This certain extent of chloride ion concentration is usually called the "threshold value" and it is reported that the value is affected by many factors such as mixture proportions, type of cement, water-cement ratio, sulfate content and so on.

After the oxide coating film on the steel is lost, the reinforcement corrosion happens because many tiny electrolytic cells are formed. In these cells, the water in the pores of the paste contains various dissolved ions and serves as the electrolyte, while heterogeneities in the surface of the steel cause some regions of the bars to act as the anodes and other regions to act as the cathodes (Carino 2004a).

At the anode, iron atoms lose electrons and move into the surrounding concrete as

ferrous ions, which is represented by the following oxidation (or anodic) reaction:

$$Fe \rightarrow Fe^{2+} + 2e^- \qquad (2.1)$$

The electrons flow through the bar to the cathode where they combine with water and oxygen, which are present in the concrete in order to produce hydroxyl cations. This reaction is as follows:

$$H_2O + 1/2O_2 + 2e^- \rightarrow 2OH^- \qquad (2.2)$$

The hydroxyl cations then combine with free ferrous ions to produce ferrous hydroxides that finally become iron oxides (or rusts). The whole process can be pictorially illustrated in Fig. 2.3 below.
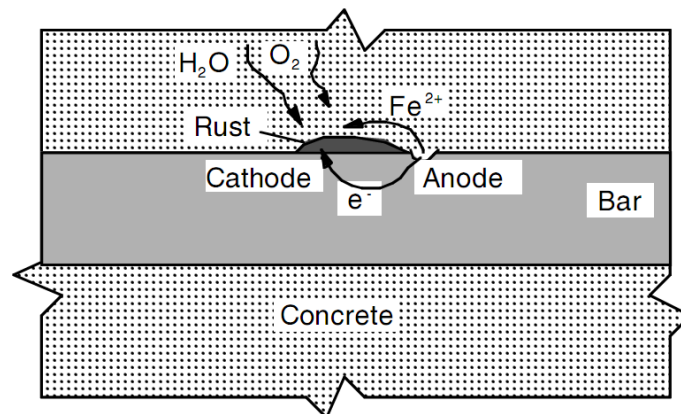
Fig. 2.3 Corrosion Process of Steel Reinforcement (Carino 2004a).

Corrosion is however just the beginning of a longer story. What happens next is that the rust, a product of corrosion, occupies much bigger volume than the original steel, and therefore produces internal stresses in the surrounding concrete, that finally causes the internal cracks to be initiated. These internal cracks are usually mistermed as

20

"delamination". At the beginning, these cracks are usually small and locate separately, but then they develop and become spalls that can be visually observed on the concrete surface.

In conclusion, the most common defects of concrete bridge decks that need to be identified during inspection are those caused by corrosion-induced deterioration. These defects include; (1) rebar corrosion, (2) concrete delamination; and (3) spalls. Since spalls can be observed by visual inspection, this study focuses on detecting early corrosion-induced deterioration, i.e., corrosion and delamination. By far, for a comprehensive assessment of concrete bridge decks, it would be desired to acquire knowledge about the chloride ingression at the reinforcement level.

2.3.2 Bridge Inspection Overview

Bridge inspection can be defined as a process in which the defects on a bridge are identified, recorded and used for assessing bridge condition. As has been seen previously, the inspection data provides required and invaluable inputs for bridge management systems. Interestingly, bridge inspection was not created because of that need. Instead, it was originally regulated for safety reasons. The event that changed US and human practices in guarantying bridge safety happened on December 15, 1967, when the Silver Bridge between Ohio and West Virginia collapsed during rush hour and caused 46 people dead in the freezing Ohio River (WSDOT 2010). This tragedy immediately brought the US government's focus on bridge safety issue. And as a consequence, on April 27, 1971, the Federal Highway Administration (FHWA) issued

the National Bridge Inspection Standards (NBIS). The purpose of this standard was to establish a program for regular and comprehensive inspections of all US federal highway bridges. The standard set forth the minimum qualifications for bridge inspectors, regulated specific types and frequencies for bridge inspection, as well as stipulated the inspection reporting format.

In 1978, the FHWA extended these requirements to all public bridges which carry vehicular traffic. In l987, when a review of the national bridge inspection programs was conducted by the Office of the Inspector General (OIG) in six states, a number of shortcomings were found. As a result, in August 1988, the FHWA issued some revisions to the NBIS (WSDOT 2010).

As just mentioned above, the National Bridge Inventory Standards (NBIS) set forth minimum inspection requirements for all public bridges in US which carry vehicular traffic. When implementing the NBIS, State Departments of Transportation (DOTs) generally expand the standards. They usually inspect more structures, perform some inspections more frequently, and place additional requirements on the qualifications of inspection personnel. The bridge inspections are normally performed for three purposes: (1) to ensure the safety of bridges, (2) to discover needs in maintenance and repair, and (3) to prepare for bridge rehabilitation (Hearn 2007).

2.3.3 Bridge Inspection Types and Intervals

There are several types of bridge inspection. Each type serves for specific purpose as previously mentioned and is performed at different frequency. Hearn (2007)

summarizes different types of bridge inspection, which are practiced in US, and their respective standard inspection frequencies. This information is described in Table 2-1 and it is noted that the frequencies for a specific inspection type may vary, depending on particular agencies.

Table 2-1 Types of Bridge Inspection in US (Hearn 2007)

Inspection	Description	Standard Inspection Interval
Damage Inspection	An unscheduled inspection to assess structural damage resulting from environmental factors or human actions	-
Fracture-Critical Member Inspection	A hands-on inspection of a fracture-critical member or member components that may include visual and other nondestructive evaluation.	24 months
Hands-On Inspection	Inspection within arm's length of the component. Inspection uses visual techniques that may be supplemented by nondestructive evaluation (NDE) techniques.	-
In-Depth Inspection	A close-up inspection of one or more members above or below the water level to identify any deficiencies not readily detectable using routine inspection procedures; hands-on inspection may be necessary at some locations.	-
Initial Inspection	First inspection of a bridge as it becomes a part of the bridge inventory to provide all Structure Inventory and Appraisal data and other relevant data and to determine baseline structural conditions.	-
Routine Inspection	Regularly scheduled inspection consisting of observations and/or measurements needed to determine the physical and functional condition of the bridge, to identify any changes from initial or previously recorded conditions, and to ensure that the structure continues to satisfy present service requirements.	24 months
Special Inspection	An inspection scheduled at the discretion of the bridge owner, used to monitor a particular known or suspected deficiency.	-
Underwater Inspection	Inspection of the underwater portion of a bridge substructure and the surrounding channel that cannot be inspected visually at low water by wading or probing, generally requiring diving or other appropriate techniques.	60 months

2.3.4 Visual Inspection Method

Visual inspection has been, and are still being, the dominant method to inspect bridges in the United States (Gucunski et al. 2009). This method does not require any special equipment while it can still provide invaluable information if the inspection is performed by experienced inspectors. Based on the observed defects, the inspector will utilize his or her knowledge about structure engineering, construction material and construction process in order to identify the probable cause of distresses and assess bridge condition. Although the method is simple and effective, it does have big limitations. It cannot detect internal flaws such as the chloride ingression, corrosions, voids, internal cracks and delamination in concrete structures. As a result, serious defects are not constantly found by this inspection method and tragic events keep happening; for example, the collapse of De la Concorde overpass in Montreal, Quebec, Canada in 2006.

Another problem of the visual inspection method is that it provides subjective information. This will affect the quality of bridge management decision–making. It is clear that the accuracy of bridge condition found by bridge inspection is a necessary requirement for making appropriate funding decision in the bridge maintenance program. Realizing this, in 2001, the FHWA conducted a comprehensive research to evaluate the reliability of visual inspection method in US (FHWA 2001). One of the main findings of that research is concerned with the accuracy of visual inspection result. It was reported that on average there were between four and five different Condition

Rating values assigned to each primary element while the overall scale is from 0 to 9. It was also stated that at least 48 percent of the individual Condition Rating for the primary elements were assigned incorrectly.

The limitations of visual inspection discussed above have motivated the bridge community to look for other inspection techniques, using either the destructive or nondestructive technologies. However, because destructive methods result in demolition of parts of bridge structures and very costly, when the destruction parts have to be repaired; nondestructive technologies are preferred. Available nondestructive evaluation (NDE) technologies for concrete bridge inspection are described and discussed in detail in the next section.

2.4   Nondestructive Evaluation Methods for Concrete Structures

According to Hellier (2003), Non-destructive Evaluation (NDE), Non-destructive Testing (NDT), Non-destructive Inspection (NDI), or Non-destructive Examination (NDE) are commonly used expressions to indicate an examination, test, or evaluation performed on any type of test object without changing or altering that object in anyway, in order to determine the absence or presence of conditions or discontinuities that may have an effect on the usefulness or serviceability of that object. For consistency, the term "NDE" is used throughout this dissertation. Although visual inspection is also a nondestructive method, according to this definition; it should be noted that whenever the term "NDE" is used in this thesis, it refers to nondestructive evaluation technologies other than visual inspection method.

Various NDE technologies have been applied for inspection of concrete structures. Typical technologies include: (1) Half-Cell Potential; (2) Concrete Resistivity; (3) Polarization Method; (4) Chain drag or hammer sounding; (5) Pulse velocity; (6) Spectral Analysis of Surface Waves; (7) Impact Echo; (8) Infrared Thermography; and (9) Ground Penetrating Radar. While detailed descriptions of these methods are provided in Appendix A, each of them is briefly described and discussed in turn in the following subsections.

2.4.1 Half-cell Potential (HP)

The half-cell potential (HP) is an electrical method that is used to delineate probable corrosion activity in concrete structures. Since this method requires the electrical access to the reinforcement and the electrical connectivity between the rebars, it is not applicable to epoxy-coated reinforcement.

Several studies have been performed investigating HP technique for inspection of concrete structures. For example, based on the results of an experimental study, Pradhan and Bhattacharjee (2009) concluded that half-cell potential is a stable indicator of rebar corrosion initiation. In another research, Pour-Ghaz et al. (2009) developed a method that quantitatively relates the potential readings on the surface of the concrete to the rate of probable localized reinforcement corrosion through concrete resistivity, cover thickness and temperature.

2.4.2   Concrete Resistivity

Because the half-cell potential method provides no indication of corrosion rate at the time of measurement, some techniques have been devised to supplement the method and one of these is the concrete resistivity test. This test is used to acquire electrical resistance of the concrete. The value of electrical resistance obtained is then used in conjunction with the half-cell potential test to estimate the corrosion rate of the reinforcement. The relationship between the concrete resistivity and the likelihood of significant corrosion is shown in Table 2.2 (Bungey and Millard 1996)

Table 2-2 Relationship between concrete resistivity and likelihood of significant corrosion (Bungey and Millard 1996)

Resistivity (kΩ-cm)	*Likelihood of Significant Corrosion (Nonsaturated concrete when steel activated)*
<5	Very high
5-10	High
10-20	Low/Moderate
>20	Low

2.4.3   Polarization Method

Like the concrete resistivity method, the polarization test provides another means to overcome the major drawback of half-cell potential method, i.e., no information about the rate of corrosion. The term "*polarization*", in corrosion science, refers to the change in the open-circuit potential as a result of the passage of current (Davis et al. 1998).

Using this method, Bungey and Millard (1996) investigated the relation between corrosion current density with the rate of corrosion penetration. The result of that research is presented in Table 2.3.

Table 2-3 Typical corrosion rate for steel in concrete (Bungey and Millard 1996)

Rate of corrosion	Corrosion current density, i_{corr} ($\mu A/cm^2$)	Corrosion penetration, p ($\mu m/year$)
High	10→100	100→1000
Medium	1→10	10→100
Low	0.1→1	1→10
Passive	<0.1	<1

2.4.4 Chain Drag and Hammer Sounding

Chain drag and hammer sounding are the simplest technique for detecting top rebar delamination of exposed reinforced concrete bridge decks. The technique is based on the sound effect when a metal chain, a steel rod, or a hammer is dragged over the surface of the concrete bridge deck. Over non-delaminated concrete areas, a clear and sharp ringing sound will be produced while in delaminated regions, the dull and hollow sound, resulting because of void and discontinuity, will be perceived. By listening and differentiating these sounds, the operator will be able to locate the delaminated areas over the entire surface of the concrete bridge deck.

Although the technique is found very effective in assessment of bare concrete decks, it is, however, reported being much less sensitive for assessment of concrete bridge decks which are overlaid with asphalt pavement (Barnes 1999). In that structure, the asphalt pavement acts as an insulator that reduces the transmission of sonic energy to the concrete and back to the surface, resulting in low amplitude volume and distorted reflecting sounds. For this practical reason, the chain drag is usually employed by transportation agencies to determine the removal areas on asphalt-covered concrete bridge decks those have been prepared for repair, after the asphalt layer has been removed.

Even in the exposed concrete bridge decks, a main drawback of the chain drag method is that the inspection result is subject to operator's technique and interpretation. Especially, with noise from traffic flow and after hours of operation, the auditory sense of the operator normally tends to become insensitive (Barnes 1999). Another big limitation of the chain drag technique is that it cannot detect reinforcement corrosion, a major type of defect for comprehensive assessment of concrete structures. When detectable depth is concerned, it was reported that the method is able to detect delamination at the depth of 1 to 3 inches, depending on the size of chain link used, with the accuracy to be within ten and twenty percent of the total delaminated area (Barnes 1999).

2.4.5 Pulse Velocity

Like the spectral analysis of surface waves and the impact echo method that will be described in the next two sections, the pulse velocity test belongs to the family of ultrasonic (or stress wave) methods. These stress waves are produced when pressure or deformation is suddenly applied to the surface of a solid. The disturbance then propagates through the solid, with the speed of propagation being a function of several factors such as the modulus of elasticity, Poisson's ratio, the density, and the geometry of the object (Davis et al. 1998). Having the knowledge of this dependence allows one to infer about the characteristics of a solid by monitoring the propagation of stress waves in the object.

Based on the above basic idea, many complicated configurations of the pulse velocity

method have been studied for specific applications. Successful applications of this method for concrete assessment, according to Naik et al. (2004), include: (1) estimate strength of concrete; (2) study the homogeneity of concrete; (3) monitor the setting and hardening process of concrete; (4) study durability of concrete; (5) measure surface crack depth; and (6) determine dynamic modulus of elasticity.

2.4.6 Spectral Analysis of Surface Waves

Also based on principle of stress wave propagation, however as its name implies, spectral analysis of surface wave (SASW) method employs some special characteristics of surface wave, i.e., Rayleigh or R-wave, to infer elastic properties of the solid object under investigation, normally a layered structural system such as soil sites, asphalt or concrete pavement systems, and concrete structural members.

The technique was extensively studied by researchers at the University of Texas at Austin in the early 1980s in which they used an impactor or vibrator to generate a range of frequencies (Davis et al. 1998). The relationship between wavelength and velocity was then investigated using advanced signal processing technique that they called spectral analysis of surface waves. Since then, this name has become popular for the method as it is being used.

2.4.7 Impact Echo (IE)

Impact Echo (IE) is the last nondestructive evaluation method of ultrasonic technique family described in this study. When a stress pulse is generated by an impact at a point,

the exited energy propagates along the test object in all direction with the hemispherical

wave fronts of P- and S-waves. When these wave fronts reach an external or internal

interface such as object boundaries, cracks or voids, there will be energy reflections or

so-called echoes from these sources. The arrivals of these reflected waves at the test

surface where the impact was generated causes displacements that are measured by a

receiving transducer and recorded by a data acquisition system (Carino 2004b).

According to Davis et al. (1998), the IE technique has been applied successfully to: (1)

determine the thickness and detect flaws in plate-like structural member such as slabs

and bridge decks; (2) detect flaws in beams, column and cylindrical structural members;

(3) assess the quality of bonds in overlays; and (4) crack depth measurement.

2.4.8 Infrared Thermography

Infrared thermography is a detection technique that works based on the principle of

electromagnetic radiation. The basic idea is that a material with subsurface

abnormalities, or defects, will affect the heat flows through its internal structures (Davis

et al. 1998). For concrete, these anomalies may include the delaminations caused by

reinforcement corrosion, honeycombs caused by poor consolidation, or pooling fluids

caused by water infiltration. As a consequence, the changes in heat flow produces

localized differences in the surface temperature. Thus, by measuring or detecting these

differences, the knowledge of presence and location of any subsurface abnormality can

be obtained. The test method for detecting delamination in bridge decks using infrared

thermography is standardized, by American Society for Testing and Material, in ASTM

31

D4788-03.

Several factors that have been found can affect the spectrum observation during the test and therefore need to be taken into consideration (Davis et al. 1998). These factors can be categorized into two groups, namely, physical factors and environmental factors. Of those, the physical parameters include the concrete surface emissivity, surface temperature, concrete thermal conductivity, concrete volumetric-heat capacity, thickness of the heated layer, and the intensity of incident solar radiation. For environmental factors, it is found that the cloud, wind and surface moisture may influence the test result.

2.4.9 Ground Penetrating Radar (GPR)

Ground penetrating radar (GPR) is a nondestructive evaluation (NDE) technology based on the propagation behavior of electromagnetic (EM) waves. When a beam of EM energy goes through an interface between two materials of different dielectric properties, a portion of energy is reflected back while the remainder penetrates into the second material. The intensity of the reflected energy, *AR*, was found depending on the intensity of incident energy, *AI*, at the interface and the relative dielectric constants of the two media, ε_{r1} and ε_{r2}. This relationship is described in Equation 2.3 (Clemeña 2004).

$$AR = AI \frac{\sqrt{\varepsilon_{r1}} - \sqrt{\varepsilon_{r2}}}{\sqrt{\varepsilon_{r1}} + \sqrt{\varepsilon_{r2}}} \qquad (2.3)$$

When the relative dielectric constant of the first material (medium) is smaller than the relative dielectric constant of the second material (medium), making the result of Equation 2.3 negative, although the shape of reflection waveform looks the same as the original pulse, their directions (or polarity) are different. This effect, in radar theory, is called change in polarity or phase reversal and should be noted when analyzing GPR signals.

In addition to dielectric constant as described above, another very important factor that affects the received signal is the electrical conductivity of propagation media. This property of particular material determines the energy loss when an electromagnetic wave propagates through its medium, as approximated by Equation 2.4 (Bungey and Millard 1993). It was also found that the conductivity of concrete increases with the increasing frequency (Halabe et al. 1993). This means the electromagnetic wave of lower frequency can penetrate deeper inside the structure than those of higher frequency.

$$\alpha = 1.69 \times 10^3 \frac{\sigma}{\sqrt{\varepsilon_r}} \qquad (2.4)$$

Where:

α = signal attenuation (dB/m)

σ = conductivity of propagating medium ($\Omega^{-1}m^{-1}$)

ε_r = relative dielectric constant of propagating medium

To inspect a structure such as a bridge deck, a ground-coupled antenna is dragged manually on a pushing cart by an operator, or a horn antenna is attached to a vehicle in order to scan with traffic speed. This antenna transmits brief pulses of electromagnetic energy into the surveyed structure. The energy reflected at various medium interfaces is then received by the antenna to produce the output signal. Since the process is repeated at a certain pulse repetition frequency (PRF), a GPR profile (linescan or B-scan) is produced when the antenna is moved along each survey path. These profiles, composed of a large number of individual GPR signals (A-scans), contain a lot of useful information for assessing bridge deck condition. An example of GPR profile for concrete bridge deck with asphalt overlay is shown in Fig. 2.4.
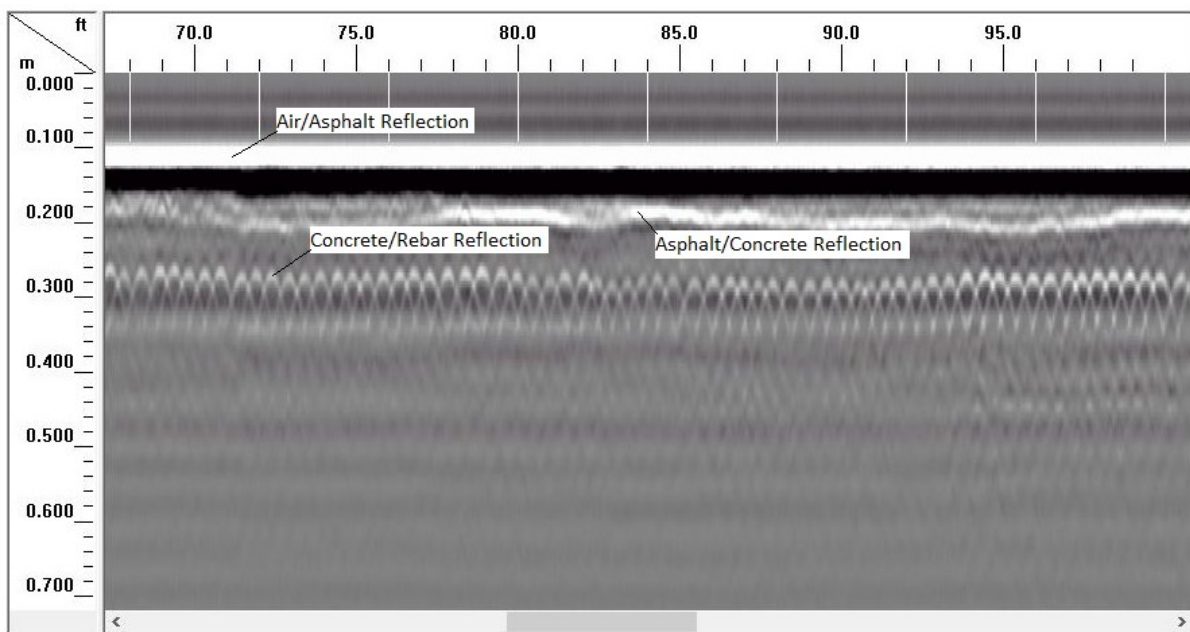
Fig. 2.4 Typical GPR profile for concrete bridge decks with asphalt overlay.

Numerous studies have been carried out to investigate methods for analyzing GPR data from concrete bridge decks. Important researches in chronological order can be found

in Canto (1982); Clemeña (1983, 1985); Carter et al. (1986); Chung et al. (1992, 1993); Maser (1995, 1996); Millard et al. (1997); SlatonBarker and Wallace (1997); Reel et al. (1997); Davidson and Chase (1998); Maser and Bernhardt (2000); Huston et al. (2000); Scott et al. (2001); Barnes and Trottier (2004); Barnes et al. (2008); Le Groupe (2010); Tarussov et al. (2013); and Martino et al. (2014). Although all of these researches were based on the same physical principles of GPR, their interpretation methods are different and can be grouped into two categories, namely (1) numerical analysis of reflection amplitude and (2) visual interpretation of GPR data. Detailed explanation for each of them is as follows.

2.4.9.1 *Numerical Analysis of Reflection Amplitude*

Numerical analysis of reflection amplitude is a technique for analyzing GPR data based on the amplitudes measured at various material interfaces. This is the most commonly used technique for evaluating GPR data of concrete slabs. Although the reflection amplitude at concrete surface, bottom rebar or slab bottom may be taken into account; most often, the analyst will infer the condition of bridge deck based on the reflection amplitude at top mat transverse reinforcing bar. The rationale behind this evaluation method is based on known effects of moisture, chloride content and rust on the recorded GPR signals. These effects are described in great detail by Tarussov et al. (2013). In short, they cause more attenuation on reflection amplitude.

Amplitude mapping consists of measuring reflection amplitudes at top rebar over the entire survey area and plotting them with contour lines. According to Parrillo et al.

(2006), however, the amount of deterioration should not be determined based solely on colors on the contour map. He pointed out that even a new deck will contain some range in rebar reflection amplitudes due to rebar depth variation. By the same reason, Geophysical Survey Systems Inc. (GSSI) recommends that amplitude interpretation technique is not appropriate for a deck with no deterioration or a deck with near total deterioration (GSSI 2012). Even for a bridge deck with average deterioration, in addition to rebar depth variation, there are still several factors that may lead to the inefficiency of analyzing reflection amplitudes (Tarussov et al. 2013). These factors include the variation of rebar depth and rebar spacing, surface properties, structural variation, construction quality, and so on. Up to the time of the current research, rebar depth variation is the only factor that has been taken into account for condition map adjustment (Barnes et al. 2008). Brief description of the adjustment method is provided below.

It is clear from the physical point of view that the reflection amplitude at each rebar depends on the distance (depth) from concrete surface to the rebar itself, if bare concrete decks are concerned. There are two physical principles governing this amplitude reduction, namely (a) inverse-square law, and (b) attenuation in the traveling medium. Possibly, because the amplitude variation due to inverse-square law is small, only attenuation in the traveling medium was taken into account in Barnes et al. (2008). Specifically, when normalized reflection amplitude for a concrete deck were plotted versus two-way travel time, a general decreasing linear trend was observed. Based on this observation, for depth correction, they proposed that first, a quantile linear

regression fitting was performed at 90th percentile as shown in Fig. 2.5. This regression line was then used for depth normalization by subtracting it from depth-dependent amplitude. The next step to produce amplitude map would be the same as the conventional amplitude method.
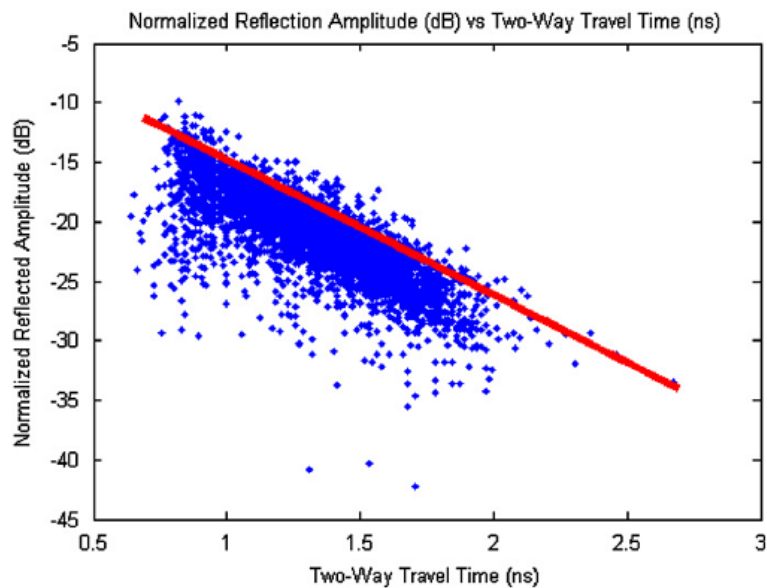
Fig. 2.5 Quantile linear regression fitting at 90th percentile (Barnes et al. 2008)

As for threshold issue, Martino et al. (2014) proposed a statistical model for threshold calibration in which GPR data was correlated with half-cell potential (HP), a well-accepted method. The purpose of the model was to use GPR as a sole tool to assess the corrosion state of bridge decks. Specifically, the model development was motivated by their observation from Fig. 2.6 that for a healthy bridge deck, the amplitude histogram was compact, quite symmetric and almost perfectly normal, while the histogram for a corroded bridge deck was spread out and leaning to one side. For a library of eight bridge decks with HP results, they then explored various descriptive statistics for

prediction purpose such as mean, standard deviation, variance, skewness and kurtosis. Based on that exploration, they came up with a linear regression formula to calculate corrosion area as shown in Fig. 2.7 in which they concluded that the product of skew and mean value of GPR amplitude data provided the best prediction performance. Finally, with corroded area percentage obtained, GPR threshold can be found through an interactive trial and error process.
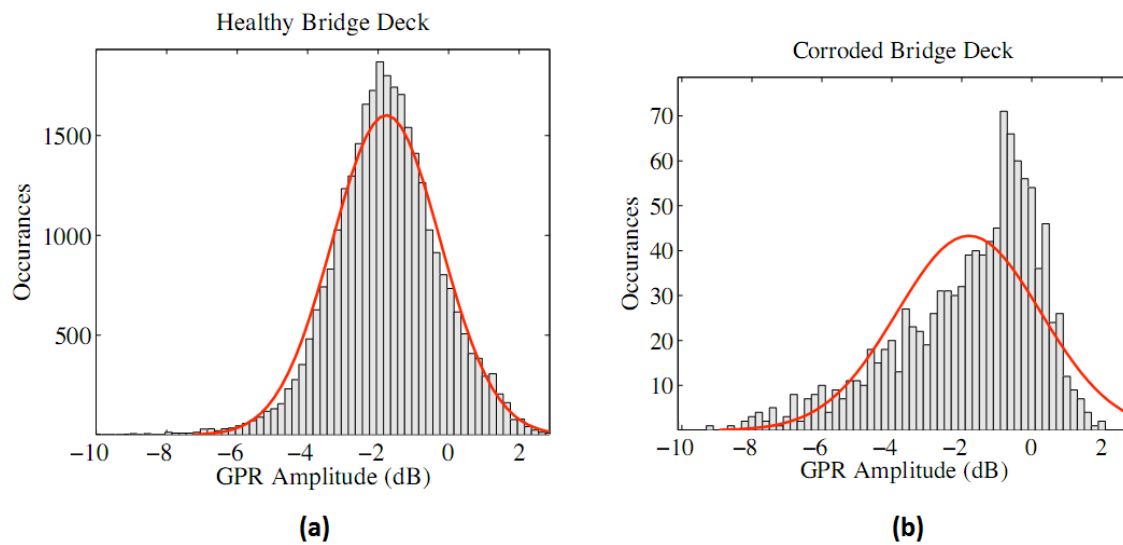
Fig. 2.6 Amplitude histogram for (a) healthy and (b) corroded bridge decks (Martino et al. 2014)

2.4.9.2 Visual Interpretation of GPR Data

Visual interpretation of GPR data refers to those techniques that are based on visual recognition of deterioration in GPR data. For example, Chung et al. (1992) developed a technique for evaluating GPR data of asphalt-covered reinforced concrete bridge deck collected with an elevated (horn) antenna. The method is based on the characteristic

"W-shape" of individual GPR signals in which any variation from this W-shape characteristic is considered indicating some signs of deterioration.
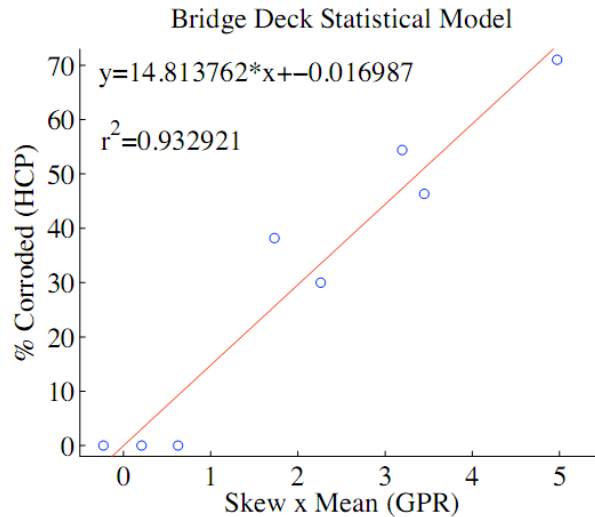
Fig. 2.7 GPR Threshold Prediction Model (Martino et al. 2014)

Also based on visual analysis of individual radar waveforms, Barnes and Trottier (2004) investigated the effectiveness of GPR to forecast repair quantities for concrete bridge decks. The research reported a varying range of forecast accuracy. Specifically, it was concluded that the method seems to work well when the decks exhibiting deterioration levels between 10 and 50%. For the decks surveyed that contain less than 10% and more than 50% deterioration of the total deck surface area, the results shown significant differences between the GPR and ground-truth survey quantities.

Because visual analysis of individual waveforms is very time-consuming and impractical to be used in bridge deck inspection, Tarussov et al. (2013) proposed a new method for mapping corrosion in concrete structures, based on linescan (B-scan) image analysis. In order to analyze GPR data for a concrete bridge deck, the analyst scrolls

through each GPR profile and marks visible anomalies based on known criteria of deterioration. This marking process is illustrated in Fig. 2.8. The processed profiles are then combined by a specialized software tool to generate a deterioration map. While the definitions of condition such as sound concrete, moderate and severe corrosion depend greatly on analyst's experience and varying case by case, typical conditions those illustrated in Fig. 2.8 can be summarized in Table 2-4.
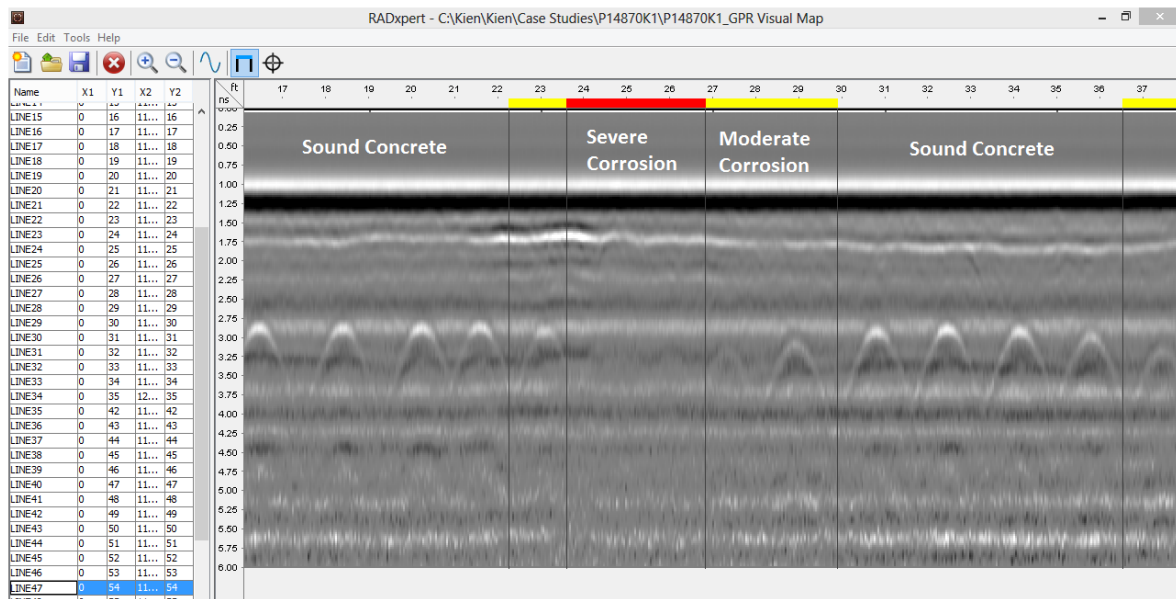
Fig. 2.8 Marked deterioration on GPR profile.

One challenge facing the analyst in some instances when he/she visually analyzes GPR profiles is that it may be difficult for him/her to clearly define the border between sound and deteriorated region. Also, it is sometime very hard for the analysts to keep their judgement constantly when they switch between profiles. In other words, visual interpretation of GPR profiles is subjective to certain extent. There may be the case where different interpreters come up with different condition maps. Obviously, this subjectivity effect is not desired and therefore should be minimized.

Table 2-4. Definition of various condition found by visual analysis of GPR profile

Sound Concrete	*Moderate Corrosion*	*Severe Corrosion*
Rebar reflection is strong and clear with hyperbola shape.	Rebar reflection is relatively weak but hyperbola shape is still clearly visible.	Strong attenuation at top rebar level; hyperbola shape from rebar reflection is distorted or almost disappear.

2.5 Bridge Condition Rating

As can be seen, the results obtained from bridge inspection are different types of structural defects. These defects, however, cannot be used directly by transportation agencies for making management decisions, i.e., for determining intervention actions and the priority order of bridge maintenance projects under their responsibility. Because of the limited financial resource and public accountability, transportation agencies need to have a firm foundation for making justifiable decisions. The solution for this is bridge condition assessment (or rating). According to the AASHTO (1994), bridge condition rating is defined as the result of determining functional capability and physical condition of bridge components.

Currently, there is variety of bridge condition rating models and it is difficult to be aware the existence of all of them. Therefore, only bridge condition assessment practices in US and Canada are described and discussed. In the United States, two most commonly used bridge condition rating systems are the NBI (National Bridge Inventory) and Pontis. The third one, actually based on Pontis database and less frequently used, is Bridge Heath Index. In Canada, according to Abu Dabous (2008), few provinces have well-developed inspection system and condition assessment methodology. Also, there is no consistency between its provinces regarding bridge condition assessment level.

Following, each of these systems will be in turn described and discussed.

2.5.1 NBI Condition Rating System

The NBI is the oldest condition rating system for bridge structures in the US. The system was developed by the Federal Highway Administration (FHWA) and its use is mandatory for all US transportation agencies. The NBI condition ratings describe the overall condition for main structural components of a bridge. The ratings are then used to calculate the bridge sufficiency rating, which in turn determines funding eligibility and priority for bridge replacement and rehabilitation (MnDOT 2009).

Typically, NBI rates a bridge in three main components, namely, deck; superstructure; and substructure. For each of them, the rating ranges from zero to nine in which nine means excellent condition (newly constructed), zero means failed condition and replacement is required. Detailed guideline for general condition ratings of those three main components, as described in FHWA (1995), are provided in Table 2.5.

As mentioned before, NBI ratings are used to calculate bridge sufficiency rating. This rating is basically a numeric value which indicates a bridge's relative ability to serve its intended purpose. The value is in percentage and ranges from 100 to 0 in which 100 percent represents an entirely sufficient bridge while zero percent indicates an entirely insufficient or deficient bridge (FHWA 1995). The sufficiency rating is the summation of four calculated values: Structural Adequacy and Safety (55%), Serviceability and Functional Obsolescence (30%), Essentiality for Public Use (15%), and Special Reductions (-13%). The formula to calculate sufficiency rating and a full list of factors

that affect this calculation can be found in Fig. 2.9.

Table 2-5 NBI Condition ratings for three main bridge components (FHWA 1995)

Rating Code	Description
N	Not applicable
9	Excellent condition
8	Very good condition (no problem noted)
7	Good condition (some minor problems)
6	Satisfactory condition (structural elements show some minor deterioration)
5	Fair condition (all primary structural elements are sound but may have minor section loss, cracking, spalling, or scour)
4	Poor condition (advanced section loss, deterioration, spalling or scour)
3	Serious condition (loss of section, deterioration, spalling or scour have seriously affected primary structural components. Local failures are possible. Fatigue cracks in steel or shear cracks in concrete may be present)
2	Critical condition (advanced deterioration of primary structural elements. Fatigue cracks in steel or shear cracks in concrete may be present or scour may have removed substructure support. Unless closely monitored it may be necessary to close the bridge until corrective action is taken)
1	Imminent failure condition (major deterioration or section loss present in critical structural components or obvious vertical or horizontal movement affecting structure stability. Bridge is closed to traffic but corrective action may put back in light service)
0	Failed condition (out of service, beyond corrective action)

The FHWA classifies deficient bridges into two categories, namely structurally deficient (SD) and functionally obsolete (FO). A structurally deficient bridge is defined as the one whose condition or design has impacted its ability to adequately carry its intended traffic loads; while a functionally obsolete bridge is the one in which the deck geometry, load carrying capacity, clearance, or approach roadway alignment has reduced its ability to adequately meet the traffic needs below accepted design standards. If a bridge meets the criteria for both SD and FO, it would only be considered as structural deficient. It means, in this case, the structural deficiency overrides the functional obsolescence and renders the bridge to be in the SD classification. In general, the lower the sufficiency rating is, the higher the priority for the bridge rehabilitation or replacement. Typically, in order to be eligible for replacement, a bridge must have a

sufficiency rating of less than 50 percent and be structurally deficient or functionally obsolete. To qualify for rehabilitation, a bridge must have a sufficiency rating of 80 percent or less and be structurally deficient or functionally obsolete. Also, it must be greater than ten years old (FHWA 1995).

Based on all the factors that are taken into account to calculate sufficiency rating, one would perceive that it is the most complicated and most comprehensive performance measure for a bridge. For example, it considers not only structural factors but also serviceability, functional performance and many others. Although this is not a wrong perception, the main problem associated with the sufficiency rating model is that it is based on NBI condition ratings.

According to Golabi and Shepard (1997), NBI condition ratings are only good for general presentational purpose. It cannot be used directly for building a performance-based decision model that includes economic considerations. Specifically, among several problems associated with the system that were pointed out are as follows.

First, NBI rates each bridge according to its major components, i.e., deck, super- and sub-structure. However, each of these components itself consists of many elements and materials and they deteriorate differently over time, depending on many factors such as their functions and environments. As a result, rating a component using one number would reduce the value of the collected data.

Second, the rating of a component does not allow specifying the required action. This is because two components with the same rating can have completely different conditions that require totally different actions. This level of detail is therefore not

sufficient to formulate repair strategies, or to estimate costs.

1. Structure Adequacy and Safety
S1 = 55% Max

59 Superstructure
60 Substructure
62 Culverts
66 Inventory Rating

2. Serviceability and Functional Obsolescence
S2 = 30% Max

28 Lanes on Structure
29 Average Daily Traffic
32 Appr. Rdwy. Width
43 Structure Type, Main
51 Bridge Rdwy. Width
53 VC over deck
58 Deck Condition
67 Structural Evaluation
68 Deck Geometry
69 Underclearances
71 Waterway Adequacy
72 Appr. Rdwy. Align
100 STRAHNET Highway Designation

3. Essentiality for public use
S3 = 15% Max

19 Detour Length
29 Average Daily Traffic
100 STRAHNET Designation

4. Special Reduction
S4 = 13% Max
19 Detour Length
36 Traffic Safety Features
43 Structure Type, Main

Sufficiency Rating = S1 + S2 + S3 – S4

Sufficiency Rating shall not be less than 0% nor greater than 100%

Fig. 2.9 Sufficiency rating formula (FHWA 1995)

Finally, the NBI condition ratings are vulnerable to subjective interpretation of bridge inspectors. The reason is that the ratings utilize multiple paths of distress and when rating, the inspector has to decide which type of distress or defect is more representative

45

of the general condition than the others. This is obviously difficult, especially when many types of defect are co-existed and equally distributed.

One more problem associated with the sufficiency rating itself is that these measures are used at the Federal level for funding allocation. The rating, however, emphasizes bridge's geometric characteristics and functionality, rendering it inappropriate for making maintenance decisions (Thompson and Shepard 2000).

2.5.2 Pontis Condition Rating System

Due to the limitations of NBI condition rating discussed above, it was decided by the FHWA and the California Department of Transportation (CalTrans), when developing the first bridge management system in US, that the system should be abandoned (Golabi and Shepard 1997). In this first bridge management system (Pontis), a standardized description of bridge elements at a greater level of detail was developed. Specifically, instead of dividing a bridge into several main components, a menu of as many as 160 elements was formulated. In this menu, a typical bridge would contain an average of about ten elements.

After several years of experience, under the FHWA guidance, a task force was created in 1993 to revise the standard. The revision, so-called the Commonly Recognized (CoRe) Structural Elements, was issued in 1994 with a smaller set (108) of standardized elements (Thompson and Shepard 2000). It was less tied to Pontis and was expected to provide a better means for recording, sharing and using of bridge inspection data. For each CoRe element, the standard specified the unit of measurement, standardized

condition states and the list of corresponding feasible actions. The last revision of the standard that replaces the 1994 version was issued in 2010. An example of condition states for an element as described in this manual is shown in Fig. 2.10.

The Pontis condition states provide input data for Pontis bridge management system. These data can then be used to identify the present maintenance needs as well as to determine the cost-effective options for a long-range bridge maintenance and improvement programs. However, it is noted from our previous discussion that, Pontis prioritizes projects based solely on cost–benefit analysis and ignores other performance measures. This has also been identified as a major drawback of Pontis system.

2.5.3 Bridge Health Index

As mentioned before, although project selection based on cost–benefit analysis is accepted by bridge management community, however it is difficult for them to justify this method to decision makers and the public, when one of the main concerns of these two groups is having the safe bridges (Scherschligt and Kulkarni 2003).. In other words, there exists a communication gap between bridge managers, elected officials and the public, if Pontis is used. To overcome this gap, the California Department of Transportation came up with a new concept, i.e., Bridge Health Index.

Basically, the Bridge Health Index is a ranking system for bridge maintenance. The index, in percentage, ranges from 0 to 100 in which the value of 100 indicates the best state while 0 means the worst condition. The basic idea of this rating is to think of the condition of a bridge or an element at a given time as a point along a continuous timeline

and the health index simply indicates where the bridge or element is along this continuum (Thompson and Shepard 2000).

Description	Element # 12/38
This element defines all reinforced concrete bridge deck/slab regardless of the wearing surface or protection systems used.	**Reinforced Concrete Deck/Slab** **Square Feet (Square Meters)** **National Bridge Elements**

Quantity Calculation
The quantity for this element should include the area of the deck/slab from edge to edge including any median areas and accounting for any flares or ramps present.

Condition State Definitions

Defect	Condition State 1	Condition State 2	Condition State 3	Condition State 4
Cracking	None to hairline	Narrow size and/or density	Medium size and/or density	The condition is beyond the limits established in condition state three (3) and/or warrants a structural review to determine the strength or serviceability of the element or bridge.
Spalls / Delaminations/ Patched Areas	None	Moderate spall or patch areas that are sound	Severe spall or patched area showing distress	
Efflorescence	None	Moderate without rust	Severe with rust staining	
Load Capacity	No reduction	No reduction	No reduction	

Feasible Actions

Condition State 1	Condition State 2	Condition State 3	Condition State 4
Do Nothing Protect	Do Nothing Protect Repair	Do Nothing Protect Repair Rehab	Do Nothing Protect Replace

Fig. 2.10 Example of condition states and feasible action (AASHTO 2010)

It was stated by the developers that the health index can be calculated for an element, a single or a group of bridges. Its computation, as shown in Equation 2.5, is based on the total element quantity, element quantity in each condition state, failure cost of each element, and the so-called condition state weighting factors. The aggregation of the index, at bridge or network level, is then based on the element weighting factors that are determined as the relative economic consequence of the failure of each element. The idea is the elements whose failure has relatively little economic effect should receive

48

less weight than the elements whose failure could threaten the public safety, or force the bridge to be closed.

$$Health\ Index\ (HI) = \frac{\sum CEV}{\sum TEV} \times 100 \qquad (2.5)$$

Where:

Total Element Value (*TEV*) = Total Element Quantity × Failure Cost of Element (FC)

Current Element Value (*CEV*) = ($\sum$ [Quantity in Condition State i × WF_i]) × FC

Weighting Factor of condition *i* (WF_i) = 1 − [(i − 1) ÷ (Number of States − 1)]

According to Roberts and Shepard (2000), the bridge health index is used in California for several purposes including: (1) as a performance measure; (2) for allocation of resource; (3) Level-of-Service indicator; (4) for showing Budget-based network condition; and (5) for measuring improved condition following preservation actions.

Although the bridge health index has been considered by the bridge management community as an excellent performance measure, this study noticed that it has some associated limitations.

Firstly, as can be seen, the way in which condition state weighting factors (WF) are calculated is very simple. This simplicity is however compromised by its inaccuracy. For example, if an element has three defined condition states and the whole element is found in condition state 2, the health index of this element would be 50 percent, meaning the element just exactly passes a half of its service life. Obviously, this is not the case

and contradicts to the basic idea of the health index stated previously. The reason to support for this argument is that normally an element will stay in each condition state not as a point in time but for a quite long period of time, except the failure condition. Drawing the health index, based on inspected condition states, as an arbitrarily pre-determined point in a continuous timeline is therefore not an appropriate conclusion. This situation is the same as when one has to guess the exact room temperature based on his sensing. For example, if someone feels the weather is hot, it is difficult for him to tell exactly what temperature the weather is because 31, 32, or 35^0C may make him feel the same thing. The circumstance like this should be best dealt with using Fuzzy theory that will be introduced later.

Secondly, although it is rational to aggregate element health indices based on economic consequences of element failure, the values of these measures are however difficult to obtain. To overcome this limitation, the Pontis system offers two options for calculating the weights, either using the failure cost (FC)-based or repair cost (RC)-based methodology (Jiang and Rens 2010). Unlike the FC-based method that takes into account both agency and user cost associated with the element failure, the RC-based method only considers the cost of the most expensive element repair action. Again, problem emerges with such simplifying solution. A more appropriate method to calculate element weights is therefore needed.

2.5.4 Bridge Condition Rating in Canada

This review of bridge condition assessment practice in Canada benefits a lot from a

previous work at Concordia University. Abu Dabous (2008), in his research, contacted four Ministries of Transportation in Canada and visited two other agencies to review their practices in bridge condition assessment and bridge management. The result was reported in his PhD thesis.

In Ontario, like most states in the US, a bridge management system has been developed. The system ranks and prioritizes bridge maintenance projects based on the so-called bridge condition index. This index is developed for an entire bridge with the basic idea similar to the bridge health index used in the US discussed before. Only a small difference is that instead of thinking the index as a point in continuous timeline, it is considered to indicate the remaining economic worth in percentage.

The Alberta Department of Transportation does not have specialized management system for bridges. However, the condition assessment of existing bridge structures is still performed and the objective, like Pontis, is to maximize bridge service life at minimum life cycle cost. Based on the inspection data, an overall bridge index is developed, which combines sub-structure and super-structure ratings.

The Ministry of Transportation of Quebec uses the bridge condition index as the principal performance measure (Ellis et al. 2008). The index is based on the same concept used in Ontario and it is computed as a weighted average of the condition state distribution of various elements. The weights are determined in the manner the same as bridge health index discussed before in which those elements have a higher replacement cost would receive a higher weighting.

With a very small territory, the Prince Edward Island's Transportation and Public

Work's department manages a total of 200 bridges in their inventory. Bridges are inspected visually every three years and a single-number overall rating will be given to each bridge. The rating values include 1, 2, and 3 in which 1 indicate significant work is required, 2 means minor work is required, and 3 corresponds to perfect condition. Nova Scotia uses a condition rating system similar to the NBI ratings described previously. The condition rating ranges from 1 to 9 in which 1 and 9 correspond, respectively, to worst and excellent conditions. Abu Dabous (2008) reported that at the time of his review, Nova Scotia Transportation and Public Works was approaching Stantec Consulting to build a customized version of Ontario bridge management system.

In order to improve the above situation, Abu Dabous developed and proposed a model, as he called, a unified bridge condition index. In this model, first the condition of each bridge element is determined, based on fuzzy membership functions of various condition states and Monte Carlo simulation method. These conditions are expressed in the form of condition vectors and the values in each condition vector indicate the probability of each element happened to be in excellent, good, fair, and poor condition, respectively. The conditions of all elements are then combined for the entire bridge, considering structural importance factors of elements as the weights, to obtain overall bridge condition rating. The structural importance factors for various elements are determined using analytic hierarchy process (AHP) approach. The final output, i.e., bridge condition index (BCI), is also expressed in form of a condition vector.

There are several issues that should be noted about the Abu Dabous' model. First, he

treated membership function of a fuzzy set as a probability distribution to perform Monte Carlo simulation. This is not an appropriate way to deal with fuzzy sets since the natures of fuzziness and randomness are not the same. Second, considering structural importance as a single factor affecting the weight of each element in the computation of the overall bridge condition index is not comprehensive. There are other indications that should be taken into account in determining the weights, for example, replacement costs and condition ratings of bridge elements.

2.6   Research Techniques in Condition Assessment

It was found during the literature search of this study that various research techniques have been applied successfully for infrastructure asset condition assessment. Typical techniques among them include regression analysis, artificial neural network (ANN), analytical hierarchy process (AHP), multi-attribute utility theory (MAUT), K-means clustering and fuzzy set theory. For example, Chughtai and Zayed (2008) developed models for assessing structural and operational conditions of sewer pipelines using multiple regression analysis; Al-Barqawi and Zayed (2006) built a condition rating model to assess underground infrastructure water mains using artificial neural network; Qasem (2011) developed performance assessment model for wastewater treatment plants using analytical hierarchy process and multi-attribute utility theory; Yan and Vairavamoorthy (2003) utilized fuzzy theory to assess pipe condition; Moselhi and Shehab-Eldeen (2000) used artificial neural network to classify defects in sewer pipes; Huang et al. (2010) used K-means clustering to group numerical data when they

explored deterioration factors of concrete bridge decks; Sasmal et al. (2006) developed condition rating model for reinforced concrete bridges based on fuzzy theory; and many others.

With such variety of techniques employed in the field of infrastructure condition assessment, this literature review presents and discusses only the selected techniques those will be used later for the present research. These selected techniques are K-means clustering and fuzzy set theory.

2.6.1 K-means Clustering

K-means Clustering is a partitioning technique that was independently discovered in various scientific fields by Steinhaus (1956), Lloyd (1982), Ball and Hall (1965), and MacQueen (1967). As the most commonly used method for cluster analysis, the K-means procedure divides N-dimensional population into K sets such that the squared error between the empirical mean of a cluster and the points in the cluster is minimized (Jain 2009). According to Jain (2009), data clustering has been used for the three main purposes: (1) to gain insight into data, generate hypotheses, detect anomalies, and identify salient features; (2) to identify the degree of similarity among forms or organisms; and (3) as a method for organizing the data and summarizing it through cluster prototypes.

Regarding the algorithm, K-means Clustering proceeds by randomly selecting k initial cluster centers (c_j) and then iteratively refining them according to two following steps (Wagstaff et al. 2011): (1) Each data point is assigned to the data set associated with the

nearest centroid where the Euclidean distance between the data point x_i and the centroid c_j of cluster j is calculated using Equation 2.6; (2) Each cluster center c_j is updated to be the mean of its constituent data points. The two steps are repeated until the centroids and data points no longer move; the clustering process stops.

$$d(x_i, c_j) = (\sum_{d=1}^{D} |x_{id} - c_{jd}|)^{1/2} \tag{2.6}$$

Where: D is the dimension of the data needed to be classified.

2.6.2 Fuzzy Set Theory

Introduced the first time by Zadeh (1965), fuzzy set theory has developed rapidly and been applied in numerous, uncountable areas. The usefulness of this theory is that it helps solve many decision making and control problems those are associated with the fuzziness and imprecision of human languages. Study efforts in application of fuzzy set theory for evaluating performance of constructed facilities in general can be found in Yao (1980), Hadipriono (1988), Tee (1988), Liang et al. (2001), Zhao and Chen (2002), Yan and Vairavamoorthy (2003), Kawamura and Miyamoto (2003), Najjaran et al. (2005); Sasmal et al. (2006), Kumar and Taheri (2007); Sasmal and Ramanjaneyulu (2008), Tarighat and Miyamoto (2009), Zhou et al. (2009), and Sun and Gu (2011).

For bridge condition assessment in particular, one of the initial and outstanding efforts that applied fuzzy set theory can be found in Tee (1988). In this study, a model to assess conditions of bridge components based on mathematical operations on fuzzy sets was

proposed. Specifically, the model makes use of fuzzy weighted average (FWA) arithmetic to combine bridge inspection ratings and their corresponding importance into overall rating for each component. For example, suppose that a bridge superstructure has three sub-components including stringers, floor beams and girders in which the stringers have a good condition rating, the floor beams have fair condition rating, the girders have a poor condition rating, and the importance coefficients of each three elements are given; using the model that he proposed will give us the answer whether that superstructure is in good, fair or poor condition. In the model, the output of fuzzy weighted average operation is also a fuzzy set. Therefore, in order to determine which language term (rating expression), i.e., good, fair, or poor, best represents the overall superstructure condition, he based on the shortest distance between this resultant fuzzy set to the fuzzy set corresponding to each linguistic rating expression. It is noted that Tee's model was aimed to support NBI rating.

Kawamura and Miyamoto (2003) developed a rating system for assessing concrete bridges based on neuro-fuzzy. In the model, bridge elements were evaluated in terms of load-carrying capability and durability, with the inputs including technical specifications, environmental conditions, traffic volume, and visual inspection. It is noted that neuro-fuzzy, also called soft-computing technique, is the fusion of fuzzy inference system and artificial neural network (ANN) in which the purpose of using neural network is to refine the knowledge base of the fuzzy system.

Tarighat and Miyamoto (2009) proposed a fuzzy inference system to evaluate

reinforced concrete bridge decks. The system utilized multi-distress inputs collected from inspection including crack-widths, spalls, delamination, hammer-tapping, and corrosion probability; with a set of 162 different rules. The output of the model is a bridge deck condition rating that ranges from 0 to 100 in which 0 and 100 mean perfect and respectively worst conditions. The proposed system was expected to provide an excellent means to assess concrete bridge decks. However, the drawback of the model is that it treats bridge decks as a whole and bases only on existing global distresses. This is not in line with current practices of bridge inspection in US and Canada which record condition states for an element according to its quantities. Therefore, it may be the case that the condition is bad with only a small deck area but good with all others. In such case, the model will rate the deck to be in bad condition.

Based on the early work of Tee (1988) and using fuzzy mathematical operations, Sasmal et al. (2006) proposed a condition assessment model for rating existing reinforced concrete bridges. The improvement of their approach was that they combined fuzzy weighted average (FWA) with an eigenvector-based priority setting methodology. In their model, each bridge is divided into three main components in which each of them in turn composed of a number of elements. The method first based on the inspected ratings and importance factors of all the elements of a component to combine these ratings into the overall component rating. The component ratings are then incorporated to produce the overall bridge rating by the same method. Because the product of such combinations is also a fuzzy set, defuzzification procedure is therefore necessary. Similar to Tee (1988), the defuzzification is also performed based on minimum

Euclidian distance.

Sasmal and Ramanjaneyulu (2008) proposed a very complicated condition rating system for evaluation of reinforced concrete bridges. The system employs analytic hierarchy process (AHP) and fuzzy logic to solve rating problem in a fuzzy environment. The rating process can be divided into several steps. First, the conditions of various reinforced concrete bridges are ranked and prioritized. Then based on the result of this prioritization, rating of the most deserved bridge is carried out using multi-attribute decision making (MADM). The inputs for the model are data collected using NBI inspection standard.

2.7 Summary of Limitations and Research Gaps

What were found from the literature strongly justify the urgent need of the current research. Specific important points relevant to this study can be summarized in the following statements. First, the most common defects of concrete bridge decks in North America that need to be identified during inspection are those caused by corrosion-induced deterioration. While these defects include rebar corrosion, concrete delamination; and spalls; by far, rebar corrosion, as early stage of deterioration, is of the most concern. Rebar corrosion is usually associated with chloride-contaminated concrete, the main root cause of concrete deterioration, which must be removed and replaced during bridge deck repair.

Second, while all bridge management systems were built based on visual inspection, this method has serious limitations when it can only detect problem when bridge decks

need major, expensive repair. Although successful application of some NDE techniques, especially GPR, to concrete bridge decks has been demonstrated in a number of researches, these technologies are still not widely accepted because of less than positive experiences, unrealistic expectations, improper use of equipment and limited data analysis methodology.

As for condition rating, although many models have been developed for bridge in general and bridge deck in particular, all of them are based on visual inspection. In addition, while the idea of bridge health index easy to understand, its computation makes it a deterministic model that does not take into account any inherent uncertainty associated with inspection result. As can be seen from the literature, this uncertainty should be dealt with using fuzzy set theory that will be explained in the next chapter.

CHAPTER 3   RESEARCH METHODOLOGY

3.1 Selection of NDE Technique

Since various NDE technologies can be utilized for inspection of concrete bridge decks and each of them has its own advantages and limitations. Principally, several techniques can be performed on the same bridge deck so as to eliminate the drawbacks of the others; however, such solution would require much more time and resources to inspect and interpret the result than the case if one single NDE method is employed. Being aware of the fact that selection of the most appropriate NDE technique should be based on a comprehensive cost-benefit analysis, however due to the unavailability of most required information, it was determined in this study that only technical criteria are considered for the selection. The methodology used in this study for selection of NDE technique is provided in Fig. 3.1.

As can be seen, the selection starts by an extensive literature research of nondestructive evaluation (NDE) technologies as has been described in the previous chapter. Then, each technology is analyzed in terms of its advantages and disadvantages for application to concrete bridge decks. In order to select the most appropriate technology, inspection requirements for concrete bridge decks are identified. These requirements, in turn, are used for establishing selection criteria. Finally, based on comparison of the capability of each NDE technology versus selection criteria set, the most appropriate NDE technique is identified and selected for this research.
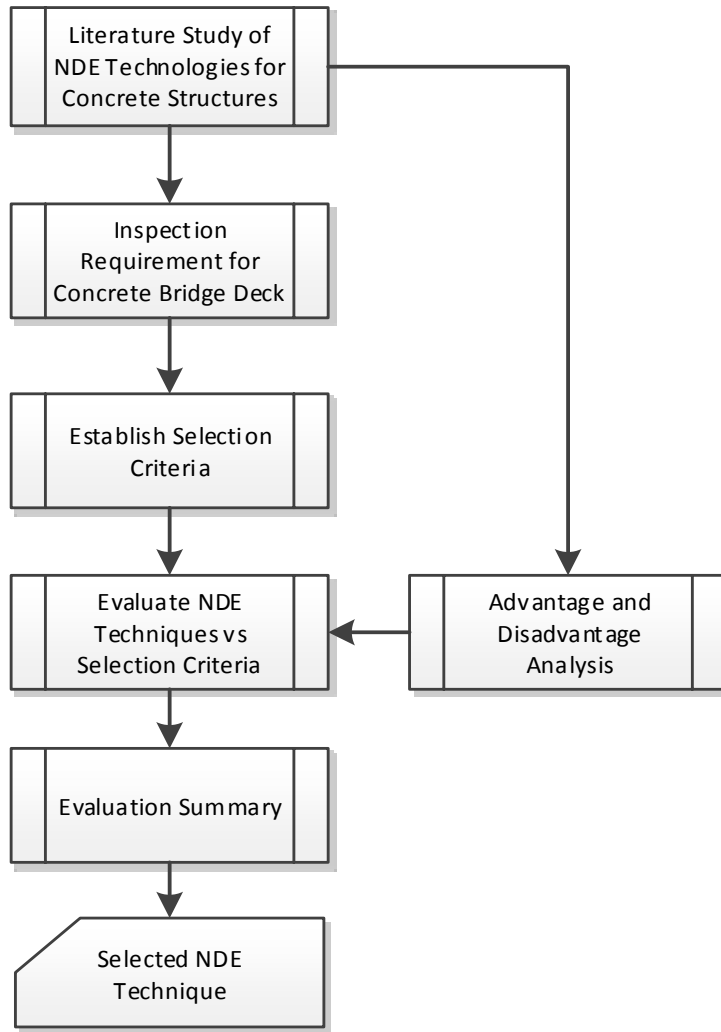
Fig. 3.1 Methodology for selection of NDE technique

3.1.1 Advantages and Limitations of Various NDE Techniques

Each technology has its own advantages and limitations. This is also the case with most

NDE technologies. For example, Half-cell Potential can provide the likelihood of

corrosion activity in concrete structure with lightweight and portable equipment,

however it is time-consuming and requires some conditions, among them connectivity

of the entire mat of embedded rebars and direct electrical connection from the

equipment with at least one rebar. The latter requirement makes the technique to be a semi-nondestructive technology when some part of concrete cover needs to be removed.

As another example, chain drag and hammer sounding are most commonly used for detecting delamination because they are effective on bare concrete and only need simple devices. However, this technology cannot be used for investigation of rebar corrosion and it is not effective when the concrete is covered with asphalt pavement. Since description like this for all techniques would be long, the readers are advised to see Appendix A. The full list of advantages and limitations of each technology described in previous chapter can be found in Table 3-1 below.

3.1.2 Inspection Requirement and Selection Criteria

As has been explained previously, only technical criteria are considered for the selection of the most appropriate NDE technique in this study. Since current research focuses only on corrosion-induced deterioration caused by deicing salt, the selection criteria were identified as follows: (1) capable of detecting chloride ingression; (2) capable of detecting corrosion; (3) capable of detecting delamination; (4) high speed of data collection and analysis; (5) inspection result can be reproducible; (6) Be able to work with asphalt overlay; (7) objective with minimal human interpretation; and (8) can be used as a stand-alone technique that does not require other tests.

Table 3-1 Advantages and limitations of different NDE techniques

Technique	Advantages	Limitations
Half-Cell Potential	Lightweight and portable equipment. Provide an indication of likelihood of corrosion activity at the time of measurement	Require a connection to the embedded reinforcement and therefore can be considered as a semi-nondestructive technique. The reinforcements have to be electrically connected. Not applicable to epoxy-coated bars. Concrete has to be moist. No indication of corrosion rates. Testing and interpretation has to be performed by experienced personnel. Time consuming.
Concrete Resistivity	Lightweight and portable equipment. Provide likelihood of corrosion rate of the activated reinforcement.	Usually used in conjunction with half-cell potential method.
Polarization method	Lightweight and portable equipment. Provide an indication of instantaneous corrosion rate at the time of measurement.	Require a connection to the embedded reinforcement and therefore being a semi-nondestructive technique. The reinforcements have to be electrically connected. Not applicable to epoxy-coated bars. No standard for interpretation of test results. Cover depth has to be less than 100 mm. Concrete surface has to be smooth, uncracked, free of impermeable coating, and free of visible moisture. Testing and interpretation has to be performed by experienced personnel. Time consuming Just provides the instantaneous corrosion rate at the time of measurement.
Chain Drag	Lightweight, simple and portable equipment. Effective method to detect delaminated areas on exposed reinforced concrete bridge decks.	Not effective on asphalt covered concrete bridge decks. Subject to operator's technique and interpretation. Cannot detect rebar corrosion. Limited detectable depth (1-3 inches)
Pulse Velocity	Lightweight and portable equipment. Relatively easy to use. Provides excellent means for investigate the uniformity of concrete structures.	Usually requires access to both sides of structure. Cannot detect reinforcement corrosion. Limited use in detecting delamination (based on literature).
Spectral Analysis of Surface Wave	Can determine the elastic properties of layered systems. Can be used to check the quality of different layers at different positions in a layered structural system.	Experienced operator is required. Cannot detect reinforcement corrosion. Difficult to obtain information about delamination. Requires complex signal processing technique.
Impact Echo	Capability of detecting variety of defects such as voids, cracks, and delamination. Only access to one face of structures is needed.	Experienced operator is required. Cannot detect reinforcement corrosion. Quite time consuming to inspect large areas.
Infrared Thermography	Capable of detecting near-surface delamination in concrete structures. Enable large areas to be surveyed in short time period and therefore cost effective.	Require favorable environmental condition. Expensive equipment. Cannot detect reinforcement corrosion. Cannot measure the depth and thickness of the detected defects. Cannot or difficult to detect the defects that locate deep inside the structure. Trained operator is needed.

Ground Penetrating Radar	Capable of fast scanning with non-contact antenna. Very sensitive to metal objects, moisture and electrical conductivity. Can easily penetrate through the air and asphalt layer Inspection result is reproducible. Commercial equipment and application software are well-developed.	Cannot directly detect thin or in-contact cracks and delamination. Requires trained operator to conduct inspection and interpret the result.

3.1.3 Evaluation and Selected Technique

As can be seen, based on comparison of individual NDE techniques to selection criteria in Table 3-2, GPR appears to be the most appropriate NDE technology for inspection of concrete bridge decks. It is noted in the table that although criteria No. 3 was not checked for GPR, Scott et al. (2001) found that the technology can detect delamination directly when it is big enough or filled with water.

Table 3-2 Comparison of NDE techniques to selection criteria

NDE Techniques	Selection Criteria (1): capable of detecting chloride ingression (2): capable of detecting corrosion (3) : capable of detecting delamination (4) : high speed of data collection and analysis (5) : inspection result can be reproducible (6) : be able to work with asphalt overlay (7) : objective with minimal human interpretation (8) : can be used as a stand-alone technique							
	(1)	(2)	(3)	(4)	(5)	(6)	(7)	(8)
Half Cell Potential		√			√		√	√
Concrete Resistivity	√	√			√		√	√
Polarization		√			√		√	
Chain Drag and Hammer Sounding			√	√				√
Pulse Velocity					√		√	√
Spectral Analysis of Surface Wave					√	√	√	√
Impact Echo			√		√	√	√	√
Infrared Thermography			√	√			√	√
Ground Penetrating Radar	√	√		√	√	√	√	√

As a validation, the above selection result is also in line with a report in the second Strategic Highway Research Program (SHRP 2) in which based on five performance measures, Gucunski (2013) concluded that GPR is the top technology for detecting and characterizing deterioration in concrete decks. The five criteria that were used for their selection include: (1) Accuracy; (2) Precision (repeatability); (3) Ease of data collection, analysis, and interpretation; (4) Speed of data collection and analysis; and (5) Cost of data collection and analysis.

3.2 GPR Inspection System

Since ground penetrating radar (GPR) is the selected NDE technology, this section presents inspection system for concrete bridge decks based on that technique. Because equipment or hardware development is not the intention of this study, only novel data analysis methods are researched. Following that direction, two data analysis approaches are studied and developed as follows.

3.2.1 Clustering-based Threshold Calibration

As can be seen from the literature, although amplitude analysis provides objective and detailed decibel scale, subjective selection of threshold value remains a limitation. While the threshold can be obtained using the model developed by Martino et al. (2014), the model itself has not been well validated. On the other hand, while visual interpretation of GPR data provides condition map with specific condition categories, that is useful for bridge managers, the determination of condition boundary is rather

subjective. In order to eliminate the subjectivity of both methods, an enhanced analysis technique is proposed in this research. The basic idea is that while detailed attenuation map in decibel scale can be used to determine relative level of deterioration between rebar picks, information from visual interpretation of GPR data will be used to determine the number of condition categories of the deck in question.

The proposed method works as follows. Once the amplitude data has been obtained for all rebar picks through conventional process of amplitude analysis, the analysts will ask themselves from visually analyzing GPR profiles: how many condition categories would be appropriate to describe the bridge deck condition. Then, the amplitude data will be grouped into that same number of clusters, using K-means, the most commonly used clustering technique described in the previous chapter. Based on the result of clustering, threshold value for each condition category will be determined and the condition map will be plotted.

Using information from both amplitude and visual interpretation, the rationale behind the proposed method is easy to understand. It is known from practice that judgment from analyst when he or she visually analyze GPR profiles can provide invaluable information. In reality, even when amplitude analysis is employed, expert analyst is still required for quality assurance (QA) in which he/she has to review manually-picked or processed rebar amplitude data in order to guarantee that amplitude change is not caused by real construction variations either designed or built into the deck.

Fig. 2.6(a) can also be used as an example for the value of visual analysis of GPR data.

Specifically, for the data in that figure, Martino et al. (2014) reported a standard deviation of 1.537 dB. Although the bridge was new and no structural anomaly was reported for the deck, the difference between rebar reflection amplitude was still up to 12 dB. While the condition of that bridge deck may be misinterpreted if only contour map of reflection amplitude is analyzed, this is usually not the case when GPR profiles are interpreted visually. The reason is, in such cases, the analyst has enough information to conclude that the amplitude variation is caused by other random factors, rather than by corrosion-induced deterioration.

For GPR image analysis, although showing great value, as discussed previously, it is challenged for the analyst to have a clearly-defined boundary between condition categories. In many instances, these boundaries are subjective and dependent greatly on the judgment of GPR experts. Hence, in case where the analysts develop condition map visually and based completely on top rebar reflection amplitude using criteria in Table 2-4, the proposed method can provide more accurate condition map.

With the above stated point concerning example deck in Fig. 2.6(a), one may consider to use bridge deck age as the main factor in order to determine the number of condition categories for clustering. However, the study conducted by Kirkpatrick et al (2002) points out that the time for chloride to reach and initiate corrosion varies greatly among bridge decks. Specifically, for some bridges, it may take only 10 years for corrosion to be initiated while in other cases, this time may be up to more than 30 years. Therefore, it is strongly recommended that determining the number of condition categories should

be based on comprehensive analysis and information, i.e., both age of bridge deck and visual analysis of GPR profiles. The suggested flowchart for determining the number of condition categories (K) is shown in Fig. 3.2. In the flowchart, the 10-year decision point can be justified when, based on previous studies (Kirkpatrick et al. 2002; Weyers 1998; Liu and Weyers 1998; Suwito and Xi 2003; Li 2003), it is very unlikely that corrosion initiates in bridge decks those are under 10 years of age.

Justification is needed for limiting the number of condition categories to only 3 while one may suggest an unlimited number of clusters. Some may think that increasing the number of clusters increases the level of detail, however two following limitations should be realized. First, larger number of clusters make it more difficult for the analysts to judge how many categories they should choose for a specific bridge deck. For example, it is always easier asking someone to simply tell whether it is hot, cold than asking him/her to specify whether it is a slightly hot, moderately hot, very hot, or very very hot, etc. Not only that, a big question should be asked if too many condition categories are used, i.e., what should be the corresponding action if concrete is found to be in a specific category. Since it is not meaningful to have two condition categories with the same implication when planning for maintenance activity, it is reasonable to define three condition categories as shown in Fig. 3.2. Corresponding maintenance strategy for each category is provided in Table 3-3.
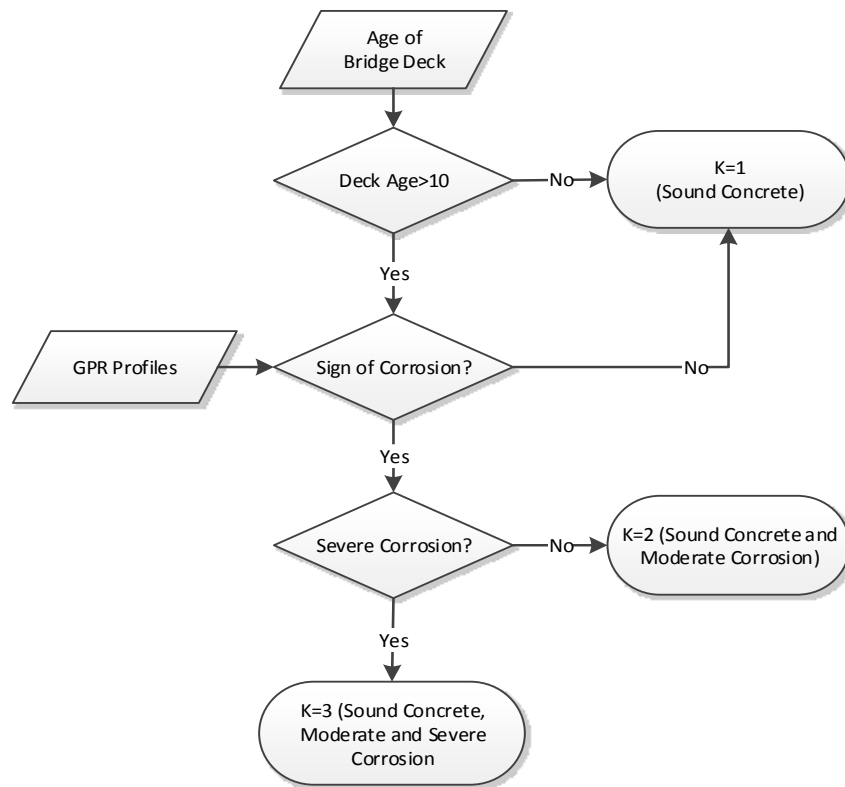
Fig. 3.2 Flowchart for determining number of condition categories (K)

Table 3-3 Condition categories and corresponding implication

Sound Concrete Area	*Moderate Corrosion Area*	*Severe Corrosion Area*
Good condition, no intervention needs to be planned.	Active corrosion exists and may develop to real damage (severe corrosion) in the short term.	Probably damaged concrete that needs to be replaced.

3.2.2 Correlation Analysis

It was realized the most ideal way to find condition change associated with any concrete bridge deck deterioration is by comparing current GPR signals with themselves, i.e. the ones at the same location, but taken previously or ideally when the bridge is newly constructed. In other words, instead of interpreting based on *relative difference* between amplitudes from only one scan, a more appropriate way should be analyzing based on *difference* between time-series data sets.

The overall workflow proposed for long-term monitoring condition of concrete bridge decks using time-series GPR data is presented in Fig. 3.3. As can be seen, when a bridge deck is still in good condition, a baseline GPR data along with scan locations, i.e. scanning paths, should be recorded and stored in the database. Periodically, each time during operation and maintenance stage or whenever the deck needs to be inspected, a new GPR data at the same scan lines using the same equipment type will be collected. Then, the comparison for each pair of GPR individual signals (A-scans) collected at the same location will be performed using the model developed in this study. Finally, based on comparison result, the condition at the inspected location will be predicted. Theoretically, it is clear that the more similarity between the two signals (new one versus baseline), the less change of the concrete condition at the inspected location. Doing it this way eliminates the need to look for sound concrete areas on the bridge to obtain the reference signals if visual analysis method is concerned. Not only that, by using original signals, abnormal signals due to structural variation can also easily be observed and differentiated with corrosion-induced defects.
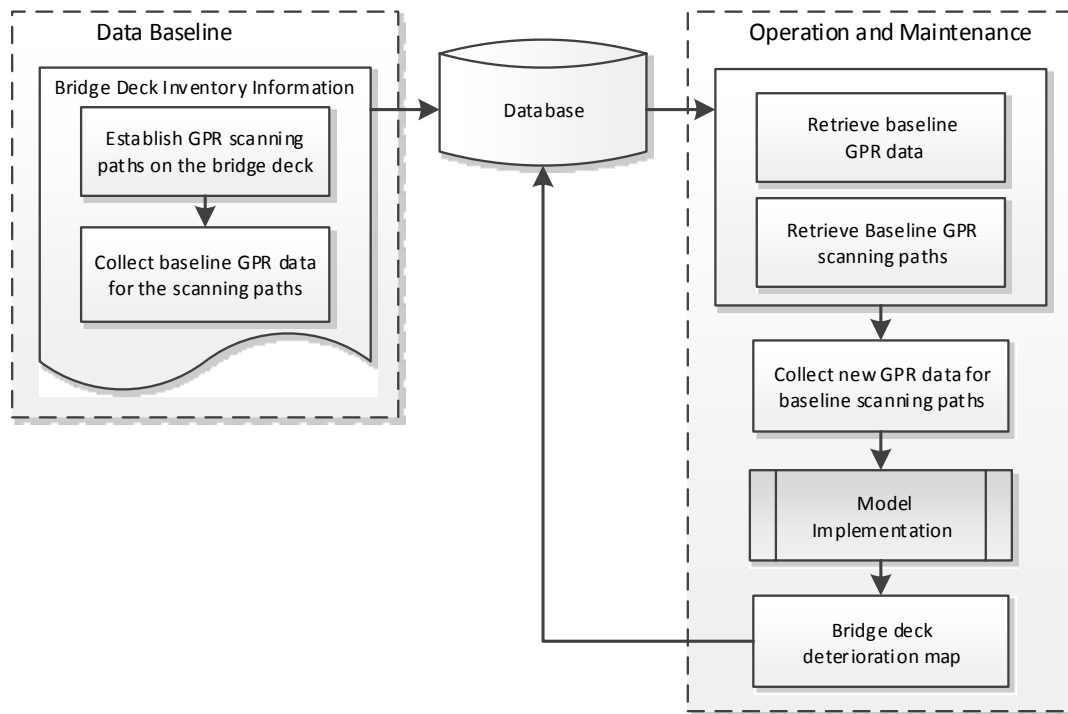
Fig. 3.3 Long-term condition assessment workflow of concrete bridge decks using GPR

In signal processing research domain, cross correlation is the technique for measuring the similarity between two signals as a function of a time-lag applied to one of them. Correlation-based methods have been used extensively for many applications such as object recognition, motion analysis, industrial inspection, and so on. For example, Tsai et al. (2003) studied the use of cross correlation for defect detection in complicated images of industrial inspection. Giachetti (2000) proposed using pattern (template) matching to compute image motion from a sequence of two or more images in which the displacement between two images was calculated based on the correlation measure between them. In a very interesting study, Brunelli and Poggio (1993) compared two different techniques for human face recognition in which the first technique was based on the computation of a set of geometrical features while the second one was based on correlation-based template matching. The same database that included frontal images

71

of 47 people was used for the two techniques. The result amazingly favored template matching in which it got perfect recognition while the method based on geometrical features obtained only 90 percent correct recognition.

Regarding computation algorithm, to compare the similarity between two signals simply without time difference, Equation 3.1 below can be used. In the equation, ρ_{xy} is the normalized correlation coefficient between two digitized signals *x(t)* and *y(t)*. Actually, it is nothing but the normalized covariance between variable *x(t)* and *y(t)*. As can be seen, the value of ρ_{xy} lies between -1 and 1 in which the closer to unity, the more similar the two signals.

$$\rho_{xy} = \frac{\gamma_{xy}}{\sigma_x \sigma_y} \tag{3.1}$$

Where:

$\gamma_{xy} = E[(x_t - \mu_x)(y_t - \mu_y)]$

μ_x and μ_y = are the means of x_t and y_t, respectively

σ_x and σ_y = are the standard deviations of x_t and y_t, respectively

Fig. 3.4 illustrates the above idea for comparing the similarity between two GPR signals in which the two waveforms needed to be compared are plotted in the same graph. The signals were collected using GSSI 1.5 GHz antenna. Each waveform is sampled and the voltage amplitudes in data unit are measured at 512 points along each scan (GPR trace or A-scan). However the first 10 samples are removed from each waveform since this

section contains a lot of noise. Using Equation 3.1, the correlation coefficient obtained for the two signals is 0.9008.

It should be noted that interpreting GPR data based on signal similarity is much more comprehensive than simply comparing amplitude. Specifically, correlation analysis takes into consideration two important pieces of information, both the amplitude and the shape of an individual signal. For example, it is known from theory and experiment that when a delamination develops in the concrete and if it is big enough or filled with water, one more reflection from this layer would be observed in the scan (Scott et al. 2001). While this reflection may affect top rebar reflection amplitude, it would be more sensitive to correlation coefficient because of change in the shape of the signal. Much more than that, while amplitude method mainly employs the signal at the center of the top rebar and then interpolate condition for other positions between bars along the same scan path and between individual scan paths themselves, correlation-based method developed above can predict condition change at any location on the profile. The reason is that if that location does not have reflection from the top rebar, it still has reflection from bottom rebar or from slab bottom. So if delamination develops or if chloride ingression cause amplitude attenuation at one of these layers, they would affect the correlation coefficient.
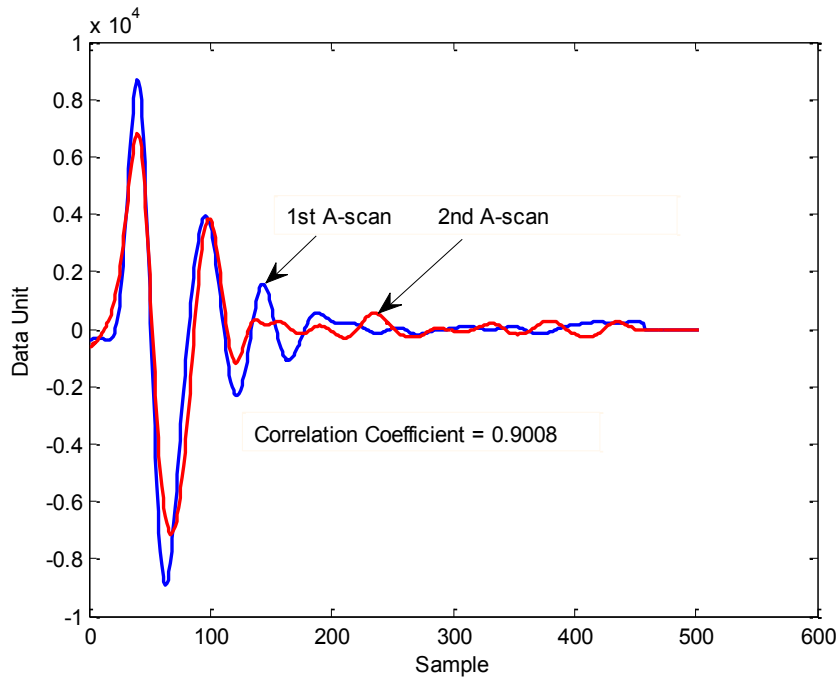
Fig. 3.4 Correlation between two GPR signals.

One more important thing should also be noted is regarding gain setting during GPR scan. This factor actually does not cause any problem for correlation-based interpretation. The reason is that, if a constant (single-point) gain is used during scanning, it may amplify or diminish the amplitude but will not make any change to the overall shape of the signal. Therefore, it has no impact to correlation coefficient. Even if one used a complicated gain setting when he or she collected the data, GSSI RADAN software has a function to restore the data as if no time-variable gain was applied to each of the unique, digitized samples along every individual GPR trace (A-scan).

After computing correlation coefficient for all locations, a contour map of correlation coefficient will be created. This contour map will delineate areas with different rates of signal changes. In principle, the lower correlation coefficient indicates the more

74

deteriorated location. However, because some signal change may be caused by error in line positioning, system instability, or electromagnetic noise in the environment instead of concrete deterioration, it is desired to calibrate a threshold of correlation coefficient for statistical-significantly confirming concrete deterioration. This threshold is to avoid false-positive diagnosis, i.e., diagnosing deterioration while in fact there is not.

3.3 Bridge Deck Corrosiveness Index (BDCI)

3.3.1 Nature of Research Question

Although corrosion maps provided by GPR are very useful for specifying MR&R actions to individual defects, a systematic framework should be developed for using them in decision making at both bridge and network levels. As discussed in Chapter 2, the ideal solution for this is an index that represents overall health of bridge decks like the one developed by California Department of Transportation (Caltrans).

For model development, it is noted again about the basic idea of bridge health index (BHI) when it uses the scale from 0 to 100 to represent the overall bridge condition. Specifically, the scale was considered by its developers as a continuous timeline in which the BHI, computed from visual inspection result, indicates the point where the bridge is during its service life. The similar question has to be answered in this research is how to convert bridge deck condition found by GPR to a numerical format of bridge deck corrosiveness index. Answering this question is however not a trivial task.

As may be noticed in Chapter 2, the way in which California bridge health index calculate condition state weighting factors (WF) makes it a deterministic method that does not model any inherent uncertainty associated with inspection result. In reality, similar to other elements, bridge decks deteriorate gradually over time. If corrosion-induced deterioration is concerned, the process starts with chloride ingression in concrete cover, then corrosion initiation, corrosion propagation, and finally, bridge deck repair or replacement. Normally, a bridge deck will stay in each stage above for a long period of time, and with current inspection method, there is no way for one to specify exactly at which point the deck is on the rating scale. In other words, uncertainty modelling is needed in order to solve the research question. It is also important to note that the uncertainty in this situation arises from fuzziness instead of randomness.

3.3.2 Fuzzy Membership Calibration

Based on the same scale used for BHI, this study visualizes each condition state of a bridge deck during its service life would occupy certain section along the continuum from 100 to 0, starting from excellent to failure condition as shown in Fig. 3.5. Since there is no way to measure directly the exact value of bridge deck condition index from GPR condition maps, expert opinion appears to be the only available option. Specifically, it was found that a group of bridge and GPR experts can be used to solicit the values regarding the boundaries of each condition state in the bridge deck condition index continuum. The sections corresponding to various condition states can then be determined based on the aggregation of these opinions.
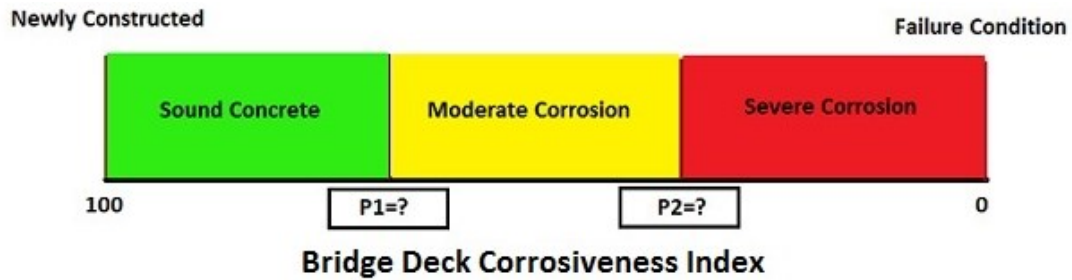
Fig. 3.5 Visualization of bridge deck corrosiveness index

According to Hisdal (1986), in order to deal with a fuzzy problem appropriately, first the source of fuzziness or uncertainty has to be identified. Specifically he provided a list of fourteen different sources of fuzziness in which three main sources were considered giving rise to membership function itself. The readers are advised to refer Hisdal (1986) for the full list of fuzziness source while the three main sources are explained here including: (1) the fuzziness due to inexact conditions of observation; (2) the fuzziness due to classification in an under- or over-dimensioned universe; and (3) the fuzziness due to the intersubject differences with respect to universe partitioning.

As the name implies, the first source of fuzziness mentioned above refers to the case when the concerned attribute values of objects can only be estimated with some possibility of making error. For example, suppose that one already has his own clear criterion for defining hot weather, for instance, greater than 30^0C. However, there would be the circumstance in which he does not know exactly the temperature and he has to judge whether the weather is hot or not, based on his perception. In such case, although the "hot" boundary is not fuzzy, the fuzziness still appears, however, as a result of non-exact conditions of observation.

77

The second type of fuzziness occurs when an attribute is classified in a universe with the number of dimensions lower than it should be for purpose of classification. Because of that, non-fuzzy classification in the lower-dimensional universe is not correct and a partial grade of membership is assigned to take into account the resulting fuzziness. This membership function is specified based on the estimated frequency of occurrence of different values in the left-out dimensions.

The problem of partitioning element health index as shown in Fig. 3.5 is related to the last type of fuzziness above. It refers to the case when the quantitative variations exist between different people in the choice of universe partitioning. For example regarding the weather again, one may consider the cool day is when the temperature lies between 15 and 25^0C while the others may choose different ranges.

It is very important to note that in comparison to visual inspection method, bridge deck inspection using NDE technologies reduces considerably the fuzziness extent, specifically the fuzziness due to inexact conditions of observation. As pointed out by the FHWA (2001), it is very difficult in many cases for bridge inspectors to determine whether a given element is in this condition state or in its adjacent ones, using visual inspection.

In industrial control and decision making, the membership functions play very important role in determining the success of fuzzy logic applications. Realizing this, numerous studies have been performed investigating techniques for membership function generation such as Yang et al. (1991), Valliappan and Pham (1993), Chen and

Otto (1995), Beliakov (1996), Tamaki et al. (1998), Arslan and Kaya (2001), Lin and Chen (2002), Dombi and Gera (2005), Yang and Bose (2006). These techniques are classified by Medasani et al. (1998) including: (1) subjective perception based; (2) heuristic based; (3) multi-dimensional histogram; (4) probability distributions to possibility distributions transformation; (5) fuzzy K-nearest neighbor techniques; (6) Neural network based; (7) clustering technique; and (8) mixture decomposition technique.

As can be seen, a vast number of techniques for generating membership function have been invented. Unfortunately, it was found that there are no guidelines or rules that can be used to select the appropriate membership generation technique. Also, Medasani et al. (1998) believed that it would be impossible to come up with a single membership generation method that would work for most applications.

Based on studying the literature, it was found that the integration of the first two techniques above can be used for generating bridge deck corrosiveness index (BDCI) membership functions in this study. These two techniques are therefore described in detail in two subsequent paragraphs.

According to Medasani et al. (1998), membership function generation based on subjective perceptions of vague or imprecise categories have been applied in many decision-making problems. In this category, several techniques can be used, for example, direct or reverse rating; polling; or relative preference method. Specifically, in the direct rating procedure, a subject is presented with a random series of objects and

then asked to indicate the membership degree to rate each one regarding an attribute. In the reverse rating procedure, the subject is presented with an ordered series of objects and asked to select the one best corresponding to the indicated degree of membership in the pre-defined category of the attribute. Thinking of membership function as a cumulative distribution function, polling technique assumes that semantic uncertainty is simply a statistical uncertainty in the information-theoretic sense.

The values of membership functions are calibrated by randomly and repeatedly presenting a subject with elements and acquiring either a 'yes' or a 'no' response to the question: Does x belong to A? The polling method implies that probability of a positive answer is proportional to membership value. Regarding relative preference method, the so-called the pairwise comparison alternative matrix, denoting as A, is used to compute membership values. In the matrix, element a_{ij} represents the relative membership value of an element x_i in a fuzzy set F with respect to the membership value of an element x_j in F. The larger the value of a_{ij}, the greater the membership of x_i compared with that of x_j. The membership values are then determined by finding the eigenvector of A.

Heuristic method assumes predefined shapes for membership functions. This technique has been employed successfully in many rule-based pattern recognition applications (Ishibuchi et al. 1993) in which some commonly used shapes for heuristic membership function include *piecewise linear functions and piecewise monotonic functions*. Realizing some clear advantages of piecewise linear membership functions such as providing a reasonably smooth transition, easily being manipulated by fuzzy operators,

however Medasani et al. (1998) also had some negative criticisms. First, because heuristic methods are chosen to fit the given problem, they work well only for problems for which they are intended. Second, the shapes of the heuristic membership functions are not flexible enough to model all kinds of data. Third, the parameters associated with the membership functions must be provided by experts and in some applications they have to be fine-tuned until the performance is acceptable. This tuning process is however not a trivial task, especially in a high-dimensional system due to interactions between variables and local minima.

The method used for finding membership function in this study is quite simple. First, it is assumed that membership functions are piecewise linear. Through a questionnaire survey, the parameters are then determined based on linear regression analysis with an assumption the same as polling technique, i.e., probability of a positive answer is proportional to the membership value.

3.3.3 Weighted Fuzzy Union (WFU) Operation

The result of concrete bridge deck inspection using GPR is area percentages of various condition states. Tee (1988) found in the literature two techniques that can be used for combining fuzzy information or knowledge, namely fuzzy weighted average (FWA) and weighted fuzzy union (WFU). Basically, the former technique is used when weighting factors are fuzzy sets themselves while the latter is more appropriate if the weights are crisp numbers. The mathematical form of WFU is presented in Equation 3.2. As can be seen, the result obtained from the equation is also a fuzzy set.

$$\bar{F} = U\left\{\sum_{i=1}^{n} W_i F_i\right\}$$
(3.2)

Where:

F_i = fuzzy set i[th]

W_i = non-fuzzy weighting factors

U = fuzzy union operator

$\bar{F}$ = resultant fuzzy set

As in the case of fuzzy inference system and fuzzy control, the resultant fuzzy output always needs to be defuzzified in order to make a concrete decision or control action. Since there is no systematic procedure for choosing a good defuzzification strategy (Lee 2005), the present study will compare the two most commonly used methods, namely centroid and bisector deffuzification. Basically, while the first technique finds the center of gravity, the bisector is the vertical line that divides the possibility distribution of the resultant fuzzy set into two sub-regions of equal area. The horizontal position of the point or the line represents the crisp output for making decision or taking control action.

CHAPTER 4   DATA COLLECTION AND CASE STUDY

4.1   System Calibration Data

As described in Chapter 3, two types of data need to be collected in this study, i.e., data for system calibration and GPR data for concrete bridge decks those will serve as the case studies. Specifically, the data needed for system calibration are described in the following subsections.

4.1.1   Correlation Coefficient Threshold

When correlation analysis is performed for two GPR data sets using the methodology developed in previous chapter, as has been explained, because some signal change may be caused by error in line positioning, system instability, or electromagnetic noise in the environment instead of concrete deterioration, it is desired to calibrate a threshold of correlation coefficient for statistical-significantly confirming concrete deterioration. This threshold is to avoid false-positive diagnosis, i.e., diagnosing deterioration while in fact there is not. The calibration method was performed by collecting data for a real concrete bridge deck in Quebec is as follows.

The deck was scanned by GPR two times on the same date with a pushing cart carrying GSSI SIR-3000 and 1.0 GHz antenna. This one-day time frame was to make sure that no deterioration would have happened on the deck and any signal difference would only be assigned to positioning error, system instability, or electromagnetic noise in the environment. Two data sets were obtained, each of them contains a total of fourteen

profiles. Necessary steps were then done to make sure that each two profiles of the two

datasets for the same scan line begin and end at the same location with same number of

samples as illustrated in Fig. 4.1. Because each profile contains 5301 samples, there are

correspondingly 148428 A-scans for 28 profiles. In other words, there are 74214

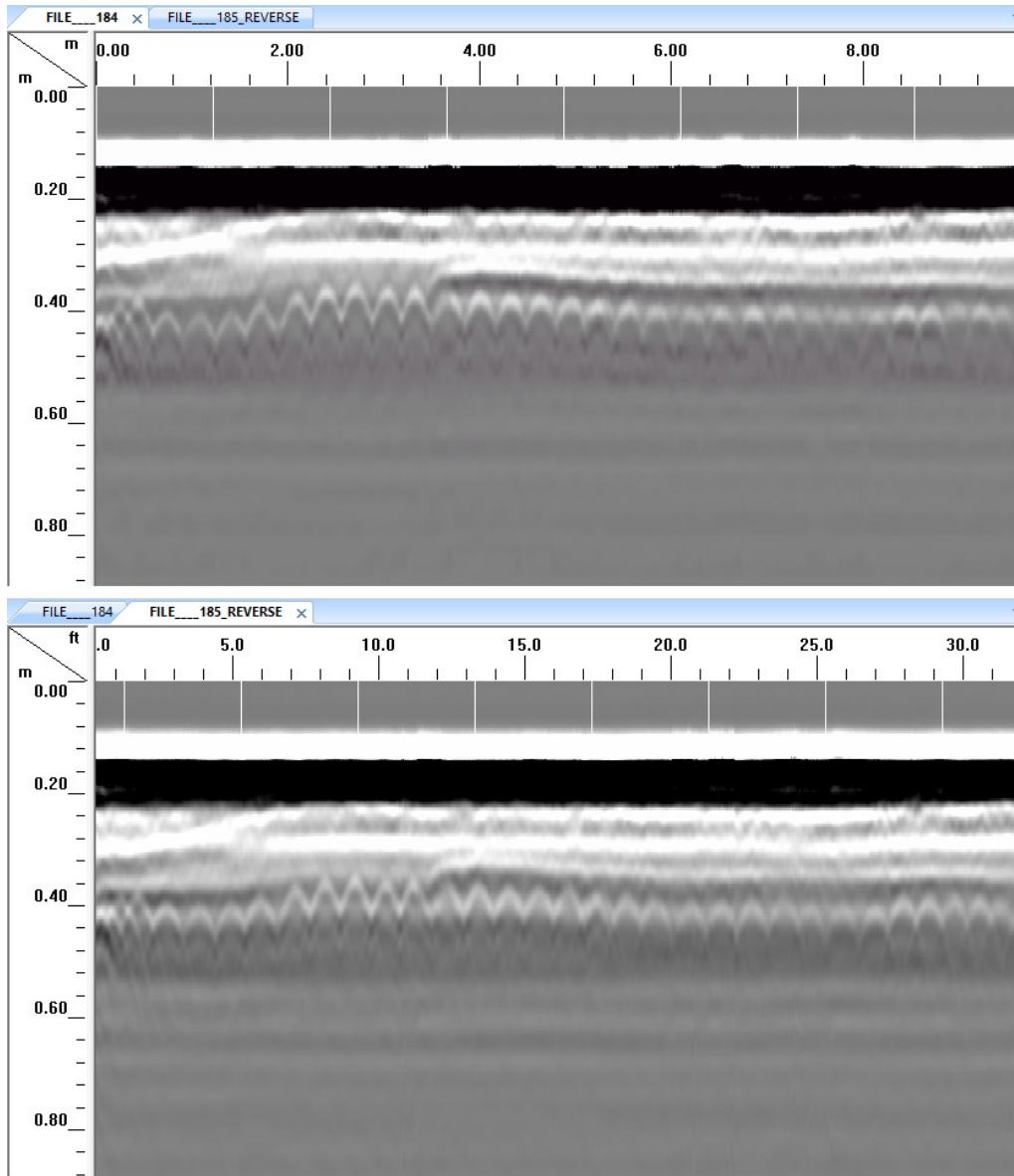couples of signals in two data sets that need to be compared.

Fig. 4.1 Two profiles with the same scan line

4.1.2 Questionnaire Survey

4.1.2.1 Survey Design

As explained in previous chapter, the main purpose of the questionnaire survey is to solicit opinions from bridge and GPR experts for building membership functions that will finally be used to convert GPR condition map to the numerical format of bridge deck condition index. However, since another research question was also raised in this study regarding how that index will be used by bridge managers for deck maintenance decision making, extra questions were added in the survey. While the web interface and entire content of the survey that was delivered online can be found in Appendix B, it is summarized including following sections and questions in each of them.

Section 1. Respondent's Information

There were three questions in this section. In Question 1, experts were asked to provide their contact information in order to correspond in case the survey solicitors would like to have further discussion. However, due to confidentiality issue, it was decided that answering this question was set "optional".

In Question 2, experts were requested about their expertise in which they have the choice for one of the following options: (1) a bridge manager; (2) a bridge engineer; (3) a bridge inspector; (4) a bridge researcher; and (5) Other that needs to be specified. The purpose of this question was not to compare the difference in opinion between expertises, but to gather as much as possible information from bridge community.

In Question 3, experts were asked about their experiences in the expertise that they selected in Question 2. The experience was based on the number of years they practiced that expertise and was divided into four categories: (1) 0-5 years; (2) 5-10 years; (3) 10-20 years; and (4) more than 20 years.

Section 2. Main Questions

Before main questions were asked in this section, GPR condition mapping was explained to bridge experts who were not familiar with GPR. In addition, respondents were also guided about the idea of the bridge deck condition index and how to complete the survey. Specifically, sing a continuous scale from 0 to 100, the same idea as California Bridge Health Index, the purpose of the survey was to map linguistic descriptions such as *sound concrete*, *moderate corrosion*, *severe corrosion* to the numerical rating of bridge deck. This scale, along with the deterioration process of a concrete bridge deck, is depicted in Fig. 4.2.

Section 2 has three questions. Question 4 required experts to provide their specific numbers about P1, P2, T1, and T2 those explained in Fig. 4.2.

In Question 5, respondents were requested to suggest intervention action for bridge decks that have condition index below the first threshold, T1. The options for answering this question included: (1) Do nothing and more frequent monitoring; (2) Repair (shallow, deep patching or full depth removal, etc.); (3) Total deck replacement; and (4) Other that needs to be specified.

The same as Question 5, in Question 6, experts were requested to suggest intervention action for bridge decks that have condition index below the second threshold, T2. The options for answering this question were: (1) Repair (shallow, deep patching or full depth removal, etc.); (2) Total deck replacement; and (3) Other that needs to be specified.
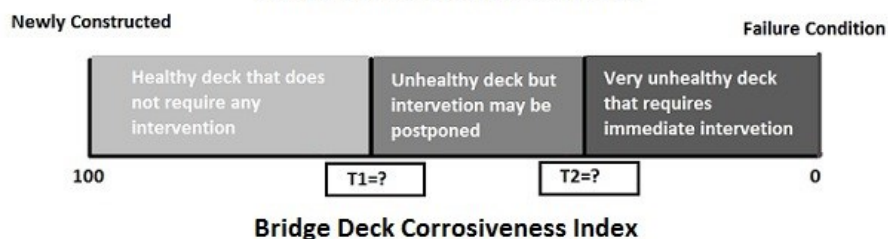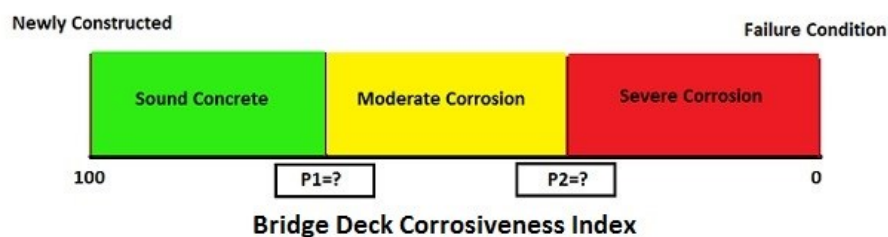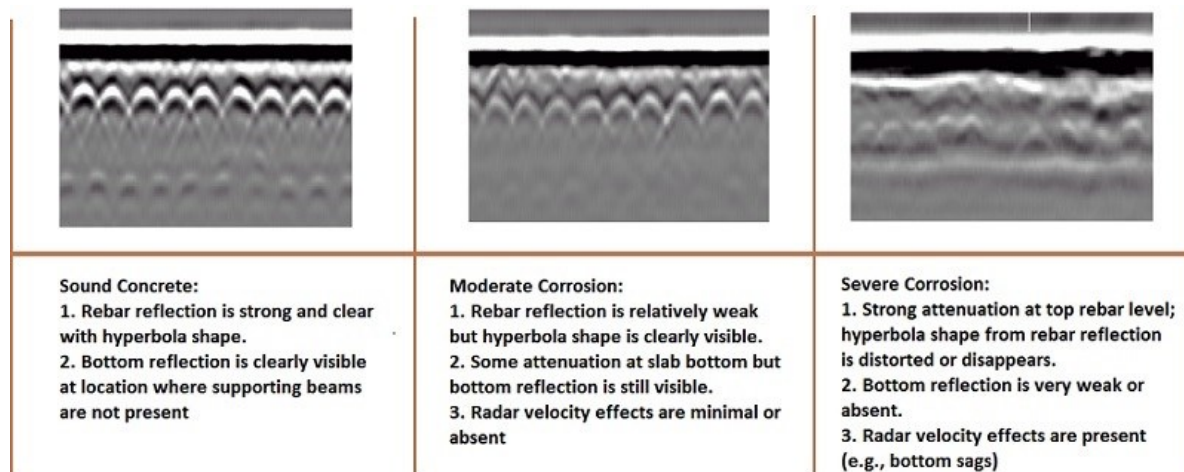

Fig. 4.2 Explanation of the survey

4.1.2.2 Survey Responses

The questionnaire survey was designed in www.surveymonkey.com website, a web

survey. The link was then delivered either directly to bridge and GPR expert, or through LinkedIn, a business-oriented social networking service. In addition to a special feedback representing collective opinion of the Ministry of Transportation of Quebec (MTQ), other received responses are described below.

Response Rate

Response rate refers to the number of experts who answered the survey divided by the number of experts in the sample. However, because of the manner in which the survey was delivered resulting in unknown sample size, the number of experts who did open the link and responded at least one question is considered instead as the number of experts in the sample. With that number being 83 and 23 experts completing the survey, the response rate is therefore 27.7% in this research.

Response rate has long been considered by many people as an indicator for the quality of a research survey. Although it is believed that higher response rates assure more accurate survey results, satisfactory number is still of controversy. To address this issue, Baruch (1999) conducted a study that explored what could and should be a reasonable response rate for academic research in which statistics from one hundred and fourty-one journal papers were investigated. Based on that study, he found that reasonable response rate for the survey that targets populations such as employees, managers or professionals was about 60 +/- 20 (%). He suggested that for future studies that use questionnaire survey, any downward deviation in response rate from this norm should be explained.

Given the suggestion from Baruch's research, there are some justification for a fairly low response rate obtained in this study. First, while many bridge experts are not familiar with GPR and cannot understand even rebar pattern in the profile, some of them had direct correspondence with the surveyors informing that they had bad experience with the technique. Second, some experts expressed their concern about the bridge deck corrosiveness index itself when in their agencies, it rarely enters the discussion on what strategies to take for planning deck intervention. Finally but possibly the main reason, many respondents may not be familiar with the way in which the main questions were asked when instead of multiple-choice options, they were requested to provide specific numbers those were proposed for the first time by this study.

Respondent's Information

Summary information on twenty-three respondents who completed the survey are presented based on their expertise in Fig. 4.3, their experience in Fig. 4.4, and their regions in Fig. 4.5 below. As can be seen, while all expertises favorable for answering the questionnaire were covered, the highest numbers of respondents were equally shared between bridge inspector and GPR expert groups, each with 26%. The numbers of bridge managers and bridge researchers participated were the same, approximately 18% for each group. Finally come bridge engineers, the last group with only 13%.

Regarding experience, interestingly, the highest participant rate belong to youngest professionals with 48% followed by the senior group with 22% responses. The most

senior respondents accounted for 17% while the experts with 5-10 years of experience shared the smallest portion of the pie with only 13%.

As for geographical distribution, most of respondents are from North America. Specifically, 52% of them come from Canada, 31% from US, and only 17% are from other regions.
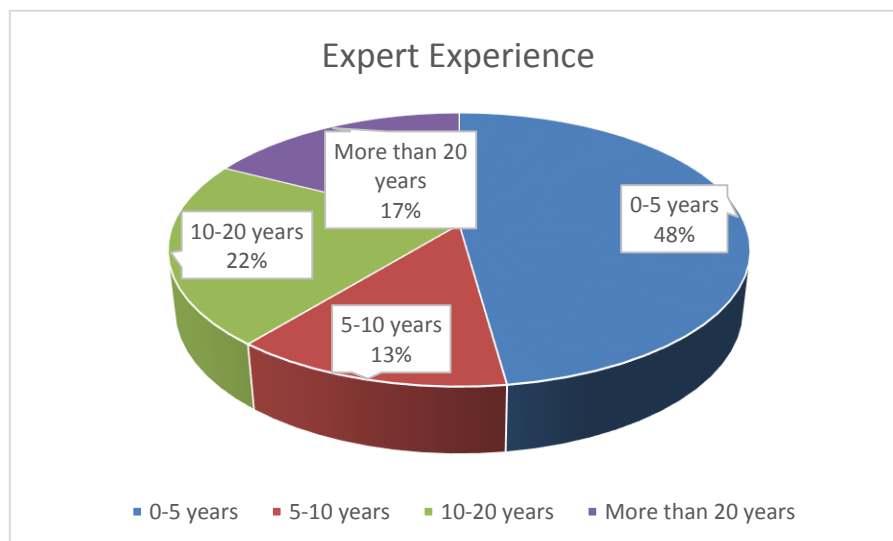

Fig. 4.3 Respondents based on expertise

Fig. 4.4 Respondents based on experience
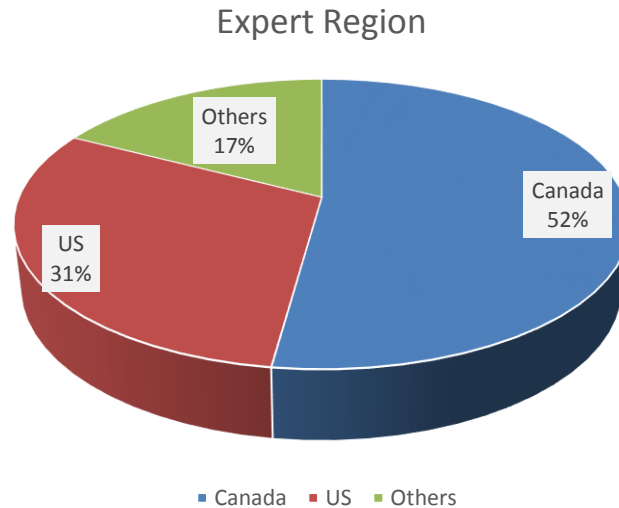
Expert Region

- Canada ■ US ■ Others

Fig. 4.5 Respondents based on region

4.2 Case Study Data

This section describes data collection for several case studies in North America, specifically, one bare (unpaved) concrete bridge deck in New Jersey, US and four asphalt-covered concrete bridge decks in Quebec, Canada. Detailed collection of data for each of them is described in turn as follows.

4.2.1 Pohatcong Bridge, New Jersey, US

The Pohatcong Bridge (Fig. 4.6) in Warren County, New Jersey, was built in 1978 with a bare concrete slab. This bridge deck was extensively studied using GPR during 2008-2013 period with four different GPR data sets, collected in May 2008, June 2012, December 2012, and September 2013, respectively. These data sets were collected at the same surveying lines using the same GSSI ground-coupled radar system. However, while the first three data sets were collected using the same machine by Rutgers

University, the fourth one was collected by Concordia University research team using the equipment loaned from Radex Detection Inc. Detailed information regarding the equipment used and setting for each data set are summarized in Table 4-1. Since the data set in 2008 covers only half of the deck width, the current research focuses on this limited area. Each data set contains 8 scan lines with 2-foot spacing, the first line was 1 foot offset from the curb. In addition, historical weather data was also searched for all data collection dates. These information, obatined from The Weather Underground Inc. (www.wunderground.com), are summarized in Table 4-2.

Fig. 4.6 Pohatcong Bridge

Table 4-1. GPR equipment and setting for each data collection

Information	May. 2008	Jun. 2012	Dec. 2012	Sep. 2013
SIR System	SIR-3000	SIR-3000	SIR-3000	SIR-3000
Antenna Model	5100 1.5 GHz	5100 1.5 GHz	5100 1.5 GHz	5100 1.5 GHz
Scans/Foot	24	60	60	72
Scans/Second	120	120	120	120
Samples/Scan	512	512	512	512
Gain (Number of Point)	1	1	1	1
Gain Value (dB)	-5	-2	-5	0
Range (ns)	10	12	12	10
IIR Filter, Vertical, High (MHz)	10	-	-	10
FIR Filter, Vertical, Low (MHz)	BOXCAR 1930	BOXCAR 1930	BOXCAR 1930	BOXCAR 1930
FIR Filter, Vertical, High (MHz)	BOXCAR 295	BOXCAR 295	BOXCAR 295	BOXCAR 295

Table 4-2 Historical weather data for each GPR data collection

Information	May. 2008	Jun. 2012	Dec. 2012	Sep. 2013
Date when data was collected	14th May	27th June	14th December	8th September
Weather on collected date	Avg. 14^0C with no rain	Avg. 19^0C with no rain	Avg. 2^0C with no rain	Avg. 19^0C with no rain
Weather one day before collected date	Avg. 13^0C with no rain	Avg. 18^0C with no rain	Avg. 2^0C with no rain	Avg. 17^0C with no rain
Weather two days before collected data	**Avg. 9^0C with rain of 8.64 mm**	**Avg. 21^0C with rain of 4.57 mm**	Avg. 2^0C with no rain	Avg. 15^0C with no rain
Weather three days before collected data			**Avg. 4^0C with rain of 0.76 mm**	Avg. 19^0C with no rain
Weather four days before collected data				Avg. 20^0C with no rain
Weather five days before collected data				Avg. 22^0C with fog
Weather six days before collected data				**Avg. 24^0C with rain of 17.27 mm**

4.2.2 Bridge A, Quebec, Canada

Bridge A (Fig. 4.7) was built in 1965 with a total length of 212 feet. It consists of four spans in the North-South direction. The bridge was formed by a deck varying in thickness (between 2' and 3'-6") resting directly on piers and abutments. The total width of the deck is 42 feet with 30 feet of traveled way. The deck was introduced by the Ministry of Transportation of Quebec (MTQ) since it is considered difficult for

inspection using GPR. The reasons include: (1) the deck is too thick that may weaken GPR signals; (2) the deck has varying thickness, causing problem to data interpretation. The bridge was last inspected in 2012 in which it was reported that although the asphalt overlay is in medium to severe condition, on average 99 percent of the concrete deck area has medium severity of deterioration and only 1 percent is in severe condition. The overall performance index for the concrete deck is 4, meaning that the current defects in the deck do not have significant impact to the deck performance. In addition, a half of the bridge was inspected in 2005 by LVM Fondatec Inc., using Half-cell Potential. The result of the test indicated that at that time 25 percent of the inspected area was in sound condition while the corrosion had initiated in the remaining 75 percent of the area.

Fig. 4.7 Bridge A

After studying the bridge deck plan, a grid of scanning paths with two-feet spacing was established. According to ASTM D6087, this spacing is acceptable for GPR inspection. There were total of fourteen paths covering 30 feet of traveled way. For each path, its two ending points were determined by a survey tape, measuring from curb to curb. Then, these points were marked. In order to scan each path with GPR, a survey string was used to make a straight line between two marked ending points. A pushing cart carrying GSSI 1.0 GHz GPR antenna was then pushed by an operator, following the survey string as shown in Fig. 4.7.

4.2.3 Bridge B, Quebec, Canada

Bridge B was built in 1966, consisting of 1-foot reinforced concrete deck with asphalt overlay that rests on five I-shaped steel girders. The deck has a width of 26 feet and a total length of 180 feet with three continuous spans. The length of the middle span is 105 feet and the other two lanes; each one is 37.5 feet long. The bridge is a little skew as shown in Fig. 4.8, with the skew angle of 3^08'. GPR scanning grid was setup with the first line that was 1.5 feet offset from the curb. Then the spacing for the lines in the middle was 1 foot. There were totally twenty-four profiles corresponding to twenty-four scanning paths.
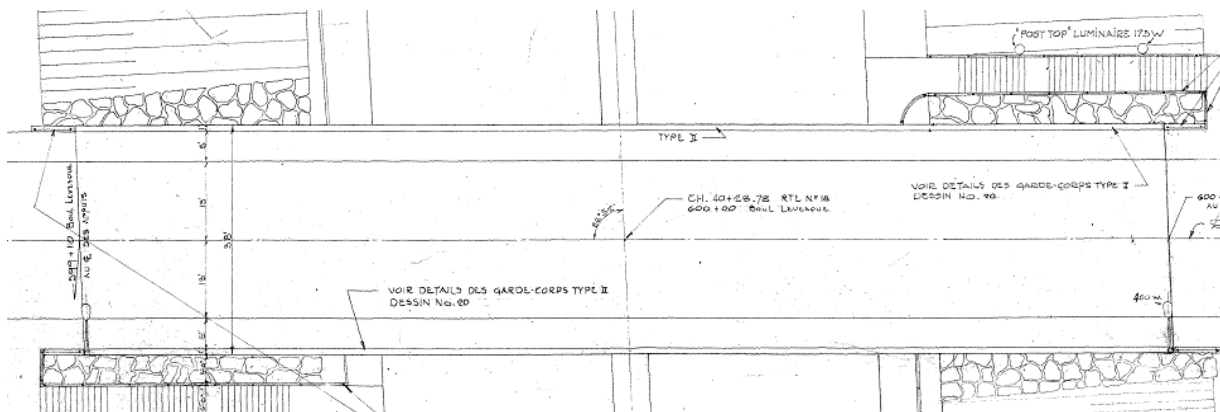

Fig. 4.8 Bridge B

4.2.4 Bridge C, Quebec, Canada

Bridge C facilitates two-way travelling with three traffic lanes for each direction, East and West. The width of traveled way for each direction is 36 feet. The bridge deck is 120 feet long and 1.5 feet deep that is supported by four longitudinal concrete walls as shown in Fig. 4.9. GPR data was collected for the entire deck with totally 68 survey lines, i.e., 34 lines for each direction.
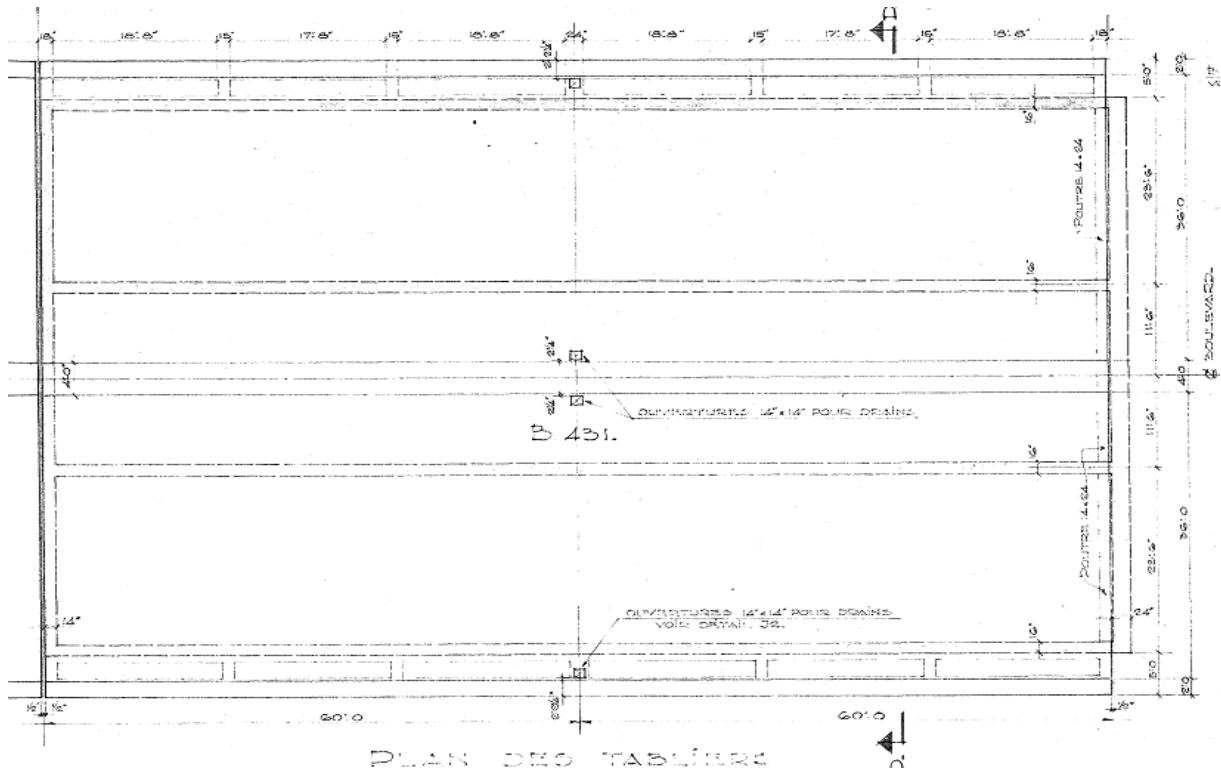
Fig. 4.9 Bridge C

4.2.5 Bridge D, Quebec, Canada

Bridge C was built in 1960. The bridge deck is about 1 foot of thickness with 45 feet in length and 32.8 feet of traveled way. While the bridge deck plan is shown in Fig. 4.10, GPR data was collected using GSSI SIR-3000 and 1.5 GHz antenna.
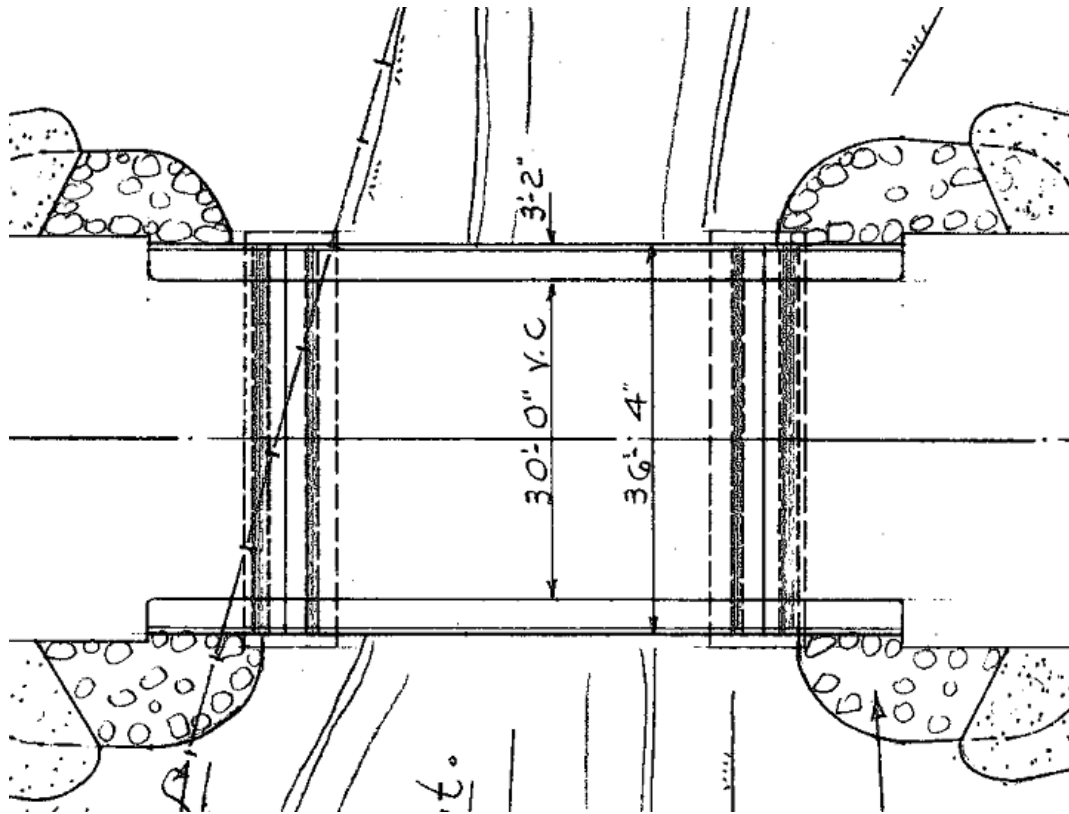
Fig. 4.10 Bridge D

CHAPTER 5   IMPLEMENTATION OF DEVELOPED MODELS

5.1 System Calibration

5.1.1 Correlation Threshold

In order to calculate correlation coefficient for 74214 couples of signals in two calibration data sets collected in previous chapter, the RADAN files were converted to ASCII format and read by MATLAB program. The distribution of correlation coefficients computed for 74214 couples of A-scans is presented in Fig. 5.1 (solid area). As can be seen, since the correlation coefficient is defined on interval [-1, 1], the most appropriate type of distribution for it is Beta distribution. This distribution type has been applied to model the behavior of random variables limited to intervals of finite length in a broad variety of disciplines. It is parameterized by two positive shape parameters, denoted by a and b. The fitting was performed in MATLAB and the result (fitting curve) is also shown in Fig. 5.1. Based on the fitted distribution, the correlation thresholds corresponding to different levels of false positive rate are calculated and presented in Table 5-1.

Table 5-1 False Positive Rates and Threshold Levels

False Positive Rate	0.1	0.05	0.02
Coefficient Threshold	0.986	0.981	0.975

As can be seen in Table 5-1, the coefficient threshold reduces when false positive rate decreases. The threshold in the model can be determined by the interpreter based on his or her desire for false alarm probability. However, it is noted that when the threshold decreases, the probability of false negative error (test result showing no problem when it exists) increases. Due to data unavailability, this issue is not resolved in the present research.

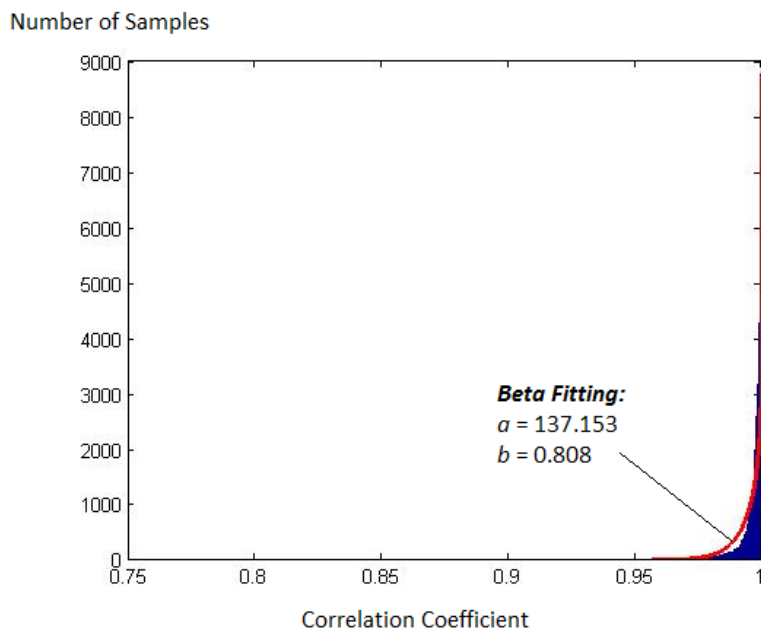**Fig. 5.1 Correlation coefficients and distribution fitting.**

5.1.2 Questionnaire Survey Analysis

5.1.2.1 Membership Function Calibration

As explained in the research methodology in Chapter 3, Question 4 is the most important question which is used to calibrate membership functions. While all the responses for this question are provided in Table 5-2, the calibration process is described as follows.

Step 1. Check the first level of consistency

As advised in the questionnaire, experts were expected to provide consistent opinions, i.e., P1 value should be greater than P2 and the same with T1, T2. However, since one expert did not know what would be the number provided by the others; as a result, the consistency should be checked at both levels, individual expert and the entire group. As can be seen in Table 5-2, for the first level check, no individual expert provided inconsistent judgment.

Table 5-2 Summary of responses for Question 4

Response No.	P1	P2	T1	T2
1	90	50	75	30
2	70	40	80	60
3	60	40	60	40
4	80	30	60	30
5	80	60	80	60
6	70	30	70	40
7	70	30	75	25
8	75	55	70	45
9	85	70	75	50
10	80	60	80	60
11	60	40	80	60
12	80	50	70	40
13	75	55	80	60
14	75	45	60	40
15	80	40	70	30
16	70	50	60	40
17	80	50	70	50
18	75	25	75	25
19	70	30	70	30
20	66	33	66	33
21	60	30	50	30
22	85	65	80	60
23	80	60	80	70

Step 2. Check the second level of consistency

In order to check the second level of consistency for the entire group, a histogram and assumed normal distribution fitting is plotted for each number couple, i.e., P1&P2 and

T1&T2. While these plots are shown in Fig. 5.2 and Fig. 5.3, as can be seen, both of them show some inconsistency at group level that need to be eliminated.
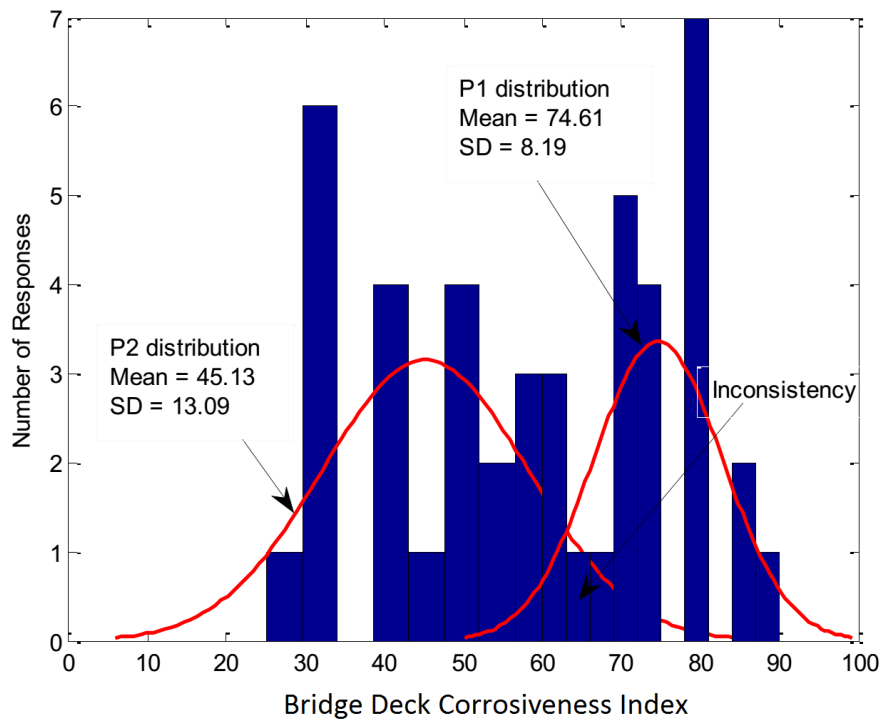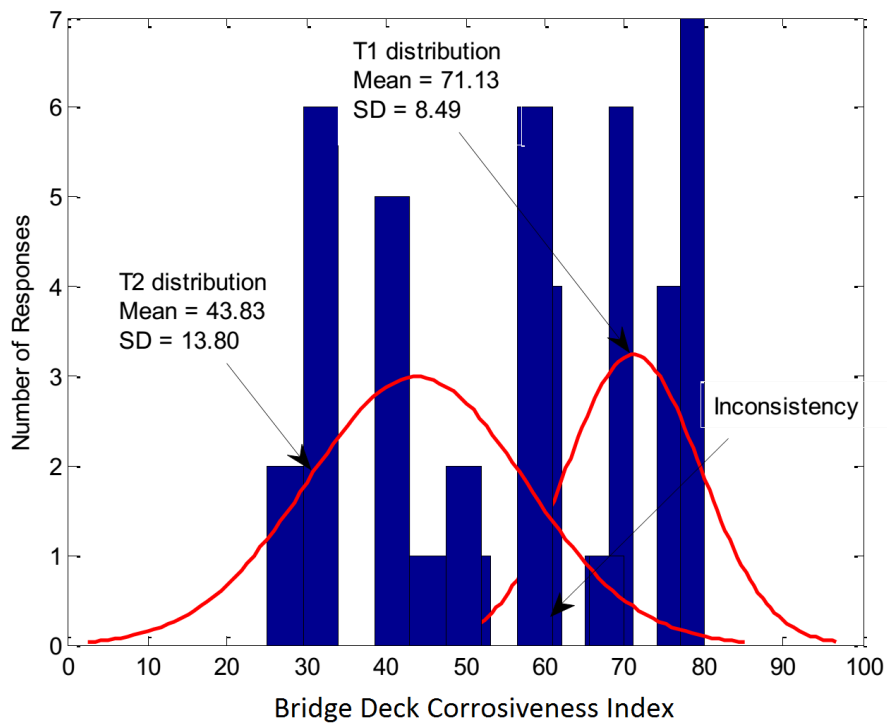

Fig. 5.2 Inconsistency between P1&P2

Fig. 5.3 Inconsistency between T1&T2

102

In order to do that, it is proposed that first, the responses in Table 5-2 are rearranged in increasing order for each column as shown in Table 5-3. Then any value in Table 5-3 that lies in inconsistency zone is highlighted and will be considered as a candidate for removal. The removal is done based on distance from normal distribution model, using standard deviations. For P1&P2 values for instance, 60 appears to be present in both P1 and P2 columns. To consider whether that value should be removed from P1 or P2 sample, a calculation illustrated in Table 5-4 is used. As can be seen, since the value, 60, is closer to the mean of P2, it should be removed from P1 sample.

Table 5-3 Rearranged responses for Question 4

Response No.	P1	P2	T1	T2
1	60	25	50	25
2	60	30	60	25
3	60	30	60	30
4	66	30	60	30
5	70	30	60	30
6	70	30	66	30
7	70	33	70	30
8	70	40	70	33
9	70	40	70	40
10	75	40	70	40
11	75	40	70	40
12	75	45	70	40
13	75	50	75	40
14	80	50	75	45
15	80	50	75	50
16	80	50	75	50
17	80	55	80	60
18	80	55	80	60
19	80	60	80	60
20	80	60	80	60
21	85	60	80	60
22	85	65	80	60
23	90	70	80	70

Table 5-4 Distance calculation for inconsistency removal

Sample	Mean	SD	Candidate Removal	Distance
	(1)	(2)	(3)	(1-3)/2
P1	74.61	8.19	60	1.78
P2	45.13	13.09	60	1.13

Following the same procedure, all the removed values from each sample are highlighted and shown in Table 5-5. As can be seen, this inconsistency removal method also result in the lowest number of responses being removed.

Table 5-5 Retained and removed values for each sample

Response No.	P1	P2	T1	T2
1	60	25	50	25
2	60	30	60	25
3	60	30	60	30
4	66	30	60	30
5	70	30	60	30
6	70	30	66	30
7	70	33	70	30
8	70	40	70	33
9	70	40	70	40
10	75	40	70	40
11	75	40	70	40
12	75	45	70	40
13	75	50	75	40
14	80	50	75	45
15	80	50	75	50
16	80	50	75	50
17	80	55	80	60
18	80	55	80	60
19	80	60	80	60
20	80	60	80	60
21	85	60	80	60
22	85	65	80	60
23	90	70	80	70

Step 3. Linear regression for determining membership function boundaries

With the retained values for each sample in Table 5-5 and since membership functions were assumed to be piecewise linear, the boundaries for membership functions are determined based on linear regression as shown in Fig. 5.4. Finally, the membership functions based on the results in Fig. 5.4 for P1&P2 and T1&T2 are shown in Fig. 5.5 and Fig. 5.6, respectively.
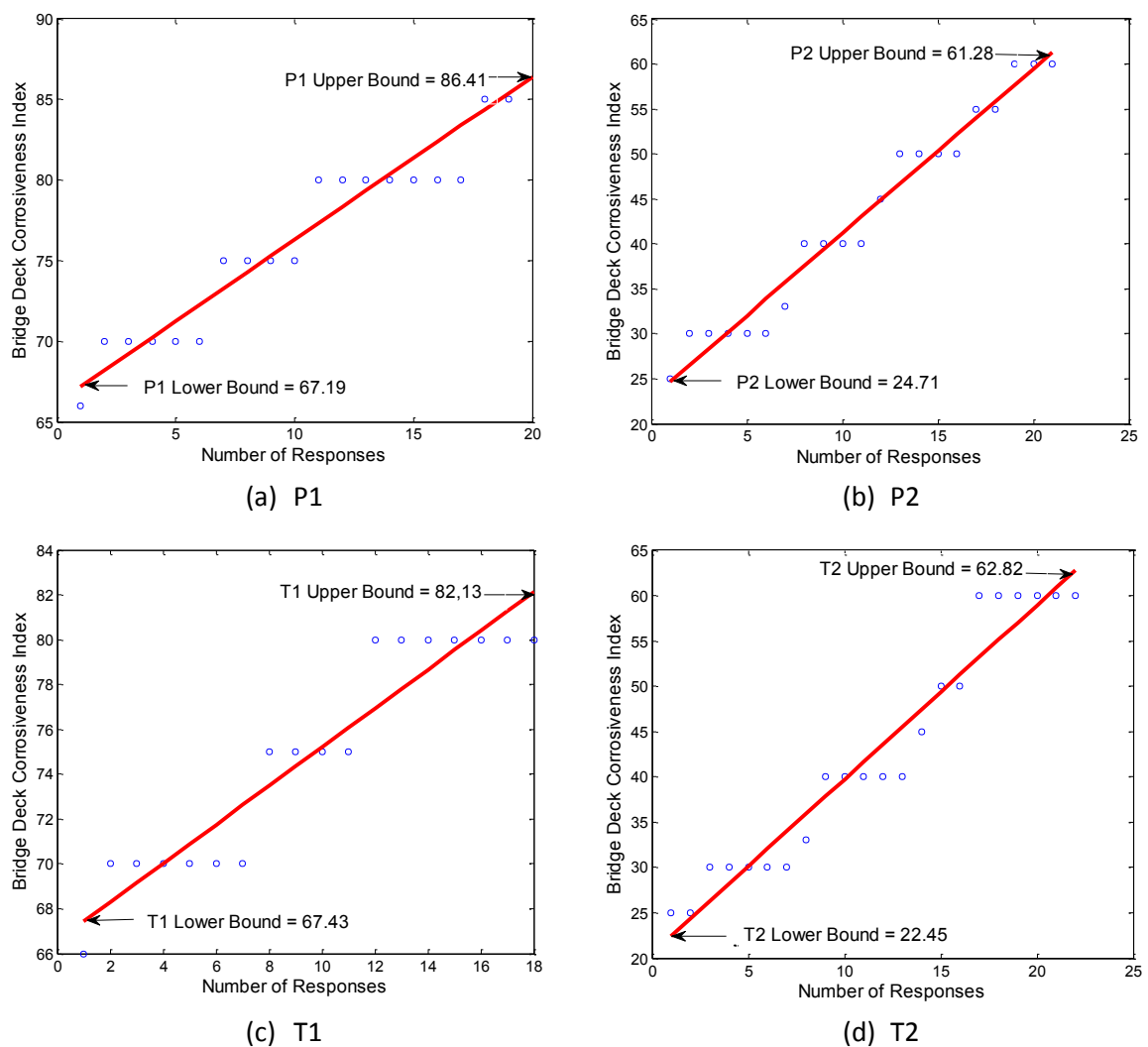

(a) P1

(b) P2

(c) T1

(d) T2

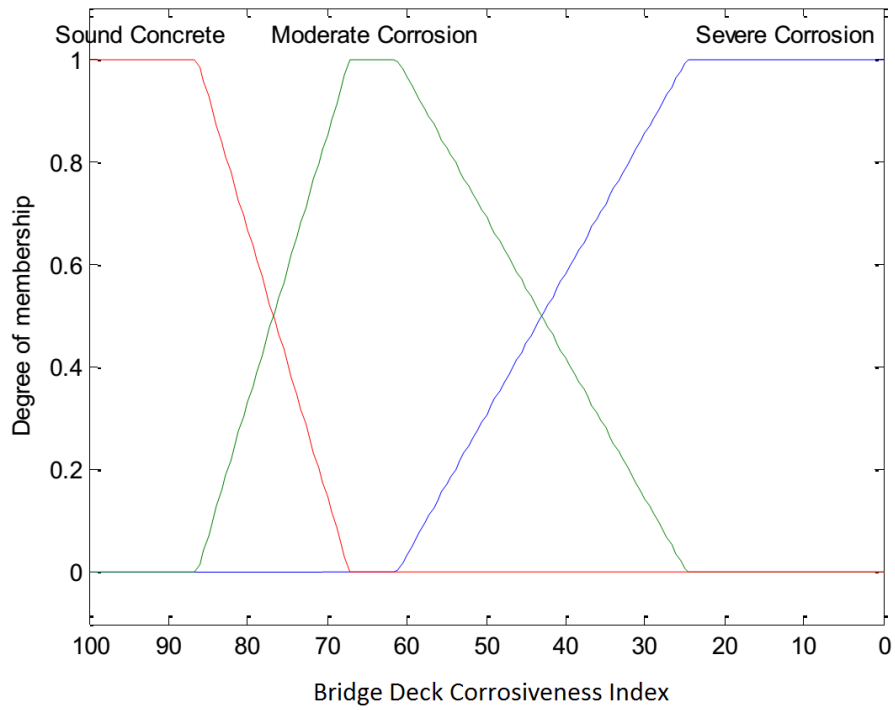**Fig. 5.4 Linear regression for membership function calibration**

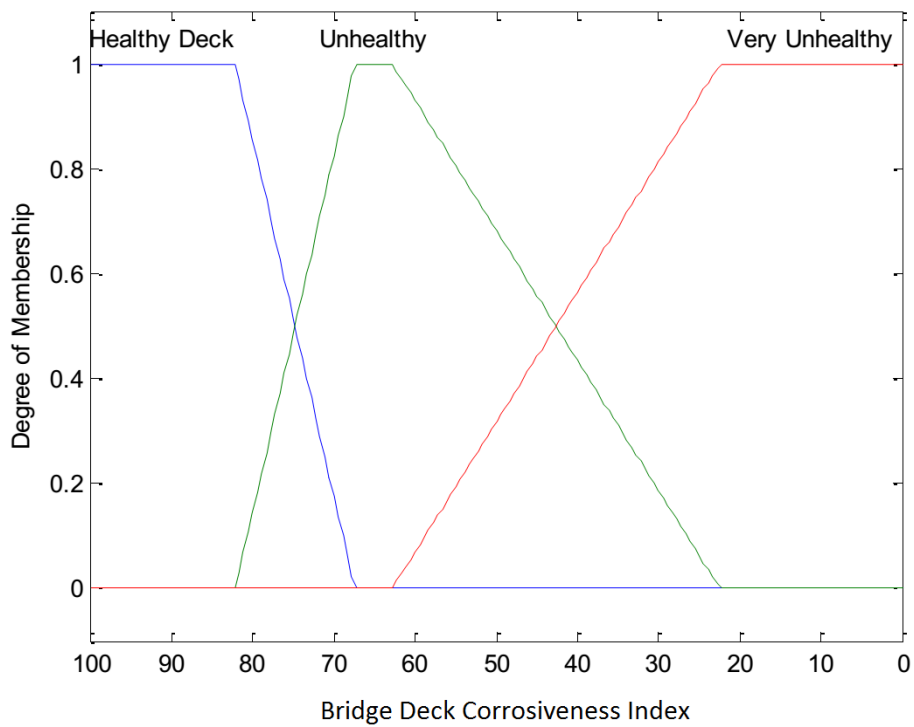**Fig. 5.5 Calibrated membership functions based on P1&P2**

Fig. 5.6 Calibrated membership functions based on T1&T2

5.1.2.2 Selection of Defuzzification Method

Ideally, the bridge deck corrosiveness index (BDCI) should have the range from 100 to 0; however, due to fuzzy information provided by GPR corrosion map, this range can never be achieved for the BDCI computed from the model. Therefore, between *centroid* and *bisector* methods for defuzzifying the resultant fuzzy set, this research selected the strategy that provides maximum range of the index. As can be seen in Fig. 5.17, although showing small difference, *bisector deffuzification* was the selected technique.
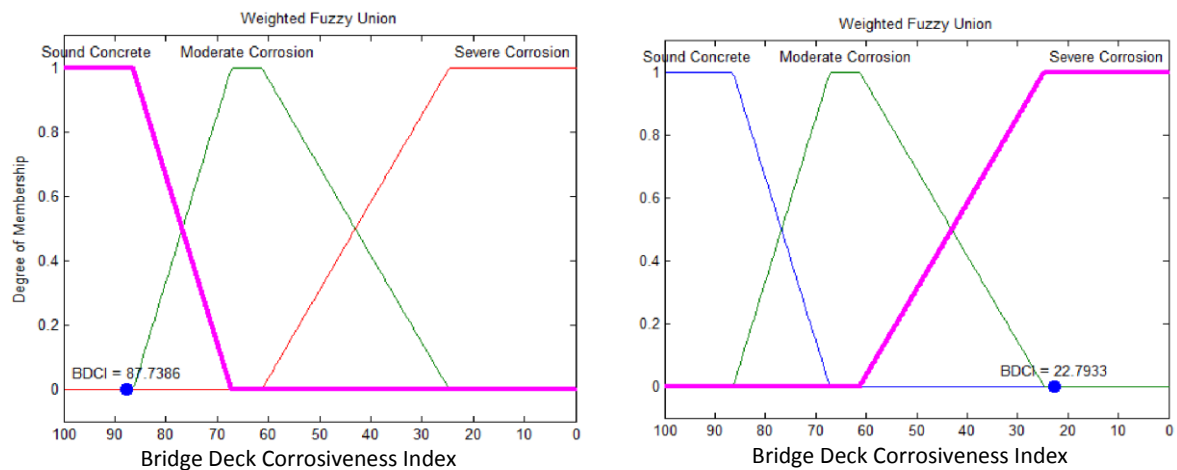
(a) Extrema of BDCI with centroid deffuzzification
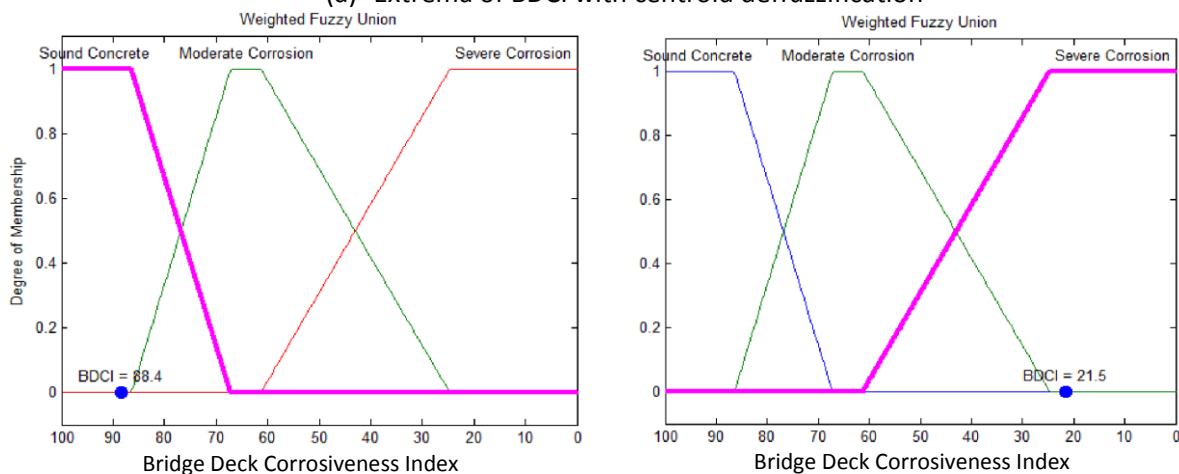
(b) Extrema of BDCI with bisector deffuzzification

Fig. 5.7 Comparison of two deffuzification methods

5.1.2.3 Intervention Actions

Beginning with Question 5 in the survey, as can be seen in Fig. 5.8, 65% respondents suggest "repair" for bridge decks those are unhealthy but intervention can still be postponed; none of them consider "total deck replacement"; 18% recommend "do nothing and more frequent monitoring"; while 17% think of other solutions such as chloride or additional NDE testings.
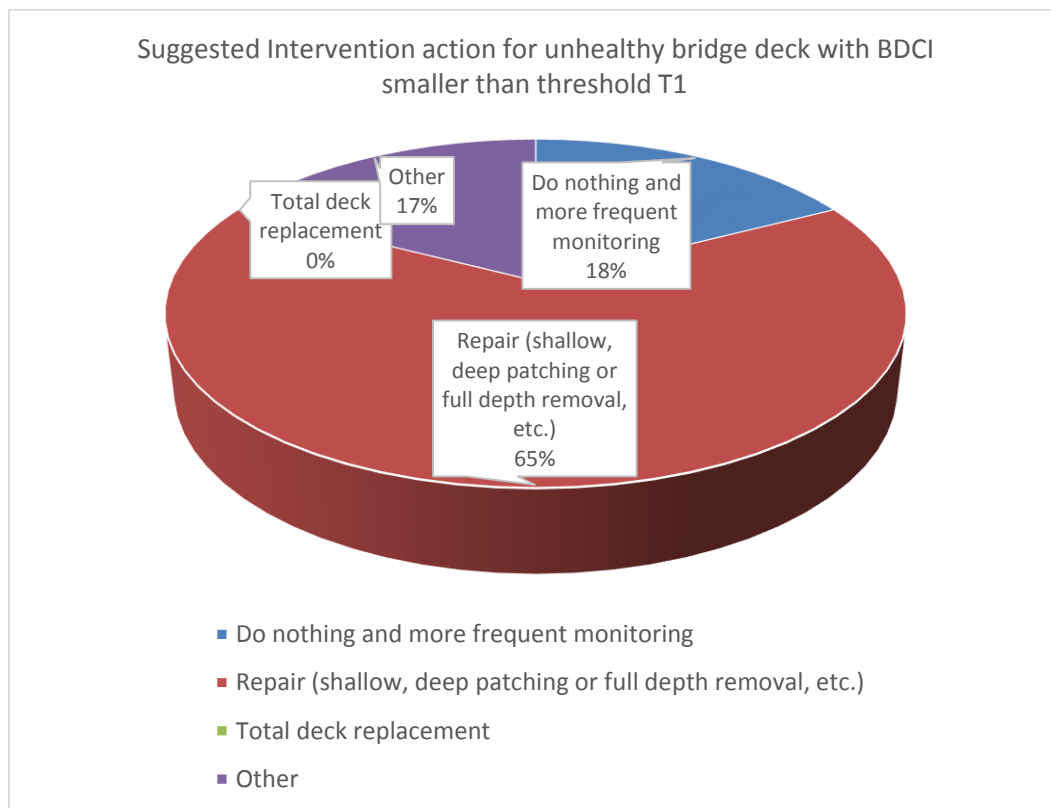

Fig. 5.8 Suggested intervention for unhealthy bridge decks

Regarding Question 6, as can be seen in Fig. 5.9, 57% of respondents suggest "total deck replacement"; 30 % of them recommend "repair" and 13% propose other actions. These newly-proposed intervention actions include (1) *deck reinforcement* and (2)

partial deck replacement for safety until plans can be developed for total deck replacement.
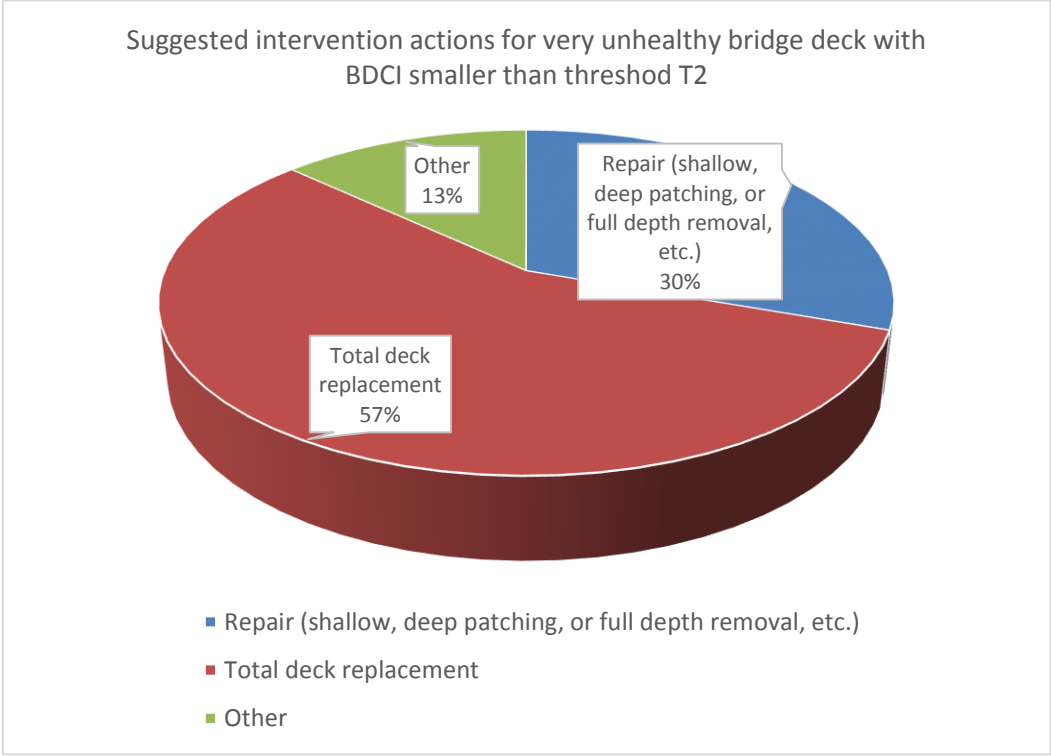

Fig. 5.9 Suggested intervention actions for very unhealthy bridge decks

Although the majority of experts responded by choosing one intervention action in the list provided by the surveyors, not all of them felt satisfactory. Their reaction for this was either (1) to correspond and discuss directly with the authors or (2) to choose an action different from those listed. Regarding BDCI thresholds and corresponding intervention actions, MTQ recommended the two following scenarios. The first scenario is when only one threshold value T is used. Then, if the BDCI is greater than T: do-nothing; otherwise, intervention should be planned in a 5-20 year horizon for the deck in question. The second scenario is the one in which two threshold values T1 and T2 are employed. Then, if BDCI is over T1: no repair or replacement intervention; if

BDCI is below T1 and over T2: an intervention planned in a 10-20 year horizon; and below T2: an intervention planned in a 5-10 year horizon.

On the contrary, the researchers also received a suggestion from an expert who participated in the survey that they should consider more decision points (thresholds), instead of the two (T1&T2) used in the questionnaire. Benefited from all these suggestions, a comprehensive strategy for using BDCI is proposed in the next section.

5.1.3   Strategic Use of Bridge Deck Corrosiveness Index (BDCI)

As can be seen in Fig. 5.6, fuzzy partitioning exist with both threshold T1 and T2 when each of them has lower and upper bound as shown in Fig. 5.4(c) and (d). What that means is, for the same BDCI value that lies in these fuzzy areas, experts do not share the same opinion regarding intervention needed for bridge deck with a specific BDCI in question. For example, if a bridge deck has a BDCI value of 80.00, some experts would consider the deck being completely healthy while others would think it is unhealthy and needs intervention. Considering these fuzzy regions along with recommendations discussed above, it is reasonable to re-define the levels of intervention needs that integrate lower and upper bounds of T1 and T2. The proposed levels of BDCI and corresponding recommended actions are provided in Table 5-6.

It is noted in Table 5-6 that at some levels of BDCI, instead of a single intervention type, a list of feasible actions may be provided. If that is the case, intervention actions are put in recommendation priority order, meaning the first type of action is recommended more strongly than the second one and so on. This approach is more practical than

providing a single action, considering the fact that bridge decks competing with each other for the limited maintenance budget.

Table 5-6 Strategic Use of BDCI and Inspection System

Level of Intervention Need (Category)	Value of BDCI	Intervention Need Description	Recommended Actions within 20-year horizon
A	100 - 82.13	Healthy deck, no intervention is required.	Do nothing, next GPR inspection is planned in 10-20 year horizon.
B	82.13 - 67.43	Slightly unhealthy deck, intervention is not yet necessary.	Do nothing, next GPR inspection is planned in 5-10 year horizon.
C	67.43 - 62.82	Unhealthy deck, intervention is needed but may be postponed.	1. Deck repair is planned in 5-10 year horizon. 2. Next GPR inspection is planned in 5-10 year horizon.
D	62.82 - 22.45	Very unhealthy deck, intervention is strongly recommended.	Total deck replacement is planned in 5-10 year horizon.
E	22.45 - 0.00	Completely unhealthy deck, immediate intervention is required.	Total deck replacement is planned in 0-5 year horizon.

As 10-year decision point used when determining the number of clusters (K) for top rebar amplitude in the preceding chapter, the same justification exists for specifying maximum 10-20 years of separation between GPR scans. With commonly high deterioration rate of bridge decks, considerable corrosion might have built up on healthy decks but undetected if this period is set too long. On the other hand, for bridge decks those have shown some unhealthy sign, Table 5-6 suggests that if intervention action is not taken, GPR inspection frequency should be increased.

In addition to provide important input that will be used by bridge maintenance planner and bridge program manager, the BDCI model developed in this research also provides an useful tool for high-level decision-makers or elected authority. For example, these agencies can use the index for communication with the public in order to gain more

attention about bridge deck condition or to justify the budget that they ask for fixing bridge problem.

5.2   System Implementation

In this section, Pohatcong bridge deck in New Jersey, the case study with most extensive data, will be used to test amplitude analysis as well as illustrate the implementation of the developed system. Basic idea is that, with time-series data collected during 5-year study period, it is assumed that deterioration progression on the deck should be somehow observed with condition assessment technique. This assumption makes it possible for various analysis results to be verified or validated as will be described and discussed.

5.2.1   Test of Amplitude Analysis

5.2.1.1 Rebar Reflection Mapping Without Depth-Correction

This is the simplest method to interpret GPR data where the effect of rebar depth variation in bridge deck is neglected. While the entire process for extracting rebar reflection amplitude using GSSI RADAN software can be illustrated in Fig. 5.10, each step for analyzing GPR data is described as follows:
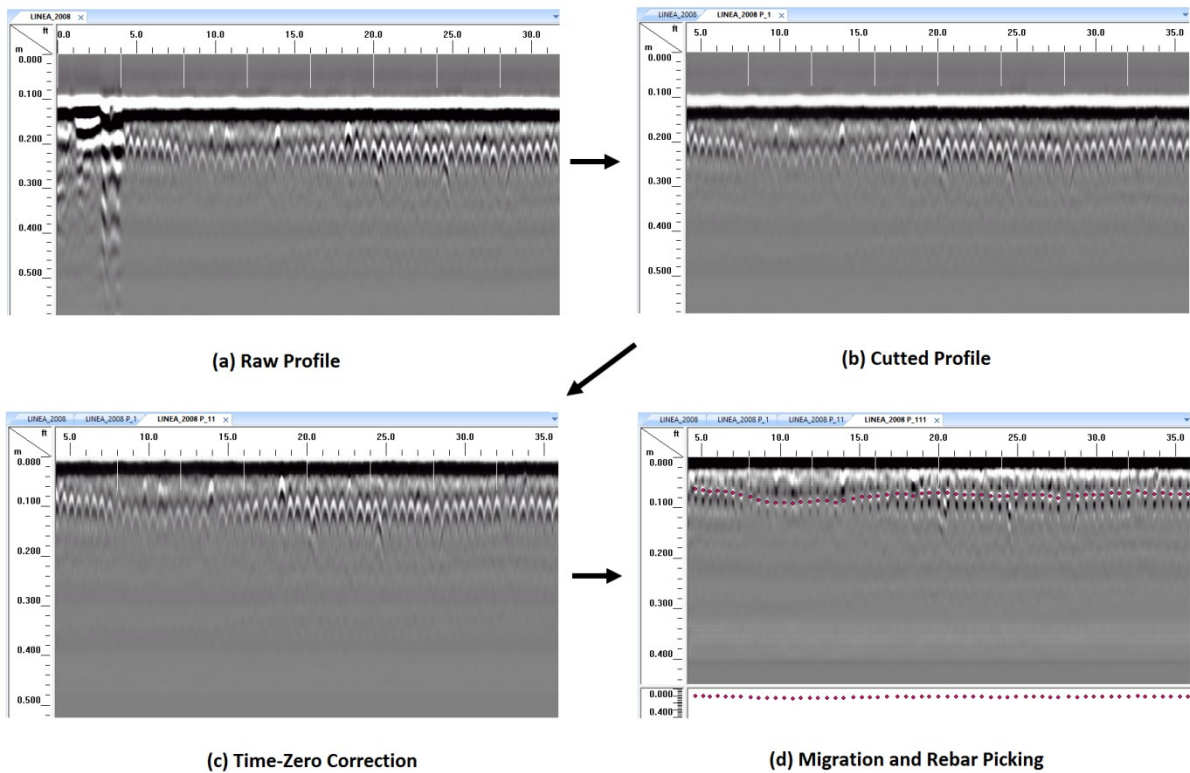
(a) Raw Profile

(b) Cutted Profile

(c) Time-Zero Correction

(d) Migration and Rebar Picking

Fig. 5.10 Process for extracting rebar reflection amplitude.

Step 1. Cut Profiles

Since each GPR profile collected on the field may begin before and end after bridge joints, this step is to guarantee that the profiles corresponds exactly to the deck's starting and ending lines.

Step 2. Time-Zero Correction

This step aims at shifting each scan of the data in order to match top of the scan to the bridge deck surface.

Step 3. Hyperbola Migration

Migration is a mathematical process to collapse hyperbolic shape associated with the rebar reflection and focus on their subsurface location. This step can also be used if signal velocity needs to be measured.

Step 4. Rebar Reflection Picking

Although the migration process above provides data containing rebar reflections that can be detected using automated algorithms in RADAN; for accuracy reason, this research employed interactive picking in which each rebar was picked manually in the migrated profile. In addition, each corresponding raw profile was checked at the same time when the picking was done. Then, information for picked rebars in each profile was exported to an ASCII comma-separated value (.csv) file. The exported information for each rebar included scan number, absolute amplitude, and 2-way travel time.

Step 5. Create Rebar Reflection Map

Once rebar picking had been done and ASCII files had been created for all the profiles, these files were then read by a MATLAB program written by the authors to create an Excel file (.xls), containing all the information about the coordinate and reflection amplitude (dB) of each rebar. Finally, for each data set, the .xls file was read by Surfer, a mapping software, to create an attenuation map. It is noted that while only the first two information of ASCII file are needed for creating rebar reflection map, the 2-way travel time may be used later on for depth correction.

The attenuation maps for four data sets obtained using the above process are shown in Fig. 5.11. As can be seen, although the shapes of the more attenuated area in the maps

in Fig. 5.11 stay quite stable over time, direct comparison of these maps is not meaningful, because of the following reasons: (1) The gain (amplification) values for different data sets are not the same, although all of them using a constant gain setting as presented in Table 4-1; (2) Even with the same gain, the power level may vary between equipment used for data collection. Therefore, in order to compare the maps, a normalization procedure is needed to eliminate the effect of those factors. At the beginning, two normalization methods were considered, namely (1) Depth-correction by Barnes et al. (2008); and (2) Direct-coupling normalization. Each of them is described in following sections.

5.2.1.2 Rebar Reflection Mapping Normalized by Depth-Correction

Although being developed originally for depth normalization, it is realized in this research that the procedure proposed by Barnes et al. (2008) can also be used for direct comparison of attenuation maps. The reason is that the procedure can eliminate the effect of transmit power and gain difference, provided that they have the same center frequency and single-point gain is used throughout various data sets. As can be seen in Table 4-1, these conditions are completely met by all four data sets. With two-way travel time information obtained previously, the maps in Fig. 5.11 were depth-corrected in the same manner as Barnes et al. (2008) and in the same MATLAB program previously mentioned. While the linear regression fitting graphs at 90th percentile can be found in Fig. 5.12, the depth-corrected attenuation maps are depicted in Fig. 5.13.
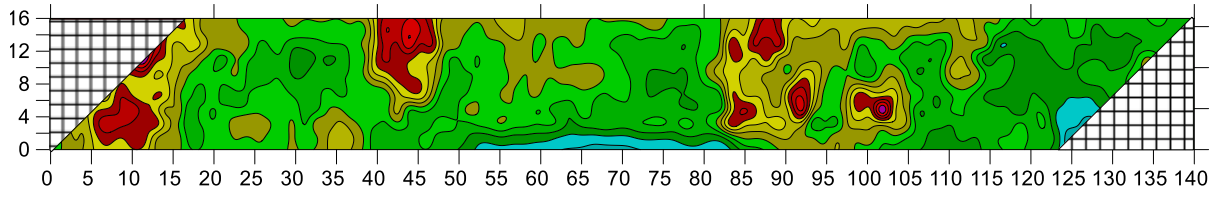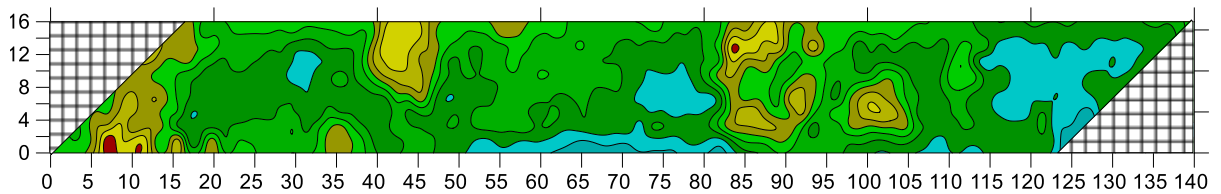
(a) Attenuation map in May 2008 without depth-correction
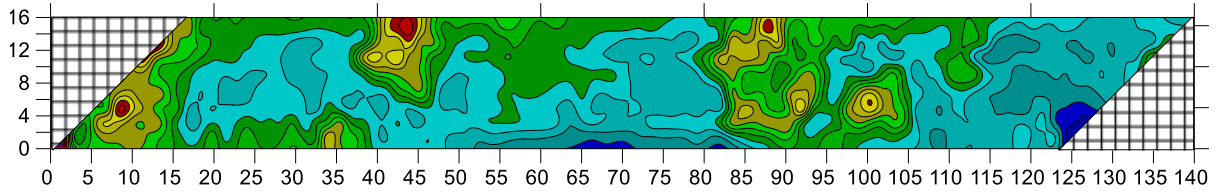
(b) Attenuation map in June 2012 without depth-correction
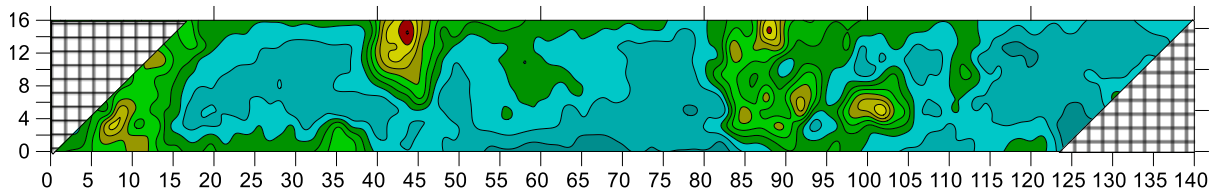
(c) Attenuation map in December 2012 without depth-correction

(d) Attenuation map in September 2013 without depth-correction

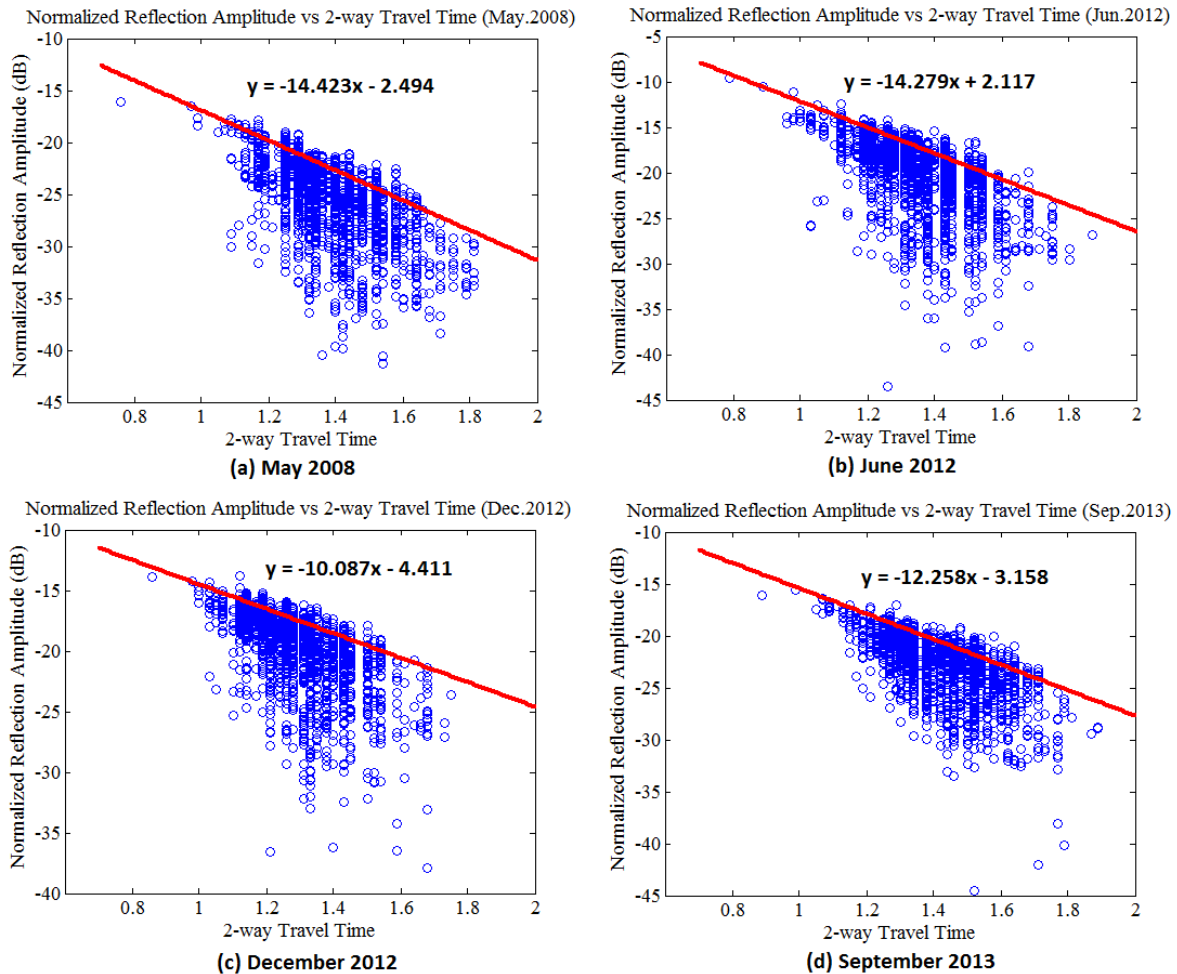**Fig. 5.11 Attenuation maps of four data sets without depth-correction.**

Fig. 5.12 Linear regression fitting at 90th percentile for four data sets.

As can be seen, the maps in Fig. 5.13 suggest some deterioration between May 2008 and June 2012, then ironically the deck condition appears to improve. Specifically, the map in September 2013 looks much better than all previous ones and its range of reflection amplitude (color spectrum) is much smaller than those of the other maps. For example, the reflection amplitude range for September 2013 data set is only 13 dB while this value for June 2012 data set is up to 20 dB. Because there was no intervention action performed on the bridge during study period, one possible explanation for this phenomenon is the difference in deterioration rate between top rebars in which good

rebars in June 2012 tend to corrode faster than already-deteriorated ones, as illustrated in Fig. 5.14. Another interesting observation is that the steepness of the fitting line in Fig. 5.12 varies between data sets. Specifically, the slope reduces from 14.423 in May 2008 to 14.279 in June 2012 and then drop significantly to 10.087 in December 2012. An increase to 12.258 can be observed in September 2013. It is noted that this variation in the steepness of the fitting line indicates change in conductivity between four data sets, i.e., the higher the steepness, the more conductive the concrete.

(a) Attenuation map in May 2008 with depth-correction

(b) Attenuation map in June 2012 with depth-correction

(c) Attenuation map in December 2012 with depth-correction

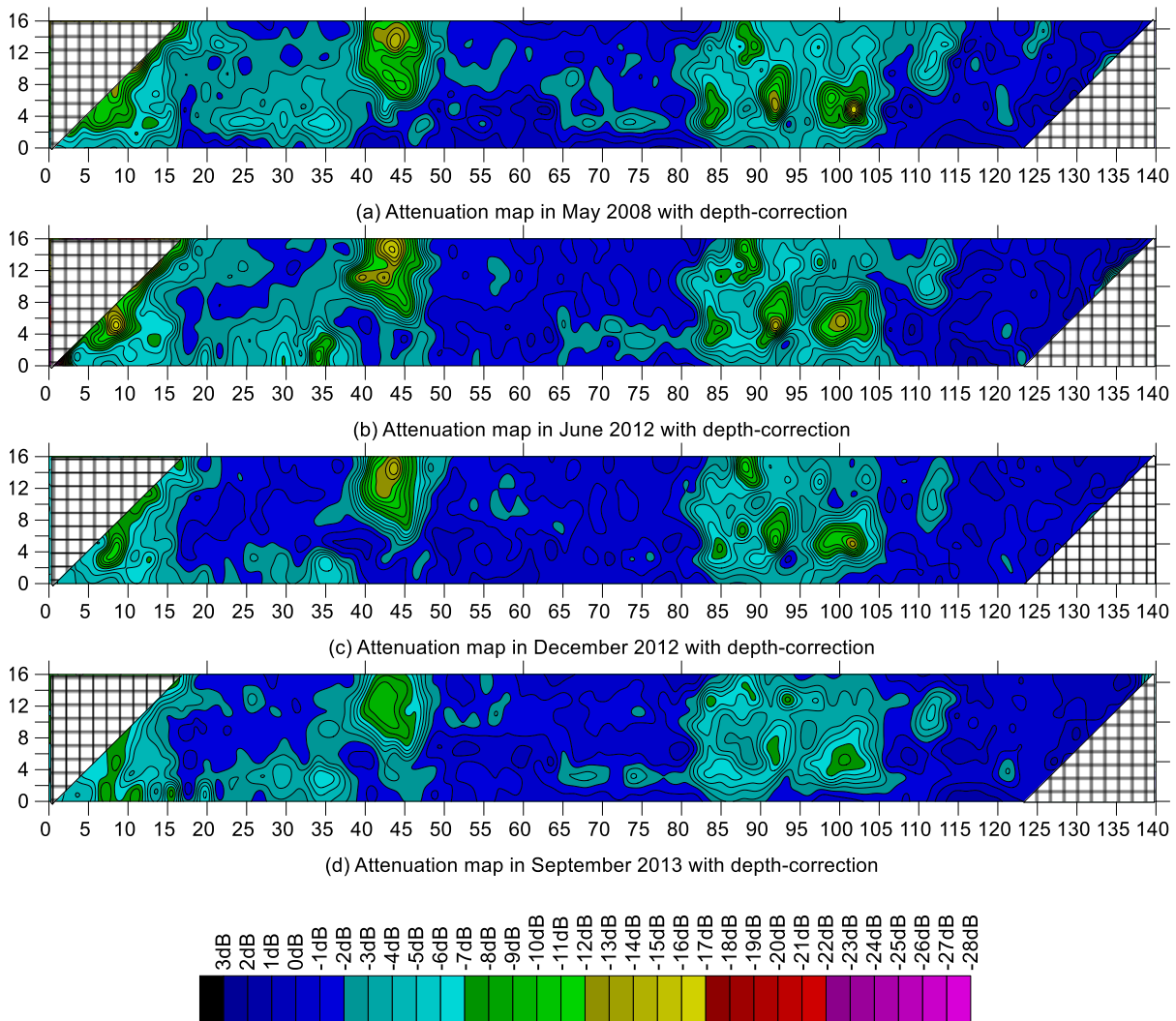(d) Attenuation map in September 2013 with depth-correction

Fig. 5.13 Attenuation maps of four data sets with depth-correction.
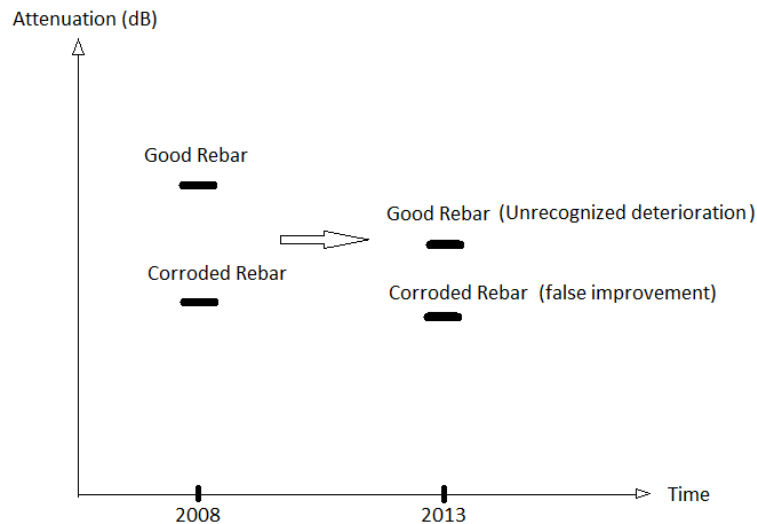
118

Fig. 5.14 Possible explanation for apparent deck improvement.

Since the effect of gain and transmit power has been eliminated by the normalization, the apparent improvement may be caused by difference in other equipment settings such as number of scans per foot, range, or filter. However, as can be seen in Table 4-1, the small difference between number of scans per foot and range between September 2013 data set with the ones in June and December 2012 would only result in a very small difference between the resolutions of GPR profiles. That should not cause much change in picked amplitude value of each rebar. In addition, it should be noted that the filters in May 2008 and September 2013 data sets were set exactly the same.

It is also possible to think of moisture in concrete cover as a cause leading to apparent deck improvement. Theoretically, this moisture may have two effects to GPR signal. First, it slows down the velocity of electromagnetic wave propagation in concrete and affects the two-way travel time measured. Second, it may increase concrete conductivity and causes more attenuation at top rebar. For these reasons, average two-way travel

time has been calculated for the four data sets. The values obtained are 1.385 ns, 1.359 ns, 1.294 ns, and 1.419 ns for May 2008, June 2012, December 2012, and September 2013, respectively. Then, to study the relationship, if any, between concrete moisture and conductivity, the average two-way travel time (moisture equivalence) is plotted against the steepness of regression fitting line (conductivity equivalence), as depicted in Fig. 5.15.

As can be seen, although having the highest moisture content, September 2013 data set does not show highest conductivity (attenuation). Therefore, it is evident that moisture content is not the main factor that causes variation in concrete conductivity in this case. Instead, if those conductivity data are analyzed in terms of season in which each data set was collected, i.e., May, June, September, December, one can easily come up the hypothesis that concrete conductivity tends to decrease after the usage of deicing salt in winter is stopped, as illustrated in Fig. 5.16.
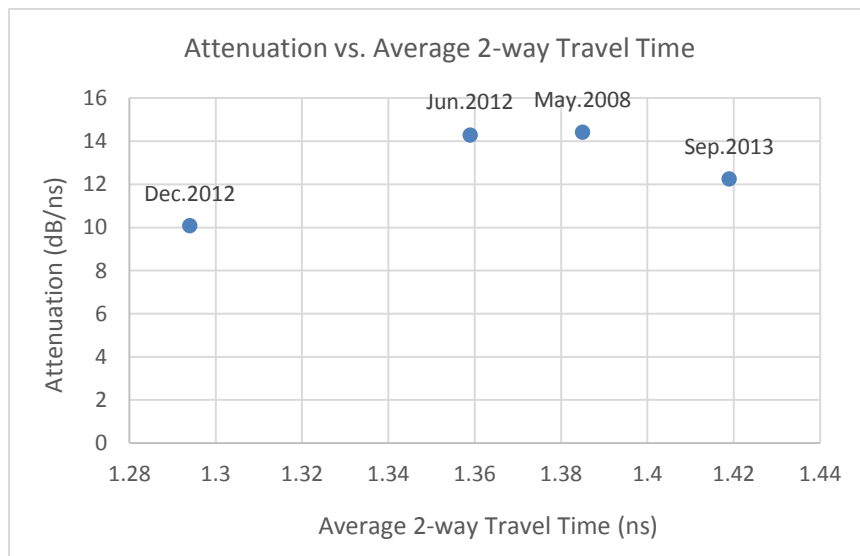

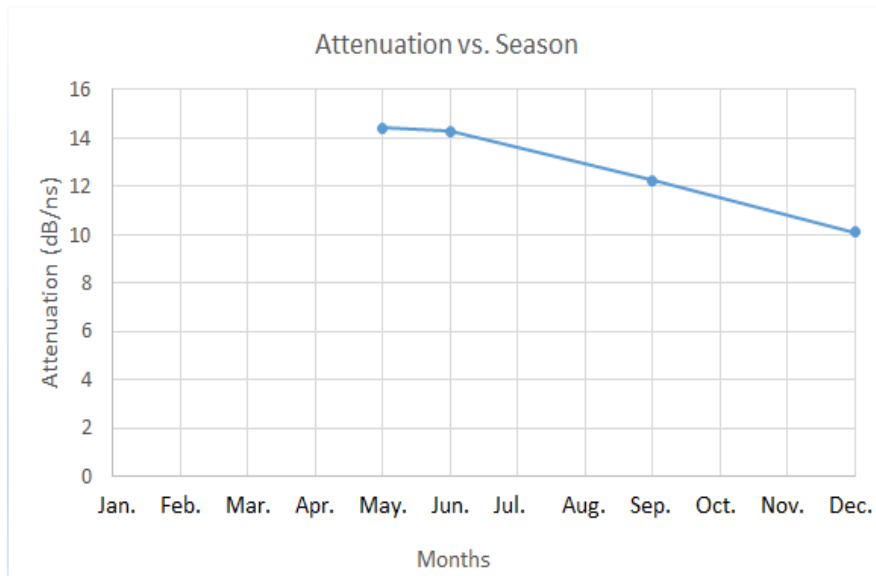**Fig. 5.15 Relationship between concrete moisture and conductivity.**

Fig. 5.16 Relationship between season and concrete conductivity.

5.2.1.3 Rebar Reflection Mapping Normalized by Direct-Coupling Amplitude

Direct-coupling normalization is the normalization method where the first (direct-coupling) reflection amplitude, in decibel, is subtracted from those of top rebar reflection. It is noted that, due to the effect of surface reflection portion, although this first reflection amplitude in radar waveform may not be constant, it still provides invaluable information regarding transmit power and therefore can be used for normalizing attenuation at top rebar. This idea can be illustrated in Fig. 5.17 where a MATLAB program was written to extract direct-coupling reflection amplitude of all A-scans and plotted as a contour map for each data set. Based on the main color, i.e., the color with highest percentage, in each contour map in Fig. 5.17 and the gain values in Table 4-1, difference in equipment transmit power can be approximated from direct-coupling amplitude without gain, as explained in Table 5-7. As can be seen, while the

equipment used to collect the first three data sets has the same transmit power, the one

used in September 2013 was about 8 dB lower.

(a) Direct-Coupling Reflection Map in May 2008

(b) Direct-Coupling Reflection Map in June 2012

(c) Direct-Coupling Reflection Map in December 2012

(d) Direct-Coupling Reflection Map in September 2013
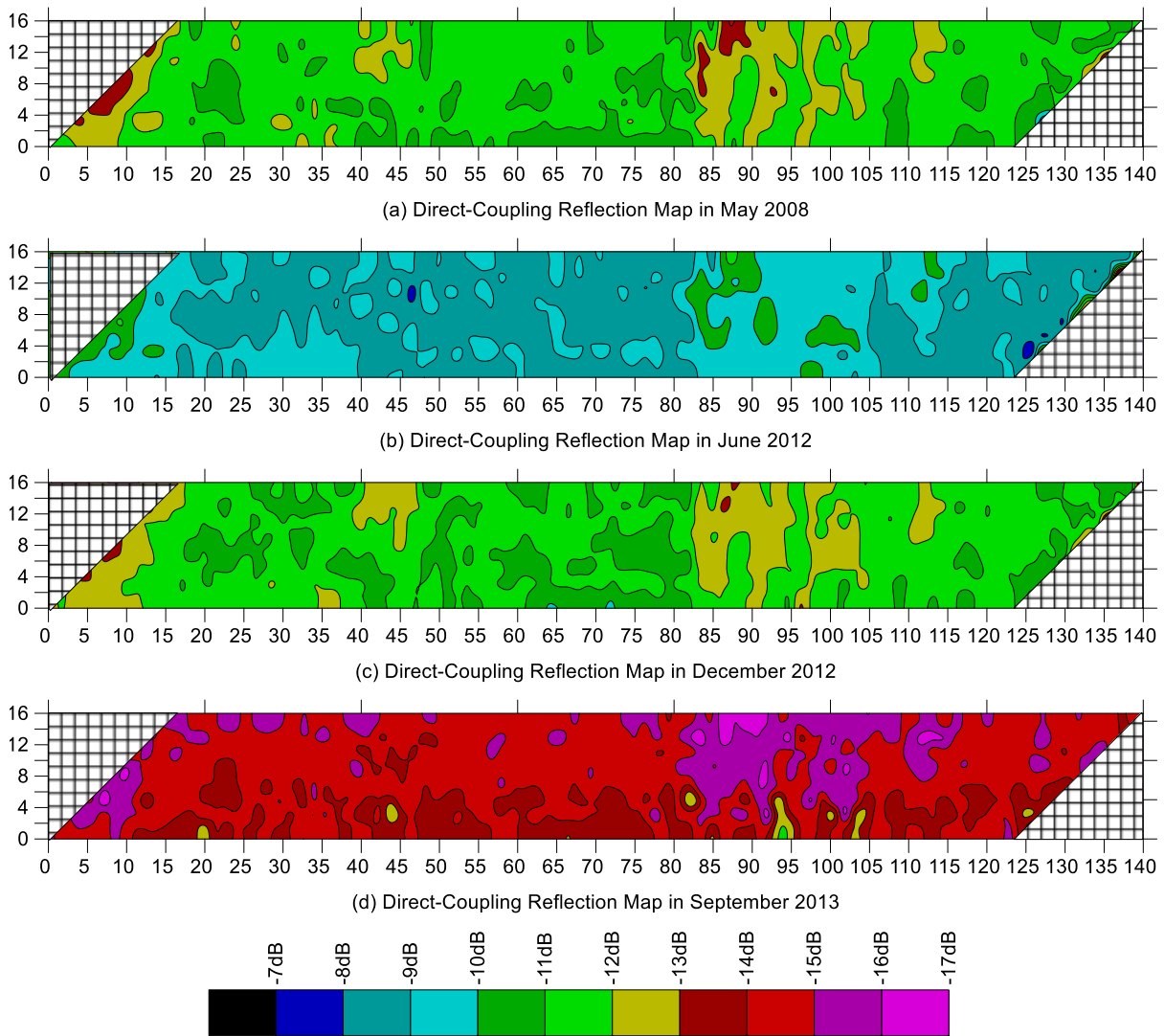
Fig. 5.17 Direct-coupling reflection maps of four data sets.

Table 5-7 Difference in transmit power approximated from direct-coupling amplitude.

Information	May. 2008	Jun. 2012	Dec. 2012	Sep. 2013
(1). Direct-coupling amplitude (dB)	-12	-9	-12	-15
(2). Gain value (dB)	-5	-2	-5	0
(3). Direct-coupling amplitude if no gain was applied (dB) = (1) - (2)	-7	-7	-7	-15

With the formula in Equation 5.1, the information in Table 5-7 can be used to adjust contour maps previously obtained in Fig. 5.11 for comparison purpose. Specifically, for each data set, direct-coupling reflection amplitude measured in decibel will be subtracted from rebar reflection amplitude. The adjusted contour maps from this process are shown in Fig. 5.18. This time, completely opposite to what was expected, it appears from all the maps that the deck condition continuously improves over time.

$$NR = 20 \times log_{10} \frac{R}{D} \tag{5.1}$$

Where: NR = Normalized rebar reflection amplitude (dB).

R = Rebar reflection amplitude (data unit).

D = Direct-coupling reflection amplitude (data unit).

Since the above result cannot be accepted, one possible reason behind this nonsensical phenomenon has been hypothesized, i.e., effect of conductivity change as discussed previously. Specifically, reduction in concrete conductivity would result in less signal attenuation in concrete cover and therefore may cause apparent improvement. With the conductivity data for each data set obtained previously, this hypothesis can be tested easily when the amplitude to plot contour maps in Fig. 5.18 are further normalized for conductivity. For example, to conductivity-normalize the amplitude of a rebar in May 2008 data set, this amplitude will be added a value equal to 14.423 (dB/ns), slope of the fitting line, multiplying with 2-way travel time (ns) at that rebar. The attenuation maps obtained from this conductivity normalization process are provided in Fig. 5.19. As can be seen, the result is still not acceptable when it shows improvement from May 2008 to

June 2012, deterioration between then and December 2012, and improvement again for

the map in September 2013.

(a) Attenuation map in May 2008 with direct-coupling normalization

(b) Attenuation map in June 2012 with direct-coupling normalization

(c) Attenuation map in December 2012 with direct-coupling normalization

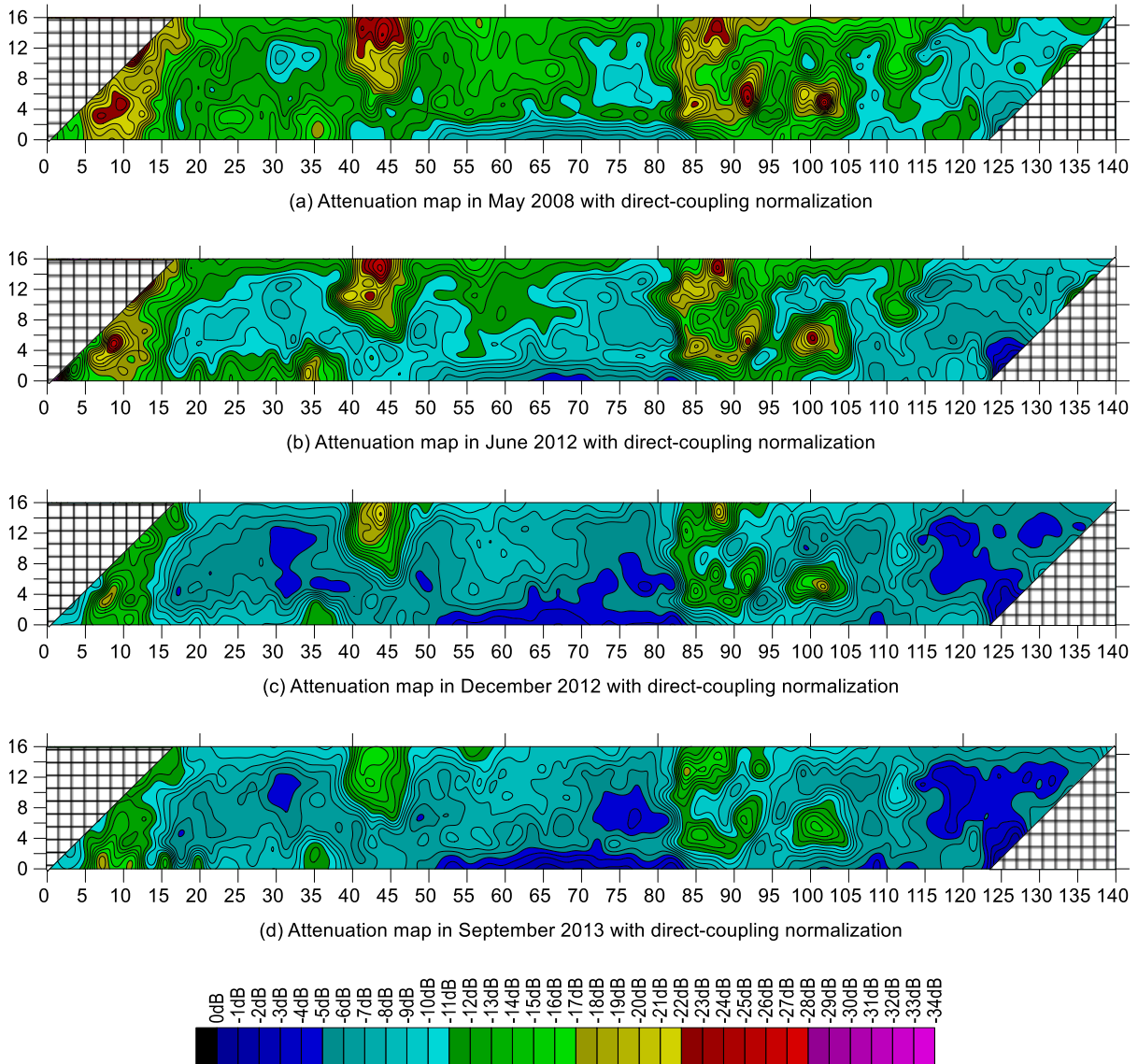(d) Attenuation map in September 2013 with direct-coupling normalization

Fig. 5.18 Attenuation maps of four data sets with direct-coupling normalization.
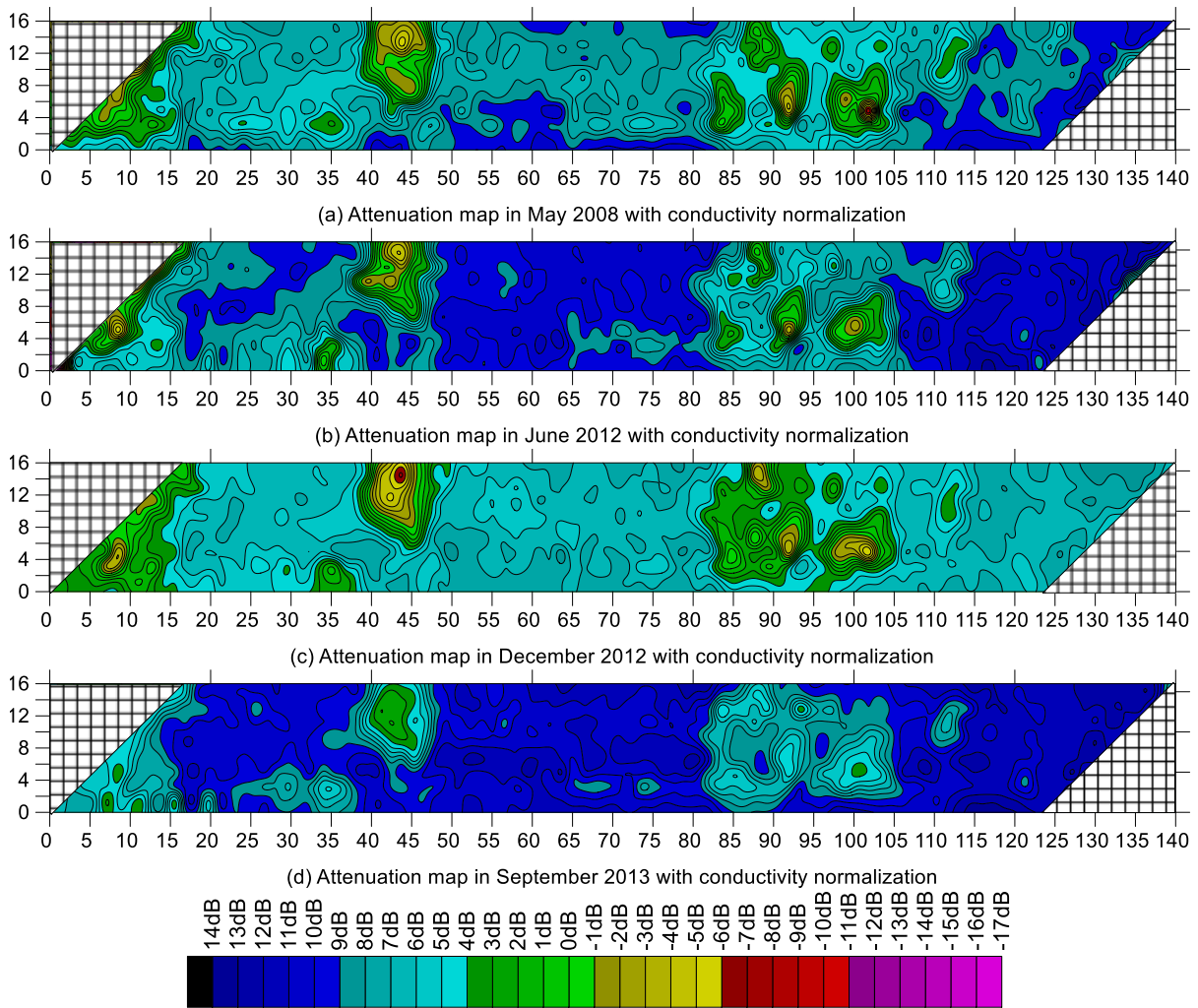
Fig. 5.19 Attenuation maps of four data sets with conductivity normalization.

5.2.1.4 Rebar Reflection Mapping without Migration

Although being a commonly used processing technique for GPR, migration was identified in this research as another possible cause behind the failure of all previous interpretation. The reason is that the migration process distorts GPR waveforms, therefore original reflection amplitudes cannot be obtained. With that possibility, while all other processing steps are the same as before, this time, the rebars were picked directly on cut profiles as shown in Fig. 5.20. The obtained attenuation maps with depth

correction, direct-coupling, and conductivity normalization are shown in Fig. 5.21, Fig. 5.22, and Fig. 5.23 respectively.
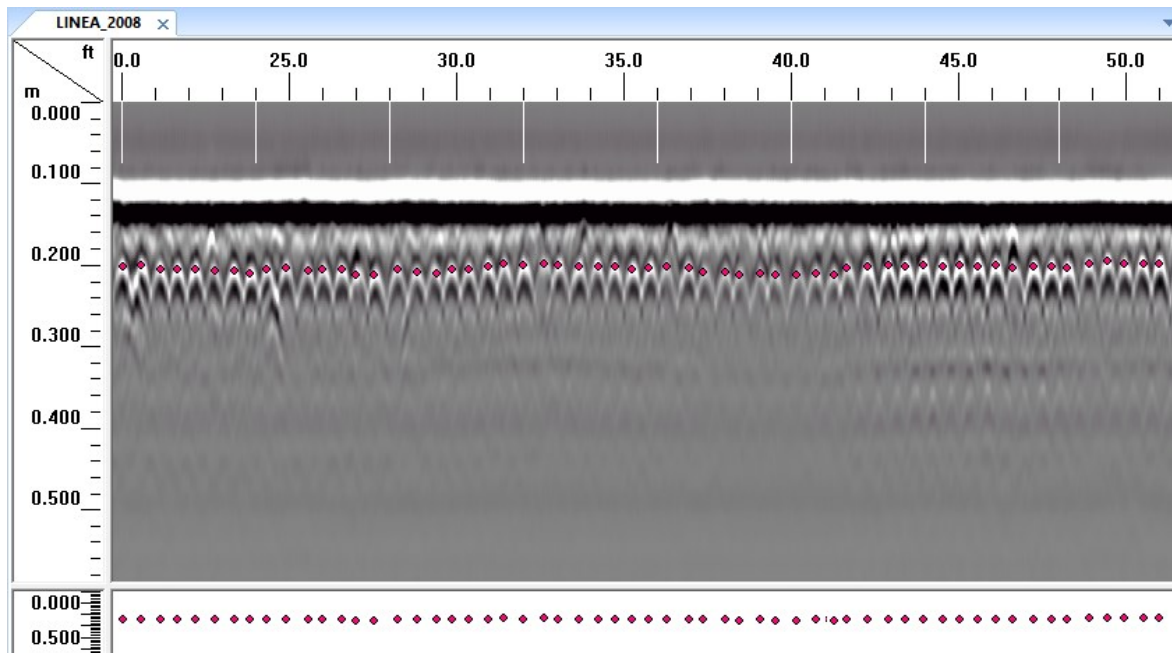
Fig. 5.20 Rebar picking for unmigrated data processing.

As can be seen from Fig. 5.13, Fig. 5.18, Fig. 5.19, Fig. 5.21, Fig. 5.22 and Fig. 5.23, with all normalization techniques, the attenuation maps in September 2013 always appear to be of best condition among the other data sets. Possible reasons for this may be the fact that (1) the 2013 data was collected by different machine, although the same system model and (2) it was collected after longest period of dry and hot weather as shown in Table 4-2.

(a) Unmigrated attenuation map in May 2008 with depth-correction

(b) Unmigrated attenuation map in June 2012 with depth-correction

(c) Unmigrated attenuation map in December 2012 with depth-correction

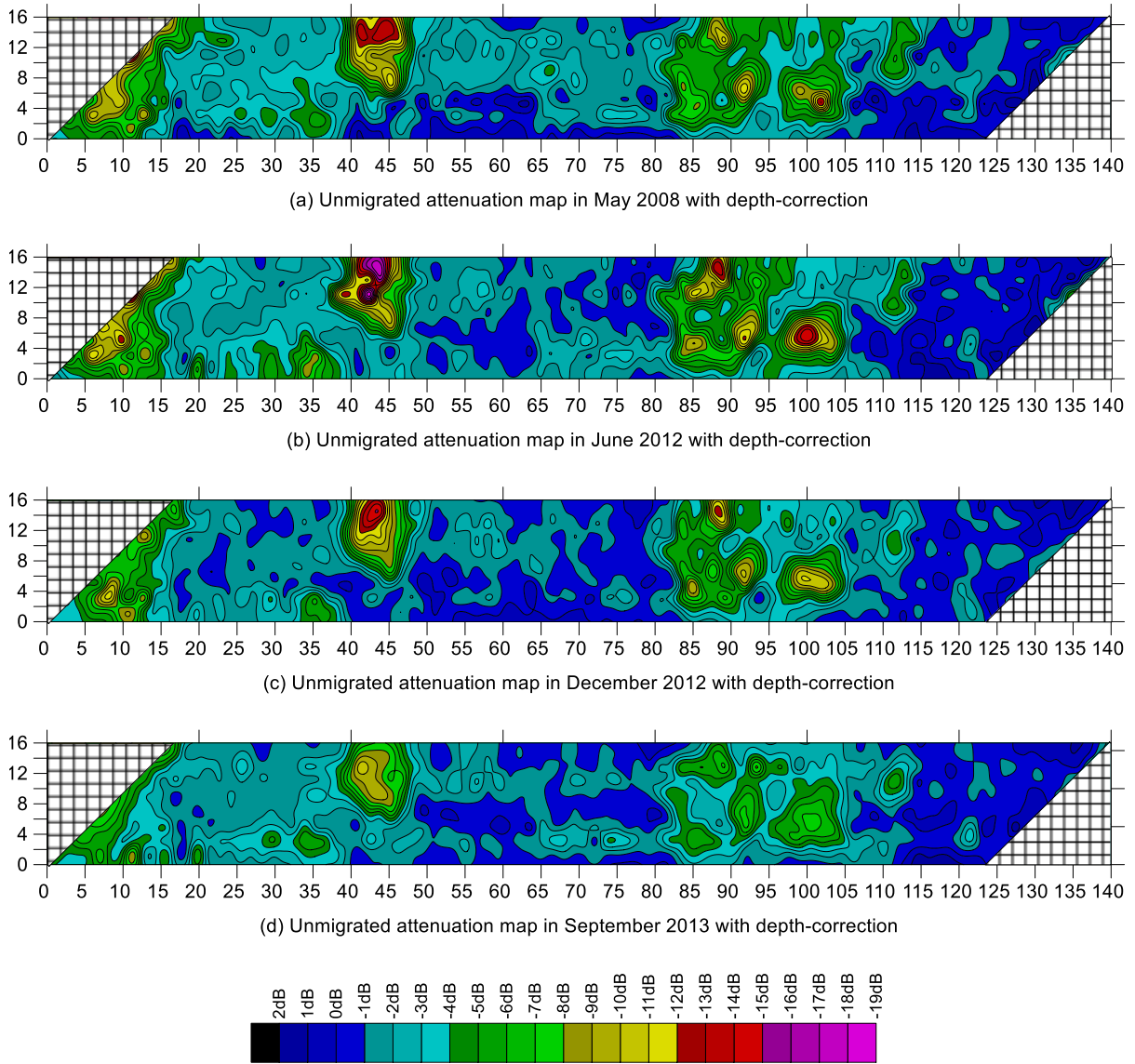(d) Unmigrated attenuation map in September 2013 with depth-correction

Fig. 5.21 Unmigrated attenuation maps of four data sets with depth-correction.

(a) Unmigrated attenuation map in May 2008 with direct-coupling normalization
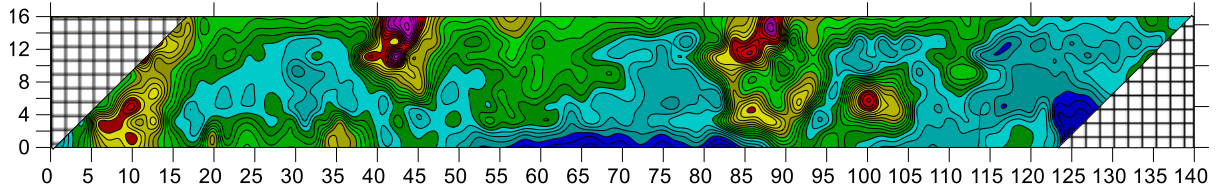
(b) Unmigrated attenuation map in June 2012 with direct-coupling normalization
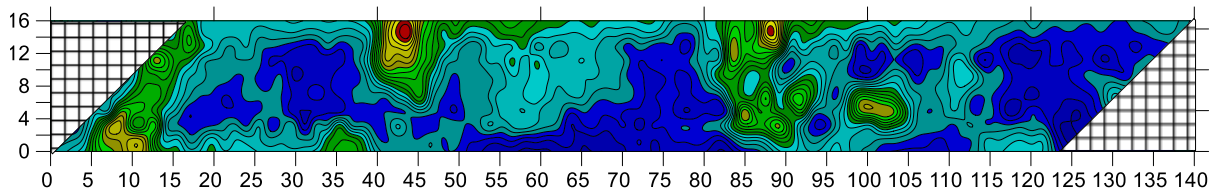
(c) Unmigrated attenuation map in December 2012 with direct-coupling normalization

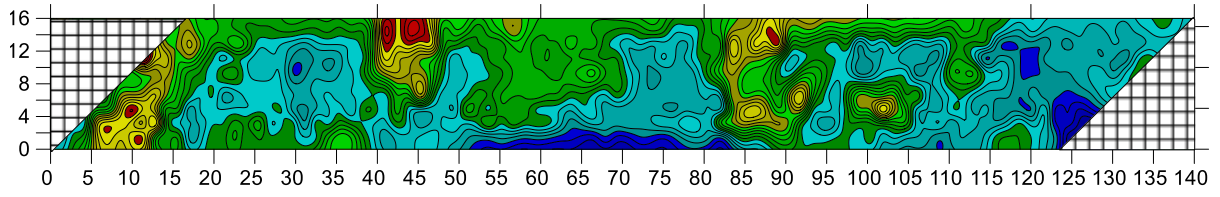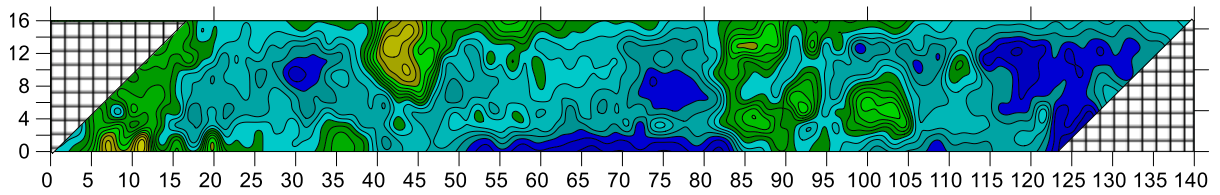(d) Unmigrated attenuation map in September 2013 with direct-coupling normalization
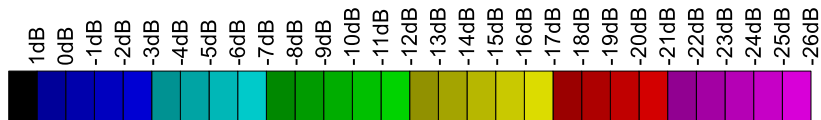
Fig. 5.22 Unmigrated attenuation maps of four data sets with direct-coupling normalization.

(a) Unmigrated attenuation map in May 2008 with conductivity normalization

(b) Unmigrated attenuation map in June 2012 with conductivity normalization

(c) Unmigrated attenuation map in December 2012 with conductivity normalization

(d) Unmigrated attenuation map in September 2013 with conductivity normalization
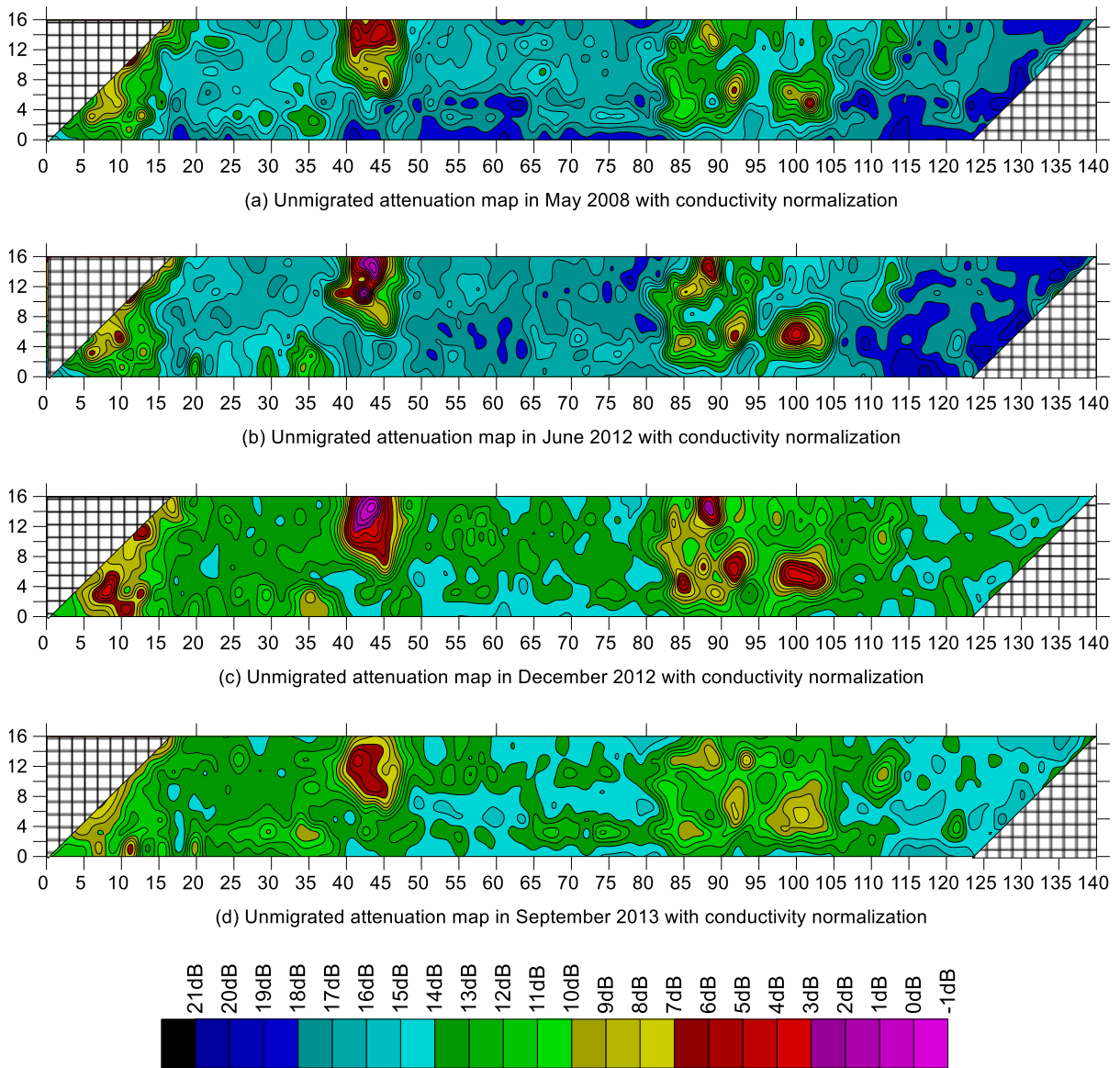
Fig. 5.23 Unmigrated attenuation maps for four data sets with conductivity normalization.

5.2.2 Implementation of Clustering-based Threshold Model

In addition to illogical improvement of the deck condition suggested by amplitude analysis, as previously mentioned, another problem exists with the maps in Fig. 5.13, regarding threshold value. In this section, based on time-series data in the case study, the threshold calibration method proposed in this research will be validated against the

model developed by Martino et al. (2014). The validation is done by comparing corrosion area estimated by each method.

5.2.2.1 Corrosion areas based on Martino et al. (2014) model

The percentage of corrosion area based on Martino et al. (2014) was calculated for each data set using the formula in Equation 5.2. The results are summarized in Table 5-8.

$$Corroded\ Percentage = 14.813762 \times (Skew \times Mean) - 0.016987 \quad (5.2)$$

It is noted that in Table 5-8, in line with apparent improvement that has been seen from previous analysis of amplitude data, the percentage of corroded area is smallest for the data set in September 2013. As can be seen, the illogical reduction of corroded area is approximately 25% between June 2012 and September 2013.

Table 5-8 Corrosion area based on Martino et al. (2014) model

Data Set	May. 2008	Jun. 2012	Dec. 2012	Sep. 2013
Percentage of corroded area (%)	59.61	79.25	64.89	54.58

5.2.2.2 Corrosion areas based on K-means clustering technique

In order to find the thresholds for each data set using the proposed method, first, bridge deck age along with all GPR profiles are thoroughly examined. For the deck in the case study, although it appears to be in good condition as shown in Fig. 4.1, with more than 30 years in service, it is reasonable to predict certain rebar corrosion has initiated in the concrete. This assumption is then checked by visual analysis of GPR profiles as illustrated in Fig. 5.24. As can be seen, though expert analysts can easily realize three levels of concrete deterioration, a problem arises with boundary determination when

130

there is no clearly-defined criteria for them to do so. However, with the proposed method, only the number of condition categories, i.e., 3, would be used for automatically grouping amplitude data. While the thresholds and area percentages of each condition category based on K-means clustering results are shown in Fig. 5.25, the condition maps for four data sets based on these thresholds are shown in Fig. 5.26.
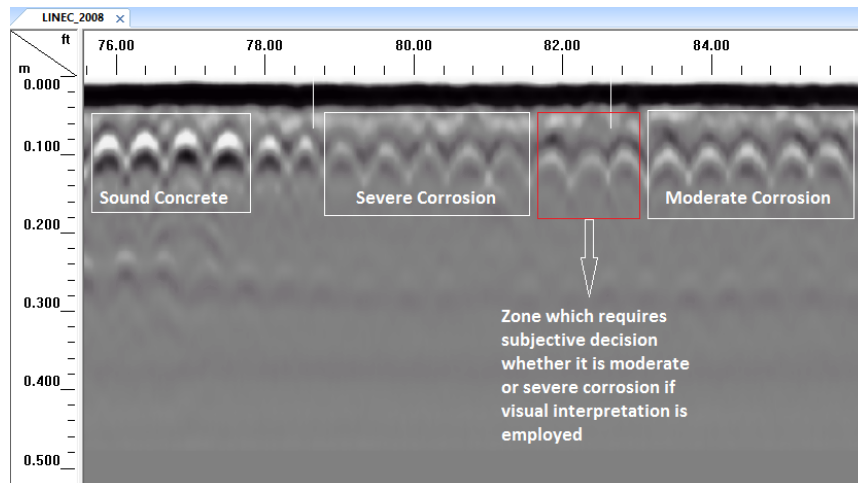
Fig. 5.24 Visual interpretation of GPR data

As can be seen from Fig. 5.25, also sharing some fluctuation in the percentage numbers of each condition category over time as the result obtained from Martino et al. (2014) model, however the proposed method provides much more stable results. Specifically, although mistakenly suggesting condition improvement for the two data sets in year 2012, the moderate corrosion (yellow) and severe corrosion (red) areas delineated by the method in Fig. 5.26 stay quite stable over a short five-year period of study. As another source of validation, the maps in Fig. 5.26 also correlate perfectly with the map provided by GPR expert analyst in Fig. 5.27 where the threshold values were subjectively selected. In addition, the GPR result is further validated when it shows

good correlation with concrete resistivity test result in Fig. 5.28. The two maps was developed by Center for Advanced Infrastructure and Transportation (CAIT), Rutgers University in year 2012.
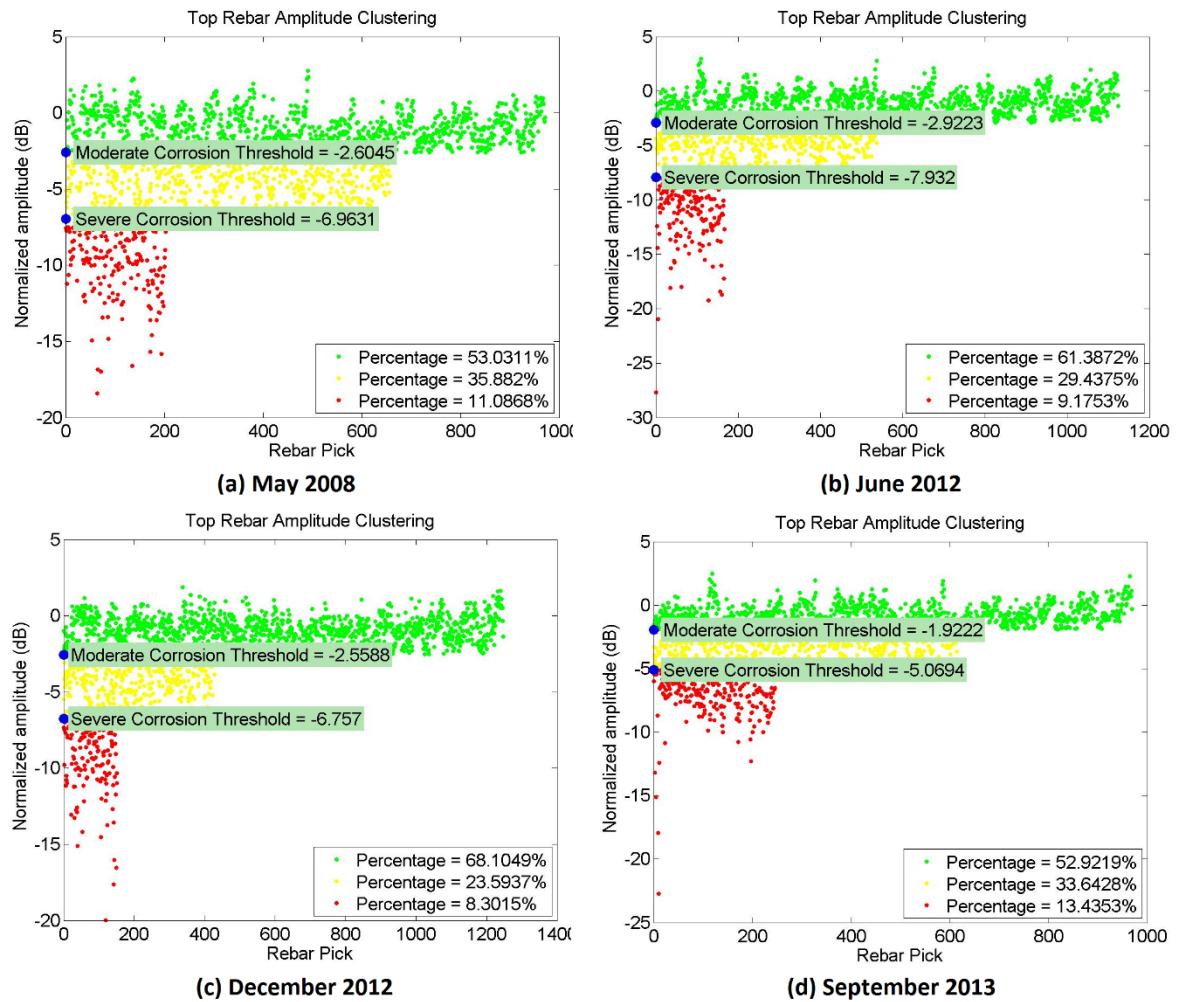
Fig. 5.25 Amplitude clustering for four data sets
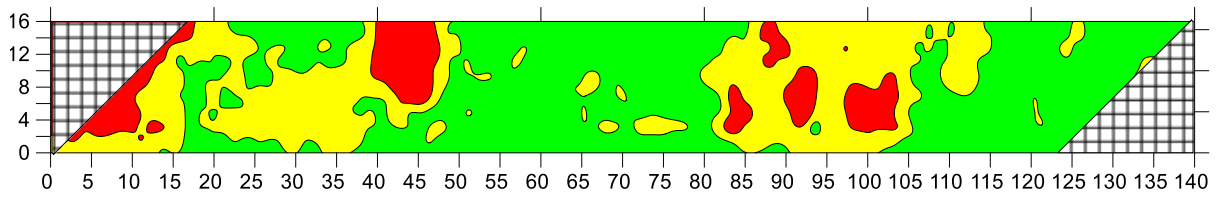
(a) Deterioration map in May 2008

-2.6dB -6.96dB -28dB
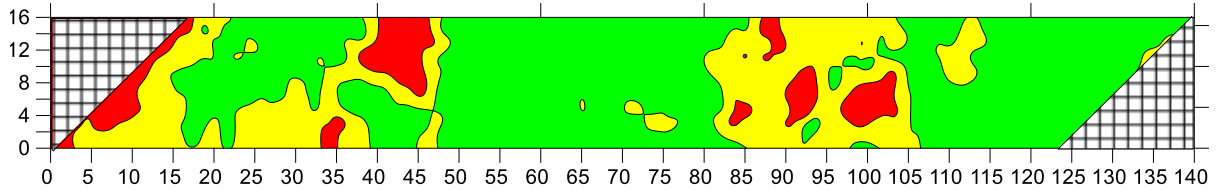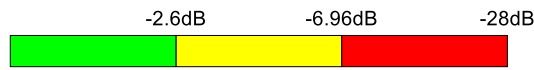
(b) Deterioration map in June 2012

-2.92dB -7.93dB -28dB
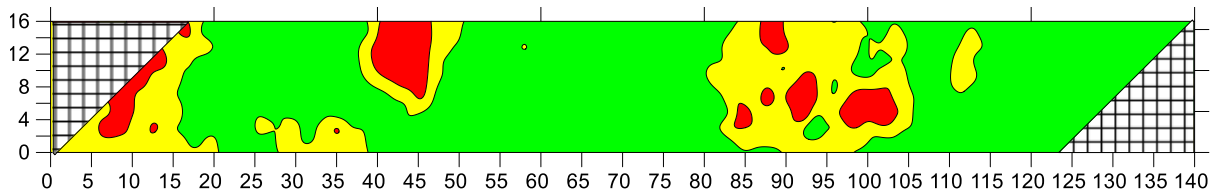
(c) Deterioration map in December 2012

-2.56dB -6.76dB -28dB
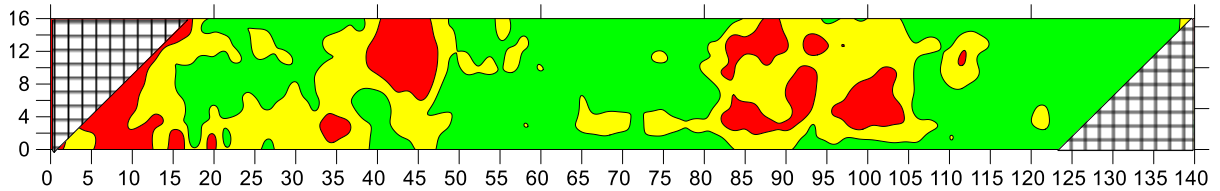
(d) Deterioration map in September 2013

-1.92dB -5.07dB -28dB

Fig. 5.26 Deterioration maps of four data sets based on threshold calibration
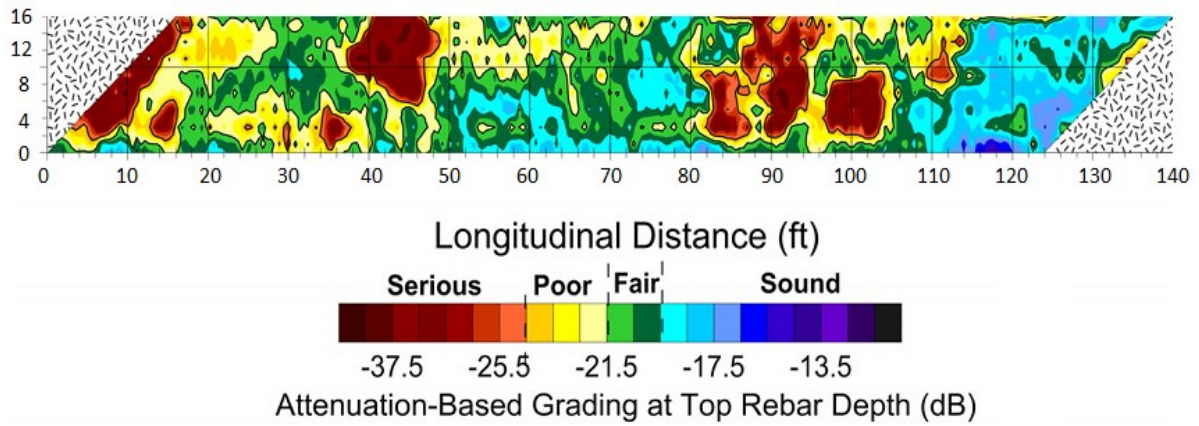
Fig. 5.27 GPR Condition map based on subjective selection of threshold values (La et al. 2013)
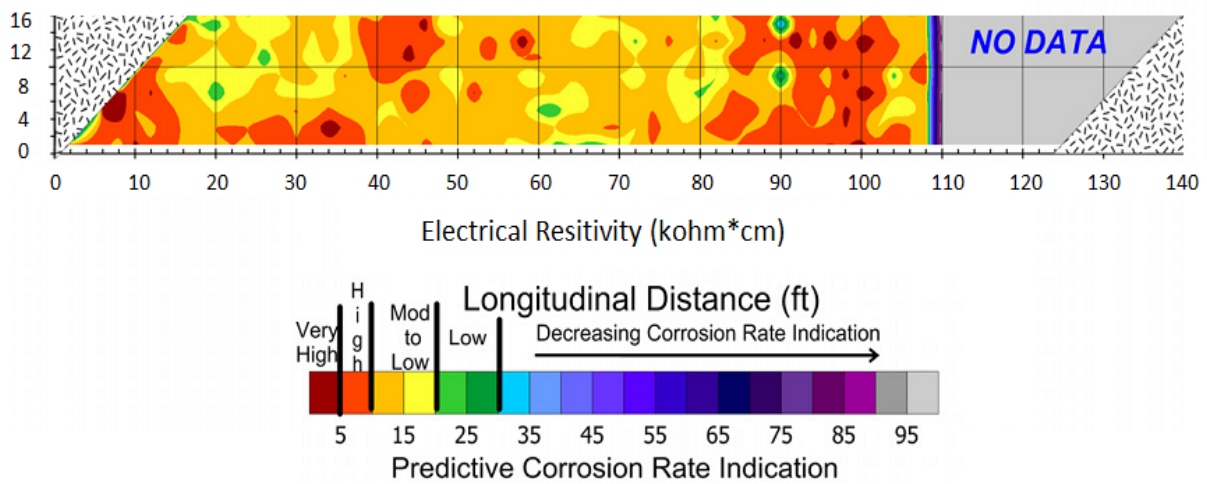
Fig. 5.28 Concrete resistivity test result (La et al. 2013)

5.2.3 Implementation of Correlation Analysis

In this section, the case study is used to illustrate the implementation of the proposed methodology based on correlation analysis. Since the ideal data set when the deck was new is not available, the one in 2008 is used as the baseline. So, the question that the correlation model developed in this study would be able to answer is how much change has happened on the deck and which regions tend to deteriorate more or less during

2008-2013 time period. It is noted that although the four data sets were collected at the same surveying lines using the same GPR system as described before, some difference in the scan setting did introduce some discrepancies in the initial data sets before processing. However, with the capability of RADAN software to apply similar post-processing parameters to these data sets, the differences have been minimized. Detailed problem and data processing are described below.

As explained in the methodology, the first and maybe the most difficult step to implement the proposed methodology is to make sure that two profiles of the two datasets for the same scan line should begin and end at the same location. In addition, in order to compare A-scans, the two profiles should have the same number of scans per unit length. These requirements are not readily met from the data collection as illustrated in Fig. 5.29. As can be seen in Fig. 5.29(a) and 5.29(b), two profiles were collected using different number of scans per unit length and they did not start at the same location or at the deck joint. However, using available functions in the RADAN software such as "distance normalization" to adjust varying data to a constant scans per unit length and "edit block" to cut profiles so that unwanted data from approach ramps and expansion joints at abutments are not included as reinforced concrete deck, the two profiles can be processed to match exactly location and number of scans as shown in Fig. 5.29(c) and 5.29(d). It is noted that some condition changes between 2008 and 2013 data sets can be visually observed from these two processed profiles.

(a) Unprocessed profile 2008

(c) Processed profile 2008

(b) Unprocessed profile 2013

(d) Processed profile 2013
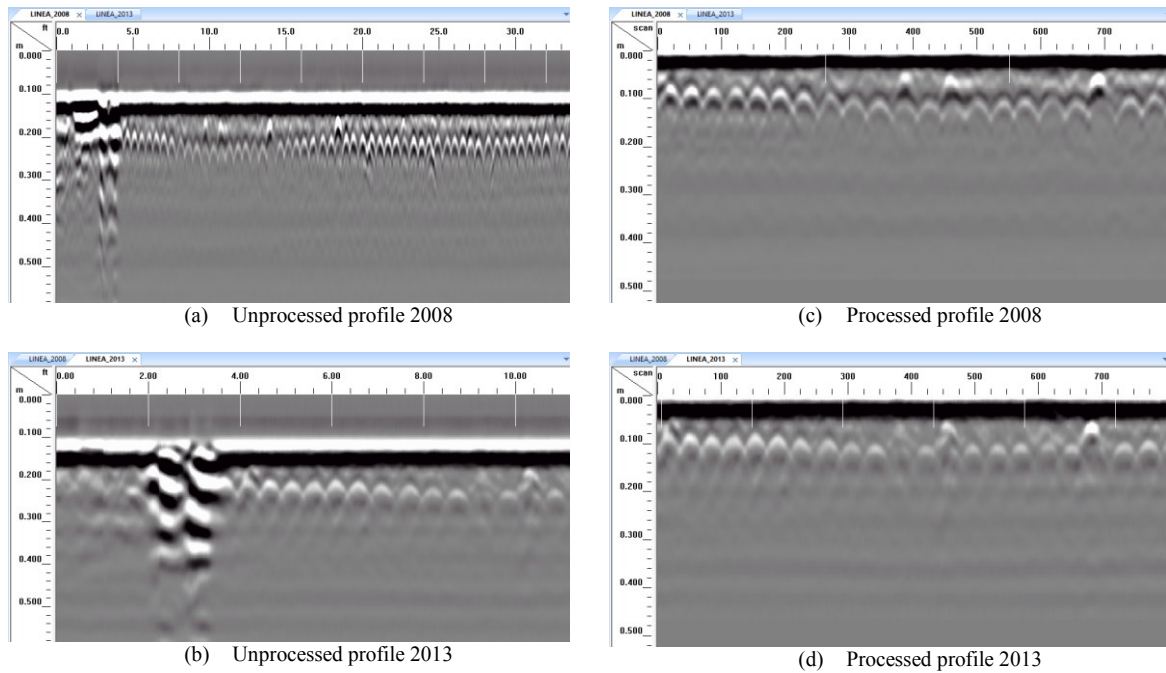
Fig. 5.29 Example of processing for two data sets

In the second step, the processed RADAN files are converted to ASCII format. These ASCII files are then read by a MATLAB program developed in this research to compute correlation coefficient and assign coordinate for each A-scan location. The output of the MATLAB program is also an ASCII file which contains information on coordinate of each A-scan couple and their corresponding correlation coefficient. This file is then read by Surfer®, a graphing and mapping software, and a contour map is produced. The final output of the proposed model is correlation coefficient maps presented in Fig. 5.30.

The map in Fig. 5.30 only shows relative deterioration between two consecutive scans. It is noted that since five years of time separation is not long enough in comparison to the average life of a bridge deck, the shapes of the contour lines in Fig. 5.30 change mainly because of random factors such as survey positioning error, signal noise, different equipment used, equipment instability, etc. In other words, in this case, random

136

error part contributes to the variation of correlation coefficient rather than slight concrete deterioration caused by five-year study period. However, the overall deterioration progression can still be confirmed with the reduction of average correlation coefficient of each data set over time. These indices were calculated and shown in Table 5-9. In addition, if the thresholds in Table 5-1 are employed, it can be said that almost the entire deck has undergone deterioration. This conclusion is illustrated in Fig. 5.31, Fig. 5.32, and Fig. 5.33, respectively for three threshold values in Table 5-1. As noted before and can be seen clearly in the maps, when the threshold based on false-positive error decreases, the probability of false-negative error increases indicated by the increasing area of green region.

Table 5-9 Decrease of average correlation coefficient over time

Relative deterioration between	*May.2008 – Jun.2012*	*May.2008-Dec. 2012*	*May.2008-Sep. 2013*
Average correlation coefficient	0.957	0.946	0.891

5.2.4 Implementation of Bridge Deck Corrosiveness Index

This section illustrates the implementation of BDCI model to the New Jersey case study in which GPR results in Fig. 5.25 and Fig. 5.26 for four data sets are used. As can be seen, the obtained values show reasonable trend between May 2008 and September 2013, however it suggests condition improvement for June and December 2012 data sets. This problem, as explained in Chapter 4, caused by some unknown variables that affect interpretation of GPR amplitude data.

(a) Correlation map between May 2008 and June 2012

(b) Correlation map between May 2008 and December 2012

(c) Correlation map between May 2008 and September 2013
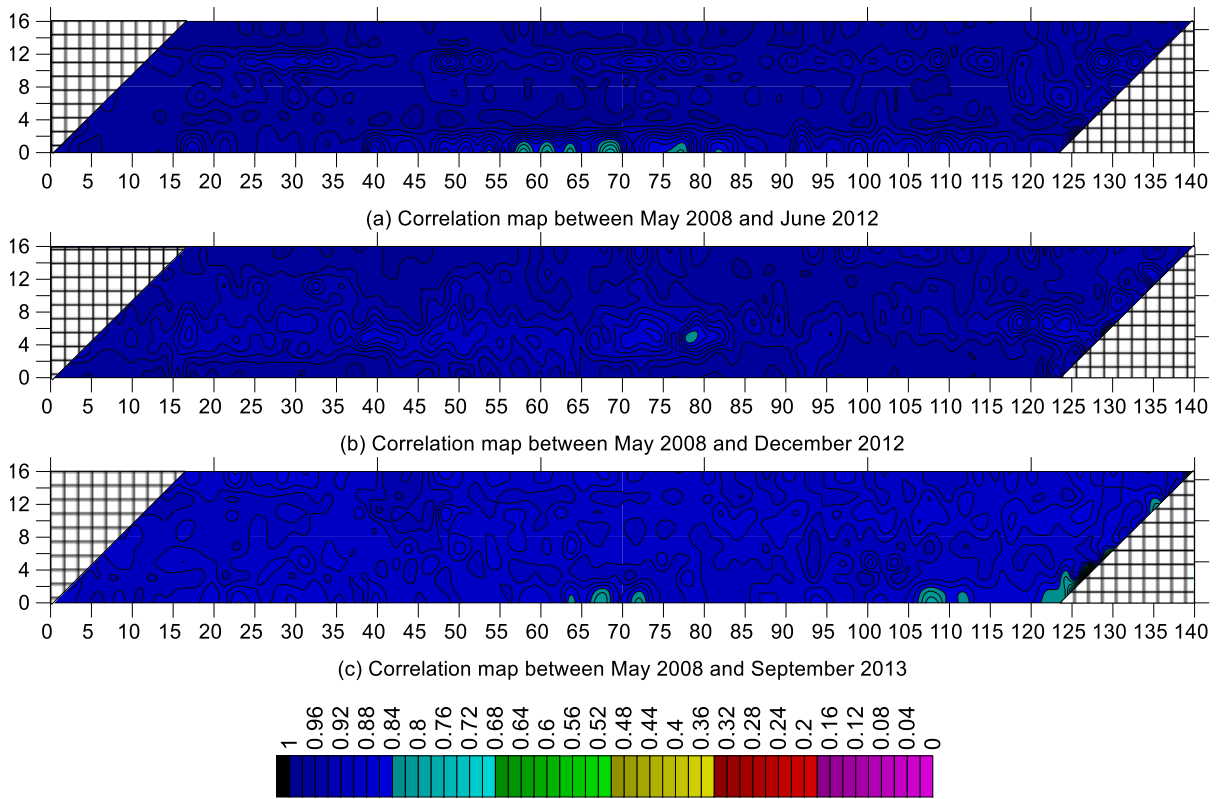
Fig. 5.30 Correlation coefficient maps

(a) Relative deterioration map between May 2008 and June 2012

(b) Relative deterioration map between May 2008 and December 2012

(c) Relative deterioration map between May 2008 and September 2013
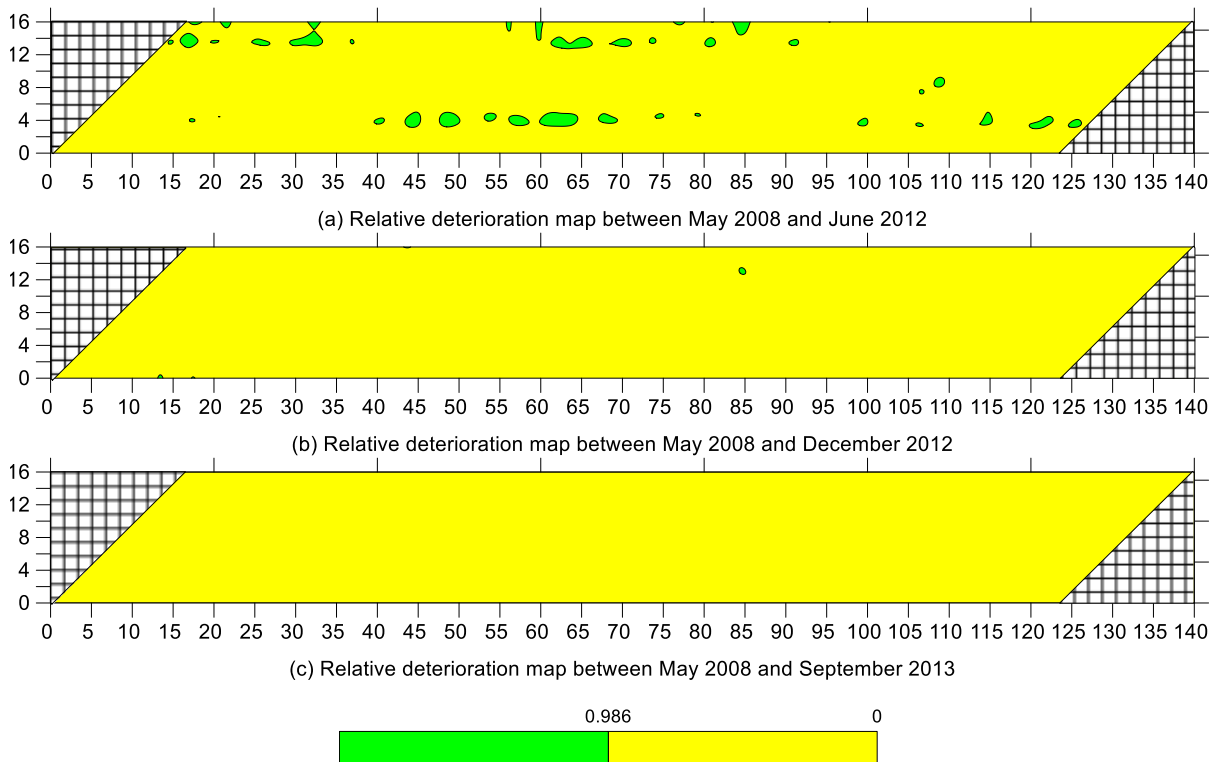
Fig. 5.31 Relative deterioration map with correlation threshold value of 0.986

(a) Relative deterioration map between May 2008 and June 2012

(b) Relative deterioration map between May 2008 and December 2012

(c) Relative deterioration map between May 2008 and September 2013

0.981   0
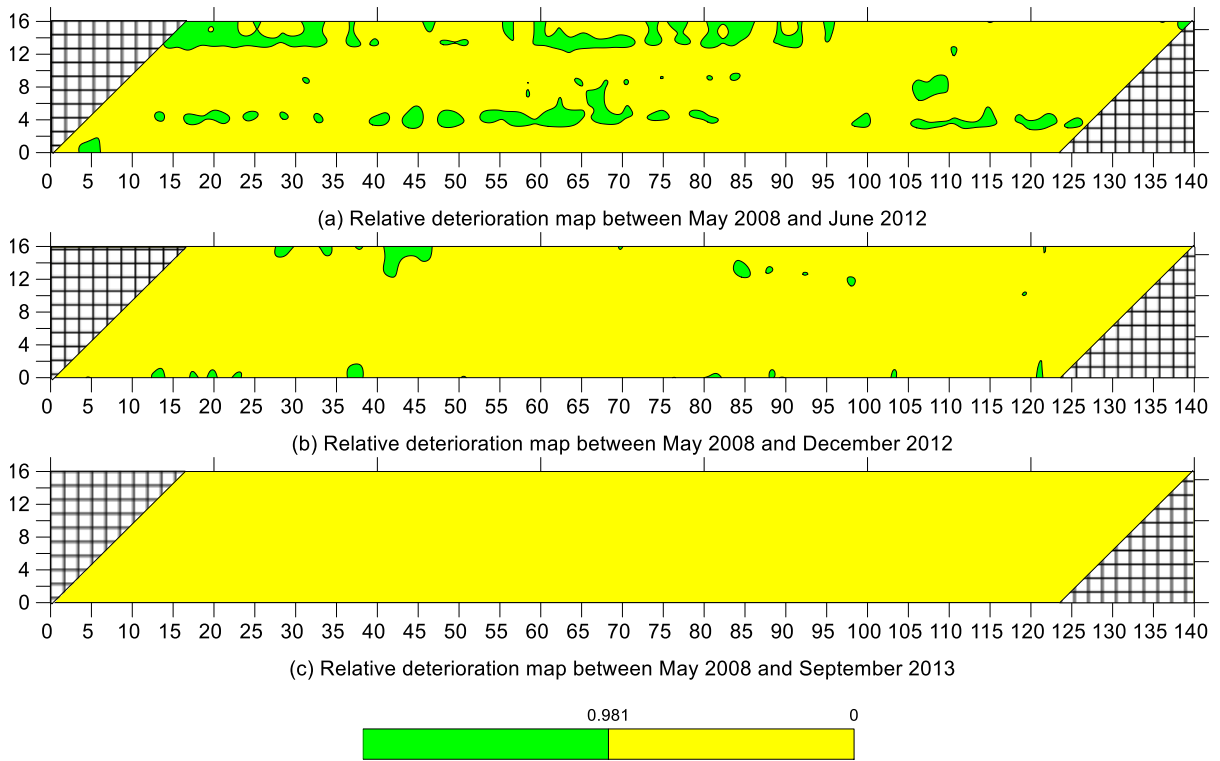
Fig. 5.32 Relative deterioration map with correlation threshold value of 0.981

(a) Relative deterioration map between May 2008 and June 2012

(b) Relative deterioration map between May 2008 and December 2012

(c) Relative deterioration map between May 2008 and September 2013

0.975   0
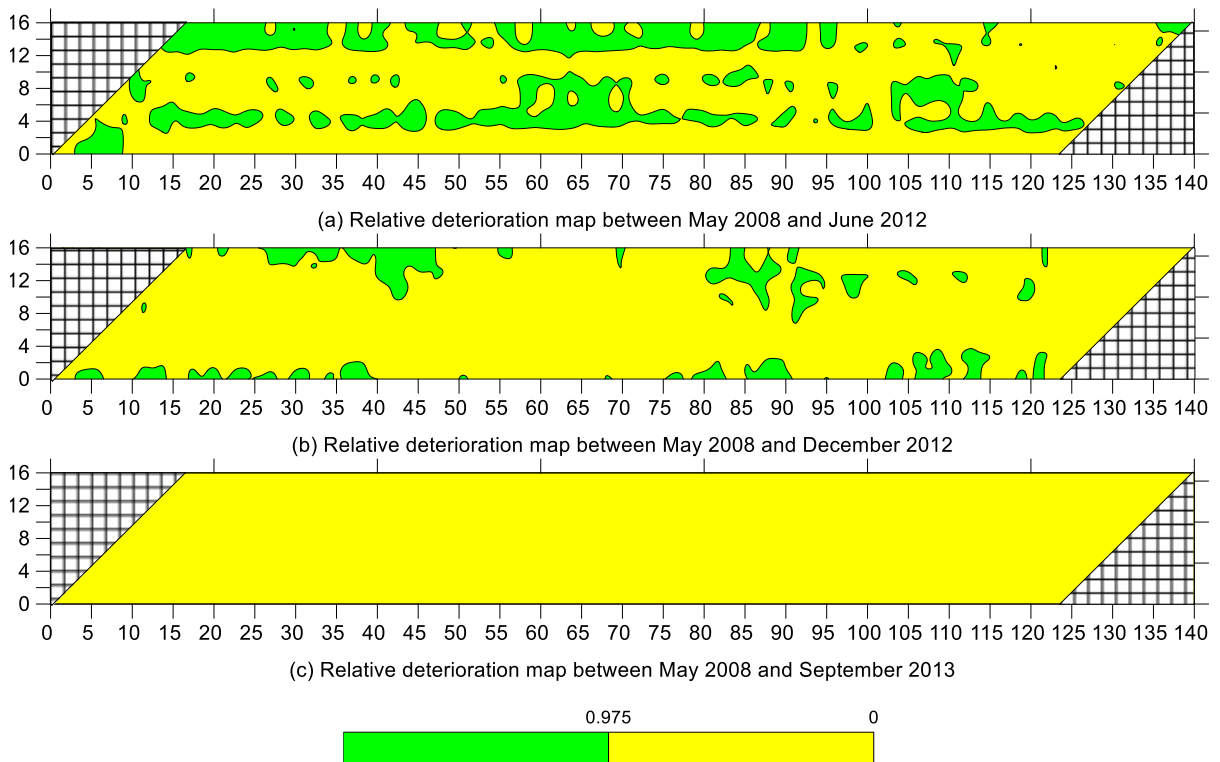
Fig. 5.33 Relative deterioration map with correlation threshold value of 0.975

Although showing some fluctuation, all BDCI values obtained in Fig. 5.34 suggest that the bridge deck is in category B of intervention need where it only expects GPR monitoring in the next 5-10 years. This outcome is reasonable, considering bridge appearance in Fig. 4.1 and concrete resistivity test result in Fig. 5.28.

(a) May 2008

(b) June 2012

(c) December 2012

(d) September 2013
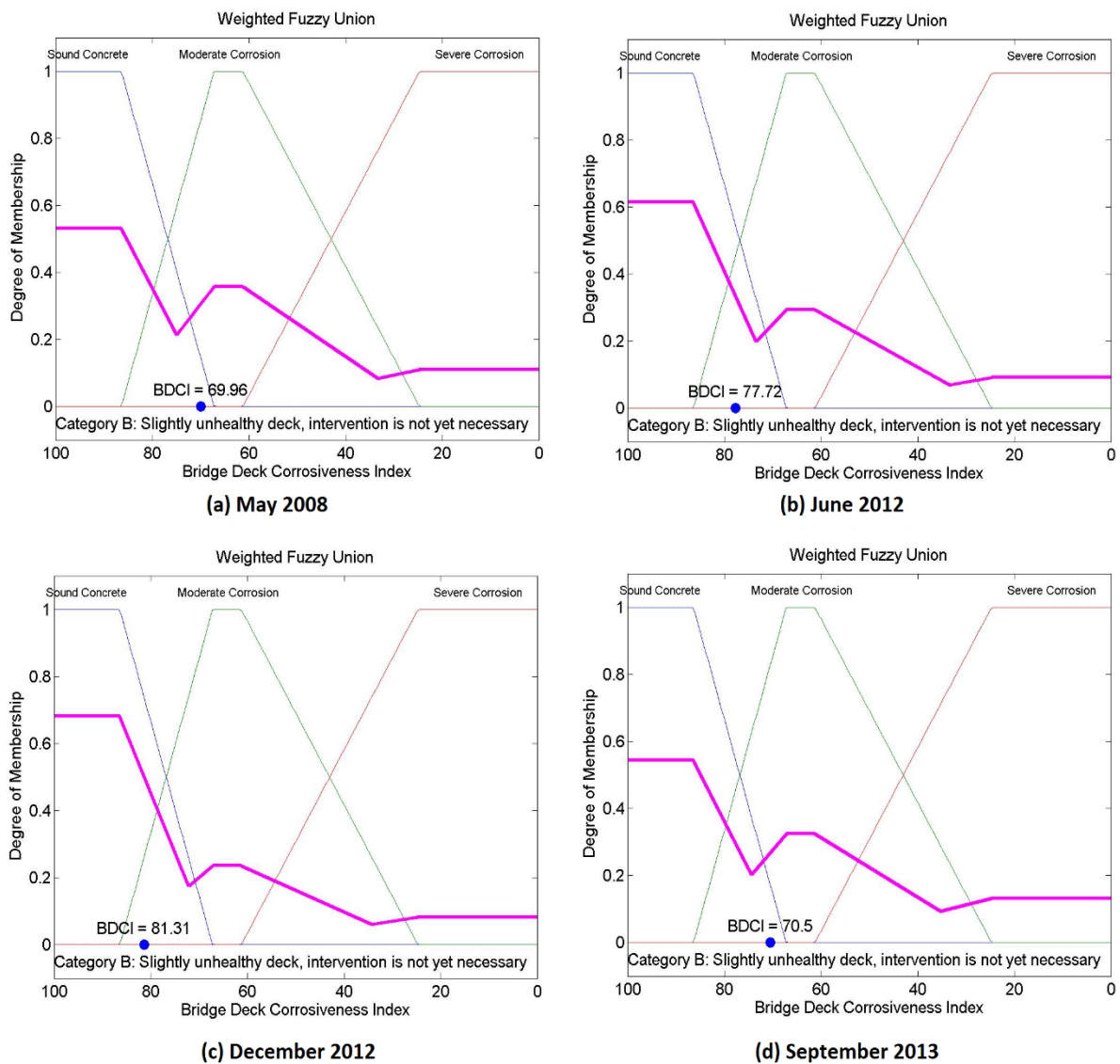
Fig. 5.34 BDCI calculation for four data sets

5.3 Discussion

The above case study clearly shows how the proposed models are implemented for a real concrete bridge deck. Regarding correlation analysis method, it can be implemented in a very short period of time with the capability to be automated by a computer-software. Specifically, using correlation method, the analyst does not need to pick the amplitude for each individual rebar, a time-consuming and tedious process. Instead, he or she just needs cut profiles in order to make sure the profiles of the two scans start and end at the same points and have the same number of scans. Furthermore, unlike the amplitude method, correlation analysis can naturally eliminate all amplitude anomalies due to rebar depth and rebar spacing variation, or those arising from structural and reinforcement layout. It can filter the defects associated with the deterioration process such as corrosion and delamination, without generating errors caused by real construction variations either designed or built into the deck. These same variations are what typically requires expert analysts to interactively interpret and/or quality assurance (QA) review manually-picked and processed rebar amplitude data. They are also the same structural features whose sudden and often unpredictable table signal features in GPR B-scan data cause automated rebar-picking programs to fail.

However, in order for the method to be added to current practice, a standard data collection procedure should be followed. First, all the data collection should use the same setting and equipment type, i.e., the same manufacturer, model and frequency. Some important settings of the system for the application of this method include gain,

range, filter, number of samples per scan, and number of scans per unit length. If one of these parameters was not set the same for time-series data, additional manipulation would be required in order to adjust the variance, and each data manipulation contributes to creating false differences between data that would not otherwise exist. A simple example has been shown in the case study when distance normalization was used because of difference in number of scans per unit length between two data sets. This function is employed in RADAN software in order to adjust varying data to a constant scans per unit length. It reduces or adds A-scans based on interpolation algorithm between adjacent waveforms. Ideally, adjustments like this should be minor, so setting the same scans per unit distance on each GPR data collection effort would be preferable to attaining equivalency via an interpolative method. Second, regarding scanning path positioning, these lines should be carefully set up at the first time, recorded and stored in the database in order to facilitate the retrieval of their location in the future. In the case study of this research, simple information recorded from previous data collection was used to locate previous scan lines. However, with the rapid advancement of modern technology such as real-time kinematic (RTK), differential global positioning system (GPS) along with the expected use of robotic data collection in the future (La et al. 2013), it is anticipated that positioning error between time-series data would be minimized. If that is the case, threshold value calibrated in this research would also need to be adjusted.

As has been seen in the amplitude analysis of the case study, weather and moisture condition are some other factors that may affect GPR signals and therefore performance

of the proposed method in this study. However, similar to positioning error, electromagnetic noise, or system instability; the effects of these factors can be taken into account in the future research with the new threshold calibration. Specifically, a longer time-frame with various weather condition will be used for calibration of the threshold. In current research, this time-frame was only one day.

Possessing the property of both amplitude and visual analysis, the basic idea behind correlation approach is very easy to understand. It predicts concrete deterioration based on any amplitude or shape change of the overall signal. The only drawback of the method is that it requires baseline data for implementation. Obviously, this will result in more inspection cost in the short-term associated with the first data collection. However, this cost is small for GPR since the time it take to scan an average deck is only several hours with one or two technician. Even if traffic control cost is taken into account for a bridge with high traffic volume, in comparison to a lot of time it will take to inspect the bridge in the future using time-consuming and expensive method such as half-cell potential, a few hours of baseline GPR data collection would still be a cost-saving option.

Separate from its use for future time-series condition assessment, other justifications exist for collecting baseline data. First, the data can be used for inspection of construction quality, i.e. voids, cracks, or other anomalies due to poor construction. In some state departments of transportation (DOTs), GPR use (1.5GHz resolution or higher) is specified for QA verification of concrete cover regarding its compliance with

construction specifications (Perkins et al. 2000). Furthermore, accurate knowledge about cover depth variation on new decks provides a basis for service life modeling based on chloride diffusion (Weyers 1998; Liu and Weyers 1998; Suwito and Xi 2003; Li 2003); though most models erroneously assume design cover or cover based on random sampling as representative of rebar depth throughout the deck. Hence, justifying multi-purpose use for the same initial, baseline GPR data makes economic sense from many perspectives.

Regarding apparent improvement of deck condition suggested by amplitude analysis method in the case study, the reason behind it is still not well understood in this research. In addition to some possible explanations those have been mentioned previously during the course of analysis such as weather, moisture, equipment, chloride or seasonal effect, there are still other unknown variables that caused the failure of all normalization methods employed in this research. While these variables should be investigated and taken into account in the future research for normalization, assessing concrete deterioration based on overall signal change is always a valid assumption.

Lastly, the inspection framework based on the correlation analysis of time-series data is considered as the main contribution of this study and should be added to practice in the long-term. However, since this framework requires baseline data that is not available for most bridge decks in service, the threshold calibration method based on K-means clustering is suggested as an alternative solution during transitional period. Consequently, the bridge deck corrosiveness index developed in this research is be

based on the GPR output provided by such alternative solution, though slight errors

associated with the method has been shown in the case study.

CHAPTER 6   AUTOMATED SOFTWARE

6.1 Prototype Software

All the methodology and analysis presented in previous chapters have been implemented through various programs written in MATLAB (**Mat**rix **Lab**oratory), a multi-paradigm numerical computing environment and high-level programming language developed by Mathworks. The problem with these programs is that they are hard-coded, meaning data values are written directly in MATLAB. In addition, even hard-coding issue is fixed and the programs obtain values from external sources or generated data, another problem would remain in which MATLAB will need to be installed on the computer running these programs.

In order to fix these issues and create a stand-alone application for the developed system, a software named *GPR-based Bridge Deck Condition Assessment System* (**GPR-BriDCAS**) has been coded in C#, a .NET programming language developed by Microsoft Corporation. This has been done easily with MATLAB Builder™ NE platform when it allows all MATLAB functions to be converted to .NET components those in turn can be embedded in .NET program. While detailed process for creating and using .NET components can be referred from Mathworks Inc. website, the main interface of the software when it starts is shown in Fig. 6.1.

As can be seen, on the very top left-hand side of the form in Fig. 6.1, there are two method options for the user to select, namely Correlation and Amplitude. These two

options correspond to the two methods proposed for analyzing bridge deck GPR data. Specifically, if the user wish to find progressive deterioration between two GPR scans, the "Correlation" radio button should be checked. Otherwise, if he/she wants to develop condition map based on top rebar amplitude, "Amplitude" radio button should be selected. While the link between various components of the software is depicted in Fig. 6.2, description for using them is provided in turn in the sections below.
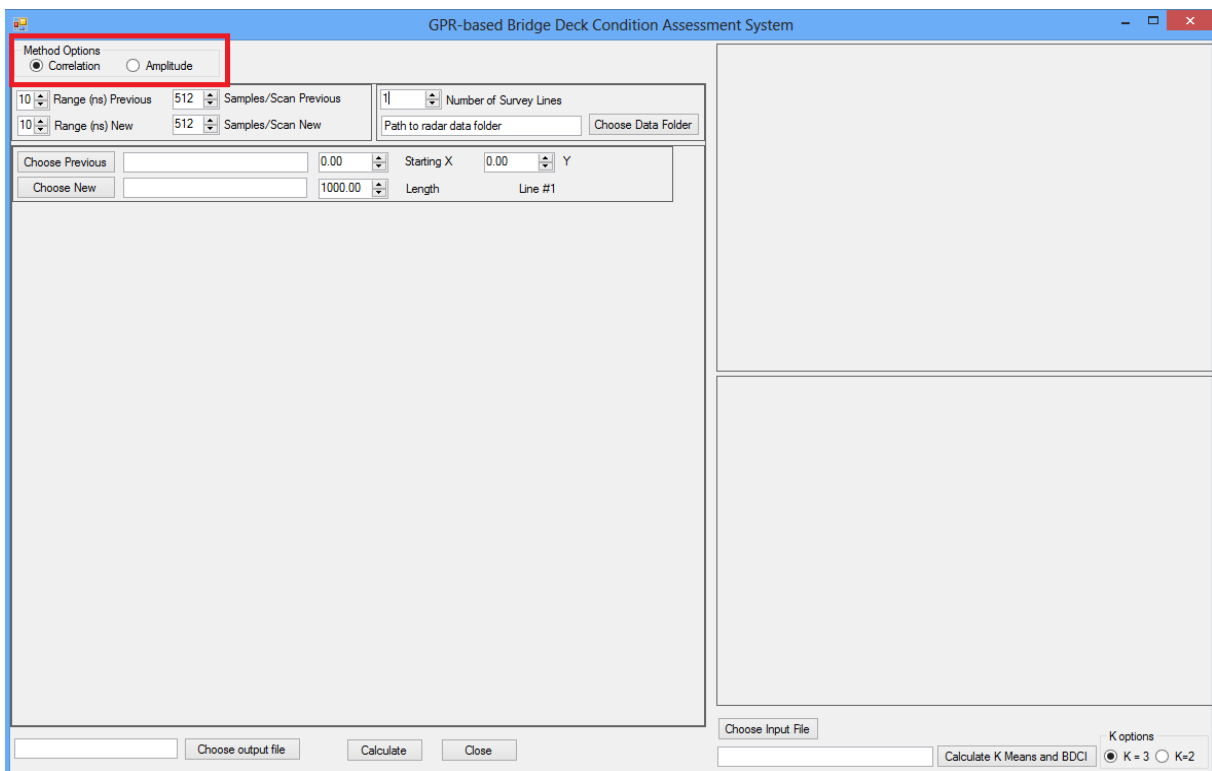
Fig. 6.1 Program Interface

6.1.1 Correlation Option

When "Correlation" method is chosen. In order to perform calculation, first, the user needs to input the information and data for the two scans. These information and data can be grouped into two categories: (1) General setting for each scan and (2) Data for

each survey line. While Fig. 6.3 shows two data categories and how to input the data in the form for the bridge deck with 8 survey lines, the needs for these information are briefly explained as follows.
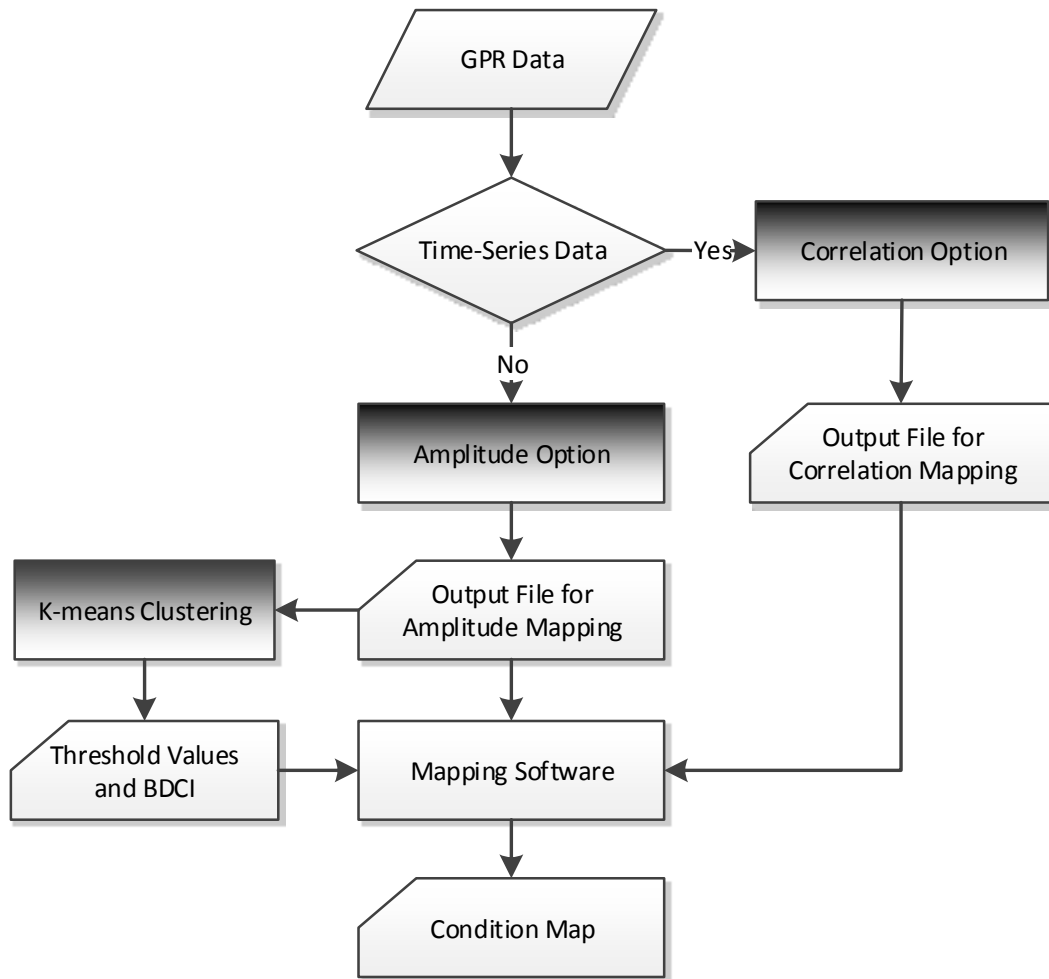
Fig. 6.2 Link between software components

General setting provides important information for each GPR dataset such as the number of survey lines used for the bridge deck in question, the range (time duration) in nano-second (ns) to record each GPR signal, and the number of samples digitized for each A-scan. Ideally, as suggested in Chapter 5, all of these settings should be fixed for all scan times, however, the software has been designed to adjust in case there is any

difference between these settings. In addition, since all GPR data for the same scan is usually put in the same directory, "Choose Data Folder" helps the user to locate the files more easily.
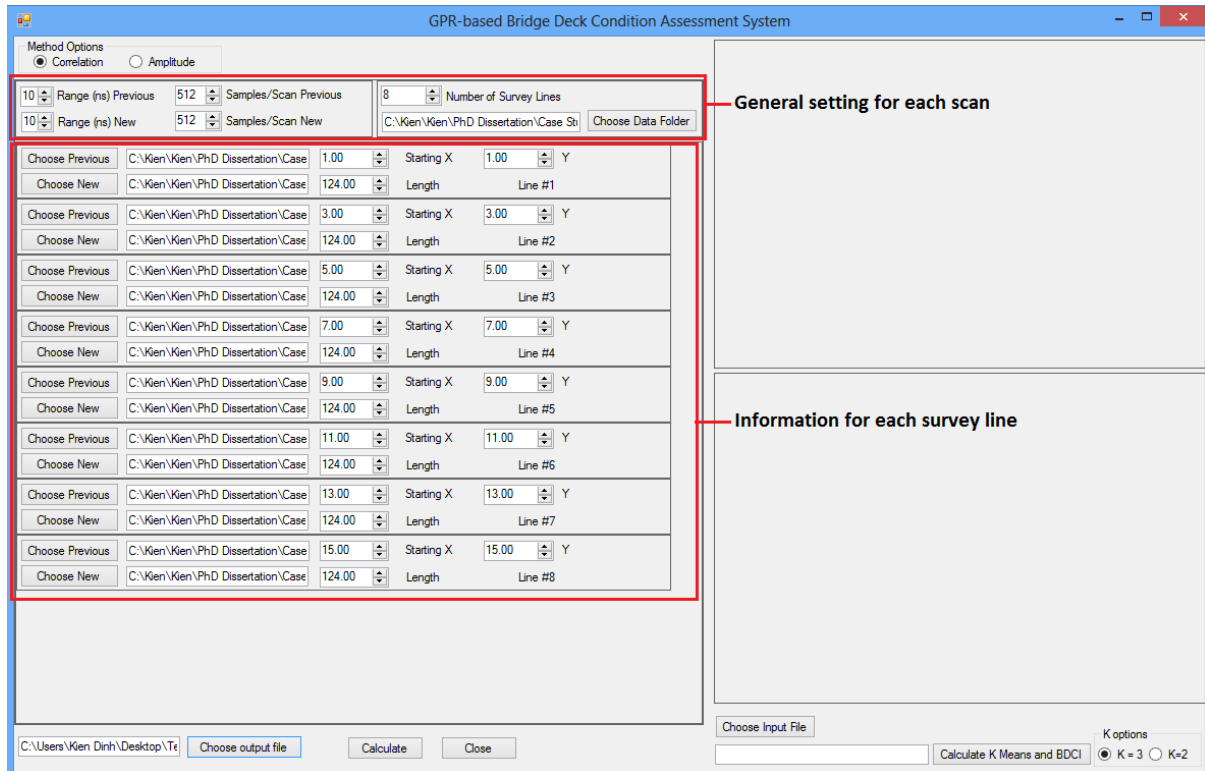
Fig. 6.3 Input for Correlation Method

For each survey line, in addition to choose the data file, the user also needs to specify the coordinate (x and y) of starting point and the length for each line. These information will be used by the software in order to calculate the coordinate of each individual waveform, along with its corresponding correlation coefficient between two A-scans. As explained in Chapter 5, the data file input in this calculation is in .txt format, converted from DZT file using GSSI software.

After all information and data have been input, the user just needs to specify output file

149

and click "Calculate" button. The result is an xls. File as shown in Fig. 6.4, containing coordinate x (first column), y (second column) and correlation coefficient (third column). This file can then be read by Surfer, mapping software, to create the correlation map as illustrated in Chapter 5.

Fig. 6.4 Example Output from Correlation Calculation

6.1.2 Amplitude Option

When "Amplitude" option is checked, the same as "Correlation" method, the user needs to specify the number of survey lines and then input the data for each line as shown in Fig. 6.5. The data file for each line in this calculation option is in .CSV format that is obtained after top rebar amplitudes have been picked and exported from GSSI RADAN software. However, in addition to input coordinate of starting point and length of each line, the user also needs to input the number of A-scans on each profile. This information is required by the software to infer the coordinate of each rebar on the profile.
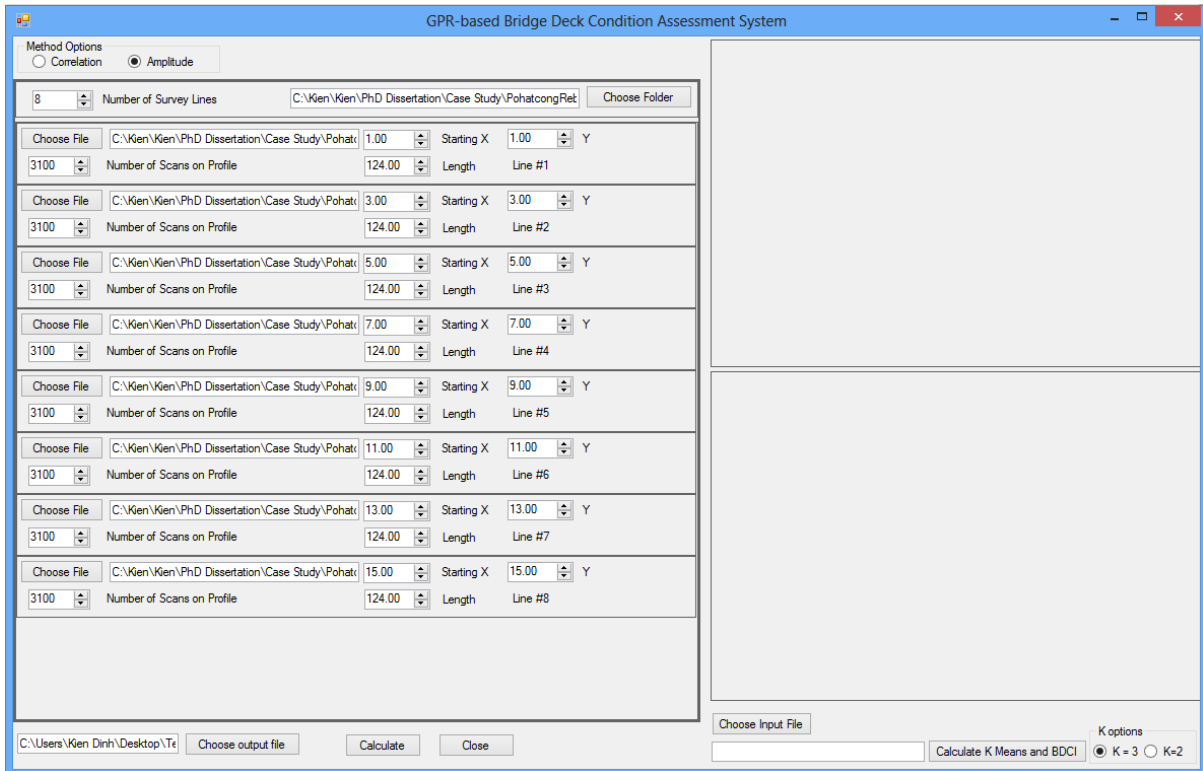
Fig. 6.5 Input for Amplitude Method

Like the correlation method, after required data has been input, the user also needs to choose output file and click "Calculate" button in order for the software to perform the calculation. In the example output shown in Fig. 6.6, the only difference from Fig. 6.4 is the third column in which instead of correlation coefficient, this column indicates depth-corrected amplitude of each rebar (in decibel).

While the file obtained above can be read by Surfer program to generate contour map of rebar reflection amplitude with constant interval between the contour lines; however, as explained in Chapter 5, the amplitude data in the third column will be used first for finding threshold values using K-means technique and then to calculate Bridge Deck Corrosiveness Index (BDCI). These two functions are described in the section below.

151
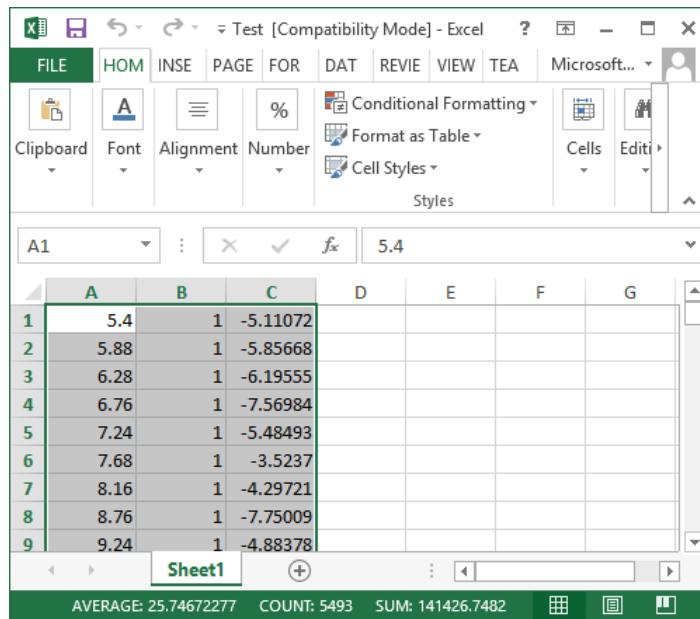
Fig. 6.6 Example Output for Amplitude Calculation

6.1.3 K-means Clustering and BDCI Calculation

The .xls file obtained from the amplitude analysis above can then be read by the software in order to perform clustering and calculate Bridge Deck Corrosiveness Index (BDCI). For doing that, the user need to choose .xls file by clicking "Choose Input File" button on the form in Fig. 6.7. After that, he/she needs to specify the number of K for clustering. Obviously, if K is equal to one, there is no need for clustering and bridge deck is considered healthy. Therefore, the form only allows the user to select the value of K being either 2 or 3. Finally, after all the inputs have been specified, the calculation will be implemented by clicking "Calculate K-means and BDCI" button. The output of this process is shown in Fig. 6.8.

152
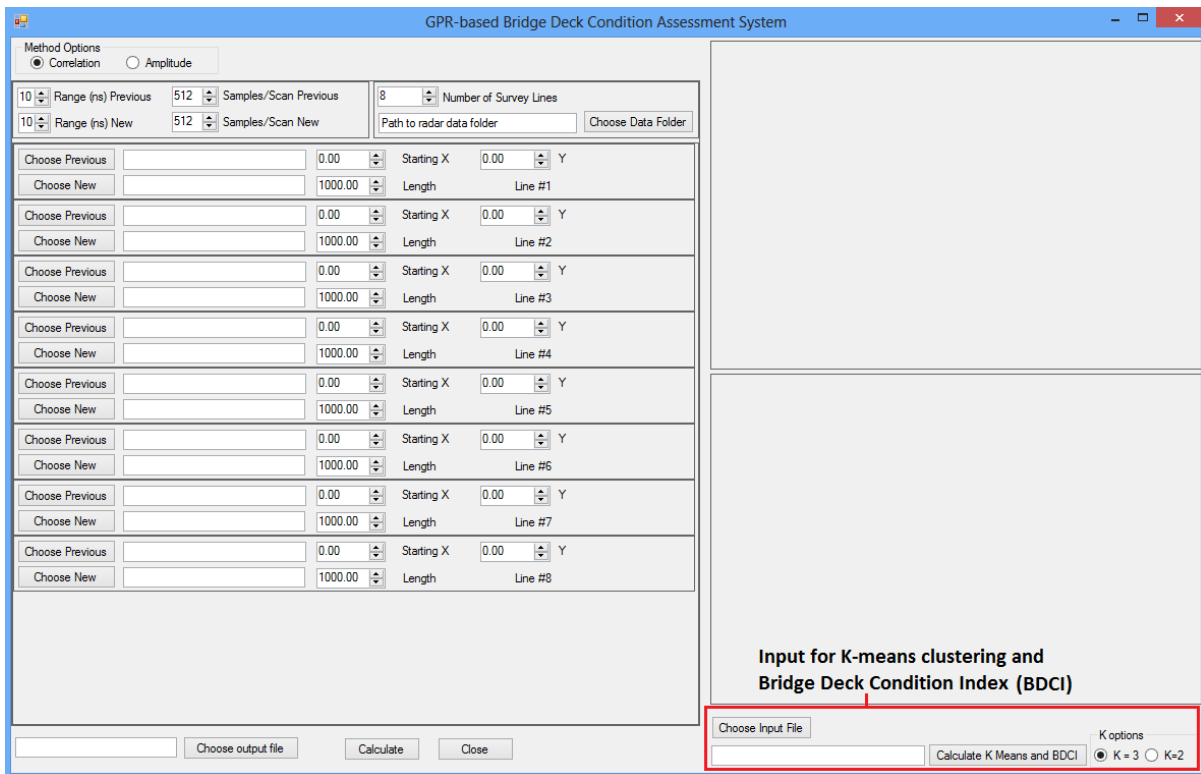
Fig. 6.7 Input for K-means clustering and BDCE Calculation

As can be seen, Fig. 6.8 provides several outputs such as the thresholds, percentages associated with various concrete conditions, and BDCI value. For visualization and condition mapping, these thresholds can be input into Surfer (mapping software) as depicted in Fig. 6.9. It is noted that the map in Fig. 6.9 is created by reading the .xls file obtained in previous step.

6.2 Software Implementation

In this section, the developed software is implemented to several case studies in Quebec where GPR data have been collected in Chapter 4. Since previous GPR data were not available for all of these bridges, only amplitude option of the software is employed.

153

The result for each case study is presented in turn as follows.
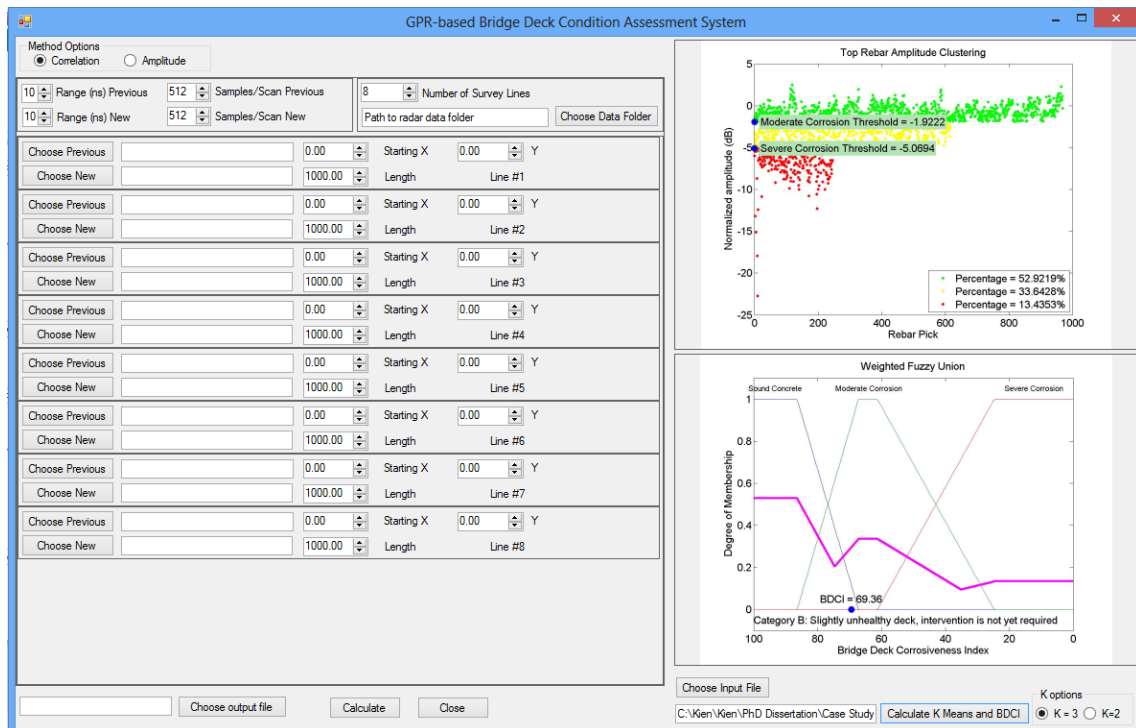
Fig. 6.8 K-means clustering and BDCI Output
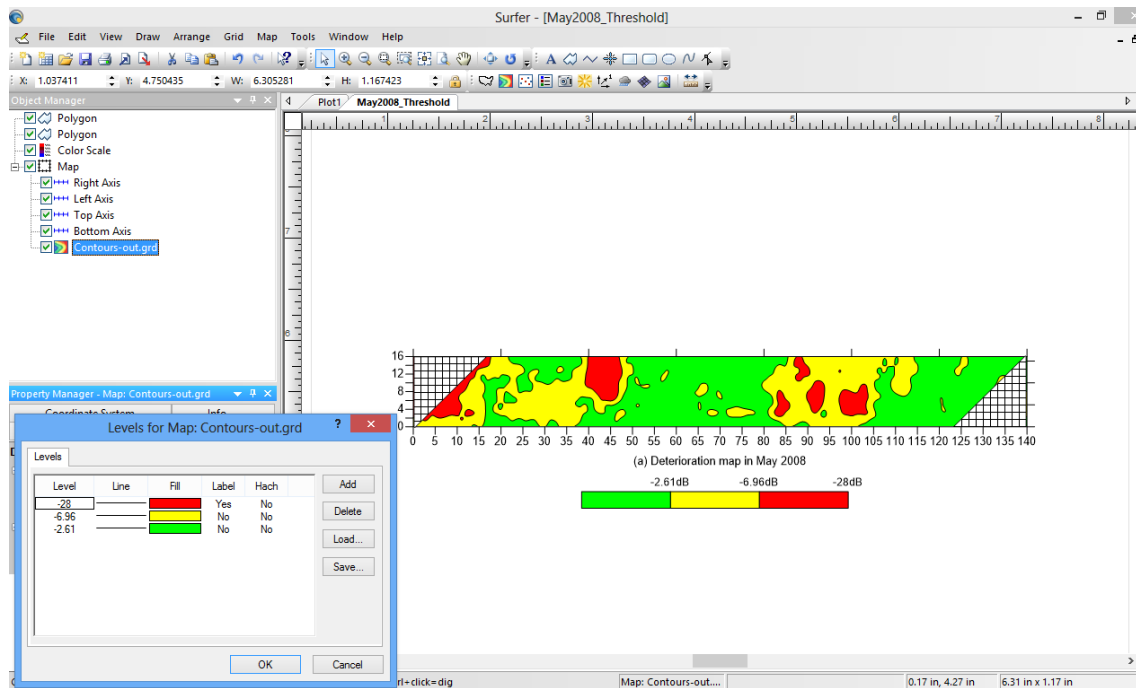
Fig. 6.9 Condition Map based on Threshold Values

6.2.1 Bridge A

As can be seen in Fig. 6.10, with BDCI value of 60.26, the deck of Bridge A is classified as category D, meaning it is a very unhealthy deck and intervention is strongly recommended. The recommendation for this deck is that it should be totally replaced in the coming 5-10 year programming period.
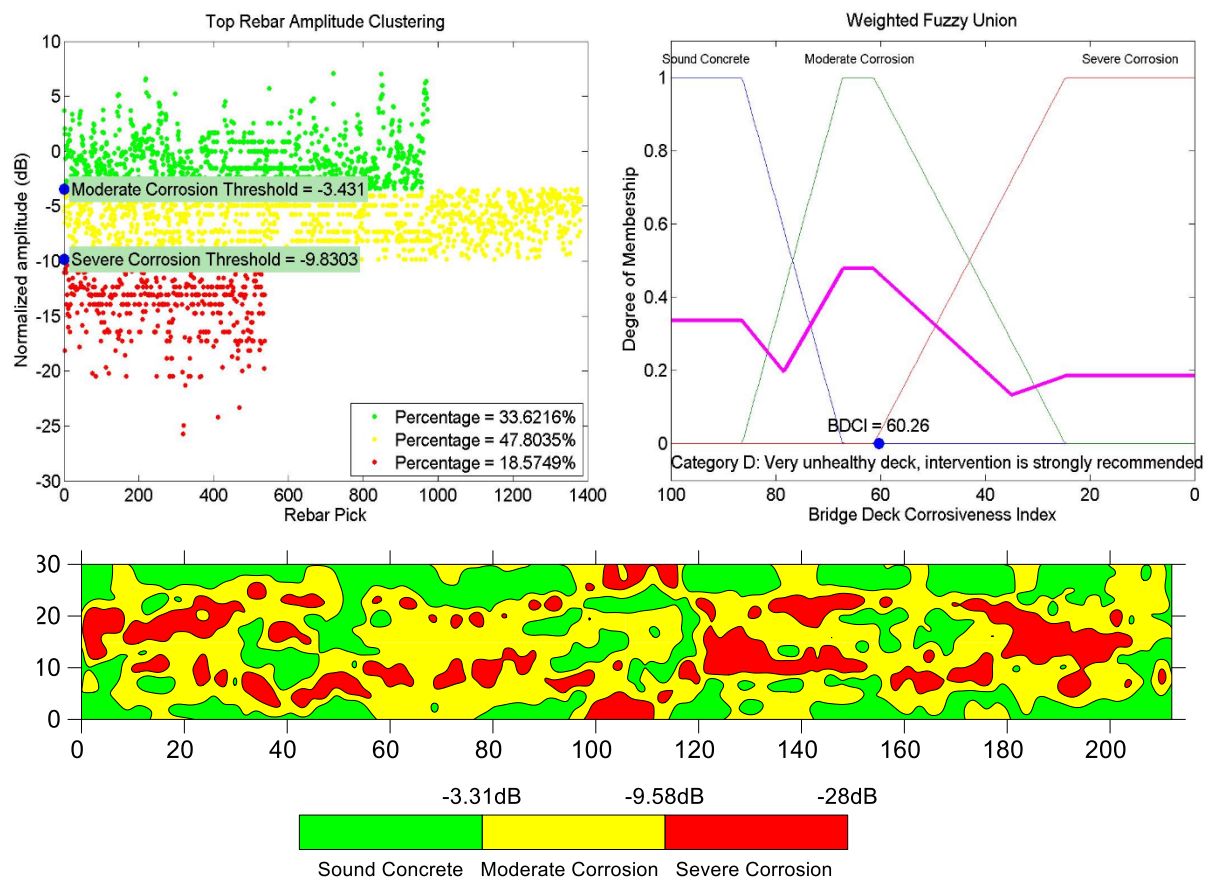
Fig. 6.10 BDCI and Corrosion Map for Bridge A

6.2.2 Bridge B

The result in Fig. 6.11 suggests that the deck of Bridge B is in category C; meaning it is unhealthy, intervention is needed but may be postponed. The recommendation for the bridge owner is that they should repair the bridge in the next 5-10 year programming

horizon using available techniques such as shallow patching, deep patching or full depth removal, etc. The selection of which technique should depend on level of chloride contamination on each specific area. However, in case the intervention is postponed, the deck should be monitored with GPR for that same period.
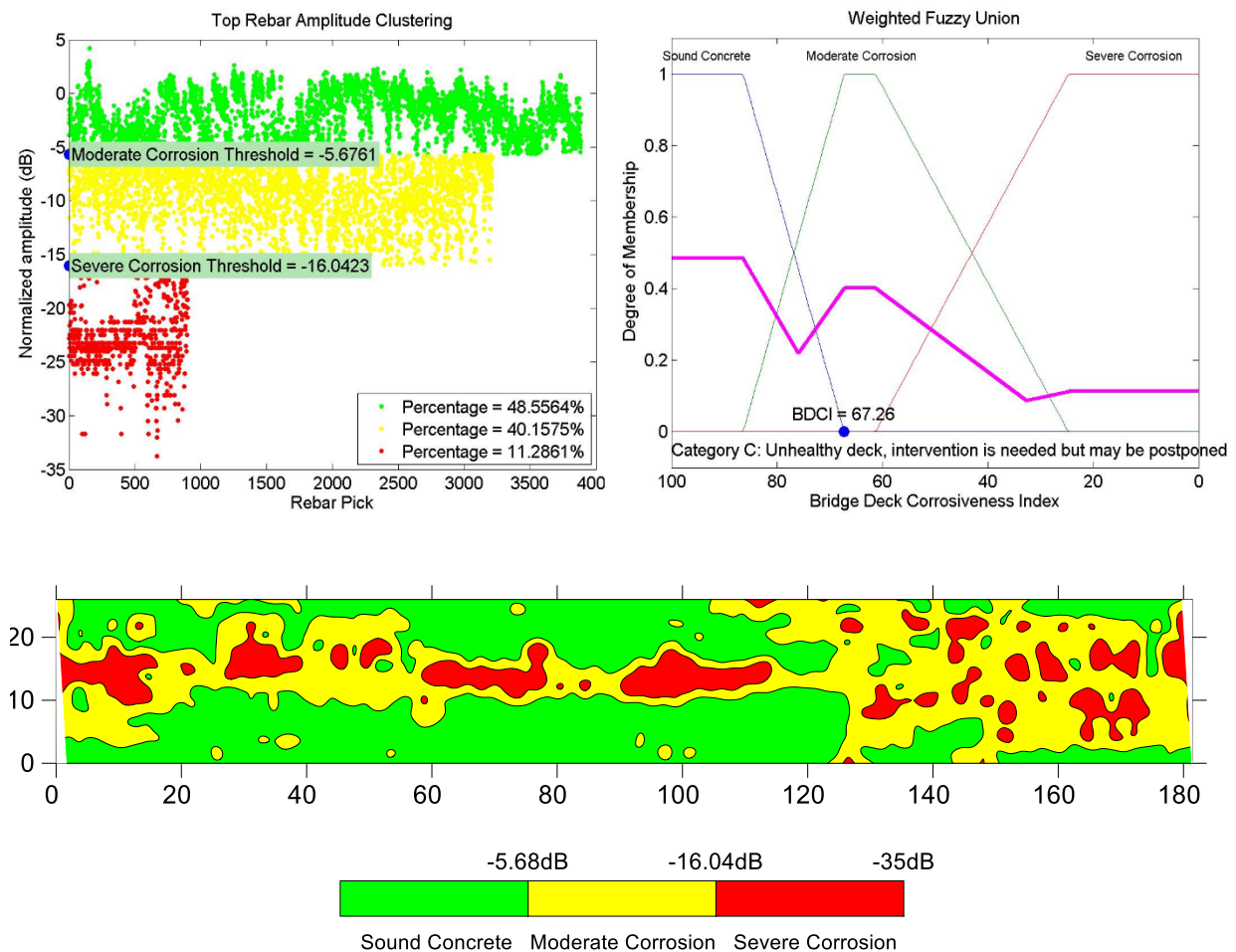
Fig. 6.11 BDCI and Corrosion Map for Bridge B

6.2.3 Bridge C

As can be seen in Fig. 6.12, BDCI value suggests the deck of Bridge C is in category D. The recommendation for this bridge deck is similar as the one of bridge A.
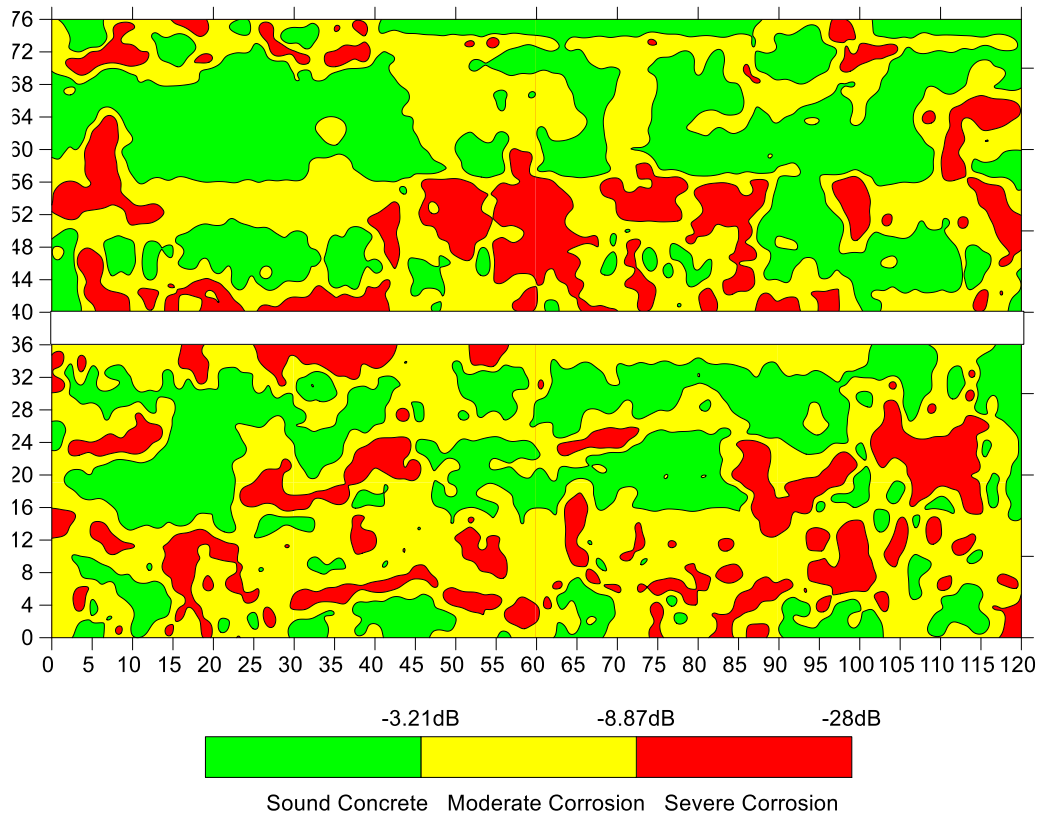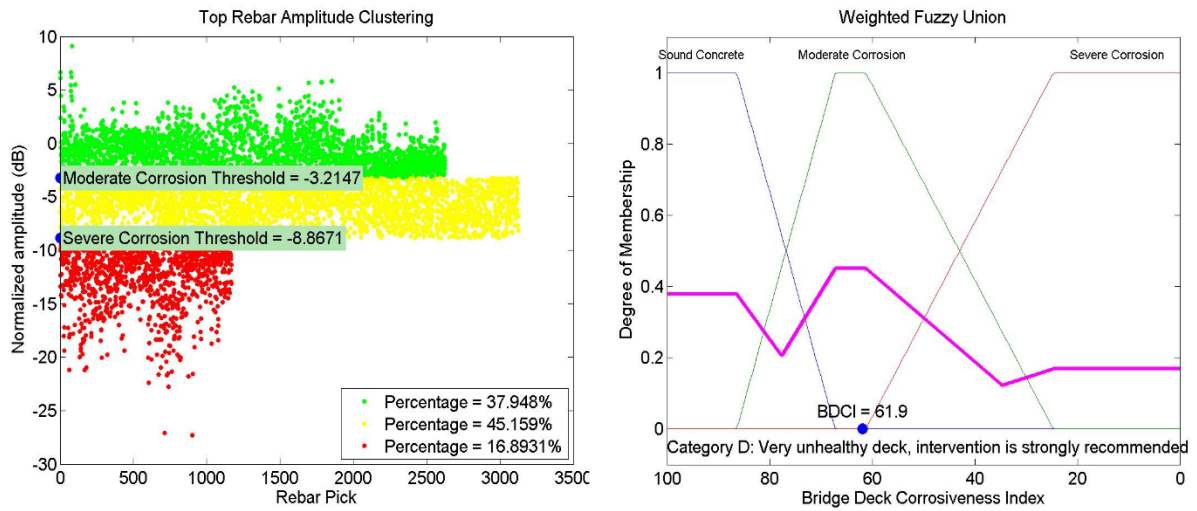
Fig. 6.12 BDCI and Corrosion Map for Bridge C

6.2.4 Bridge D

Since the result in Fig. 6.13 suggests the deck to be classified as category B, only

monitoring with GPR in the next 5-10 year programming period is required.
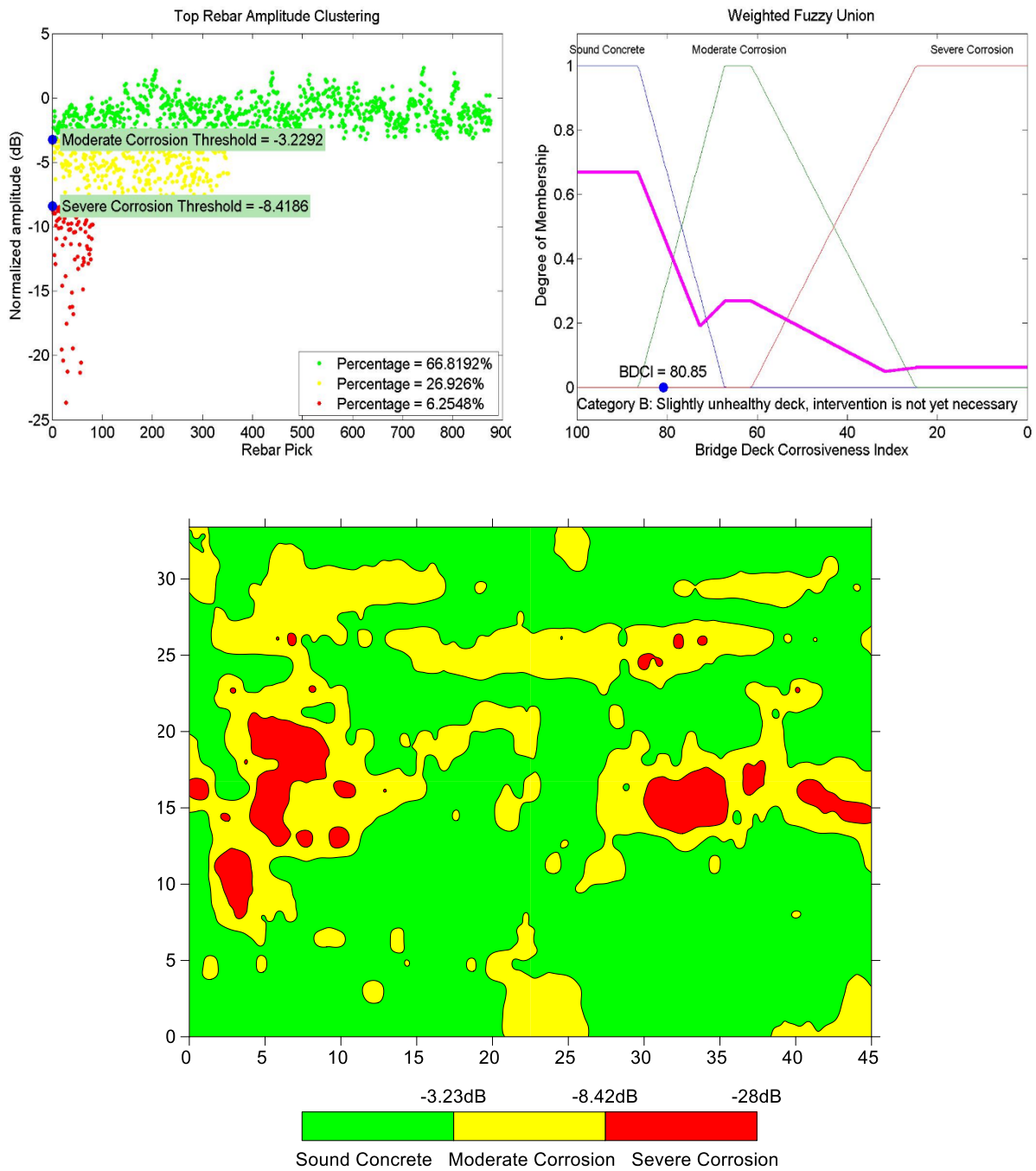
Fig. 6.13 BDCI and Corrosion Map for Bridge D

CHAPTER 7   CONCLUSIONS, CONTRIBUTIONS AND FUTURE RESEARCH

7.1   Conclusions

The main goal of the current research was to develop a condition assessment system for concrete bridge decks using NDE technology. Based on study of literature, model development, data collection and case study, the following conclusions can be drawn:

- Among various NDE technologies, ground penetrating radar (GPR) was found to be the most appropriate technique for inspection of concrete bridge decks. Based on principles of electromagnetic wave propagation, this technology allows concrete bridge decks to be scanned in a very short period of time and with high level of acquisision precision. The sensitivity of GPR to chloride presence and concrete corrosion makes the technology an ideal tool for concrete bridge deck inspection.

- Although being the most commonly used method for interpreting GPR data from concrete bridge decks, top rebar amplitude analysis has several limitations, including: (1) subjective selection of threshold value; (2) can only assess relative corrosion severity between individual rebars; and (3) the effect of unknown variables to amplitude data.

- Threshold calibration technique developed in this study based on K-means clustering not only resolves subjectivity problem in selecting threshold value, but also facilitates the automatic calculation of area percentage for each

condition category. These percentages are utilized for computation of bridge deck corrosiveness index later on.

- For New Jersey case study, although also showing some fluctuation in the percentage numbers of each condition category over time as the result obtained from available threshold model in literature, however the proposed calibration method, based on K-means clustering, provided reasonable and much more stable results.

- With the ability to compare the similarity of two GPR waveforms, correlation analysis of time-series GPR data developed in this research can be used for both condition assessment and condition monitoring of concrete bridge deck. For the concrete bridge deck in New Jersey, unlike amplitude interpretation, correlation analysis provided expected outcome where average correlation coefficient of the deck decreased with time. The only problem with the method is that it requires baseline GPR data to be collected.

- Collecting expert opinion proves to be an effective approach for solving condition rating problem. A simple method for using these opinions has been illustrated in this research where the combination of polling technique and heuristic method was used for calibration of fuzzy membership functions.

- With the automated software and recommended action scale, the proposed BDCI would be very useful for transportation agencies when it can be used to plan MR&R activity of an individual bridge, or to be incorporated into the analysis at network level. The implementation of the software for four asphalt-covered

concrete bridge decks in Quebec, Canada showed that it provides invaluable outputs with required functionality.

In summary, concrete bridge deck inspection based on GPR, a nondestructive evaluation technology, provides much more accurate and objective information about bridge deck condition and therefore enhances public safety. The proposed system improves the quality of decision making when it directs transportation agencies toward identifying critical deficiencies and focusing constraint funding on most deserving assets. As a result, bridge decks can be preserved and maintained more efficiently, leading to significantly reduced life-cycle costs of bridge structures.

7.2 Research Contributions

The inspection and condition rating system for concrete bridge decks developed in this study is sufficiently novel for contribution to knowledge. It is expected to provide a more accurate solution than the current practice of bridge condition assessment solely based on visual inspection. The main contributions of this research can be summarized as follows:

- A comprehensive assessment of amplitude analysis, the most commonly used method for analyzing GPR data of concrete bridge decks;

- An enhanced technique for analyzing GPR data in which amplitude thresholds are obtained based on K-means clustering.

- A novel framework for collecting and interpreting GPR data in which time-series

data is analyzed using correlation coefficient between A-scans.

- A fuzzy model for interpreting bridge deck corrosiveness index (BDCI) from GPR condition maps

- A scale in which intervention need and suggested action for a bridge deck can be determined based on the value of its BDCI index.

7.3 Limitations and Recommendation for Future Work

7.3.1 Limitations of Developed System

Based on all findings during the course of this study, several limitations of the developed system were identified as follows:

First and most importantly, because true baseline data was not available, the analysis method based on correlation of A-scans has not been fully developed in this study. Specifically, while the method requires GPR data collected when bridge decks are new, the baseline data used in this research was 30 years old. Under this condition, only relative deterioration between two scans can be observed and there is no way to calibrate the correlation thresholds from this data, those would differentiate severe corrosion from moderate deterioration or in turn moderate corrosion from sound concrete. This was the reason why bridge deck corrosiveness index (BDCI) model developed in this study was input by condition maps obtained from amplitude analysis of GPR data.

Second, there are still unknown variables that affect GPR amplitude data at top rebar level. Although several normalization methods were devised and explored, it still

appears that bridge deck condition in the case study improves at some points in time. However, because of limited information with only four time-series data sets used in this study, it was unable to explore and model random variables that affect amplitude data.

7.3.2 Future Work

Potential improvements and extensions of this study, recommended future work, can be divided into two areas as follows:

7.3.2.1 Current Research Enhancements

First, in order to fully develop correlation analysis approach proposed in this study, a long-term research project should be performed in which true baseline data is collected for typical bridge decks in North America.

Second, extensive time-series data collection and analysis should be implemented to identify and model random, unknown variables that affect amplitude data. In addition, with this data, the effect of weather or moisture in concrete slabs can be taken into account for calibration of correlation coefficient threshold.

Since the strategy for intervention actions was adjusted and proposed by the author after collecting and analyzing the survey, it is recommended that the second-round survey should be performed. This second survey would allow the strategy to be reviewed and refined by experts in the field.

Finally, although the automation tool developed in this study functioned well and provided required output for the case studies, it should be enhanced to be more user-friendly as a professional, commercial software package.

7.3.2.2 Current Research Extensions

While the current research focused only on using GPR for concrete bridge decks, the proposed system can be extended to other concrete bridge elements such as girders, piers, abutments, towers (pylons) and so on. Since that may be the case, there should be an approach to aggregate condition indices of all these elements that forms the condition index of the entire bridge structure. Analytical Network Process (ANP) would be a rational technique for such integration.

Since robotic data collection has been developed recently for various NDE technologies, including GPR, there is an opportunity for the system developed in this study to be incorporated into such program. Because the robot bases on global positioning system (GPS) technology for automatically navigating on bridge deck surface, it provides much more accurate positioning. If robotic integration is really the case, the simplicity of the developed system makes it possible for GPR data to be analyzed with condition maps and BDCI being output in real time.

REFERENCES

AASHTO (1994). "Manual for Condition Evaluation of Bridges." 2nd Ed. American Association of State Highway and Transportation Officials, Washington, D.C.

AASHTO (2010). "AASHTO Bridge Element Inspection Manual." 1st Ed, American Association of State Highway and Transportation Officials, Washington, D.C.

Abu Dabous, S. (2008). "A Decision Support Methodology for Rehabilitation Management of Concrete Bridges." Ph.D thesis, Concordia Univ., Montreal, Canada.

Al-Barqawi, H., and Zayed, T. (2006). "Condition Rating Model for Underground Infrastructure Sustainable Water Mains." *Journal of Performance of Constructed Facilities*, ASCE, Vol. 20, No. 2, May, pp. 126-135.

A1-Qadi, I.L, Prowell, B.D., Weyers, R.E., Dutta, T., and Gouru, H. (1993). "Concrete Bridge Protection and Rehabilitation: Chemical and Physical Techniques." *Strategic Highway Research Program*, National Research Council, SHRP-S-666.

Agrawal, A.K., Kawaguchi, A., and Chen, Z. (2010). "Deterioration Rates of Typical Bridge Elements in New York." *Journal of Bridge Engineering*, ASCE, Vol.15, No.4, pp. 419-429.

Ariaratnam, S.T., El-Assaly, A., and Yang, Y. (2001). "Assessment of Infrastructure Inspection Needs Using Logistic Models." *Journal of Infrastructure Systems*, ASCE, Vol. 7, No. 4, December, pp. 160-165.

Arslan, A., and Kaya, M. (2001). "Determination of fuzzy logicmembership functions

using genetic algorithms." *Fuzzy Sets and Systems*, Elsevier, Vol. 18, Iss. 2, March, pp. 297-306.

ASCE. (2013). Report Card for America's Infrastructure. American Society of Civil Engineering, http://www.infrastructurereportcard.org/bridges/ Accessed May 12, 2014.

ASTM C 597 – 02 (2005). "Standard Test Method for Pulse Velocity through Concrete." *Annual Book of ASTM Standards*, West Conshohocken, PA, ASTM, Vol. 04.02.

ASTM C 876 – 91(1999). "Test Method for Half-Cell Potentials of Uncoated Reinforcing Steel in Concrete." *Annual Book of ASTM Standards*, West Conshohocken, PA, ASTM, Vol. 04.02.

ASTM C 876 – 09 (2007). "Standard Test Method for Corrosion Potentials of Uncoated Reinforcing Steel in Concrete." *Annual Book of ASTM Standards*, West Conshohocken, PA, ASTM, Vol. 03.02.

ASTM D4580 – 03 (2007). "Standard Practice for Measuring Delaminations in Concrete Bridge Decks by Sounding," *Annual Book of ASTM Standards*, West Conshohocken, PA, ASTM, Vol. 04.03.

ASTM D4788 – 03 (2007). "Standard Test Method for Detecting Delaminations in Bridge Deck Using Infrared Thermography." *Annual Book of ASTM Standards*, West Conshohocken, PA, ASTM, Vol. 04.03.

ASTM D6087 – 08 (2010). "Standard Test Method for Evaluating Asphalt-Covered Concrete Bridge Decks Using Ground Penetrating Radar," *Annual Book of ASTM*

Standards, West Conshohocken, PA, ASTM, Vol. 04.03.

Ball, G. H., & Hall, D. J. (1965). "ISODATA, a novel method of data analysis and pattern classification." STANFORD RESEARCH INST MENLO PARK CA.

Barnes, C.L. (1999). "A Study of the Effectiveness of Ground Penetrating Radar for Assessing Asphalt Covered Reinforced Concrete Bridge Deck Deterioration." M.S thesis, Dalhousie University – DALTECH, Halifax, Nova Scotia, Canada.

Barnes, C. L. and Trottier, J. F. (2000). "Ground-Penetrating Radar for Network-Level Concrete Deck Repair Management." *Journal of Transportation Engineering*, ASCE, Vol. 126, No. 3, May/Jun. pp. 257-262.

Barnes, C. L. and Trottier, J. F. (2002). "Phenomena and Conditions in Bridge Decks that Confound GPR Data Analysis." *Transportation Research Record*, No. 1795, Transportation Research Board, Washington D.C. pp. 57-61.

Barnes, C. L. and Trottier, J. F. (2004). "Effectiveness of Ground Penetrating Radar in Predicting Deck Repair Quantities." *Journal of Infrastructure Systems*, ASCE, Vol. 10, No. 2, June, pp. 69-76.

Barnes, C., Trottier, J. F., and Forgeron, D. (2008) "Improved Concrete Bridge Deck Evaluation Using GPR by Accounting for Signal Depth-Amplitude Effects." *NDT & E International*, Vol. 41, No. 6, September, pp. 427-433.

Baruch, Y. (1999). "Response rate in academic studies-A comparative analysis." *Human Relations*, Vol. 52, No. 4, pp. 421-438.

Beliakov, G. (1996). "Fuzzy Sets and Membership Functions Based on Probabilities." *Information Sciences*, Elsevier, Vol. 91, Iss. 1-2, May, pp. 95-111.

Briechle, K., and Hanebeck, U. D. (2001). "Template Matching Using Fast

Normalized Cross Correlation."*Proceedings of SPIE: Optical Pattern Recognition

XII*, Vol. 4387, March, pp. 95-102.

Brunelli, R., and Poggio, T. (1993). "Face Recognition: Features versus Templates."

IEEE Transactions on Pattern Analysis and Machine Intelligence, Vol 15, No. 10,

October, pp 1042-1052.

Bungey, J. H., and Millard, S. G. (1993). "Radar Inspection of Structures."

Proceedings, Institute of Civil Engineers, Structures and Buildings Journal

London, Vol. 99, May, pp. 173-186.

Bungey, J.H., and Millard, S.G. (1996). "Testing of Concrete in Structures." 3rd Ed.,

Chapman & Hall.

Carino, N.J. (2004a). "Method to Evaluate Corrosion of Reinforcement." In:

Handbook on Nondestructive Testing of Concrete, Malhotra, V.M and Carino,

N.J., ed., 2nd Ed., ASTM & CRC.

Carino, N.J. (2004b). "Stress Wave Propagation Methods." In: *Handbook on

Nondestructive Testing of Concrete*, Malhotra, V.M and Carino, N.J., ed., 2nd Ed.,

ASTM & CRC.

Canto, T.R. (1984). "Review of Penetrating Radar as Applied to Nondestructive

Evaluation of Concrete." In: *In Situ/Nondestructive Testing of Concrete*, V. M.

Malhotra, ed., ACI SP-82, American Concrete Institute, Farmington Hills, Mich.,

pp. 581-601.

Cantor, T.R., Kneeter, C.P. (1982). "Radar as Applied to Evaluation of Bridge

Decks." *Transportation Research Record,* No. 853, Washington, D.C., pp. 27-32.

Carter, C.R., Chung, T., Holt, F.B., Manning, D. (1986)."An Automated Signal

Processing System for the Signature Analysis of Radar Waveforms from Bridge

Decks." *Canadian Electrical Engineering Journal*, Vol. 11, No. 3, pp. 128-137.

Chung, T., Carter, C.R., Masliwec, T., Manning, D.G. (1992) "Impulse Radar

Evaluation of Asphalt-Covered Bridge Decks." *IEEE Transactions on Aerospace*

and Electronic Systems, Vol. 28, No. 1, January, pp. 125-137.

Chung, T., Carter, C.R., Reel, R., Tharmabala, T., Wood, D. (1993). "Impulse radar

signatures of selected bridge deck structures." *Canadian Conference on Electrical*

and Computer Engineering, Vol. 1, September, pp. 59-62

Chughtai, F., and Zayed, T. (2008). "Infrastructure Condition Prediction Models for

Sustainable Sewer Pipeline." *Journal of Performance of Constructed Facilities*,

ASCE, Vol. 22, No. 5, October, pp. 333-341.

Clemeña, G.G., Jackson, D.R., and Crawford, G.C. (1992). "Benefits of using Half-

Cell Potential Measurement in Condition Surveys of Concrete Bridge Decks."

Transportation Research Record, No. 1347, Transportation Research Board,

Washington, D.C., pp. 46-55.

Clemeña, G.G. (1983). "Nondestructive Inspection of Overlaid Bridge Decks with

Ground Penetrating Radar." *Transportation Research Record,* No. 899,

Washington, D.C., pp. 21-32.

Clemeña, G.G. (1985). "Survey of Bridge Decks with Ground Penetrating Radar: A

Manual." FHWA/VA-86/3, *Virginia Highway and Transportation Research*

Council, Charlottesville, Virginia.

Clemeña, G.G. (2004)."Short-Pulse Radar Methods." In: *Handbook on Nondestructive Testing of Concrete*, Malhotra, V.M and Carino, N.J., ed., 2nd Ed., ASTM & CRC.

Daniels, D.J., ed. (2004). "Ground Penetrating Radar." 2nd Ed., The Institution of Electrical Engineers, London, United Kingdom.

Davidson, N.C., Chase, S.B. (1998). "Radar Tomography of Bridge Decks." *Structural Materials Technology III – An NDT Conference*, SPIE Volume 3400, March, pp. 250-256.

Davis, A. G., Ansari, F., Gaynor, R. D., Lozen, K. M., Rowe, T. J., Caratin, H., … & Sansalone, M. J. (1998). "Nondestructive Test Methods for Evaluation of Concrete in Structures." *American Concrete Institute*, ACI, 228.

Dinh, K., Zayed, T., and Tarussov, A. (2013). "GPR Image Analysis for Corrosion Mapping in Concrete Slabs." *CSCE Conference*, Montreal, Quebec, Canada, May 29th - June 1st.

Dombi, J., and Gera, Z. (2005). "The approximation of piecewise linear membership functions and Łukasiewicz operators." *Fuzzy Sets and Systems*, Elsevier, Vol. 154, Iss. 2, September, pp. 275-286.

Ellis, R.M., Thompson, P.D., Gagnon, R., and Richard, G. (2008). "Design and Implementation of a New Bridge Management System for the Québec Ministry of Transport." Transportation Research Circular E-C128, pp. 77 – 86.

Ellis, R. M., & Thompson, P. D. (2007). "Bridge Asset Valuation and the Role of the Bridge Management System." In Annual Conference and Exhibition of the

Transportation Association of Canada: Transportation-An Economic Enabler.

FHWA (1995). "Recording and Coding Guide for the Structure Inventory and Appraisal of the Nation's Bridges." FHWA-PD-96-001, *Federal Highway Administration*, U.S Department of Transportation.

FHWA (2001). "Reliability of Visual Inspection for Highway Bridges, Volume I: Final Report." FHWA-RD-01-020, *Federal Highway Administration*, U.S Department of Transportation.

FHWA (2006). "Highway Concrete Pavement Technology Development and Testing: Volume IV – Field Evaluation of Strategic Highway Research Program (SHRP) C-206 Test Sites (Bridge Deck Overlays)." FHWA-RD-02-086*, Federal Highway Administration*, U.S Department of Transportation.

FHWA (2013). FHWA Bridge Programs Count, Area, Length of Bridges by Highway System. Federal Highway Administration, http://www.fhwa.dot.gov/bridge/fc.cfm Accessed May 12, 2014.

Forman, E., and Peniwati, K. (1998). "Aggregating individual judgments and priorities with the Analytic Hierarchy Process." *European Journal of Operational Research*, Elsevier, Vol. 108, Iss. 1, July, pp. 165-169.

Giachetti, A. (2000). "Matching techniques to compute image motion." *Image and Vision Computing*, Elsevier, Vol. 18, Iss. 3, February, pp 247-260.

Golabi, K. and Shepard, R. (1997). "Pontis: A System for Maintenance Optimization and Improvement of US Bridge Networks." *Interfaces*, Vol. 27, No. 1, Franz Edelman Award Papers January - February, pp. 71-88.

Gucunski, N., Feldmann, R., Romero, F., Kruschwitz, S., Abu-Hawash, A., & Dunn, A. (2009). "Multimodal condition assessment of bridge decks by NDE and its validation." *Proc. 2009 Mid-Continent Transportation Research Symp.*, Ames, Iowa, 18p (Vol. 261, No. 5).

Gucunski, N. (2013). "Nondestructive testing to identify concrete bridge deck deterioration." Transportation Research Board, Washington D.C.

Gucunski, N., Romero, F., Imani, A. S., & Fetrat, F. (2013). "NDE-Based Assessment of Deterioration Progression in Concrete Bridge Decks." *Transportation Research Board 92nd Annual Meeting* (No. 13-3043).

Hadipriono, F.C. (1988). "Fuzzy Set Concepts for Evaluating Performance of Constructed Facilities." *Journal of Performance of Constructed Facilities*, ASCE, Vol. 2, No. 4, November, pp. 209-225.

Hammad, A., Yan, J., & Mostofi, B. (2007). "Recent development of bridge management systems in Canada." *Annual Conference and Exhibition of the Transportation Association of Canada: Transportation-An Economic Enabler*.

Halabe, U. B., Sotoodehnia, A., Maser, K. R., and Kausel, E. A. (1993). "Modeling the Electromagnetic Properties of Concrete." *ACI Materials Journal*, Vol. 90, No. 6, Nov.-Dec., pp. 552-563.

Hearn, G. (2007). "Bridge Inspection Practices." *National Cooperative Highway Research Program*, Transportation Research Board, NCHRP Synthesis 375.

Hellier, C.J. (2003). "Handbook of Nondestructive Evaluation", McGRAW-HILL, Vol. 10, NY.

Hisdal, E. (1986). "Infinite-valued logic based on two-valued logic and probability, Part 1.2." *International Journal of Man-Machine Studies*, Elsevier, Vol. 25, Iss. 2, August, pp.113-138.

Horhota, D.J. (1996). "Evaluation of Spectral Analysis of Surface Waves (SASW) Test Method for Florida Department of Transportation (FDOT) Application." Ph.D thesis, University of Florida, Florida, USA.

Huang, R. Y., Mao, I., & Lee, H. K. (2010). "Exploring the deterioration factors of RC bridge decks: a rough set approach." *Computer-Aided Civil and Infrastructure Engineering*, Vol. 25, No. 7, pp. 517-529.

Hudson, R.W., and Carmichael, R.F., Hudson, S.W., Diaz, M.A., and Moser, L.O. (1993). "Microcomputer Bridge Maintenance Management." *Journal of Transportation Engineering*, ASCE, Vol.119, No.1, pp. 59-76.

Huston, D., Hu, J.Q., Maser, K., Weedon, W., and Adam, C. (2000). "GIMA ground penetrating radar system for monitoring concrete bridge decks." *Journal of Applied Geophysics*, Elsevier, Vol. 43, Iss. 2–4, March, pp. 139–146.

Ishibuchi, H., Nozaki, K., and Tanaka, H. (1993). "Efficient fuzzy partition of pattern space for classification problems." *Fuzzy Sets and Systems*, Elsevier, Vol. 59, Iss. 3, November, pp. 295-304.

Jain, A. K. (2010). "Data clustering: 50 years beyond K-means." *Pattern Recognition Letters*, Vol. 31, No. 8, pp. 651-666.

Jiang, X., and Rens, K.L. (2010). "Bridge Health Index for the City and County of Denver, Colorado. I: Current Methodology." *Journal of Performance of*

Constructed Facilities, Vol. 24, No. 6, December, pp. 580-587.

Kawamura, K., and Miyamoto, A. (2003). "Condition state evaluation of existing reinforced concrete bridges using neuro-fuzzy hybrid system." *Computers & Structures*, Elsevier, Vol. 81, Iss. 18–19, August, pp. 1931-1940.

Kirkpatrick, T. J., Weyers, R. E., Anderson-Cook, C. M., & Sprinkel, M. M. (2002). "Probabilistic model for the chloride-induced corrosion service life of bridge decks." *Cement and concrete research*, Vol. 32, No. 12, pp. 1943-1960.

Koo, D.H., and Ariaratnam, S.T. (2006). "Innovative method for assessment of underground sewer pipe condition." *Automation in Construction*, Elsevier, Vol. 15, Iss. 4, pp. 479-488.

Kumar, S., and Taheri, F. (2007). "Neuro-Fuzzy approachs for pipeline condition assessment." *Nondestructive Testing and Evaluation*, Taylor & Francis, Vol. 22, No. 1, March, pp. 35-60.

La, H. M., Lim, R. S., Basily, B., Gucunski, N., Yi, J., Maher, A., and Parvardeh, H. (2013). "Autonomous robotic system for high-efficiency non-destructive bridge deck inspection and evaluation." *Automation Science and Engineering (CASE),* IEEE International Conference, August, pp. 1053-1058.

Le Groupe, S. M. (2010). "Évaluation de l'état des ponts autoroutiers par méthode RADAR: corrélation entre les méthodes de traitements qualitatives et normalisées." MTQ Annual Convention, Quebec, QC.

Lee, K.H. (2005). "First Course on Fuzzy Theory and Application." Springer, Germany.

Liang, M., Wu, J., and Liang, C. (2001). "Multiple Layer Fuzzy Evaluation for Existing Reinforced Concrete Bridges." *Journal of Infrastructure Systems*, ASCE, Vol. 7, No. 4, pp. 144-159.

Li, C. Q. (2003). "Life cycle modeling of corrosion affected concrete structures-initiation." *Journal of Materials in Civil Engineering*, ASCE, Vol. 15, No. 6, December, pp. 594-601.

Lin, C.C., and Chen, A.P. (2002). "Generalization of Yang et al.'s method for fuzzy programming with piecewise linear membership functions." *Fuzzy Sets and Systems*, Elsevier, Vol. 123, Iss. 3, December, pp. 347-352.

Liu, Y., and Weyers, R. E. (1998). "Modeling the time-to-corrosion cracking in chloride contaminated reinforced concrete structures." *ACI Materials Journal*, Vol. 95, No. 6, pp. 675-680.

Lloyd, S. (1982). "Least squares quantization in PCM." *Information Theory*, IEEE Transactions, Vol. 28, Iss. 2, 129-137.

Lounis, Z. (2013). "Critical concrete infrastructure: extending the life of Canada's bridge network." Construction Innovation, Vol. 18, No. 1.

MacQueen, J. (1967). "Some methods for classification and analysis of multivariate observations." *Proceedings of the fifth Berkeley symposium on mathematical statistics and probability*, Vol. 1, No. 14, pp. 281-297.

Mahafza, B.R. (2000). "Radar Systems Analysis and Design Using MATLAB." Chapman & Hall/CRC, Boca Raton, FL.

Martino, N., Birken, R., Maser, K., and Wang, M. (2014). "Developing a deterioration

threshold model for assessment of concrete bridge decks using ground penetrating radar." *Transportation Research Board 93rd Annual Meeting* (No. 14-3861).

Maser, K. R., and Roddis, W. M. K. (1990). "Principles of Thermography and Radar for Bridge Deck Assessment." *Journal of Transportation Engineering*, ASCE, Vol. 116, No. 5, Sept.-Oct., pp. 583-601.

Maser, K.R. (1995). "Evaluation of bridge decks and pavements at highway speed using ground penetrating radar." *Proceedings of the SPIE Conference on Nondestructive Evaluation of Aging Infrastructure*, Vol. 2456, June, pp. 237-248.

Maser, K.R. (1996). "Condition Assessment of Transportation Infrastructure Using Ground Penetrating Radar." *Journal of Infrastructure Systems*, ASCE, Vol.2, No.2, June, pp.94-101

Maser, K., and Bernhardt, M. (2000). "Statewide Bridge Deck Survey Using Ground Penetrating Radar." *Structural Materials Technology IV - An NDT Conference*, Atlantic, NJ, pp. 31-37.

Medaglia, A.L., Fang, S.C., Nuttle, H.L.W, and Wilson, J.R. (2002). "An efficient and flexible mechanism for constructing membership functions." *European Journal of Operational Research*, Elsevier, Vol. 139, Iss. 1, May, pp. 84-95.

Medasani, S., Kim, J., and Krishnapuram, R. (1998). "An overview of membership function generation techniques for pattern recognition." *International Journal of Approximate Reasoning*, Elsevier, Vol. 19, Iss. 3-4, Nov-Dec, pp. 391-417.

Millard, S.G., Bungey, J.H., Shaw, M.R., Thomas, C., and Austin, B.A. (1997). "Interpretation of Radar Test Results." In: *Innovations in Nondestructive Testing*

of Concrete, Pessiki, S. and Olson, L., ed., Vol. 168, ACI.

Montgomery, D.C., and Runger, G.C. (2003). "Applied Statistics and Probability for Engineers." 3rd Ed., John Wiley & Sons, Hoboken, NJ.

Moselhi, O., and Shehab-Eldeen, T. (2000). "Classification of Defects in Sewer Pipes using Neural Networks." *Journal of Infrastructure Systems*, Vol. 6, No. 3, September, pp. 97-104.

MnDOT (2009). "Bridge Inspection Manual." *Minnesota Department of Transportation*, Version 1.8, October.

Naik, T.R, Malhotra, V.M, and Popovics, V.S. (2004). "The Ultrasonic Pulse Velocity Method" In: *Handbook on Nondestructive Testing of Concrete,* Malhotra, V.M and Carino, ed., 2nd Ed., ASTM & CRC, NJ.

Najjaran, H., Sadiq, R., and Rajani, B. (2005). "Condition Assessment of Water Mains using Fuzzy Evidential Reasoning." *Systems, Man, and Cybernetics*, IEEE International Conference, October, Vol. 4, pp. 3466-3471.

Parrillo, R., Roberts, R. and Haggan, A. (2006). "Bridge Deck Condition Assessment using Ground Penetrating Radar." *ECNDT Conference Proceeding*, Berlin, Germany, pp. 25-29.

Patidar, V., Labi, S., Sinha, K.C., and Thompson, P.D. (2007). "Multi-Objective Optimization for Bridge Management Systems." *National Cooperative Highway Research Program*, Transportation Research Board, NCHRP Report 590.

Perkins, A. D., Amrol, J. J., Romero, F. A., & Roberts, R. L. (2000). "DOT Specification Development Based on Evaluation of Ground-Penetrating Radar

System Performance in Measuring Concrete Cover (Reinforcement Depth) on New Bridge Deck Construction." *Structural Materials Technology—NDT Conference*, February, pp. 53-60.

Penttala, V. (2009). "Causes and mechanisms of deterioration in reinforced concrete." In: *Failure, distress and repair of concrete structures*, CRC, Woodhead Publishing Limited, pp. 3-31.

Pour-Ghaz, M., Isgor, O.B., and Ghods, P. (2009). "Quantitative Interpretation of Half-Cell Potential Measurements in Concrete Structures." *Journal of Materials in Civil Engineering*, ASCE, Vol. 21, No. 9, September, pp. 467-475.

Pradhan, B., and Bhattacharjee, B. (2009). "Half-Cell Potential as an Indicator of Chloride-Induced Rebar Corrosion Initiation in RC." *Journal of Materials in Civil Engineering*, ASCE, Vol. 21, No. 10, pp. 543-552.

Qasem, A. (2011). "Performance Assessment Model for Wastewater Treatment Plants." Ph.D thesis, Concordia Univ., Montreal, Canada.

Qian, S. (2004). "Preventing Rebar Corrosion in Concrete Structures." NRCC, <www.nrc-cnrc.gc.ca/obj/irc/doc/pubs/nrcc47625/nrcc47625.pdf> (Mar. 21, 2012).

Reel, R., Tharmabala, T., Wood, I., Chung, T., and Carter, C.R. (1997). "New Impulse Radar Strategies for Bridge Deck Assessment." In: *Innovations in Nondestructive Testing of Concrete*, Pessiki, S. and Olson, L., ed., Vol. 168, ACI.

Roberts, J.E, and Shepard, D. (2000). "Bridge Management for the 21st Century." *Transportation Research Record*, No. 1696, Transportation Research Board,

Washington, D.C., pp. 197-203.

Ryall, M.J (2010). "Bridge Management." 2nd Ed., Butterworth-Heinemann, Oxford, UK.

Saaty, T.L. (2001). "Decision Making with Dependence and Feedback – THE ANALYTIC NETWORK PROCESS." 2nd Ed., RWS Publications, Pittsburgh, PA.

Saaty, T.L., and Vargas, L.G. (2006). "DECISION MAKING WITH THE ANALYTIC NETWORK PROCESS - Economic, Political, Social and Technological Applications with Benefits, Opportunities, Costs and Risks." Springer, NY.

Saaty, T.L. (2008). "The Analytic Hierarchy and Analytic Network Measurement Processes: Applications to Decisions under Risk." *European Journal of Pure and Applied Mathematics*, Vol. 1, No. 1, pp. 122-196.

Sasmal, S., Ramanjaneyulu, K., Gopalakrishnan, S., and Lakshmanan, N. (2006). "Fuzzy Logic Based Condition Rating of Existing Reinforced Concrete Bridges," Journal of Performance of Constructed Facilities, Vol. 20, No. 3, August, pp. 261-273.

Sasmal, S., and Ramanjaneyulu, K. (2008). "Condition evaluation of existing reinforced concrete bridges using fuzzy based analytic hierarchy approach." *Expert Systems with Applications*, Vol. 35, Iss. 3, October, pp. 1430-1443

Scherschligt, D. and Kulkarni, R.B. (2003). "Pontis-based Health Indices for Bridge Priority Evaluation", *9th International Bridge Management Conference*, Transportation Research Board, pp. 29-45.

Scott, M., Rezaizadeh, A., and Moore, M. (2001). "Phenomenology Study of

    HERMES Ground Penetrating Radar Technology for Detection and Identification

    of Common Bridge Deck Features," FHWA-RD-01-090, *Federal Highway*

    Administration, U.S. Department of Transportation.

SlatonBarker, A.B., and Wallace, J.W. (1997). "Nondestructive Testing of Bridge

    Decks Using Dual Frequency Radar." In: *Innovations in Nondestructive Testing of*

    Concrete, Pessiki, S. and Olson, L., ed., Vol. 168, ACI.

Smadi, O., Stein, P. and Kallam, K. (2008). "Iowa DOT Bridge Asset Management

    Using Pontis: Data Integration, Performance and Decision Support Tools." Final

    Report, *Centre for Transportation Research and Education*, Iowa State University.

USFHA (1999). "Asset Management Primer.", a report submitted to US Department

    of Transportation, Federal Highway Administration, Office of Asset Management.

Sharp, S.R. (2004). "Evaluation of two corrosion inhibitors using two surface

    application methods for reinforced concrete structures." Final Report submitted to

    Virginia Transportation Research Council.

Steinhaus, H. (1956). "Sur la division des corp materiels en parties." Bull. Acad.

    Polon. Sci, No. 1, pp. 801-804.

Sun, L., and Gu, W. (2011). "Pavement Condition Assessment Using Fuzzy Logic

    Theory and Analytic Hierarchy Process." *Journal of Transportation Engineering*,

    ASCE, Vol. 137, No. 9, September, pp. 648-655.

Suwito, A. and Xi, Y. (2003). "Service life of reinforced concrete structures with

    corrosion damage due to chloride attack." *Life-cycle performance of deteriorating*

structures, ASCE, pp. 207-218.

Tarighat, A., and Miyamoto, A. (2009). "Fuzzy concrete bridge deck condition rating method for practical bridge management system." *Expert Systems with Applications*, An international Journal, Elsevier Ltd, pp. 12077-12085.

Tarussov, A., Vandry, M. and De La Haza, A (2013). "Condition assessment of concrete structures using a new analysis method: Ground-penetrating radar computer-assisted visual interpretation." *Journal of Construction and Building Materials*, Elsevier Vol. 38, pp. 1246–1254.

Tamaki, F., Kanagawa, A., and Ohta, H. (1998). "Identification of membership functions based on fuzzy observation data." *Fuzzy Sets and Systems*, Elsevier, Vol. 93, Iss. 3, February, pp. 311-318.

Tee, A.B. (1988). "The Application of Fuzzy Mathematics to Bridge Condition Assessment," Ph.D thesis, Purdue Univ., West Lafayette, Ind, US.

Thompson, P.D and Shepard, R.W. (2000). "AASHTO Commonly-Recognized Bridge Elements, Successful Applications and Lessons learned." paper prepared for the National Workshop on Commonly Recognized Measures for Maintenance.

Tinkey, Y., and Olson, L.D. (2010). "Vehicle-Mounted Bridge Deck Scanner." Final Report for Highway IDEA Project 132, Highway IDEA Program, Transportation Research Board, USA.

Tsai, D. M., Lin, C. T., and Chen, J. F. (2003). "The evaluation of normalized cross correlations for defect detection." *Pattern Recognition Letters*, Elsevier, Vol. 24, Iss. 15, November, pp. 2525-2535.

Tsai, D. M., Lin, C. T. (2003). "Fast normalized cross correlation for defect detection." *Pattern Recognition Letters*, Elsevier, Vol. 24, Iss. 15, November, pp. 2625-2631.

Valliappan, S., and Pham, T.D. (1993). "Constructing the Membership Function of a Fuzzy Set with Objective and Subjective Information." *Computer-Aided Civil and Infrastructure Engineering*, Wiley, Vol. 8, Iss. 1, January, pp. 75-82.

Vanier, D.J. (2000). "Asset Management 101: A Prime, Inovations in Urban Infrastructure", Seminar of the APWA International Public Works Congress, Louisville, KY, USA, pp.1-14 <www.nrc-cnrc.gc.ca/obj/irc/doc/pubs/nrcc44300.pdf> (Mar. 21, 2012).

WSDOT. (2010). "Washington State Bridge Inspection Manual." Washington State Department of Transportation.

Weather History for Allentown, Pennsylvania, The Weather Underground Inc. <http://www.wunderground.com/history/airport/KABE> (Mar. 10, 2014).

Wagstaff, K., Cardie, C., Rogers, S., and Schrödl, S. (2001). "Constrained k-means clustering with background knowledge." In ICML, June, Vol. 1, pp. 577-584.

Weil, G.J. (2004). "Infrared Thermographic Techniques." In: *Handbook on Nondestructive Testing of Concrete*, 2nd Ed., ASTM & CRC.

Weyers, R. E. (1998). "Service life model for concrete structures in chloride laden environments." *ACI Materials Journal*, Vol. 95, Iss. 4, pp. 445-453.

Yan, J.M., and Vairavamoorthy, K. (2003). "Fuzzy Approach for Pipe Condition Assessment," *ASCE International Conference on Pipeline Engineering and*

Construction, pp. 466-476.

Yang, C.C., and Bose, N.K. (2006). "Generating fuzzy membership function with self-organizing feature map." *Pattern Recognition Letters*, Elsevier, Vol. 27, Iss. 5, April, pp. 356-365.

Yang, T., Ignizio, J.P., Kim, H.J. (1991). "Fuzzy programming with nonlinear membership functions: piecewise linear approximation." *Fuzzy Sets and Systems*, Elsevier, Vol. 41, Iss. 1, May, pp. 39-53.

Yao, I. (1980). "Damage Assessment of Existing Structures." *Journal of the Engineering Mechanics Division*, Vol. 106, No. 4, pp. 785-799.

Younis, R., and Knight, M.A. (2010). "A probability model for investigating the trend of structural deterioration of wastewater pipelines." *Tunnelling and Underground Space Technology*, Elsevier, Vol. 25, Iss. 6, December, pp. 670-680.

Zadeh, L.A. (1965). "Fuzzy Sets." *Information and Control*, Vol. 8, No. 3, pp. 338-353.

Zayed, T.M. (2001). "Assessment of Productivity for Concrete Bored Pile Construction," Ph.D thesis, Purdue Univ., West Lafayette, Ind, U.S.

Zhao, Z., and Chen, C. (2002). "A fuzzy system for concrete bridge damage diagnosis." *Computers & Structures*, Elsevier, Vol. 80, No. 7-8, pp. 629-641.

Zhou, Y., Vairavamoorthy, K., and Grimshaw, F. (2009). "Development of a Fuzzy Based Pipe Condition Assessment Model Using PROMETHEE." *Proceedings of World Environmental and Water Resources Congress*, ASCE, pp. 4809-4818.

Zhu, C., Wang, Z., and Shan, X. (2011). "Evaluation of Rail Network Based on

Analytic Network Process." *Proceedings of the Third International Conference on*

Transportation Engineering (ICTE), ASCE, pp. 31-36.

A. Description of NDE Techniques for Inspection of Concrete Bridges

A.1. Half-cell Potential (HP) Method

The Half-cell Potential (HP) is an electrical method that is used to delineate probable areas on concrete structures with rebar corrosion. It is known that corrosion is an electrochemical process that involves flow of charges, i.e. electrons and ions, at many tiny electrolytic cells. At the anode of each of these electrolytic cells, iron atoms lose its electrons and move into surrounding concrete as ferrous ions. The free electrons left from this process remain in the rebar and give the rebar negative charge. The half-cell potential method is therefore based on detecting of these negative charges to find out the regions with likely corrosion activities. The instrument for half-cell potential method is described in ASTM C 876 and is illustrated in Fig. A.1. As can be seen, the apparatus consists of a coper-coper sulfate half-cell, connecting wires, and a high-impedance voltmeter. The positive terminal of the voltmeter is attached to the reinforcement and the negative one is attracted to the coper-coper sulfate half-cell. The reason high-impedance voltmeter is used is to limit the current flowing through the circuit. The half-cell makes the electrical contact with the concrete by means of a porous plug and a sponge that is moistened with a wetting solution.

If the rebar is corroding, the free electrons would tend to flow from the rebar to the half-cell and then they would be consumed in a reduction reaction, making the copper ions in the copper sulfate solution to be transformed into copper atoms that deposit onto the

rod. Because of the way the terminals of the voltmeter are connected in the circuit as previously described, the voltmeter would indicate a negative value. The more negative the voltage reading, the higher likelihood that the rebar is corroding.
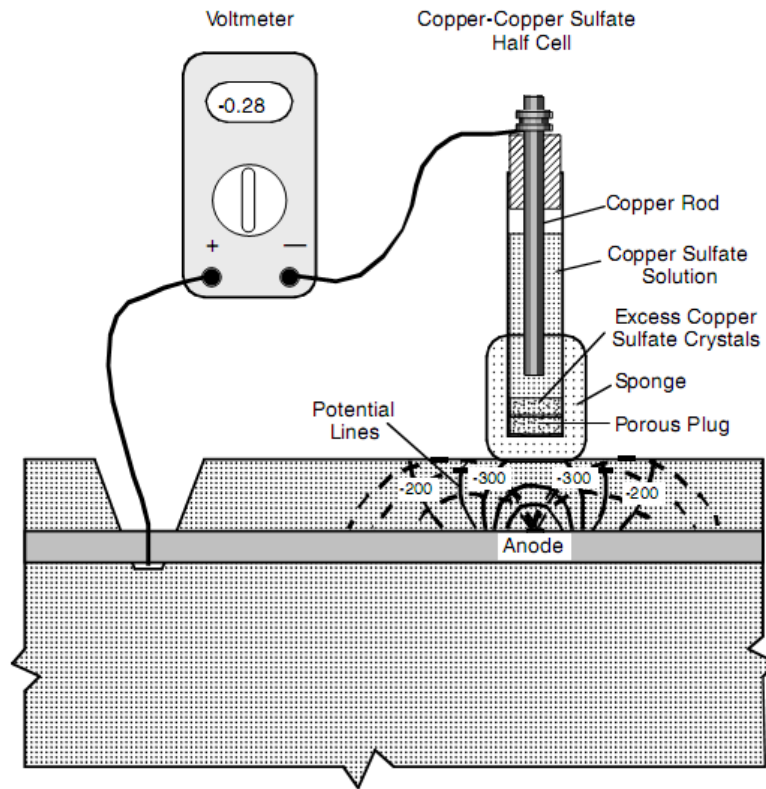

Fig. A. 1 Apparatus for Half-cell Potential method (ASTM C 876)

As can be seen in Fig. A.1, the half-cell potential method needs the electrical access to the reinforcement. It is therefore not applicable to epoxy-coated reinforcement, and in order for the method to work, the electrical connectivity between the rebars is also required. In using the method, testing is usually performed at points arranged in a grid. The required spacing between these testing points depends on specific structures, and for concrete bridge decks, ASTM C 876 recommends a spacing of 1.2 m. If the differences in voltages between adjacent points are greater than 150 mV, it suggests that

a closer spacing is necessary.

Another key requirement of half-cell potential test is that the concrete has to be sufficiently moist. If the measured potential at a test point does not change by more than ±20 mV within 5-minute period, the moisture is considered sufficient (ASTM C 876). Otherwise, the concrete surface has to be wetted, using one of two approaches described in ASTM C 876. One other issue has to be taken into consideration is when the test is performed outside of the range of 17 to 28^0C, a correction factor will have to be applied to the measured voltages.

The data from half-cell potential survey can be presented using either one of two methods, namely, equipotential contour map, or cumulative frequency diagram. The equipotential contour map, more commonly used method, first draws test points on scaled plan view of the tested area. The half-cell potential reading at each point is then marked on the plan and then equipotential contours are created. Example of equipotential contour map is taken from FHWA (2006) and shown in Fig. A.2. The Fig. illustrates an equipotential contour map for a concrete bridge deck with the contour interval of -0.05 V, and the negative sign is omitted before each number.
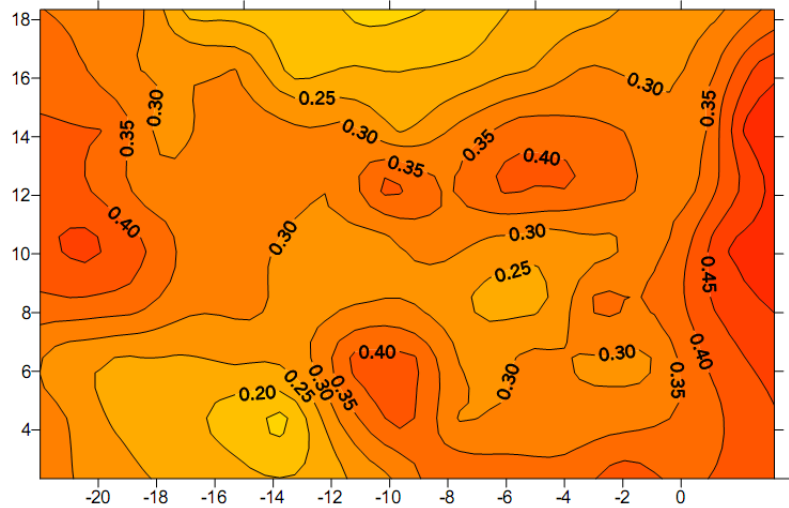
Fig. A. 2 Example of equipotential contour map (FHWA 2006)

The cumulative frequency diagram is a plot used to determine the distribution of the measured half-cell potentials. It is created by plotting the test data on normal probability paper and then a straight line that best fits to the data is drawn. Fig. A.3 provides an example of cumulative frequency diagram, taken from Sharp (2004), for three samples of half-cell potential data. What is provided in cumulative frequency diagram is the percentage of potential readings that are more negative than a certain value.
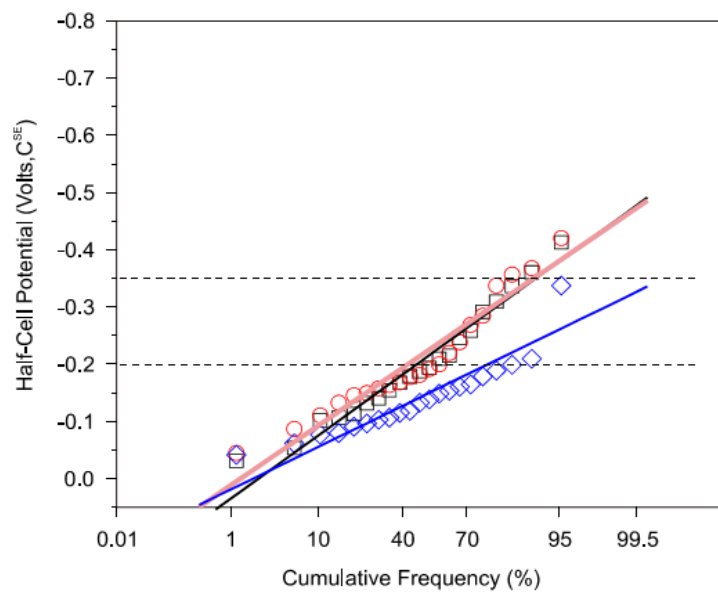
Fig. A. 3 Example of cumulative frequency diagram (Sharp 2004)

Regarding data interpretation, according to ASTM C 876, to formulate appropriate conclusions about corrosion activity, half-cell potential method should be used in combination with other data such as chloride content, depth of carbonation, delamination survey, and the exposure condition of the inspected concrete structures. There are two major techniques, or combination of the two, for interpretation of test results, namely, numeric magnitude technique and potential difference technique.

In numeric magnitude technique, the value of half-cell potential reading is used as an indicator of likelihood of corrosion activity. Specifically, if an area has the potential readings that are more positive than − 200 mV, there is likelihood, more than 90% probability, that no corrosion is occurring at the time of measuring. If the readings are more negative than − 350 mV, there is likelihood that it has active corrosion. Lastly, when the value lies between the two, the existence of corrosion activity is not known with certainty.

In potential difference technique, the areas of active corrosion are diagnosed based on its high potential gradients. These regions can easily be delineated on the contour map where the voltage contours get closer to each other.

A.2. Concrete Resistivity

Because half-cell potential method provides no indication of corrosion rate at the time of measurement, some techniques have been devised to supplement the technique and one of these is concrete resistivity test. It is known that when the reinforcement loses its natural passive oxide coating film, the corrosion activity will depend on the

availability of oxygen for cathodic reaction and also on electrical resistance of the concrete, the factor that controls the transportation of ferrous ions from anodes to cathodes. Concrete resistivity method is used to acquire this information, i.e. electrical resistance of the concrete.

Currently, there is no ASTM test method for measuring resistivity of in-place concrete (Carino 2004a). Instead, the classical technique to measure soil resistivity is normally used. The apparatus for this test, as shown in Fig. A.4, includes four equally spaced electrodes that electrically connected to the concrete surface when tested, using a conducting cream. As can be seen, the outer electrodes are connected to a source of alternating current and an Ammeter, while a Voltmeter is used to connect the inner electrodes.
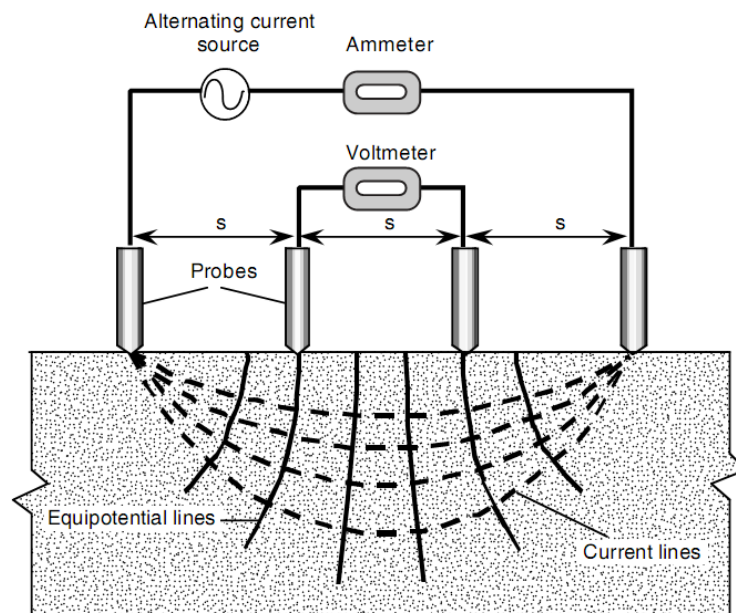

Fig. A. 4 Apparatus for Resistivity Test (Bungey and Millard 1996)

The result of the test displayed by Ammeter (I) and Voltmeter (V) are used to calculate

electrical resistance of a unit cube (ρ) of the concrete, employing Equation A.1

$$\rho = \frac{2\pi sV}{I} \qquad\qquad (\text{A.1})$$

The value of electrical resistance obtained is then used in conjunction with the half-cell potential test to estimate the corrosion rate of the reinforcement.

A.3.   Polarization Method

Like concrete resistivity method, polarization test provides another means to overcome the major drawback of half-cell potential method, i.e., no information about the rate of corrosion. The term "*polarization*", in corrosion science, refers to the change in the open-circuit potential as a result of the passage of current (Davis et al. 1998). For a small perturbation of the open circuit potential, there is a linear relationship between the change in voltage, ΔE, and the change in applied current per unit area of electrodes, ΔI, and this ratio is called the polarization resistance, R_p, and (Carino 2004a).

Fig. A.5 shows the instrumentation to perform the polarization test. The test involves the following main steps: (1) Making an electrical connection to the reinforcement; (2) Locate the rebar whose corrosion rate to be measured, wet the surface and place the equipment over the center of the rebar; (3) Measure the open-circuit half-cell potential, E_o, as illustrated in Fig. A.5(A); (4) Switch on to make a close circuit that produces a small change in voltage, ΔE, and measure the current, I_p, as shown in Fig. A.5(B); (5) Repeat the above steps for different values of potential; (6) Calculate the area of the rebar that is affected by the measurement; and finally (7) Plot the potential vs. the current per unit area of the bar and determine the best-fit straight line. This straight line

represents the polarization resistance and in terms of the unit it can be visualized through Equation A.2. The polarization resistance is then used to calculate the corrosion rate, i_{corr}, using Equation A.3.
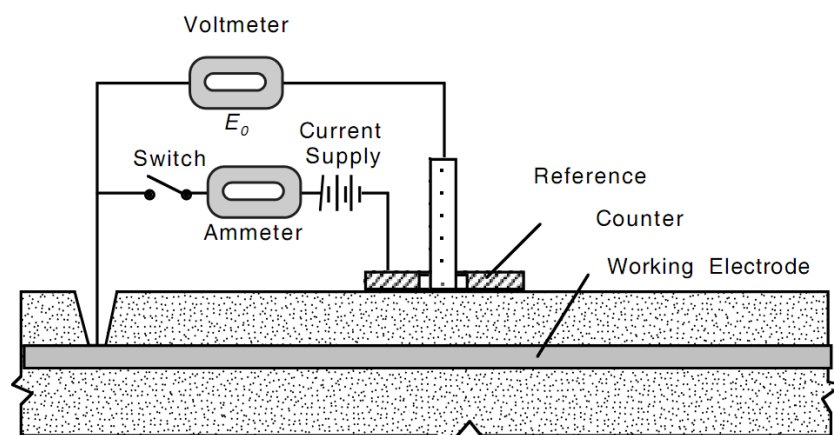
$$R_p = \frac{\Delta E}{\Delta i} \qquad \text{(A.2)}$$

$$i_{corr} = \frac{B}{R_p} \qquad \text{(A.3)}$$

Where:

i_{corr}: corrosion current density (ampere/cm^2)

B: is a constant (Volt)

R_p: Polarization resistance (ohms .cm^2)

(A) Measure open circuit potential, E_o

192

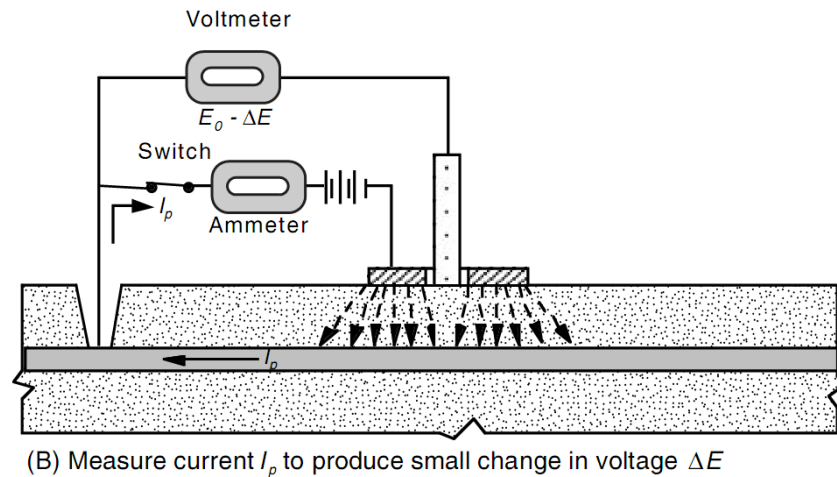(B) Measure current I_p to produce small change in voltage ΔE

Fig. A. 5 Polarization Test (Carino 2004a)

A.4. Chain Drag Method

The chain drag is maybe the simplest technique for detecting top rebar delamination of exposed reinforced concrete bridge decks. The apparatus and procedure to perform this test is described in ASTM D4580 – 03 (2007). The technique is based on sound effect when a metal chain, a steel rod, or a hammer is dragged over the surface of the concrete bridge deck. Over non-delaminated concrete areas, a clear and sharp ringing sound will be produced while in delaminated areas, the dull and hollow sound, resulting because of void and discontinuity, will be perceived. By listening and differentiating these sounds, the operator will be able to locate the delaminated areas over the entire surface of the concrete bridge deck.

Although the technique is found very effective in assessment of bare concrete decks, it is, however, reported being much less sensitive for assessment of concrete bridge decks that are overlaid with asphalt pavement (Barnes 1999). In those structures, the asphalt pavement acts as an insulator that reduces the transmission of sonic energy to the

concrete and back to the surface, resulting in low amplitude volume and distorted reflecting sounds. For this practical reason, the chain drag is usually employed by transportation agencies to determine the removal areas on asphalt-covered concrete bridge decks those have been prepared for repair, after the asphalt layer has been removed.

Even in exposed concrete bridge decks, a main drawback of the chain drag method is that the inspection result is subject to operator's technique and interpretation. Especially, with noise from traffic flow and after hours of operation, the auditory sense of the operator normally tends to become insensitive. Another big limitation of the chain drag technique is that it cannot detect reinforcement corrosion, a major type of defect for comprehensive assessment of concrete structures. When detectable depth is concerned, it is reported that the method is able to detect delamination at the depth of 1 to 3 inches, depending on the size of chain link used, with the accuracy to be within ten and twenty percent of the total delaminated area (Barnes 1999).

A.5.   Pulse Velocity Method

Like spectral analysis of surface waves and impact echo method that will be described in the next two sections, the pulse velocity test belongs to the family of ultrasonic (or stress wave) methods. These stress waves are produced when pressure or deformation is suddenly applied to the surface of a solid. The disturbance then propagates through the solid and the speed of propagation, in an elastic solid, has been found, is a function of several factors such as the modulus of elasticity, Poisson's ratio, the density, and the geometry of the object (Davis et al. 1998). Having the knowledge of this dependence

allows one to infer about the characteristics of a solid by monitoring the propagation of stress waves in the object.

According Naik et al. (2004), there are three types of stress wave propagation, including: (1) compressional waves (also called longitudinal or P-waves); (2) shear waves (also called transverse or S-waves); and (3) surface waves (also called Rayleigh waves). Each of these waves has its own characteristics in which the compressional waves propagate through the solid medium in a manner similar to how sound propagates through the air. In terms of velocity, for a given solid, compressional waves have the highest velocity while the surface waves have the lowest rank.

The basic idea on which the pulse velocity method is built is that the velocity of a pulse of compressional waves propagating through an elastic medium depends on the elastic properties and the density of the medium as represented in Equation A.4. In a concrete element, variations in density can arise as a result of non-uniform consolidation while variations in elastic properties can occur because of variations in aggregate sizes, mix proportions or curing. Therefore, by measuring the pulse velocity at different points in a concrete element, it is possible to make inferences about concrete uniformity and quality.

$$V = \sqrt{\frac{KE}{\rho}} \qquad\qquad (A.4)$$

Where:

V = compressional wave velocity

$K = (1 - \mu)/\big((1 + \mu)(1 - 2\mu)\big)$

E = dynamic elasticity modulus

ρ = density

μ = dynamic Poisson's ratio

The most basic configuration for pulse velocity test, adapted from ASTM C 597 – 02, is shown in Fig. A.6. As can be seen, the instrument consists of two transducers, one for transmitting and one for receiving ultrasonic pulse. These transducers primarily generate compressional waves at predominantly one frequency with most of the ultrasonic energy directed along the axis orthogonal to the transducer face. The frequency that is used for testing concrete structures normally range between 25 and 100 kHz (Naik et al. 2004). Along with two transducers, the instrument also comes with time measuring circuit and time display unit. These units allow travel time between two transducers to be measured and recorded. The known distance between two transducers is then used to calculate compressional wave velocity using Equation A.5.
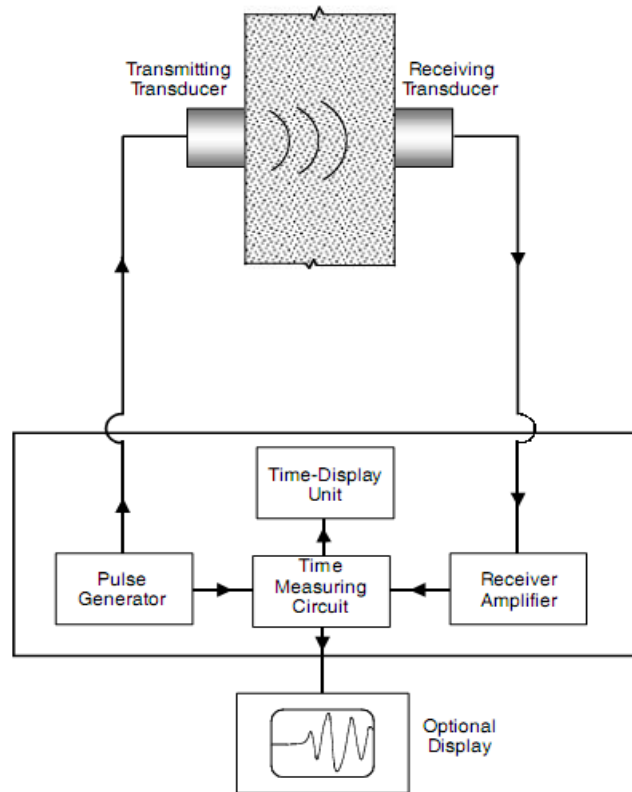
Fig. A. 6 Schematic diagram of pulse velocity test (ASTM C 597-02)

$$V = \frac{L}{\Delta t} \qquad \text{(A.5)}$$

Where:

L = distance between two transducers

Δt = pulse travel time between two transducers

Based on the basic idea as described above, many more complicated configurations of the pulse velocity method have been studied for specific applications. Successful applications of the method for concrete assessment, according to Naik et al. (2004), include: (1) estimate strength of concrete; (2) study the homogeneity of concrete; (3) monitor the setting and hardening process of concrete; (4) study durability of concrete; (5) measure surface crack depth; and (6) determine dynamic modulus of elasticity.

A.6.   Spectral Analysis of Surface Waves

Also based on principle of stress wave propagation, however as its name implies, spectral analysis of surface wave (SASW) employs some special characteristics of surface wave, i.e, Rayleigh or R-wave, to infer elastic properties of the solid object under investigation, normally a layered structural system such as soil sites, asphalt or concrete pavement systems, and concrete structural members. To have a better understanding how the method works, the characteristics of each stress wave type are going to be described in the following paragraph.

According to Horhota (1996), when an impact or a deformation is created in a solid, the particle motion of P-wave is push-pull movement that is parallel to the direction of wave propagation. Conversely, the particle movement of S-wave is in shearing manner that is normal to the propagating direction. For R-wave, it is found having both vertical and horizontal components, and the path of its motion is a retrograde ellipse. A very special characteristic of surface wave that makes it different from P- and S-waves is that it only exists in region near the solid surface and the affected depth is dependent on the frequency of vibration, as being found almost equal to one wavelength (l). It is also found that while P- and S-waves generated by an impact propagate outward along a hemispherical wave front, that wave front of R-waves has a cylinder shape.

Coming back to the main idea of SASW method, it is known from previous discussion on pulse velocity method that the velocity of stress wave propagation is dependent on the elastic properties of the solid medium. In layered systems, these properties change between different layers and this offers an ideal opportunity for the application of

surface wave theory. The principle is that, by varying the vibration frequency, the resulting wavelength or the depth of surface wave penetration will change. Once this penetration depth changes, the average elastic properties of the medium over its length will be affected, depending on the number of layers it covers. As a result, the surface wave velocity, measured at different frequency, will not be the same. This principle of the SASW method is called "dispersion" and it can be visualized as shown in Fig. A.7. The configuration for the SASW test, based on dispersion principle above, has progressed over time. During early days of the SASW method development, an impactor or vibrator that generates a single frequency is used. For each frequency, to determine its wavelength, the receivers need to be moved and adjusted until the phase difference between them is 360 degree. Knowing the frequency and the wavelength allows the surface wave velocity corresponding to that wavelength to be calculated. By varying the generated frequency and using the same computing procedure, the dispersion curve, i.e., surface wave speed vs. wavelength, will be plotted. A process, called inversion, will finally be used to obtain the approximate stiffness profile of the system. The process to attain the dispersion curve in this manner is, however, very time consuming. As a result, in the early 1980s, researchers at the University of Texas at Austin began studies of a surface wave technique that can use an impactor or vibrator to generate a range of frequencies (Davis et al. 1998). The relationship between wavelength and velocity was then investigated using advanced signal processing technique that they called spectral analysis of surface waves. Since then, this name has become popular for the method as it is currently being discussed. The configuration to

perform the test that developed at University of Texas at Austin is going to be presented in the next paragraphs.
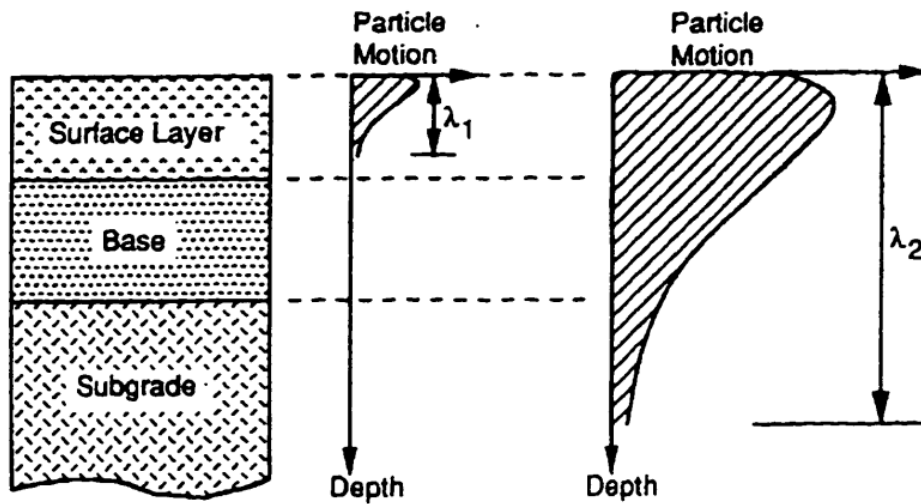

Fig. A. 7 Principle of dispersion for a layered system (Horhota 1996)

As can be seen in Fig. A.8, the apparatus for the test includes an impactor or vibrator to generate surface waves, two receivers that are geophones or accelerometers to monitor the motion as the surface waves propagate along the surface, and a two-channel spectral analyzer to process and analyze the received signals. It is known from elementary vibration theory that the impactor will generate a range of frequencies and the longer contact time of the impact, the broader range of the frequency spectrum will be generated. This property can be used to control a specific application.

As explained previously, a layered system is a dispersive medium for R-waves in which different frequency components propagate at different speeds. For each frequency component, the so-called phase velocity is calculated by measuring the time for its corresponding surface wave to travel between two receivers. As can be seen in Equation A.6, in order to perform that calculation, first the phase differences need to be obtained

by computing cross-power spectrum recorded at two receivers. The phase difference, as a function of frequency, is represented by the phase portions of this resulting spectrum.
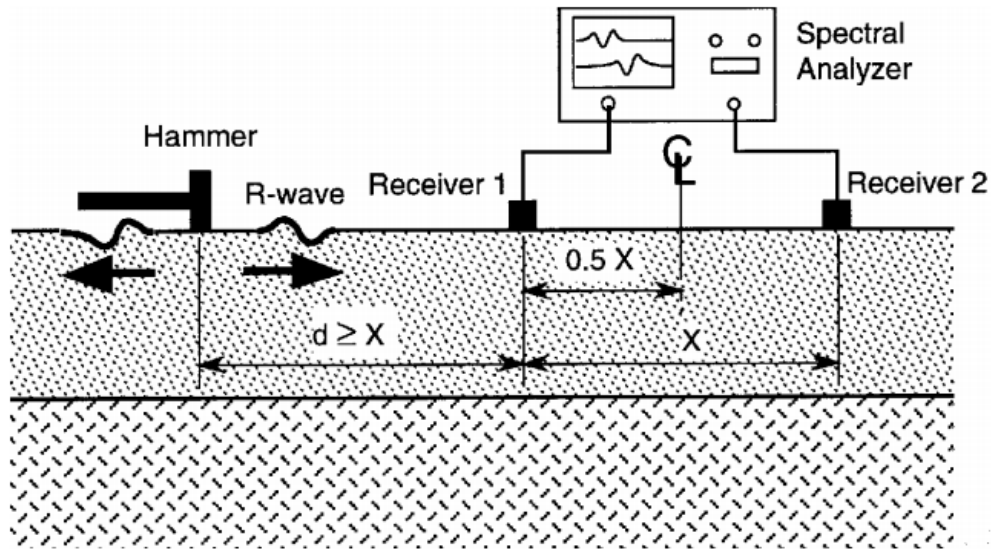

Fig. A. 8 Schematic of SASW method as described in Davis et al. (1998)

$$C_{R(f)} = X \frac{360}{\emptyset_f} f \qquad \text{(A.6)}$$

Where:

$C_{R(f)}$ = surface wave speed of frequency componenet f

X = distance between two receivers

$\emptyset_f$ = phase angle of frequency component f

With respect to procedure to perform inversion, the tested structure is modeled as layers of varying thickness and each layer is assigned a density and elastic constants (Davis et al. 1998). Using this information for the assumed layered system, surface wave

propagation is simulated and theoretical dispersion curve is determined. This theoretical curve is then compared with the experimental one. If they match, the assumed stiffness profile is considered correct and the inversion process ends. Other while, the assumed layered system is refined and the same process continues. Fig. A.9 presents an example of SASW test result for a concrete pavement system that is described in Davis et al. (1998). As can be seen, Fig. A.9(a) shows the calculated dispersion curve while Fig. A.9(b) presents S-wave speeds computed from inversion process. These S-wave speeds can be seen well correlating with the soil profile obtained from field boring as illustrated in Fig. A.9(c).
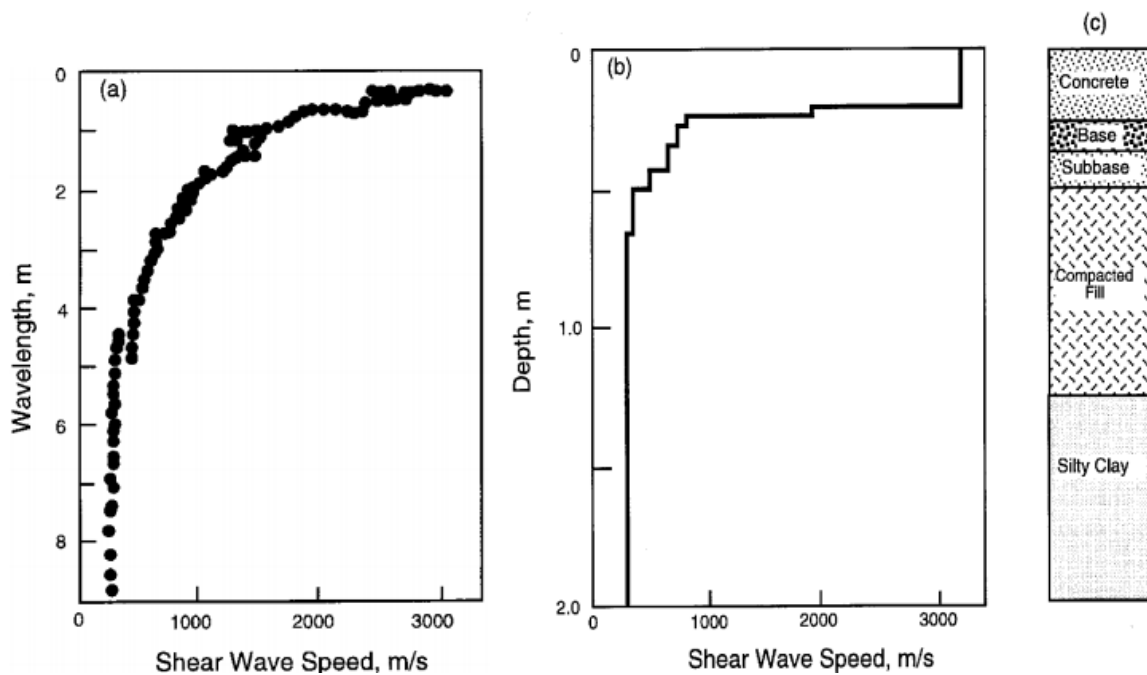

Fig. A. 9 Example of SASW test result described in Davis et al. (1998)

A.7.   Impact Echo (IE) Method

Impact Echo (IE) is the last nondestructive evaluation method of ultrasonic technique family described in this study. It is observed from many previous studies that when a

stress pulse is generated by an impact at a point, the exited energy propagates along the test object in all direction with the hemispherical wavefronts of P- and S-waves. When these wave fronts reach an external or internal interface such as object boundaries, cracks or voids, there will be energy reflections or so-called echoes from these sources. The arrivals of these reflected waves at the test surface where the impact was generated causes displacements that are measured by a receiving transducer and recorded by a data acquisition system (Carino 2004b). It is found that when the receiving transducer is placed adjacent to the impact point, the displacement is dominated by P-wave reflections. The impact echo method is therefore based on principle and property of P-wave propagation as illustrated in Fig. A.10.
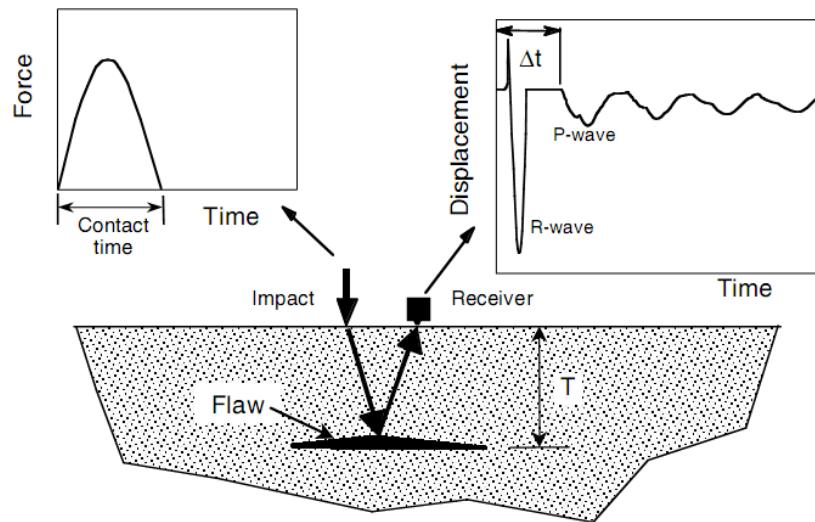

Fig. A. 10 Principle of impact echo method (Carino 2004b)

Regarding signal analysis and data interpretation, during early days of impact echo method development, the analysis is performed in time domain in which the arrival time of reflected wave is used. This method, however, has shown only feasible for very thick

members such as piles and drilled shafts because in such cases there is sufficient time between the generated pulse and the reflected wave. This is obviously not the case for thin structural members such as walls or slabs and therefore the better solution was in need. The new approach, that is much simpler and quicker, based on frequency analysis of displacement waveforms (Davis et al. 1998). Its underlying principle is that the stress pulse generated by an impact will reflect back and forth between the test surface and the medium interfaces, i.e., flaws or boundaries. Because the frequency of the arrival of reflected wave depends on the wave speed and the distance between the interfaces, the displacement waveform recorded at the receiver is the combination of many frequency components. This condition is ideal for application of frequency analysis technique. Specifically, the time domain waveform recorded at the receiver is transformed to frequency domain using Fast Fourier Transform (FFT) algorithm. The output of this transform is an amplitude spectrum that provides the relative amplitude of various frequency components contained in the recorded waveform. The shortest path, or thickness, among many reflections would correspond to the peak in the amplitude spectrum. The thickness, D, is then calculated by using the formula in Equation A.7. It is very important to note about the impact echo method that the frequency being discussed is called "thickness" frequency, instead of vibration frequencies as contained in the generated pulse.

$$D = \frac{C_p}{2f} \qquad\qquad (A.7\,)$$

Where:

D = distance, or thickness, between test surface to reflecting interface

C_p = the speed of P-wave propagation

f = peak frequency in the amplitude spectrum

Fig. A.11 provides an example of frequency analysis, described in Carino (2004b), with two amplitude spectra. The Fig. on top illustrates the test over a solid portion of a concrete slab while the Fig. at the bottom shows the test result for a portion of the same slab embedded with a simulated defect. As can be seen, for the solid part, the peak frequency is at 3.42 kHz, corresponding to the echo from slab bottom. This peak is clearly shifted to the higher value, 7.32 kHz, when the simulated void is introduced, meaning the shorter reflecting distance.
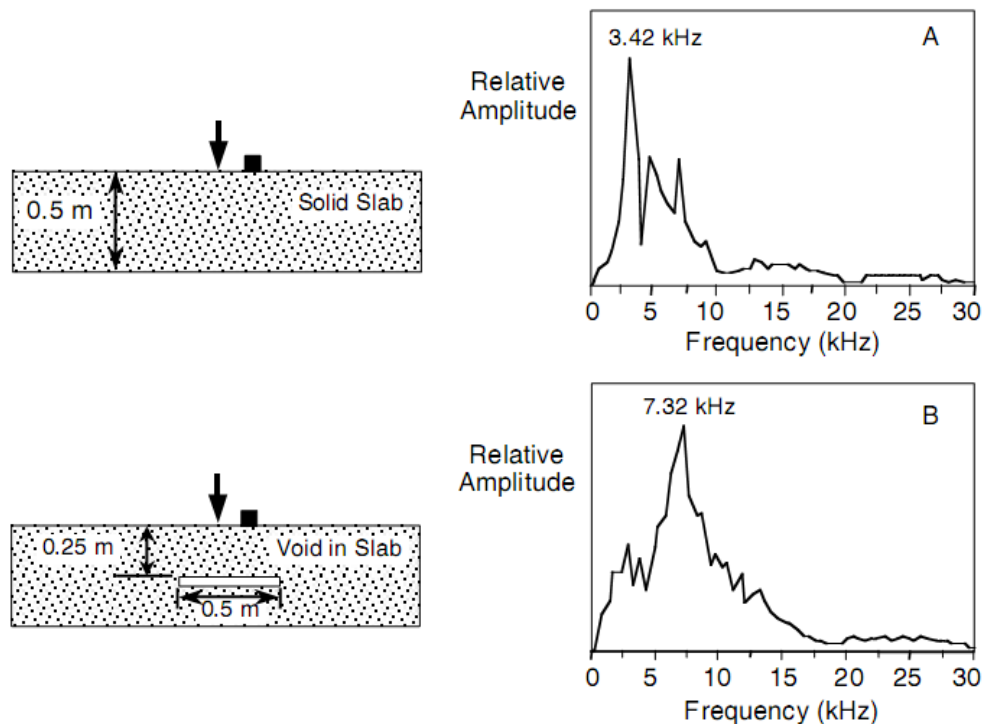

Fig. A. 11 Example of frequency analysis (Adapted from Carino 2004b)

The description above clearly introduces the idea of impact echo method. According to

Davis et al. (1998), the technique has been applied successfully to: (1) determine the thickness and detect flaws in plate-like structural member such as slabs and bridge decks; (2) detect flaws in beams, column and cylindrical structural members; (3) assess the quality of bonds in overlays; and (4) crack depth measurement.

A.8.   Infrared Thermography Method

Infrared thermography technique has proved itself to be an effective, convenient and economical method for testing of concrete structures (Weil 2004). There are two basic principles associated with the technique (Davis et al. 1998). The first principle is that when an object emits energy from its surface, this energy is in form of electromagnetic radiation. It was found that the rate of emitted energy per unit surface area conforms to Stefan-Boltzmann law while the wavelength of radiation depends on the object temperature. When this temperature increases, the radiation wavelength becomes shorter and at a sufficiently high temperature, the object will emit the wavelength that is in the visible spectrum. This high temperature, however, is not usually the case for normal or room condition when concrete is inspected. As a result, the emitted radiations observed during inspection are normally in the range of infrared spectrum. This clearly explains the origin of the name of the method.

The second principle of the technique states that a material with subsurface abnormalities, or defects, will affect the heat flows through its internal structures as illustrated in Fig. A.12. For concrete, these anomalies may include delamination caused by reinforcement corrosion, honeycombs caused by poor consolidation, or pooling fluids caused by water infiltration. As a consequence, the changes in heat flow produces

206

localized differences in surface temperature. Thus, by measuring or detecting these differences, the knowledge of presence and location of any subsurface abnormality can be obtained. The test method for detecting delamination in bridge decks using infrared thermography is standardized, by American Society for Testing and Material, in ASTM D4788-03.
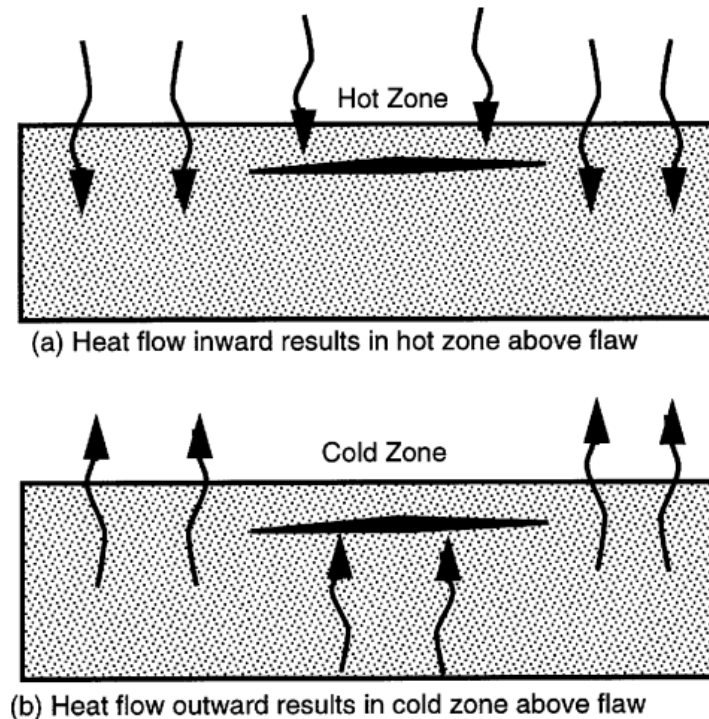

(a) Heat flow inward results in hot zone above flaw

(b) Heat flow outward results in cold zone above flaw

Fig. A. 12 Effect of internal defects on surface temperature during heat flow (Davis et al. 1998)

Regarding the heat source to create the heat-flow condition for the test, although sometimes heating lambs maybe used, it is much convenient and economical to use natural source, i.e., solar energy. Based on solar heating, the test can be performed during day-time when the heat flows into the structure, or during night-time when the heat flow is in the reverse direction. In order for the test to be effective, it is also

recommended that the test should be conducted when the largest heating or cooling gradients are present. Under such condition and if the test is implemented in day-time, the concrete surface above the abnormal area would be hotter than the region with sound concrete. Obviously, the reverse observation will be true if the test is performed in cooling condition.

Several factors that have been found can affect the spectrum observation during the test and therefore need to be taken into consideration (Davis et al. 1998). These factors can be categorized into two groups, namely, physical factors and environmental factors. Of those, the physical parameters include concrete surface emissivity, surface temperature, concrete thermal conductivity, concrete volumetric-heat capacity, thickness of the heated layer, and intensity of incident solar radiation. For environmental factors, it is found that cloud, wind and surface moisture may influence the test result.
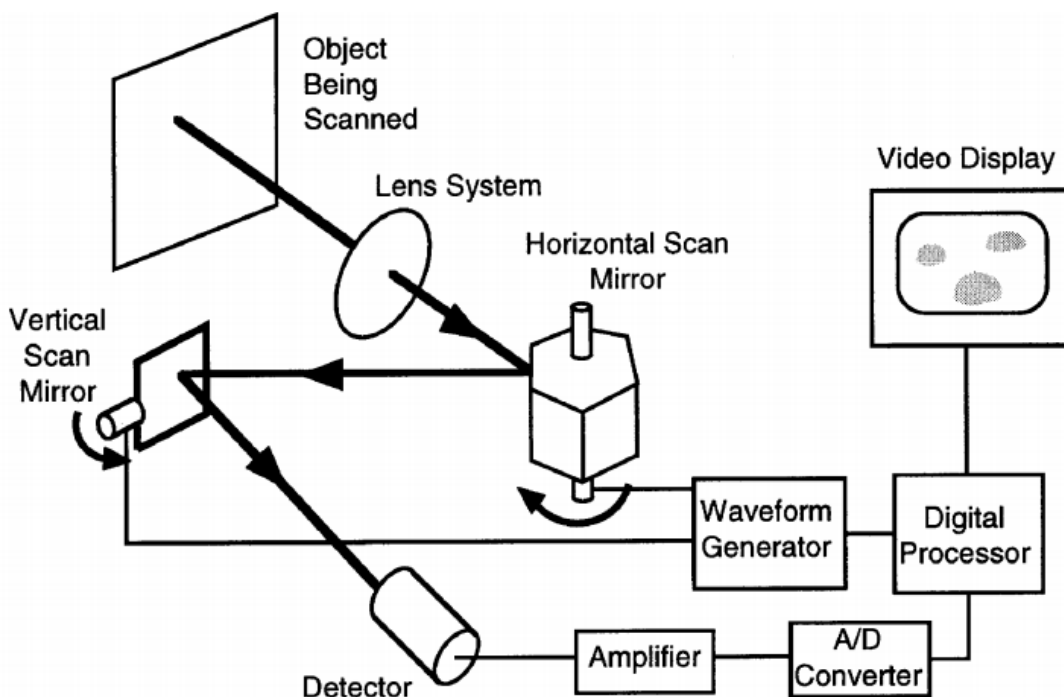
Fig. A. 13 Schematic Infrared Scanner System described in Davis et al. (1998)

With the basic ideas described above, the equipment to perform the test, as described in Davis et al. (1998), consists of three main components: (1) a scanner/detector unit, (2) a data acquisition/analysis device, and (3) a visual image recorder. The complete system is shown in Fig. A.13. The infrared scanner head is an optical camera, with lenses that allows only infrared radiation with wavelengths in the range of 3 to 5.6 μm (shortwave), or 8 to 12 μm (medium wave) to be transmitted. The data acquisition and analysis unit consists of an analog-to-digital (A/D) converter, a computer with a high resolution monitor and a data storage device, along with data analysis software. In order to rapidly scan large areas such as highway or airfield pavements, these instruments can be mounted on a high speed vehicle. Once data have been obtained by the infrared scanner, it is digitized by A/D converter and displayed either using a shaded gray or a color image, depending on data analysis software. Cooler or hotter regions can then be identified by different gray-levels or by various colors. Along with infrared image recording, visual images are also collected, either using videotape recorder, a film or a digital video camera. The images, infrared and visual one, are then compared. The purpose of this is to ensure that the apparent temperature differences in the infrared image are not caused by differences in surface emissivity. An example for this is illustrated in Fig. A.14. As can be seen, if only looking at the infrared image shown in Fig. A.14(b), one would mistakenly conclude that the asphalt patch areas are delamination. Obviously, he would not make that same mistake if the visual image, shown in Fig. A.14(a), is provided.
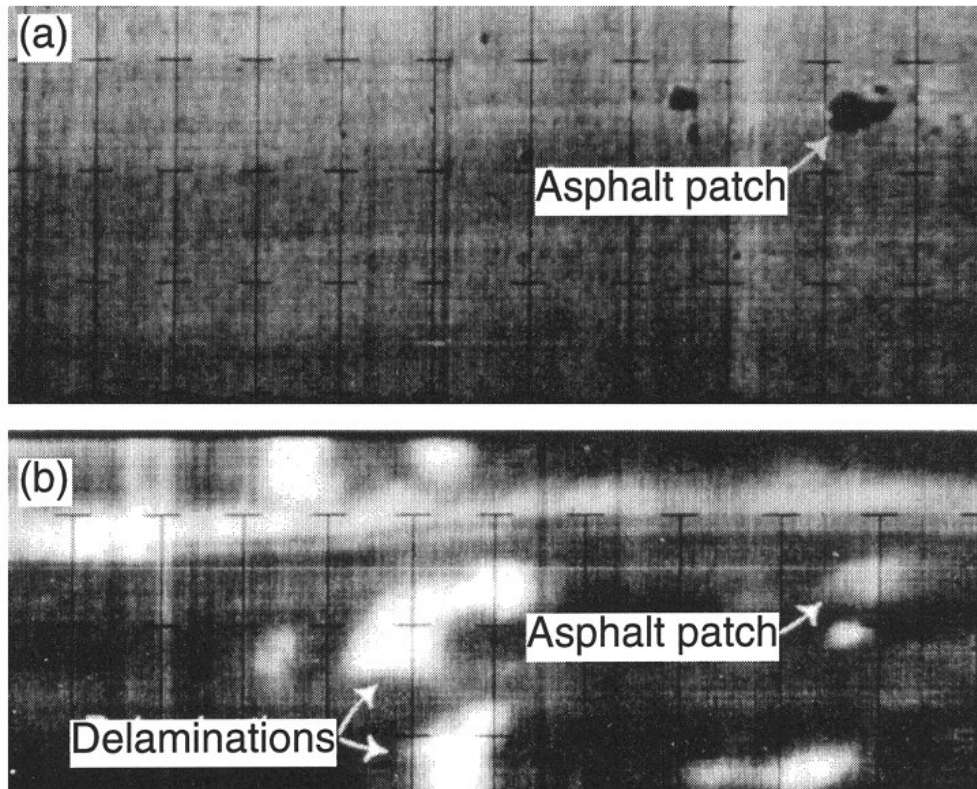
Fig. A. 14 Example of Infrared Thermography (Davis et al. 1998)

A.9. Ground Penetrating Radar (GPR)

Radar is an object-detection technique that was developed before and during World War
Two for military purpose. The term "radar" stands for **ra**dio **d**etection **a**nd **r**anging and
as this full name implies, the technique uses electromagnetic (radio) waves as a means
to detect the presence and location of concerned objects. The earliest civil engineering
application of radar, according to ACI 288.2R-98, was for probing into soil to detect
buried pipelines and tanks. Later, many studies have been performed in this area such
as for detecting cavities below airfield pavements, determining concrete thickness,
locating voids or reinforcing bars, and identifying deterioration.

Unlike traditional radar that detects objects in very long distances, objects or defects in

civil engineering that need to be discovered usually locate inside the structures and at a relatively shallow depth below the surface. To ensure the resolution for clearly differentiating between adjacent objects, the radars designed for civil engineering application therefore need to emit only a very short pulse of electromagnetic energy. As a result, the name short-pulse radar has frequently been used for these types of radar. The more commonly used name for the technique is, however, ground penetrating radar (GPR). It is explained that when detecting civil engineering objects, the antenna is normally coupled towards the ground or the structures instead of being coupled upward into the air like conventional radars.

The fundamental working principle of radar is based on the propagation behavior of electromagnetic (EM) wave. It is observed that when a beam of EM energy encounters an interface between two mediums of different dielectric constants, a portion of energy is reflected back while the remainder penetrates through the interface and goes into the second medium. The intensity of reflected energy, AR, is found depending on the intensity of incident energy, AI, at the interface and the relative dielectric constants of the two mediums, ε_{r1} and ε_{r2}. This relationship is described in Equation A.8 (Clemeña 2004).

$$AR = AI \frac{\sqrt{\varepsilon_{r1}} - \sqrt{\varepsilon_{r2}}}{\sqrt{\varepsilon_{r1}} + \sqrt{\varepsilon_{r2}}} \tag{A.8}$$

Fig. A.15 clearly illustrates the principle above. To inspect a structure such as pavement or bridge deck, an antenna is dragged manually over the inspected surface or attached to a vehicle in order to scan with much higher, or traffic, speed. This antenna transmits

a short pulse of electromagnetic energy into the surveyed structure. The energy reflected at various material interfaces is then received by another antenna, or sometime by the same antenna, to produce the output signal that is proportional to the amplitude of the reflected electromagnetic field. By analyzing these received signals, the objects, defects, or different material layers hidden inside the structure can be identified.

It should be noted in Fig. A.15 that, although the shapes of reflection signal at different interfaces look the same, their directions (or polarity) are however different. This effect, in radar theory, is called *change in polarity* or *phase reverse* and it happens when the relative dielectric constant of the medium before reflection is smaller than the relative dielectric constant of the medium after reflection, making the result of Equation A.8 negative. Specifically, it can be seen in the Fig. that the polarity of surface reflection is different from those of original pulse as well as interface and bottom reflection. This is explained because the dielectric constant of air (the first medium) is smaller than the dielectric constant of concrete (the second medium).
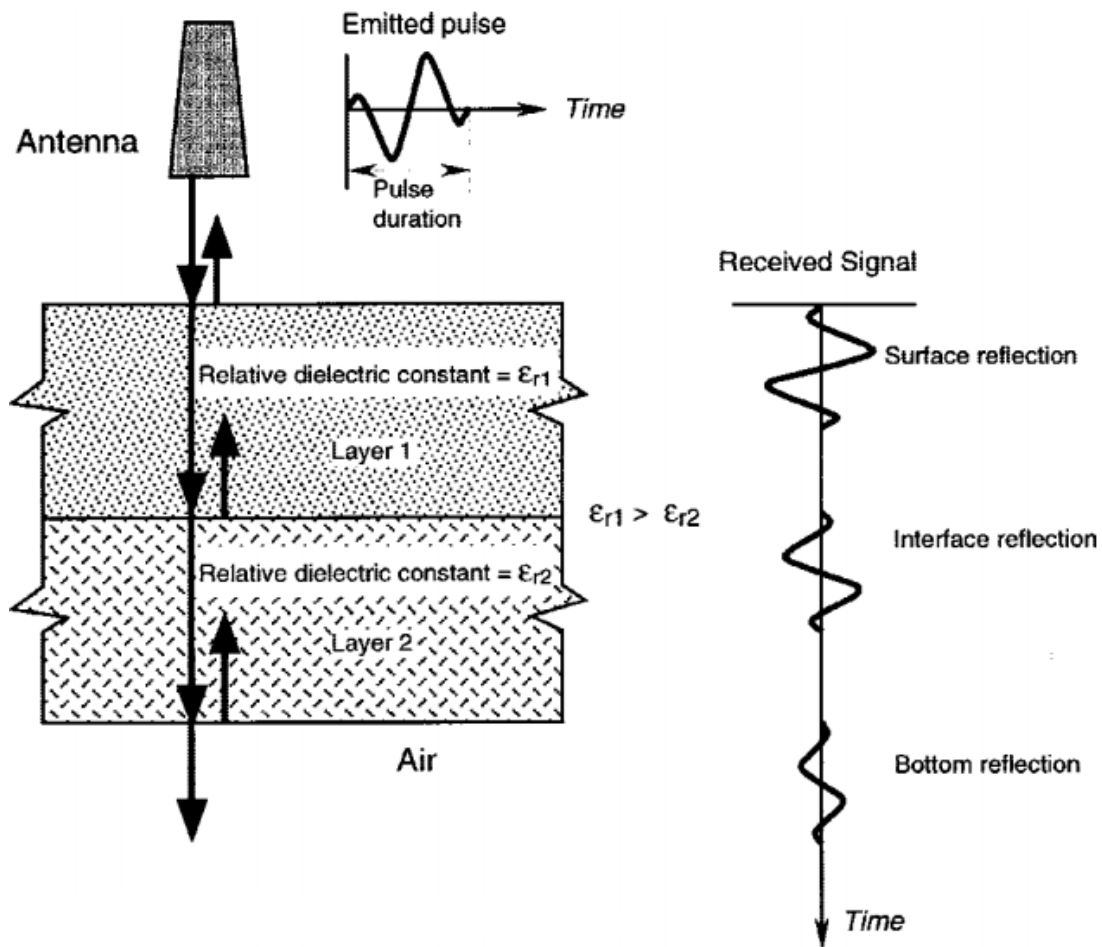
Fig. A. 15 Principle of GPR method (Davis et al. 1998)

In addition to dielectric constant as described above, another very important factor that affects the received signal is the electrical conductivity of different propagation mediums. This property of particular material determines the energy loss when an electromagnetic wave is propagated through its medium, as approximated by Equation A.9 (Bungey and Millard 1993). Interestingly, it was found that the conductivity of concrete increases with the increasing frequency (Halabe et al. 1993). This also means that the electromagnetic wave of lower frequency can penetrate deeper inside the structure than those of higher frequency.

$$\alpha = 1.69 \times 10^3 \frac{\sigma}{\sqrt{\varepsilon_r}} \qquad\qquad (A.9)$$

Where:

α = signal attenuation (dB/m)

σ = conductivity of propagating medium ($\Omega^{-1}m^{-1}$)

ε_r= relative dielectric constant of propagating medium

Based on the fundamental principles and physical properties of electromagnetic waves explained above, typical instrumentation for a GPR system includes: an antenna unit, a control unit, a displace equipment, and a storage device. While the antenna unit, as has been described, emits and receives electromagnetic energy, the control unit is the heart of the system. It plays many roles such as providing electrical power to create the pulse; controlling pulse repetition frequency, acquiring and amplifying the received energy, and finally transferring the output to the displace equipment. Regarding storage device, GPR data may be stored in an analog recorder or in a digital storage device for later analysis and interpretation. The data, according to Davis et al. (1998), can then be presented by the displace equipment using either oscillographs that plot a succession of recorded waveforms (topographic or waterfall plot), as illustrated in Fig. A.16, or graphic facsimile recorders that provide a cross-sectional representation of the tested object. An example of the latter technique is presented in Fig. A.17. As can be seen, Fig. 2.20(b) shows time history of the received waveform from a test object containing a simulated delamination provided in Fig. A.17(a). This received waveform is then thresholded and when the amplitude exceeds the threshold range, the pen of the graphic

recorder plots a solid line on the recording paper. The line is plotted in varying gray level depending on the actual amplitude of the signal. When the GPR system scans across the test object above, the output obtained is displayed on graphic recorder as shown in Fig. A.17(c).
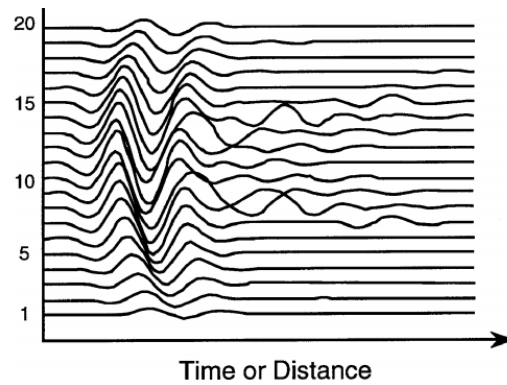

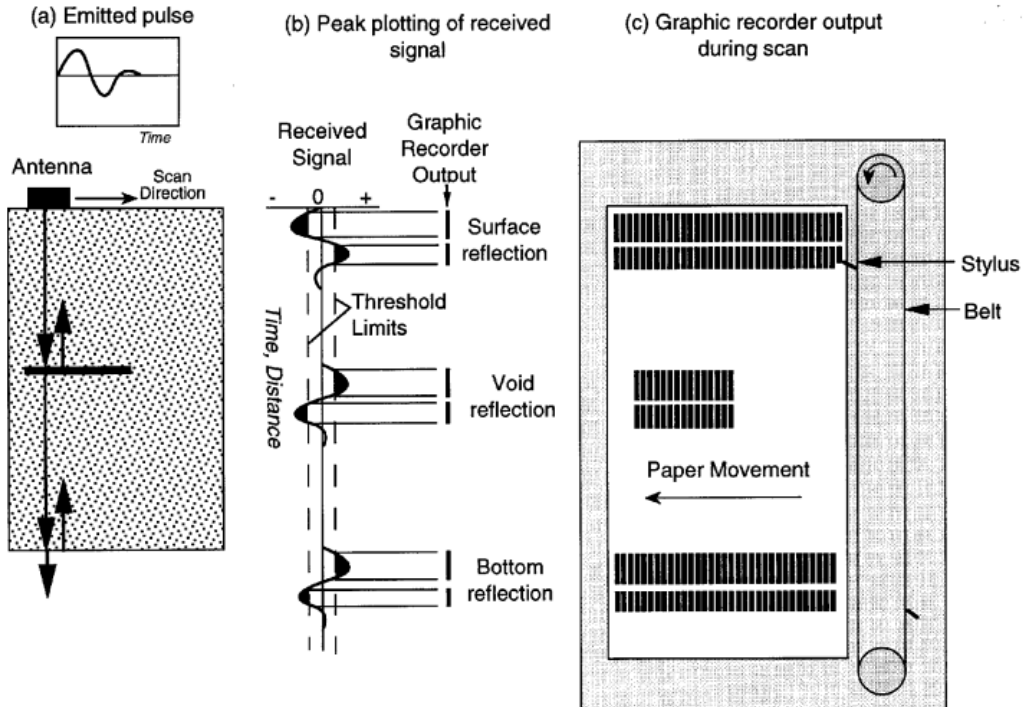**Fig. A. 16 Topographic plotting of GPR data described in Davis et al. (1998)**

Fig. A. 17 Graphic facsimile recorder technique described in Davis et al. (1998)

Modern GPR system, however, presents GPR data using a gray or color image. In order to do so, first the amplitude values are measured at 256 or 512 points along each scan. This is done electronically in analog form, by voltage measurement. Next, the voltages are digitized in 16-bit format as integers (-32768 to +32768). These integers can then be used directly for display by a 16-bit image or be converted to be displayed in an 8-bit image. In the image, each of these integers represents the intensity of each pixel. It is noted that while the height (number of pixels) of the image is either 256 or 512, depending on the number of points chosen from beginning, the width of the image varies, subject to the length of each scanning pass. Example of GPR image for reinforced concrete structure is shown in Fig. A.18. Another option for displaying data by modern GPR systems is that the operator can choose to display only an individual waveform. Example of this can be seen in Fig. A.19.
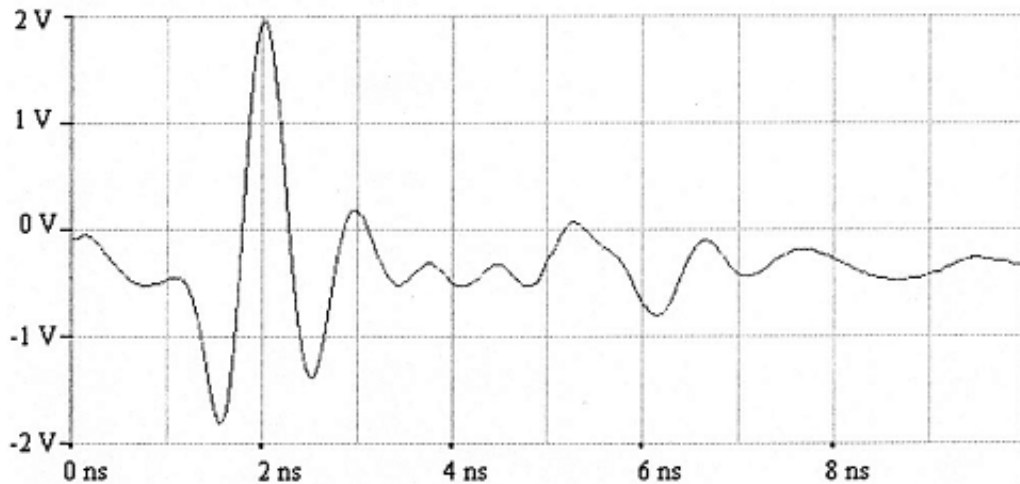

Fig. A. 18 Example of GPR image

216

Fig. A. 19 Example of individual GPR waveform

Regarding data analysis and interpretation, since GPR has a high rate of pulse generation repetition, it produces a huge amount of data. Traditional interpretation techniques, as described in Davis et al. (1998), include: (1) cluster analysis; (2) topographic plotting; (3) Quantitative peak tracking; and (4) peak plotting.

Cluster analysis is basically a method for comparison between individual signals. It was proposed by Cantor (1984) in which individual waveforms are clustered into groups of similar signals based on the result of direct comparison. Each group is then correlated with the reference signals caused by known condition obtained from visual inspection, coring or excavation. The final output of this technique is a strip chart that indicates, at each test position, type of defect and confidence measure of the prediction. Mathematically, this confidence measure indicates the closeness of fit of the individual signal at that position to the reference signal associated with that cluster.

Topographic plotting, as shown in Fig. A.16, may be one of the oldest techniques used for GPR data interpretation. Basically, the technique continuously displays or prints

radar traces at fixed distance like a topographic drawing. The picture or drawing is then visually analyzed and if the traces are found parallel to one another, a unique material is assumed (Cantor 1984). Otherwise, structural anomalies or defects are indicated. Currently, the most commonly used interpretation method is however quantitative peak tracking. Fundamentally, this technique bases on signal processing to quantitatively compute the amplitudes and arrival times of significant reflection peaks in the radar waveform (Davis et al. 1998). These computed numbers are then used to calculate and display structural properties as a depth profile that is illustrated in Fig. A.20, or a plan view contour map as shown in Fig. A.21.

The last technique for interpretation of GPR data, peak plotting, is based on graphic facsimile recorder described previously. It is remembered from our previous description that the output represented on the graphic recorder is a series of dashes, and each two consecutive dashes are associated with an echo, as shown in Fig. A.17. Therefore, like topographic plotting, based on visual analysis of graphic recorder output, any anomaly can be detected.
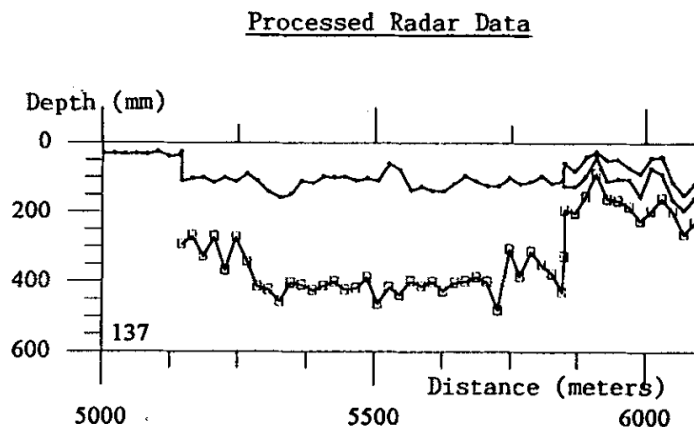

218

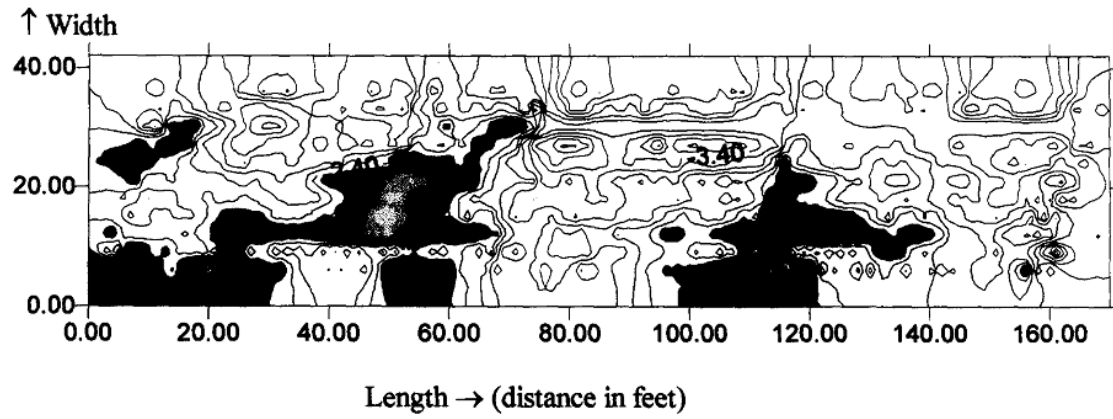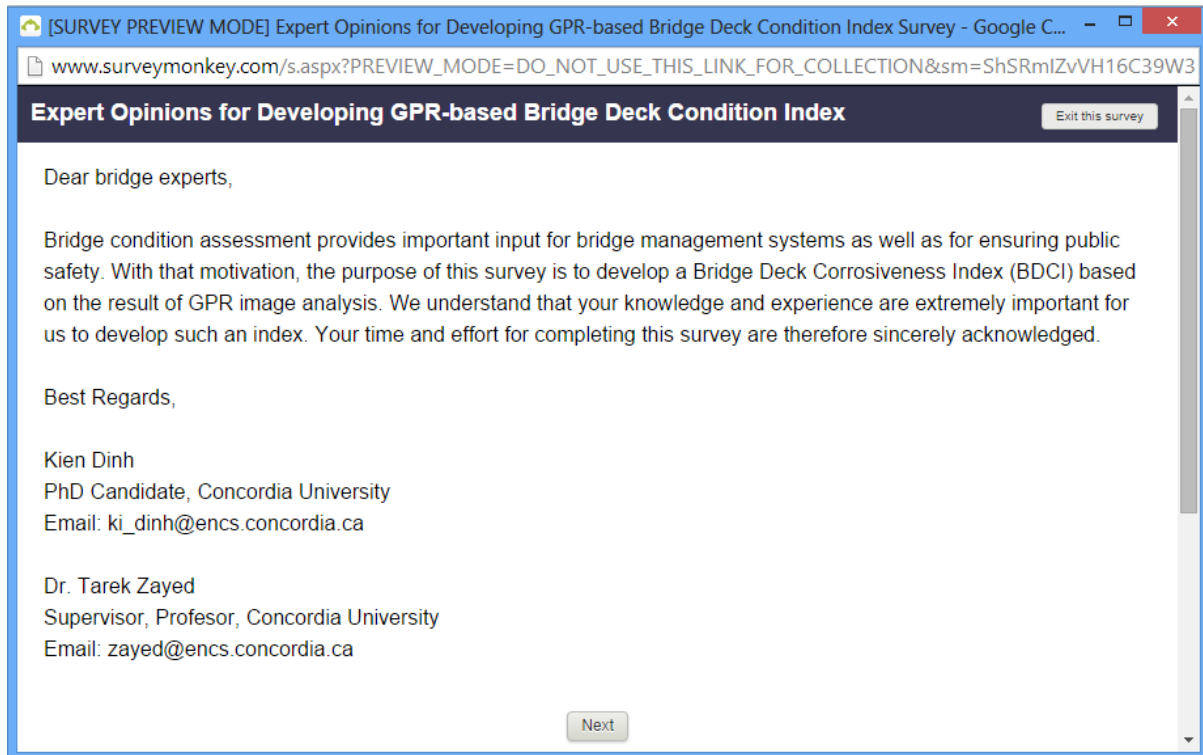**Fig. A. 20 Depth profile of structural properties (Maser 1996)**

Fig. A. 21 Contour map of reinforcement depth (Maser 1996)

APPENDIX B

www.surveymonkey.com/s.aspx?PREVIEW_MODE=DO_NOT_USE_THIS_LINK_FOR_COLLECTION&sm=ShSRmIZvVH16C39W3

Expert Opinions for Developing GPR-based Bridge Deck Condition Index

Exit this survey

1. Contact information (optional)

*2. Which option following best describes your expertise?

○ A bridge manager

○ A bridge engineer

○ A bridge inspector

○ A bridge researcher

○ Other (please specify)

*3. How many years of experience you have with this expertise?

○ 0-5 years

○ 5-10 years

○ 10-20 years

○ More than 20 years

Prev   Next

---

www.surveymonkey.com/s.aspx?PREVIEW_MODE=DO_NOT_USE_THIS_LINK_FOR_COLLECTION&sm=ShSRmIZvVH16C39W3

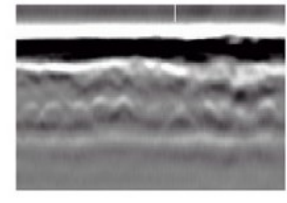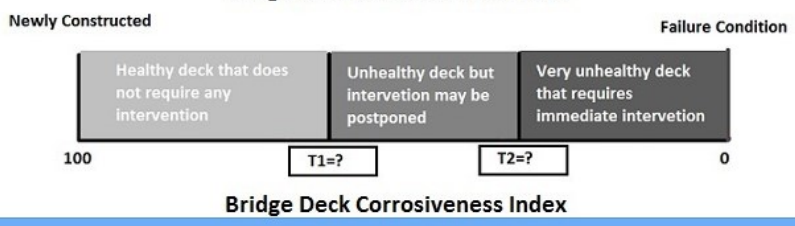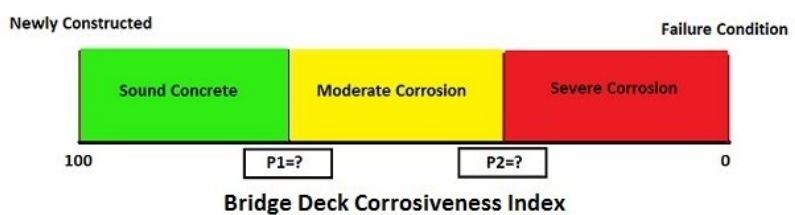**Expert Opinions for Developing GPR-based Bridge Deck Condition Index**

Exit this survey

Ground Penetrating Radar (GPR) has long been a recommended technology for condition assessment of concrete bridge decks subjected to corrosion-induced deterioration. Based on visual analysis of GPR profiles (images), we have developed several linguistic terms describing three possible condition states of concrete bridge decks, as shown in the below figure. Using a continuous scale from 0 to 100, the same idea as Bridge Health Index, our purpose is to map those linguistic descriptions to the rating of bridge deck. This scale, along with the deterioration process of a concrete deck, is depicted in the same figure.

Since linguistic terms are very fuzzy, your expert opinions in this survey would be used later to convert them to crisp number. To fill out this form, number P1 in the next question, for example, you should imagine what would be possibe range of bridge deck corrosiveness index (BDCI) if the entire deck is found in sound condition. If you think the range is from 100 (newly constructed) to 80, P1 would be 80 in your response. If that is the case, the BDCI index for a deck with entire moderate corrosion would occupy the range from 80 (P1) to P2, where P2 value has to be smaller than P1.

Next, suppose that BDCI for a bridge deck has been obtained based on the information you provided (P1 & P2) and percentage of each condition state found by GPR, please give us the two BDCI levels (thresholds), T1 and T2, as illustrated in the figure. First, the one at which you consider the bridge deck is not healthy but intervention can be postponed (T1). And second, the one at which you think the deck would require immediate intervention (T2).

[SURVEY PREVIEW MODE] Expert Opinions for Developing GPR-based Bridge Deck Condition Index Survey - Google ...

www.surveymonkey.com/s.aspx?PREVIEW_MODE=DO_NOT_USE_THIS_LINK_FOR_COLLECTION&sm=ShSRmIZvVH16C39W

Sound Concrete:
1. Rebar reflection is strong and clear with hyperbola shape.
2. Bottom reflection is clearly visible at location where supporting beams are not present

Moderate Corrosion:
1. Rebar reflection is relatively weak but hyperbola shape is clearly visible.
2. Some attenuation at slab bottom but bottom reflection is still visible.
3. Radar velocity effects are minimal or absent

Severe Corrosion:
1. Strong attenuation at top rebar level; hyperbola shape from rebar reflection is distorted or disappears.
2. Bottom reflection is very weak or absent.
3. Radar velocity effects are present (e.g., bottom sags)

Newly Constructed   Failure Condition

| Sound Concrete | Moderate Corrosion | Severe Corrosion |

100   P1=?   P2=?   0

Bridge Deck Corrosiveness Index

Newly Constructed   Failure Condition

| Healthy deck that does not require any intervention | Unhealthy deck but intervention may be postponed | Very unhealthy deck that requires immediate intervention |

100   T1=?   T2=?   0

Bridge Deck Corrosiveness Index

* **4. Please fill out your numbers (as explained above) in the boxes below.**

P1   [ ]

P2   [ ]

T1   [ ]

T2   [ ]

* **5. What is your recommended action for a deck with BDCI below T1?**

◯ Do nothing and more frequent monitoring

◯ Repair (shallow, deep patching or full depth removal, etc.)

◯ Total deck replacement

◯ Other (please specify)

[ ]

* **6. What is your recommended action for a deck with BDCI below T2?**

◯ Repair (shallow, deep patching, or full depth removal, etc.)

◯ Total deck replacement

◯ Other (please specify)

[ ]

Survey Completed. Thank you very much for your precious time.

Prev   Done